The Role of JAK2^{V617F}-positive Endothelial Cells in Aberrant Haemostasis and Thrombosis

Megan Elizabeth Cosgrove

Doctor of Philosophy

University of York
Biology

July 2016

Abstract

Endothelial cells (ECs) are a key component in maintaining proper haemostasis and thrombosis. During homeostasis, EC surfaces are anti-thrombotic, preventing platelet activity and activation of coagulation. On injury, EC surfaces become pro-thrombotic, enhancing platelet activation and mediating the adhesion of haematopoietic cells to the injured surface. Together, ECs and haematopoietic cells maintain blood fluidity in the absence of injury, but promote thrombus formation to prevent excessive blood loss on injury. The mechanisms behind these processes are tightly regulated and any perturbations can have devastating consequences to patient health, such as stroke, infarction or bleeding diathesis.

Myeloproliferative neoplasms (MPNs) are a class of haematological malignancies characterised by hyper-proliferation of myeloid cells, most commonly caused by a mutation in the non-receptor tyrosine kinase Janus kinase 2 (JAK2), $JAK2^{V617F}$. Patients with MPNs often suffer from complications due to dysfunctional haemostasis and thrombosis; therefore, patient treatment is aimed at preventing these events. $JAK2^{V617F}$ has been identified in both haematopoietic and ECs of a subset of patients with MPNs. Given the role of both cell types in maintaining physiological haemostasis and thrombosis and the common occurrence of dysfunctional haemostasis and thrombosis in patients with MPNs, it is reasonable to suspect that mutant haematopoietic and ECs may contribute to these disease manifestations.

Here, $JAK2^{V617F}$ -positive ECs were found to contribute to the dysfunctional haemostasis observed in a mouse model of MPNs. Further investigation into the mechanisms of $JAK2^{V617F}$ EC activation *in vitro* showed that permeability is increased in HUVECs expressing $JAK2^{V617F}$, which may be caused by an increase in inflammation. ECs generated from patient blood samples were shown to have varying levels of $JAK2^{V617F}$, which was inversely related to proliferation of cells. ECs which expressed high $JAK2^{V617F}$ allelic burden did not proliferate and showed features of EC senescence. Further investigation into $JAK2^{V617F}$-positive ECs will elucidate the mechanisms of $JAK2^{V617F}$ -induced EC inflammation, permeability and senescence.

Table of Contents

Figures

Tables

Acknowledgements

I know that I will always look back fondly on the 5 years I spent doing my PhD, and I owe this to the many people I have met and formed both professional and personal friendships with along the way. Firstly, many thanks are owed to my supervisor Ian Hitchcock. In the beginning, you saw a potential in me that I could not recognise in myself. Thank you for your patience, encouragement and support and for inviting me to come to Hogwarts with you to finish my PhD. I have enjoyed every step of the journey, from lab lunches in Port Jefferson to Sunday Roast at the Lamb and Lion. Your guidance as a supervisor and friend have helped form me into the scientist and person I am today.

To my Mom, who has always been an important part of my life journey, there is no page limit that would suffice for me to describe how grateful I am to have you as my Mom. Your continued love and support throughout my life are the foundation for my success. I took your "stay in school" advice quite literally and because of this I will live confidently knowing I can always depend on myself. Many thanks are owed to my brother James, for reminding me that what I do is "cool" and for believing that my work is important. You make me feel like a science rock star, which certainly helped push me through days I was feeling discouraged. Thank you to my Dad, for your love and support. I think I finally learned how "not to sweat the small stuff."

I would also like to thank my friends and extended family, on both sides of the Atlantic. Thank you to my sorority sisters, in particular Jaclyn Zimmel, Jessica Hurley and Margo Lacure; I am a better person and friend because I know you. My colleagues and friends in the CII, the Q Crew, thank you for making this a truly enjoyable place to work. Thank you to Elizabeth Gothard, who has relieved me of my fear of statistics and renewed my love of maths and to Katrina Reilly, my fellow weekend warrior, for your support and friendship during the last months of my PhD.

Lastly, thank you to Veena Sangkhae and Leah Etheridge, who together with the Hitchcock boys became my second family. Home never seemed far away, as you quickly made England a place I will always feel at home. Along with cream tea, fascinators and my hot water bottle, I bring our memories and friendships back with me to America.

Author's Declaration

All of the work presented in this thesis was performed by myself, with the exception of the following: LC-MS analysis in Chapter 4, which was performed by Adam Dowle (Proteomics Core, University of York) RNA purification and library preparation for RNA sequencing in Chapter 4, which was performed by Dr Sally James (Genomics Core, University of York), RNA sequencing statistical analysis in Chapter 4, which was performed by Dr Sandy Macdonald (Bioinformatics Core, University of York) and phase focus ptychography in Chapter 5, which was performed by and Dr Rakesh Suman (Phasefocus, Sheffield, United Kingdom). All sources are acknowledged as references. This thesis has not been submitted for any other degrees. Some of the data has been published in a peer reviewed journal as listed below.

Etheridge SL, Roh ME, Cosgrove ME, et al. JAK2V617F-positive endothelial cells contribute to clotting abnormalities in myeloproliferative neoplasms. *Proc Natl Acad Sci U S A*. 2014;111(6):2295-2300.

CHAPTER 1 INTRODUCTION

1.1 Haemostasis and Thrombosis: An Overview

Haemostasis and thrombosis are essential physiological processes. Haemostasis is the collective organisation of blood fluidity maintenance, sustaining adequate blood flow and promoting thrombus formation when vessels are injured. Thrombosis is the process of thrombus formation and in healthy humans, this occurs only when there is vessel injury. Both processes are highly regulated and insults which disrupt the balance between blood flow and thrombus propagation have severe consequences.

1.1.1 Virchow's triad

Pathological thrombus formation has long been recognised as a cause of human disease and morbidity. In the mid-1800's Rudolf Virchow described three contributing mechanisms of venous thrombosis: blood hypercoagulability, static blood flow and vessel wall injury, which were later referred to as "Virchow's triad"(Figure 1.1).[1] Indeed, evidence supports the role of individual protein factors, or lack thereof, in promoting a hypercoagulable environment.[2] Deficiencies in antithrombin, protein C or protein S or increased expression of coagulation factors such as factor VIII all contribute towards a hypercoagulable vessel environment. Static blood flow, caused by inactivity or immobilisation, can aid accumulation of protein factors leading to thrombus formation.[3] This risk factor is particularly important in venous thrombosis, where normal blood flow is already reduced due to a farther distance from the heart and lower blood pressure. The last principle included in Virchow's triad, vessel wall injury, may help to promote thrombus formation in both physiological and pathological situations. In pathology, vessel inflammation, injury after plaque rupture and altered expression of endothelial surface molecules all promote thrombus formation. Any single component of Virchow's triad can contribute towards the disruption of the haemostatic balance and as additional components become involved, patient health may become severely compromised.

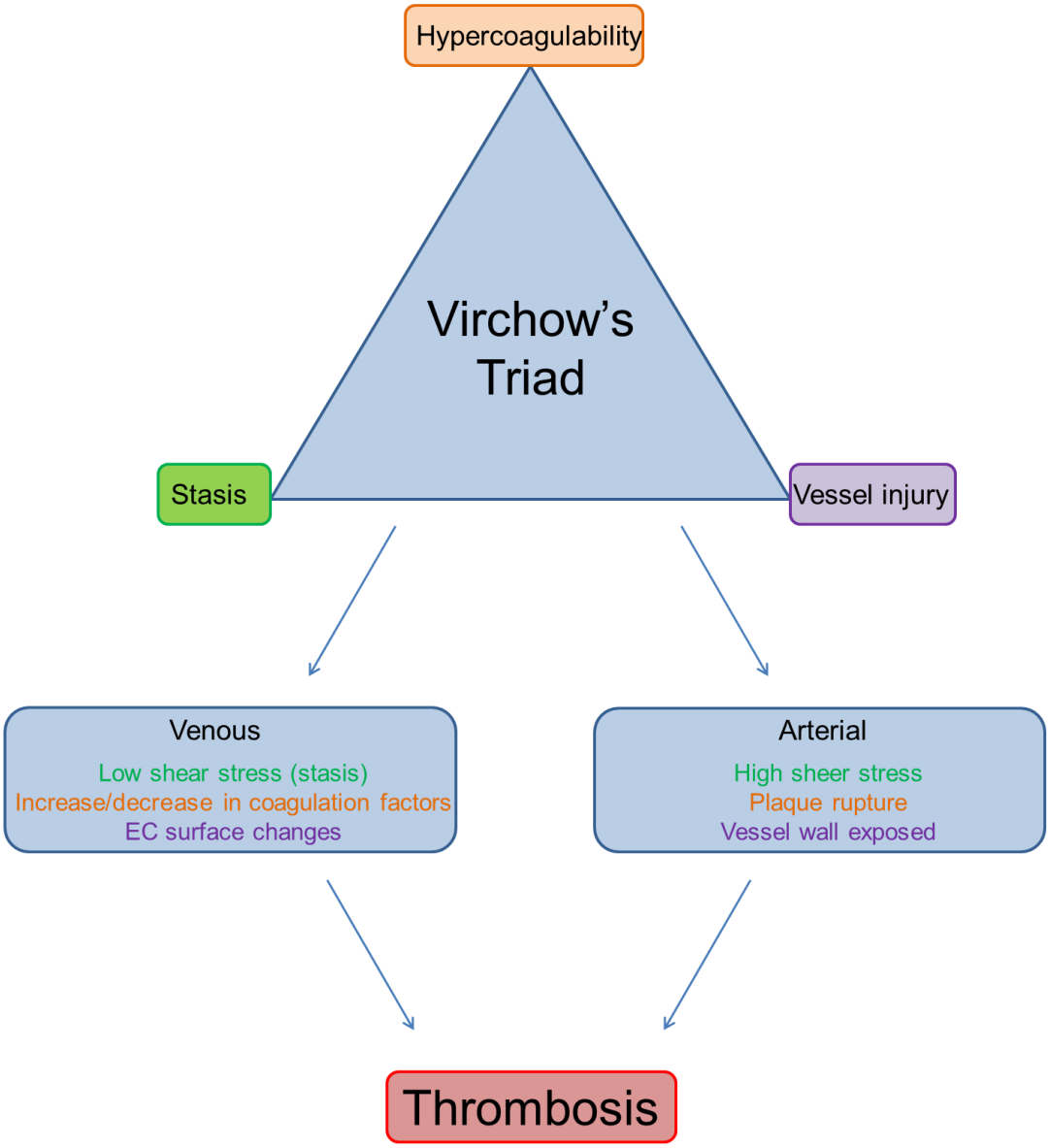

Figure 1.1 Virchow's triad
Rudolf Virchow described 3 factors contributing to venous thrombosis: hypercoagulability, stasis and vessel injury. Although the mechanisms behind venous and arterial thrombosis differ, they can both be related to these founding principles in "Virchow's triad."

1.1.2 Types of thromboses

Although Virchow's triad was first used to describe venous thrombosis, arterial thrombosis is also reflected by changes in hypercoagulability, stasis and vessel wall integrity. Often arterial thrombi form when atherosclerotic plaques rupture, exposing an injured vessel wall and releasing a storm of pro-coagulant factors. Platelet adhesion and activation are crucial steps in arterial thrombus formation, due to the high sheer stress in arteries. "White clots" form in arteries because platelets are integrated in the growing thrombus.[4] In contrast, venous thrombi consist mainly of red blood cells and fibrin deposition, leading to "red clot" formation. Both white and red clots result in disruptive blood flow and can have devastating consequences to patient health.

In addition to atherothrombosis which is often the result of a combination of high shear stress and plaque rupture, arterial thrombi can form in regions of low shear stress as in atrial fibrillation. Embolism of clots from the heart to the brain is a concern for patients which develop thrombi due to stasis in the heart atria.[5] Thrombosis in veins includes both venous thromboembolism (VTE) and deep vein thrombosis (DVT), often in the veins of the leg. Similar to cardioembolism, thrombi in veins can dislodge and travel further downstream and may lead to pulmonary embolism (PE). Emboli such as these are a leading cause of death worldwide.[6] Thrombi which remain lodged in deep veins can lead to swelling and oedema in patients.

1.1.3 Haemorrhaging

As destructive as pathological thrombus formation is to health, haemorrhaging can be equally as dangerous to patients. Haemorrhaging can lead to permanent tissue and organ damage and can result in hypovolemic shock due to systemic blood loss. The brain, in particular, is extremely susceptible to adverse effects of haemorrhage as the body has evolved to prevent such damage through the enhanced tight junctions of the blood brain barrier.[7] Inherited bleeding disorders, such as haemophilia, are often caused by a deficiency or dysfunction of one or several coagulation factors or blood cell types.[8] Acquired bleeding disorders are often secondary to primary diseases, including renal and liver disease. Thrombophilia, which may lead to increased thrombosis, may instead lead to an acquired bleeding disorder caused by scavenging of the coagulation protein von Willebrand Factor (vWF) by platelets.[9] Even in healthy

patients, trauma-induced haemorrhage can be life-threatening when treatment is inadequate or delayed.

1.1.4 Impact of cardiovascular disease on the National Health Service

Diseases of haemostasis and thrombosis are broadly classified as cardiovascular disease. Risk factors of cardiovascular disease include age, obesity, inactivity and smoking. Additionally, clotting and bleeding are often co-morbidities associated with diseases unrelated to the cardiovascular system such as cancer. In the United Kingdom, cardiovascular disease is the second leading cause of death, responsible for 28% of deaths in 2012 (British Heart Foundation, BHF).[10] It is second only to cancer (29%); however, when combined with cancer-related causes of thrombosis and haemostasis abnormalities, the number of clotting and bleeding related deaths may actually be greater. In England, expenditure for cardiovascular disease within the NHS was greater than £6.8 billion in 2012 (BHF).[10] In Wales, Northern Ireland and Scotland £442.3, £393 and £750 million were a cost to the NHS, respectively (BHF).[10]

Complications associated with thrombosis and haemostasis are leading causes of disability and death across the world.[5] Mechanisms contributing to these complications include both dysfunctional intrinsic haemostasis and thrombosis and secondary effects of unrelated diseases. In both situations, the delicate balance of blood fluidity and thrombus formation is disrupted and patients suffer severe consequences. Research into these processes is essential for understanding the mechanisms of their deregulation, prevention of adverse events and improving treatment of at-risk or ill patients.

1.2 Mechanisms of Haemostasis

Haemostasis consists of three major steps: vasoconstriction, platelet adhesion/activation and coagulation. A fourth step, fibrinolysis, completes the cycle, degrading the fibrin-rich clot to resume blood flow. Together, these four steps ensure that blood flow ceases when vessels are injured and blood fluidity is maintained in the absence of injury. The four steps of haemostasis are described in more detail in the following sub-sections.

1.2.1 Vasoconstriction

The initial physiological response to vessel injury is vasoconstriction and this process is regulated mainly by signalling between endothelial cells (ECs) and smooth muscle cells (Figure 1.2).[11] Endothelin-1 (ET-1) is produced and released by ECs in response to inflammation and binds to receptors on both smooth muscle and ECs.[12] Thromboxane (TxA2) produced by the cyclooxygenase (COX) enzymes in ECs acts on thromboxane-prostanoid receptors present on platelets and smooth muscle cells. Both ET-1 and TxA2 cause an influx of calcium into smooth muscle cells inducing constriction of these cells, narrowing the vessel lumen. Vasoconstriction is the first line of defence against blood loss and brings cells and proteins involved in clotting closer together, enhancing their capacity to interact. In constrast, nitric oxide (NO), prostacyclin (PGI2) and endothelium derived hyperpolarizing factor (EDHP) promote vasodilation by ECs.[13] NO is produced by endothelial NO synthase (eNOS) and is vasoprotective; it causes smooth muscle cells to dilate and inhibits platelet aggregation, leukocyte adhesion and exocytosis of Weibel-Palade bodies, which contain pro-coagulant proteins. PGI2, the alternative product to TxA2, causes vasodilation albeit to a lesser extent when compared to NO. EDHP hyperpolarises the cell membrane by minimising calcium influx to the cell through induction of potassium efflux from the cell.[11] EC hyperpolarisation induces smooth muscle cell hyperpolarisation, the effects of which are vasodilatory. Following the theme of balance in haemostatic processes, vasodilation and vasoconstriction are also regulated such that blood fluidity is maintained and perfusion of tissues and organs is adequate. On vessel injury, this balance favours vasoconstriction.

1.2.2 Primary haemostasis

Following vasoconstriction, primary haemostasis occurs and results in the generation of a platelet plug to seal off the injured site (Figure 1.3). This stage primarily involves platelets and their interaction with the exposed subendothelial layer. Healthy human adults have ~150-400x10^9 platelets per litre of blood and ~10^{11} of these platelets are replaced each day.[14] Production of platelets occurs in the bone marrow and begins with differentiation of myeloid progenitors to megakaryocytes. This occurs through endomitosis, whereby cells synthesize DNA, prepare for mitosis

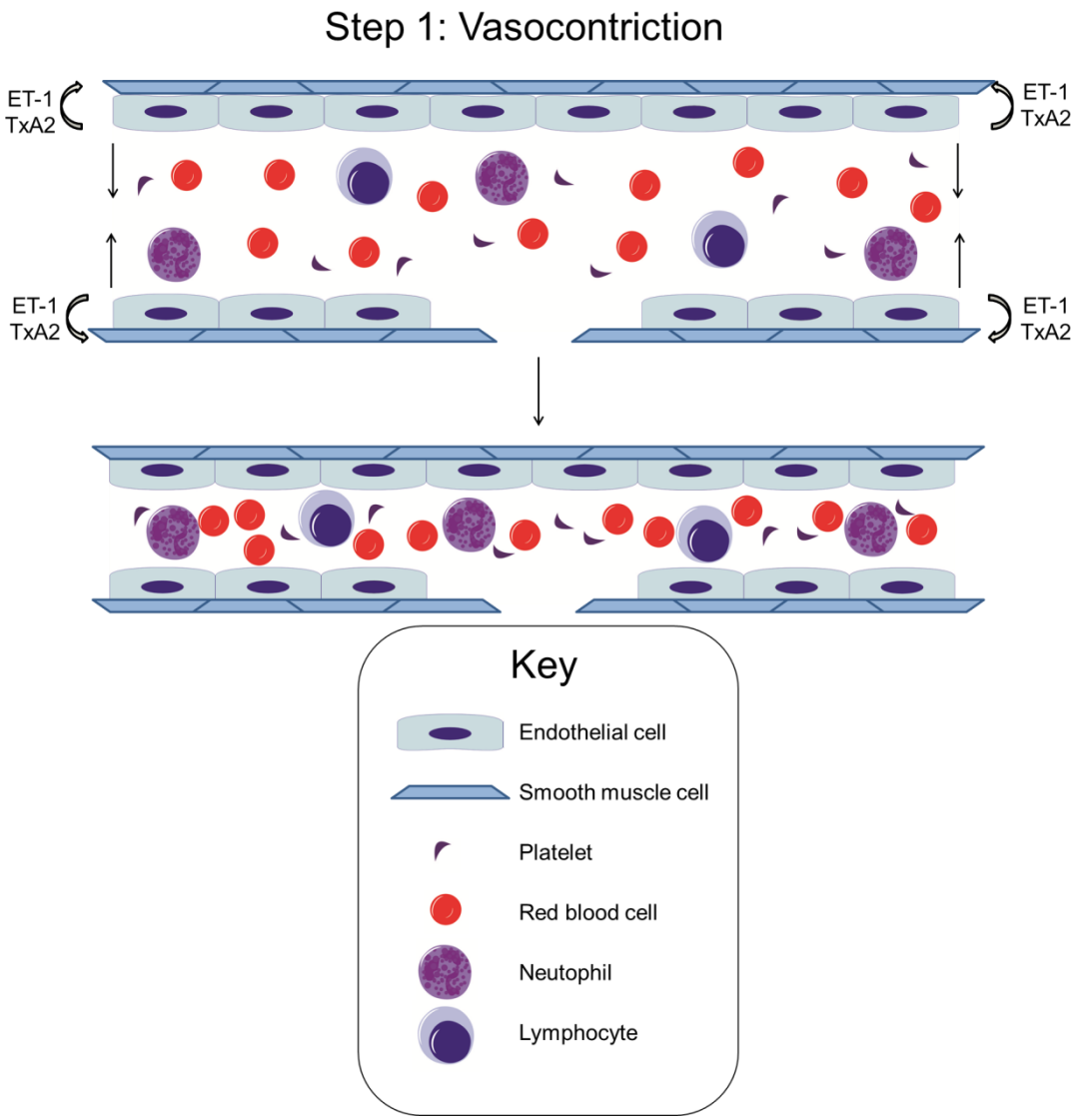

Figure 1.2 Haemostasis step 1: vasoconstriction
Vasoconstriction is the first step of haemostasis and is mainly controlled by EC-smooth muscle cell interactions. Vasoconstriction results in vessel narrowing, bringing cellular and coagulation factor components in close proximity.

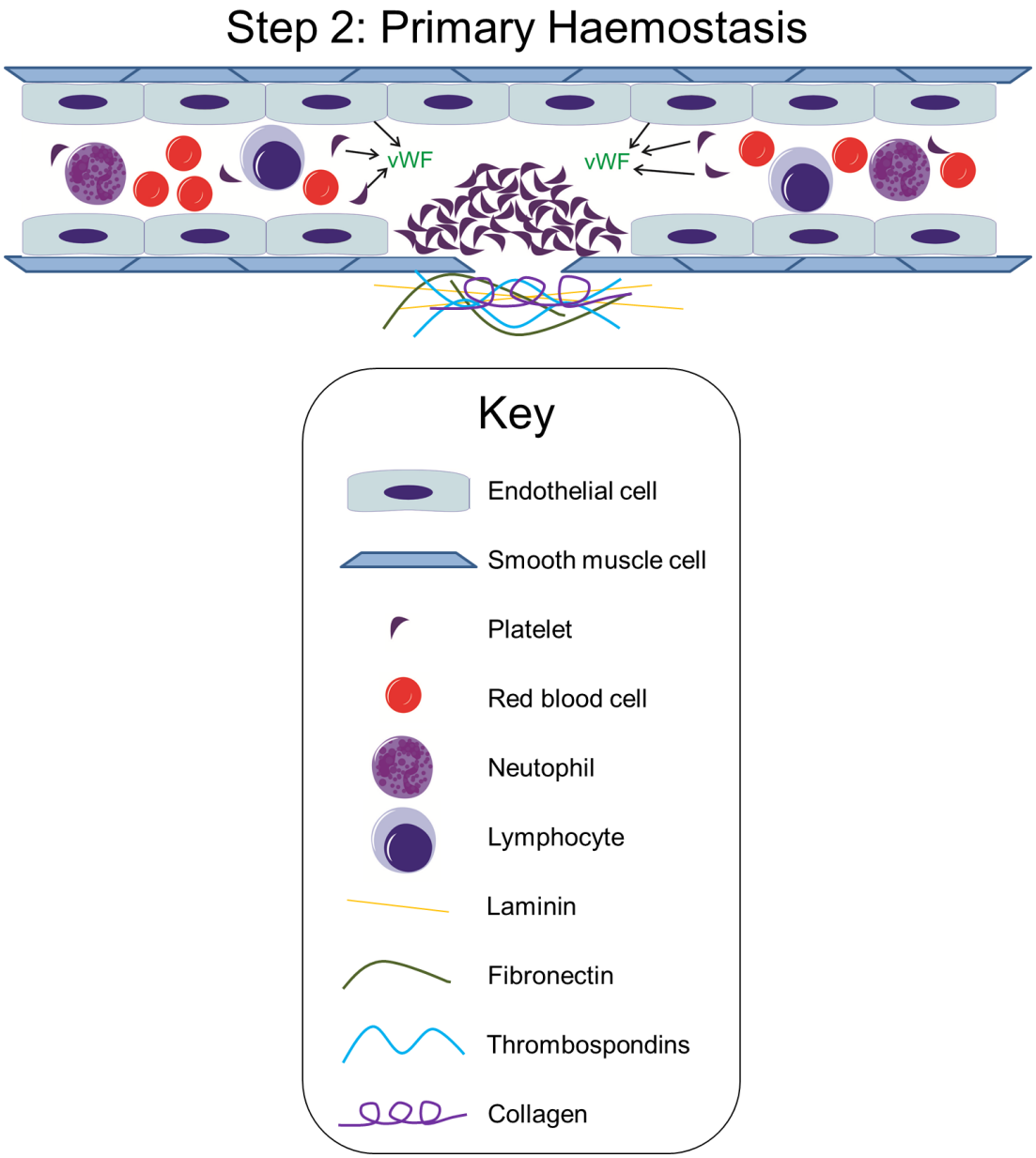

Figure 1.3 Haemostasis step 2: primary haemostasis
The second step of haemostasis, called primary haemostasis, requires cellular interactions with the damaged vessel surface. Platelet adhesion to the subendothelial layer is mediated by interactions with collagen and vWF. Binding of these components begins secondary activation of platelets, which results in more stable interactions of platelets with collagen, laminin, fibronectin and thrombospondins. Primary haemostasis results in formation of the platelet plug.

but never complete the cell cycle.[15] The result is megakaryocyte enlargement and polyploidy. Mature megakaryocytes then travel to bone marrow sinusoids, where they fragment into platelets in circulation. Platelets are therefore cell fragments; they do not contain a nucleus however they have the ability to respond to extracellular stimuli and undergo dynamic cellular changes to respond to these cues. Through these effects platelets elicit their role in platelet plug formation and provide a scaffold for coagulation, the third stage of haemostasis.

Intact vessel walls separate blood from extracellular matrix components. However on injury, blood is exposed to these components and their interaction helps to initiate thrombosis. The subendothelial layer consists of laminin, thrombospondins, fibronectin, and collagen and immobilised protein factors, which are typically dissolved in plasma but become recruited to the extracellular matrix when exposed.[16,17] One such protein is vWF.

vWF is synthesized by ECs and megakaryocytes and stored in Weibel-Palade bodies of ECs and α-granules in platelets.[18] ECs constitutively secrete a basal level of vWF, but can be stimulated to secrete additional vWF on injury. Constitutive secretion occurs across both surfaces, apical and basolateral.[19] Apical release of vWF circulates in plasma and basolateral release of vWF becomes incorporated into the extracellular matrix of the subendothelial layer. In the subendothelium, vWF binds collagen type VI and likewise, when this layer is exposed plasma vWF becomes immobilised by binding collagen type VI and collagen types I and III in layers beyond the subendothelium. [20,21] In addition to collagen binding sites, vWF contains binding sites for the platelet glycoprotein (GP)Ibα and integrin $\alpha_{IIb}\beta_{III}$.[22] vWF-platelet interactions facilitate initial platelet tethering to the injured site; this interaction is especially important in arterial thrombosis, where shear stress is high. vWF undergoes extensive post-translational processing to form ultra-large molecular weight multimers that can be as large as 20,000kDa.[19] In plasma, vWF is cleaved to multimers of different sizes by **a** **d**isintegrin-like **a**nd **m**etalloprotease domain with **t**hrombo**s**pondin type-1 motif, number **13** (ADAMTS13).[23] Ultra large molecular weight vWF is most active in platelet tethering; therefore cleaving multimers to smaller sizes by ADAMTS13 reduces their ability to bind platelets and collagen. vWF-platelet interactions are transient; platelets require additional mechanisms of adhesion and activation to secure the platelet plug. These interactions are mediated by platelets binding to other

components of the subendothelial layer. Platelet GPVI and integrin $\alpha_{II}\beta_I$ bind collagen, resulting in both adhesion and activation of platelets.[24] Platelet integrin $\alpha_V\beta_I$ binds fibronectin and subsequent activation of platelets allows for the interaction of integrin $\alpha_{IIb}\beta_{III}$ with fibronectin.[25,26] Thrombospondin-2, another component of the subendothelial layer binds platelets and thrombospondin-1, secreted by activated platelets binds neighbouring platelets and potentiates platelet aggregation.[27] Similar to platelets binding collagen, platelets form additional interactions with the basement membrane protein laminin through GPVI and $\alpha_{VI}\beta_I$.[28] Lastly, platelets adhere to fibrinogen through $\alpha_{IIb}\beta_{III}$.[29]

On activation, platelet intracellular signalling triggers degranulation of dense and α-granules, storage organelles in platelets. Contents stored in these granules are pro-coagulant and they subsequently bind to platelets and neighbouring cells to potentiate platelet aggregation. Potent platelet agonists, which are stored and released by platelets, include adenosine diphosphate (ADP) and TxA2.[30] Activation of platelets by ADP and TxA2 is especially important for sustained platelet activation, ensuring progression of haemostasis to step three, coagulation. Activation of platelets also provides the negatively-charged phospholipid membrane scaffold, which protein factors use for their enzymatic reactions in the coagulation cascade.

1.2.3 Coagulation

During primary haemostasis, platelets first become tethered to the injured surface by their interactions with vWF. This facilitates more secure platelet adhesion through additional glycoprotein and integrin interactions with subendothelial matrix proteins. Finally, platelets undergo the initial stages of activation when their receptors bind proteins of the subendothelial layer, resulting in intracellular and cell surface changes which promote the third phase of haemostasis, coagulation.

The coagulation cascade consists of a series of enzymatic proteins and their cofactors, which cleave proteins in a series that results in production of insoluble fibrin (Figure 1.4). There are two mechanisms of activating coagulation: the extrinsic pathway, induced by tissue factor (TF) and the intrinsic pathway, induced by thrombin.[31] TF, located in the subendothelium, is exposed on injury and forms a complex with factor VII. This facilitates conversion of VII to VIIa in the presence of

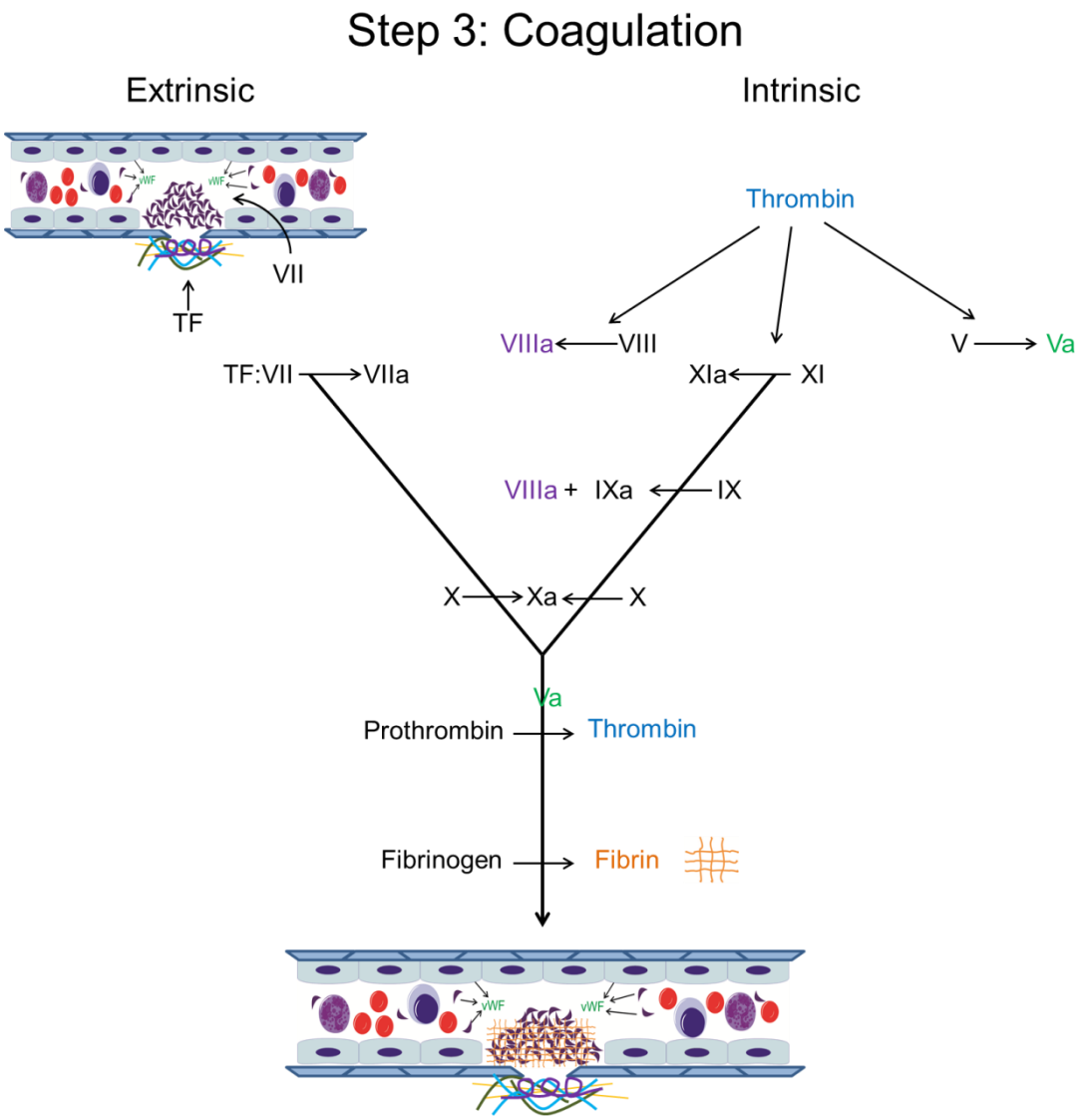

Figure 1.4 Haemostasis step 3: coagulation
Coagulation is an enzymatic cascade of serine proteases which results in fibrin deposition in the growing thrombus. In this diagram, both the extrinsic and intrinsic coagulation pathways are shown, mediated by TF and thrombin, respectively. Conversion of each inactive protein to its active form is illustrated from top to bottom of each angled line, with the product of one reaction facilitating the reaction of the subsequent reaction. When cofactors are required, these are written above arrows depicting the enzymatic reaction. Coagulation results in stable, fibrin-rich thrombus formation.

its co-factor, a calcium ion. Factor VIIa-TF then converts factor X to Xa. Together with factor Va, Xa converts prothrombin to thrombin which then cleaves soluble fibrinogen to insoluble fibrin. Fibrin can then be incorporated into the growing thrombus. Alternatively, thrombin can activate factor XI to XIa, which can convert factor IX to IXa. This leads back to the common coagulation pathway with the conversion of factor X to Xa. The end result of both intrinsic and extrinsic pathways is fibrin deposition, resulting in stable thrombus formation. An important principle of blood coagulation is amplification; once the pathway is activated factors react again with earlier factors to amplify the signal. This further ensures the response results in stable thrombus formation.

1.2.4 Fibrinolysis

Haemostasis comes full circle when the fibrin-rich thrombus is degraded and blood flow is restored to normal (Figure 1.5). Fibrin is degraded by plasmin, a serine protease generated from enzymatic cleavage of its zymogen, plasminogen.[32] Two main proteases facilitate this enzymatic reaction: tissue-type plasminogen activator (tPA) and urokinase (UK). tPA is synthesized and secreted mainly in ECs and tPA in circulation is associated with plasminogen activator inhibitor 1 (PAI-1).[33,34] UK is synthesized by fibroblasts, epithelial cells, monocytes and macrophages of the urinary tract.[35-37] Once activated, tPA and UK cleave plasminogen to plasmin, the active molecule which degrades fibrin. Both coagulation and fibrinolysis rely heavily on cleavage of inactive zymogens to release the active enzyme. Similar to coagulation, zymogen activation allows for amplification of fibrinolysis, resulting in efficient breakdown of the fibrin-rich clot.

1.3 Cellular Components of Haemostasis

Haemostasis is a coordinated process of both cellular and plasma protein constituents. In the previous section, these components were discussed collectively to give a brief overview of the four stages of haemostasis. Here, the functions of individual cell types are reviewed more closely.

1.3.1 Platelets

Platelets in circulation have the ability to adhere to injured surfaces but they have an even greater capacity to aggregate and integrate into a growing thrombus when they

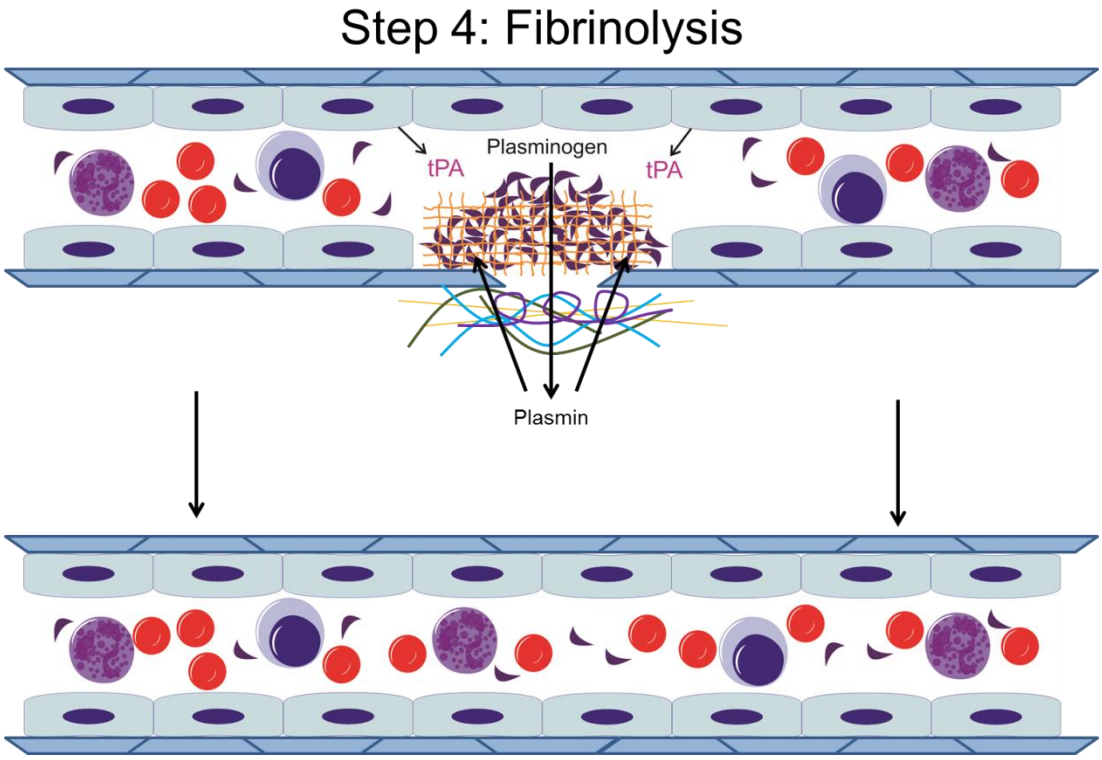

Figure 1.5 Haemostasis step 4: fibrinolysis
After the vessel is healed, fibrinolysis occurs to break down the thrombus. Fibrin degradation is accomplished through plasmin, which is activated by tPA produced by ECs. This results in thrombus degradation and restoration of blood flow.

become activated. As discussed in the previous section, platelets can bind to vWF, collagen, laminin and fibronectin in the subendothelial matrix even before they are activated. However, these interactions are greatly enhanced when platelets are activated and their receptors are better primed for stable interactions with their ligands. Initial adhesion of platelet GPVI to collagen causes an influx of calcium ions into platelets, leading to conformational changes in α2β1 which can bind collagen more stably (Figure 1.6).[38-40]

Platelets are further activated by agonists binding to their cognate receptors. These agonists include thrombin, ADP, prostaglandins and epinephrine. Thrombin, a serine protease, activates the protease-activated receptors (PAR) 1 and 4, which are G-protein coupled receptors.[41,42] Thrombin is a strong platelet agonist, resulting in the characteristic platelet-shape change from round cell fragments to elongated fragments with projections of cytoplasm from the centre. These changes are mainly the result of calcium influx, one effect of thrombin activation of PARs. ADP binds three platelet receptors, $P2X_1$, $P2Y_1$ and $P2Y_{12}$.[43] Similar to PARs, $P2Y_1$ and $P2Y_{12}$ are G-protein coupled receptors which activate phospholipase Cβ and inhibit adenylyl cyclase, respectively. In contrast to PARs, $P2X_1$ is a calcium ion channel which may result in calcium influx directly; however this has not been shown. Prostaglandins, specifically TxA2 binds its receptor TP on platelets, another G-protein coupled receptor.[44] Epinephrine binds α_2A-adrenergic receptors, also coupled to G-proteins.[45] Platelet activation is synergistic; to make use of full platelet activation potential several agonists are needed to activate multiple G-protein coupled receptors.

Many of the agonists and components of platelet activation are synthesized by none other than the platelets themselves. These proteins are stored in either dense or α-granules. Among other components, dense granules contain ADP, ATP and calcium and α-granules store fibrinogen, vWF, factor V and thrombospondin.[46,47] Initial platelet adhesion and activation leads to platelet degranulation and the release of dense and α-granule components. Therefore, platelets aid in their own activation by releasing components which can subsequently bind and enhance platelet activation. Collectively, platelets undergo primary and secondary stages of activation. In the primary stage, platelets bind to subendothelial matrix components via receptors which do not require activation-induced conformational change. This

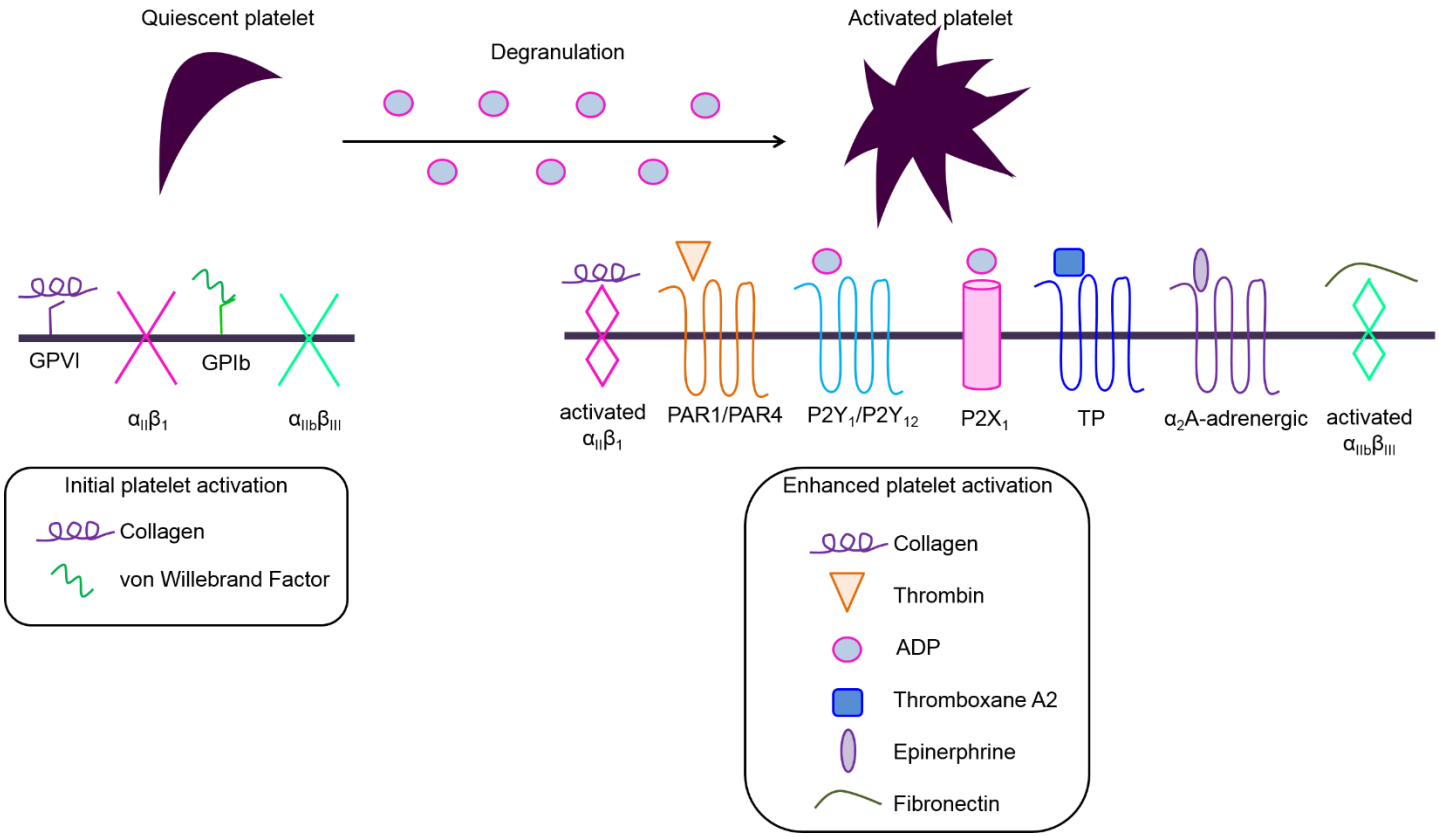

Figure 1.6 Platelets in haemostasis

Platelets are key components in primary haemostasis and coagulation. Primary adhesion of platelets is mediated by interactions of platelet GPVI with collagen and platelet GP1b with vWF in the subendothelial layer. This results in conformational changes in integrins, such as $\alpha_{II}\beta_1$ and $\alpha_{IIb}\beta_{III}$, which can form stable interactions with collagen and fibrinogen, resepctively. Activated platelets undergo shape changes and degranulate, releasing other platelet agonists. Platelets are further activated by binding these agonists, including thrombin, ADP, thromboxane A2, epinephrine.

results in primary platelet activation, whereby receptor conformational changes are induced and degranulation occurs. In the second stage, platelets bind additional subendothelial matrix components with increased affinity and bind platelet agonists made available through degranulation. These effects result in irreversible platelet activation and allow for stable platelet aggregation.

1.3.2 Monocytes

Monocytes are a type of leukocyte in peripheral blood, which translocate into nearby tissues and differentiate into macrophages. They are well-known for their contributions to the immune response, but their role in peripheral blood extends beyond inflammation. Monocytes produce TF, the potent initiator of extrinsic coagulation, in response to activation by either haemostatic or inflammatory mediators.[48] Monocytes are activated by interleukin (IL)-1 or tumour necrosis factor (TNF)-α, but also by the haemostatic agonists thrombin and factor Xa. When activated, monocytes express TF on their surface and release factors to promote inflammation. During vessel injury, monocytes adhere and form stable interactions with both platelets and endothelial cells through chemokine ligand/receptor interactions and integrins.[49] Overlap between haemostasis and inflammation in monocytes aids in amplification of both responses.

1.3.3 Endothelium

For some time, the endothelium was regarded as simply the barrier between the blood and underlying tissues. It is now known to be a highly active and dynamic cell type, possessing many of its own functions and the ability to alter those functions when necessary. ECs are found throughout the entire body forming the inner layer of all blood vessels. Collectively, the endothelium contributes to haemostasis and thrombosis, angiogenesis, leukocyte transmigration and permeability.[11] However, it is important to note that although the endothelium as a whole performs these functions, it is a heterogeneous cell type and the mechanisms behind these functions are vessel and organ specific.[50,51]

1.3.3.1 Pro-thrombotic properties of ECs

ECs were previously mentioned in regard to their role in vasoconstriction during the first phase of haemostasis. Whilst signalling smooth muscle cells to induce

vasoconstriction, ECs themselves become activated and contribute to platelet and protein coagulation factor activation (Figure 1.7).[11] Additional ultra-large vWF multimers are mobilised from EC Weibel-Palade bodies and platelet activating factor (PAF) is synthesised and released.[52,53] Upregulation of intercellular adhesion molecule-1 (ICAM-1), vascular cell adhesion molecule-1 (VCAM-1), P-selectin and E-selectin promotes platelet and leukocyte adhesion and activation.[54] ECs contribute to anti-fibrinolysis through thrombomodulin (TM)-thrombin cofactor activation of thrombin-activatable fibrinolysis inhibitor (TAFI) and through expression of PAI-1.[55,56] Taken together, ECs promote clot formation and maintenance on injury by changing their own phenotype to be pro-thrombotic and anti-fibrinolytic and by providing the necessary scaffold for coagulation reactions and cell binding.

1.3.3.2 Anti-thrombotic properties of ECs

ECs are the barrier between fluid blood and subendothelial vascular matrices. As such, their phenotype is critical to maintaining blood fluidity. To this end, ECs express and secrete factors which prevent unnecessary activation of coagulation factors and blood cells (Figure 1.7). These factors include tissue factor pathway inhibitor (TFPI), ecto-ADPase (CD39) and tPA. Additionally, ECs provide a surface for the activation of several other factors, including protein C (PC) and antithrombin (AT).

TF, the main agonist for the extrinsic pathway of coagulation, is inhibited by TFPI. TFPI is produced mainly by microvascular ECs and binds to both FXa and the TF-FVIIa complex to inhibit coagulation.[57] Patients with Texas bleeding disorder were shown to have increased TFPI-FV interactions, which resulted in a decrease in the generation of thrombin and an increase in circulating TFPI.[58] These effects contributed to bleeding diatheses in patients with this disease. ADP, an agonist for platelet activation, is hydrolysed to adenosine monophosphate (AMP) by CD39, an ecto-ADPase expressed on the surface of ECs.[59] AMP cannot activate platelets, therefore CD39 promotes platelet quiescence. In a vessel injury mouse model, expression of CD39 was shown to prevent occlusive thrombus formation.[60] This effect was reversed when the mice were treated with a non-hydrolysable form of ADP. ECs also contribute to the final stage of haemostasis, fibrinolysis, through release of tPA. Expression of tPA is particularly noted in lung microvascular

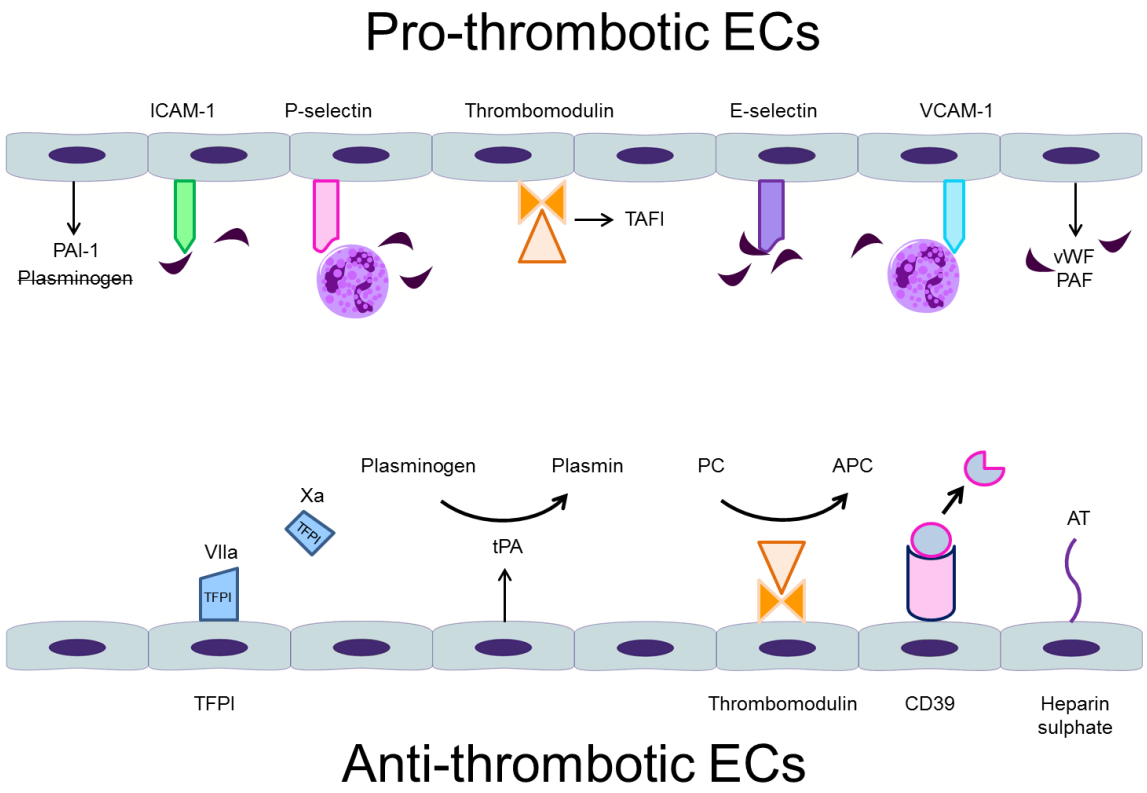

Figure 1.7 EC Pro-thrombotic and anti-thrombotic functions

ECs have both pro-thrombotic and anti-thrombotic properties. Normally, ECs express and secrete numerous factors which promote platelet quiescence: TFPI, tPA, CD39, heparin sulphate. On vessel injury, ECs change phenotype to express and secrete pro-thrombotic molecules: PAI-1, ICAM-1, VCAM-1, P-selectin, E-selectin, vWF, PAF. Thrombomodulin-thrombin contributes to both phenotypes. On the anti-thrombotic surface it promotes PC conversion to APC. Its interactions with thrombin also help prevent it from binding to platelets. On the pro-thrombotic surface, thrombomodulin-thrombin activate TAFI. ECs are dynamic and their role in haemostasis is dependent on the stage

endothelium and is increased when stimulated with thrombin.[61,62] tPA has been used as a thrombolytic agent for decades, however treatment needs to be carefully monitored as this increases patient risk for intracranial haemorrhage.[63]

AT is a serine protease inhibitor (serpin), which inhibits coagulation.[64] Although produced by the liver, AT activity is greatly enhanced when bound to heparin or heparin sulphate proteoglycans, the latter of which is expressed by ECs. AT targets several activated coagulation factors including Xa, IXa, XIa, XIIa, TF-VIIa complex and thrombin, preventing excessive amplification of the coagulation cascade. PC, another factor produced by the liver, has powerful anti-thrombotic properties when activated (activated protein C, APC). Conversion of PC to APC is mediated by TM-thrombin and is enhanced by additional interactions with endothelial protein C receptor (EPCR), an integral membrane protein of ECs.[65] APC inhibits factors VIIIa and Va, preventing excessive Xa and thrombin generation.

1.3.3.3 EC shear stress

ECs throughout the body contribute to the pro-thrombotic and anti-thrombotic functions discussed however there are vessel- and tissue-specific phenotypes that direct EC function in particular vascular niches. The vasculature is a closed system, blood flows from arteries and arterioles where pressure is high and blood oxygen content is rich, through capillary beds where nutrient/waste exchange occurs between blood and tissues, to venules and veins where pressure and blood oxygen content are low. In large vessels, three distinct layers of tissue are observed: the tunica adventitia, the outermost layer where collagen fibrils are stored, the tunica media, the middle layer where smooth muscle cells control vasomotor reactions and the tunica intima, the innermost layer consisting of a single layer of ECs and a basement membrane.[50] Arteries which sustain high shear stress from blood pumped from the heart are thicker in diameter and vessel wall architecture. Veins are farther from the heart and have low shear stress; veins require valves to keep blood flow moving and to minimise stasis. Capillaries consist of only a single monolayer of endothelial cells, basement membrane and interspersed pericytes to control constriction and dilation in these small vessels. ECs have specific roles in the normal physiology of each vessel type.

ECs have mechanosensors to identify changes in shear flow. ECs display an anti-thrombotic phenotype when they sense unidirectional, laminar flow; however

they display a pro-thrombotic phenotype when they sense multidirectional, oscillatory flow.[66,67] The latter is often accompanied by lower flow rates and is often associated with curved vessel regions. These areas are particularly susceptible to EC changes and atherosclerotic plaque formation.[68] The effects of high shear versus low shear, unidirectional flow versus oscillatory flow include changes in EC proliferation, permeability, morphology, motility and phenotype.[66] In laminar flow, EC proliferation is inhibited and permeability is decreased, resulting in a quiescent phenotype. In contrast, oscillatory flow enhances EC proliferation and permeability and EC interaction with platelets and leukocytes is promoted. Some vessel regions are spatially susceptible to oscillatory flow; however temporal changes may enhance the susceptibility to flow disturbances.

1.3.3.4 EC permeability

Endothelial cell-cell contacts control vascular permeability and can be described as continuous, discontinuous, fenestrated or non-fenestrated.[50] Continuous endothelium provides a strong barrier between blood and underlying tissue and consists of tight and adherens junctions. Paracellular transport is inhibited and transport of nutrients/waste across the endothelium must occur through diffusion and endocytosis through caveolae. Endothelium is particularly continuous in regions of high shear stress (arteries) and in the blood brain barrier, where permeability is kept at a minimum.[69] Fenestrations are small pores in the endothelium and these pores increase permeability in vessels and tissues whose functions rely on the transport of materials across the EC membrane. ECs in the intestine, for example, have fenestrae which allow for more efficient absorption of nutrients from digested food. Although fenestrae form pores in ECs, they still maintain structural integrity through fenestral diaphragms.[70] Discontinuous endothelium has true gaps, allowing even more unbiased solute transport.[50] This type of endothelium exists in sinusoidal vasculature, such as in the liver where filtration is the main function. Similar to the ability of ECs to change phenotype on vessel injury, ECs can change the degree to which their cell-cell interactions are continuous by responding to inflammatory cytokines, allowing increased leukocyte migration.[11,50] Similar to haemostasis, permeability is a dynamic function of ECs.

1.3.3.5 EC heterogeneity

All cells are subject to specific regulation by their microenvironment and ECs are no different. Although all ECs contribute to haemostasis, the mechanisms by which ECs of different vessel types and vascular beds achieve these functions are location-specific. vWF is commonly used to identify ECs, but expression is not homogeneous throughout the body. In general, vWF expression is higher in venous circulation when compared to arterial and studies in mice show that the vascular bed with the highest vWF expression is the lung.[50,51,71] TFPI expression is also high in the lung and in the placenta, implicating a role for TFPI in mediating haemostasis in microvessels.[50] Contrarily, EPCR expression is highest in large vessels of lung, liver heart and placenta, contributing towards blood fluidity in macrocirculation of these organs.[50] Spatial distribution of haemostatic factors is further regulated by temporal demands of the body; EC response to disease or vessel injury is dependent on both the intrinsic properties of ECs in that location and how the microenvironment influences those cells to respond. This heterogeneous distribution of endothelial pro- and anti-thrombotic factors results in site-specific mechanisms of haemostasis and thrombosis in both health and disease.

1.3.3.6 Circulating ECs (CECs) and endothelial progenitor cells (EPCs)

ECs have proliferative potential. During angiogenesis, when widespread vessel growth occurs and during vessel injury, when localised vessels re-grow, ECs become more proliferative to add to or repair vessels. Circulating cells were first described as having endothelial-regenerating capabilities by Asahara et al. in 1997.[72] This seminal research led to the identification of EPCs as circulating cells with the ability to differentiate into ECs and incorporate into vessel walls. Since then, a number of groups have attempted to further define the expression profile and function of this cell population to better understand the biology of EPCs and to harness their therapeutic potential.

Defining EPC surface expression is challenging. As early EPCs mature and differentiate they lose haematopoietic-derived markers and gain expression of markers associated with mature *bona fide* endothelium. When Asahara and colleagues first identified and isolated EPC-like populations, they used CD34 expression to define early stem/progenitor cells.[72] CD34-positive cells were collected from human

peripheral blood mononuclear cells (PBMCs) by magnetic activated cell sorting and grown *in vitro* on either fibronectin or collagen coated surfaces. After just one week, cells which attached to fibronectin-coated surfaces expressed several endothelial-derived markers including: CD31 (platelet endothelial cell adhesion molecule [PECAM]-1), Flk-1 (vascular endothelial growth factor receptor [VEGFR]-2), Tie-2 (angiopoietin receptor) and E selectin.

Since 1997, additional markers have been investigated for expression on EPCs. Along with CD34, CD133 is known to be expressed by haematopoietic stem cells (HSCs) and expression of both these markers is lost as HSCs differentiate into mature blood cells.[73] In an attempt to isolate a more primitive cell population, co-expression of CD34 and CD133 was used to identify cells which have not differentiated into either haematopoietic or endothelial lineages, but possess the ability to give rise to either.[74] To discriminate against cells which may be prematurely destined to the haematopoietic lineage, CD45, the common leukocyte antigen was used as an exclusion marker. Similarly, cells that were predestined for the endothelial-lineage were identified through expression of Flk-1.[75,76] $CD34^+CD133^+$ cells constitute a small population in the periphery and the additional criteria of $CD45^-Flk\text{-}1^+$ further limit the number of cells that could potentially be isolated, emphasising the rarity of the EPC population.

The original method of isolating and growing PBMCs on fibronectin-coated plates led to the identification of EPCs as a cell type in circulation and the development of an assay for the enumeration of EPCs in circulation.[72] $CD34^+$ cells alone were able to attach and form spindle-like structures, but when plated in co-culture with $CD34^-$ cells, colonies form which contain an inner cluster of round cells and spindle-type cells radiating from the centre. Asahara and colleagues compared these colonies to "blood-islands," the structures which give rise to both blood and endothelial lineages in the developing embryo. A few years later, Hill and colleagues perfected the method of EPC colony generation and used the enumeration of EPCs as a diagnostic tool in cardiovascular patients.[77] These colonies, now termed colony forming unit (CFU)-Hill colonies, are the current standard method for identifying and enumerating EPCs in circulation.

One pitfall of the CFU-Hill assay, however, is the inability of these cells to expand in culture. Therefore, the research and therapeutic potential of these cells were limited and new methods to isolate and expand this coveted cell population were investigated. [78,79] In this method, whole PBMC isolates were grown *in vitro* on collagen type I coated plates for 2-3 weeks, after which colonies arose which displayed an endothelial-like cobblestone morphology similar to cells derived from human umbilical vein endothelial cells (HUVECs). These cells were passaged and expanded to generate cultures of blood-derived endothelium, which express endothelial surface markers. These cells also performed well in endothelial functional assays forming tubes *in vitro* on 3D-matrices and incorporating into vessels in mice *in vivo*.

CECs are different from EPCs; CECs are mature cells derived from the vessel wall that have become mobilised to enter circulation following endothelial denudation (Figure 1.8). In healthy individuals, low numbers of CECs are found in circulation, but this number is increased in patients who have certain diseases, such as cancer, or in patients who have experienced vessel injury.[80] Similar methods to isolating EPCs have been employed to isolate CECs, mainly cell sorting by fluorescent antibodies and magnetic beads.[81,82] CECs are non-proliferative and cannot contribute to vessel growth and repair. Similar to mature ECs throughout the body, CECs are heterogeneous and their phenotype can define their origin and potentially provide more information about an individual's disease state. Therefore, isolating and identifying CECs from diseased patients have the ability to serve as biomarkers of disease.

1.3.3.7 Endothelial development: the haemangioblast

Similarities between haematopoietic and endothelial development have been observed by researchers for over a century; however the interrelatedness of these two developmental processes remains controversial (Figure 1.8). Most of what we know about vascular and haematopoietic development is derived from mouse embryonic studies; however despite evidence supporting a similar developmental pattern in the

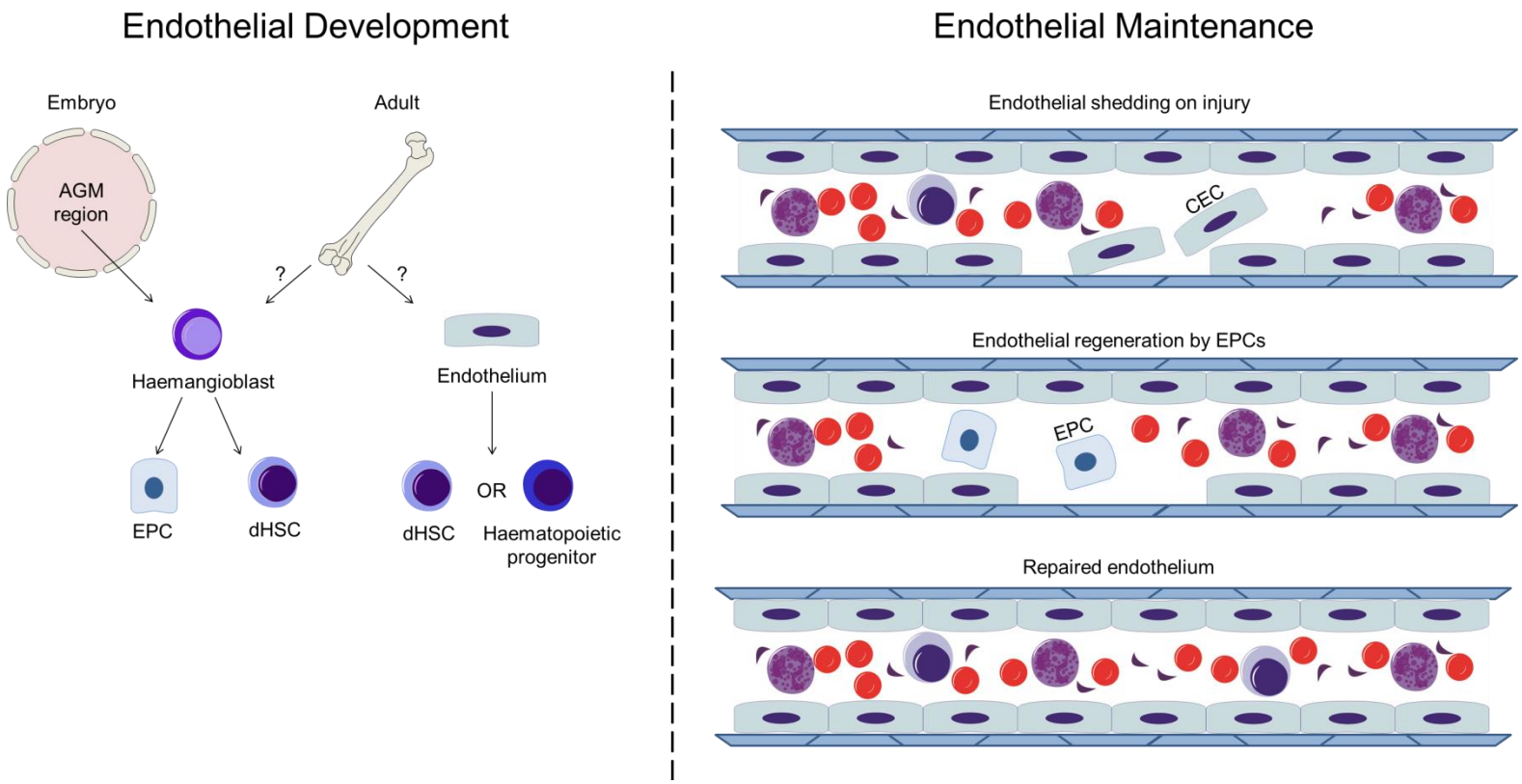

Figure 1.8 Endothelial development and maintenance

(Left) In the embryo, ECs and HSCs arise from similar regions. In the AGM region, where dHSCs first emerge, ECs also differentiate and give rise to vessels. In the adult, it is not known if cells retain the ability to differentiate into both structural endothelium and haematopoietic cells. (Right) It is known, however, that ECs can shed from the vessel wall, enter circulation and EPCs contribute to the regeneration of injured vessel walls. The origin of EPCs is not well understood.

embryo, very little is known about the convergence or divergence of these two processes in adults.

A haemangioblast refers to a single cell which can give rise to both haematopoietic and endothelial lineages and haemogenic endothelium refers to the development of blood cells from mature endothelium.[83] It is generally accepted that haemogenic endothelium gives rise to blood cells in the embryo, however it is not known if this cell type continues to produce blood cells in post-primitive haematopoiesis.[84] Investigation into the existence of a haemangioblast and/or haemogenic endothelium in adults remains a current research topic.

Emergence of HSCs in the embryo defines the beginning of definitive haematopoiesis. Prior to this, erythroid/myeloid progenitors (EMPs) give rise to functional myeloid cells to provide nutrients and oxygen to the developing foetus. [85] When treated with vascular endothelial growth factor (VEGF) and stem cell factor (SCF), precursors derived from embryonic stem cells generate blast colony-forming cells (BL-CFCs). These colonies were identified as arising from primitive cells which were capable of producing the primitive erythroid cells in embryos and eventually HSCs. Further treatment of BL-CFCs can lead to differentiation towards haematopoietic and endothelial cell types, evidenced by expression of endothelial-lineage markers and adherent cell populations in culture.[86] Both studies demonstrate that there exists a cell type in the embryo which can give rise to both endothelial and haematopoietic progenitors.

Separate studies have identified different vascular sites in the embryo with the ability to generate blood cells. On their search to identify the origin of embryonic definitive HSCs, Gordon-Keylock and colleagues identified the umbilical cord and vitelline arteries as the site of definitive haematopoietic stem cell (dHSC) production.[87] Rhodes and colleagues showed that endothelial cells in the placenta can give rise to dHSCs and that they arise independently from functional circulation.[88] Yet another study identified ECs within the aorta-gonad-mesonephros (AGM) region as HSC-generating, which suggests that generation of HSCs was dependent on endothelial expressing cells.[89] Together, these studies support the emergence of dHSCs from endothelial cells in the developing embryo.

Considerable effort has been made to support haemangioblast existence in the adult. Loges and colleagues cultured single CD133+ cells from adult blood and showed that about 2% of the total number of single cells analysed differentiated into both granulocyte and endothelial cells.[90] In a separate study, bi-potential cells were isolated from the mouse uterus, providing support for adult haemangioblast-type cells in the mouse.[91] Culture of blood outgrowth endothelial cells (BOECs) shows that EPCs exist in peripheral blood.[79] Although it is not known whether EPCs and HSCs derive from a common progenitor in adults, their common origin in the embryo suggests that it is possible.

There is evidence to support both the haemangioblast and haemogenic theories of developmental relatedness between haematopoiesis and vasculogenesis. Lancrin and colleagues provided evidence that perhaps these two theories are not separate, suggesting that endothelial and haematopoietic cells emerge from an intermediate cell type which originates from the haemangioblast.[92] This converging theory is supported by a study which used time-lapse photography to image BL-CFCs, showing that colony formation results from a transitory phase where both endothelial and haematopoietic markers are expressed. Stem cells expressing Flk1 and brachyury were induced by *Scl* to form haemogenic endothelium, characterised by expression of Tie2 and c-kit. This cell-type could then be induced by *Runx1* expression to form dHSCs which express CD41 and CD45. This study also showed that without *Runx1* expression, dHSCs could not be produced and instead haemogenic endothelium gave rise to primitive EMPs. In contrast, Chen and colleagues showed that dHSCs and EMPs differentiate through different haemogenic endothelial intermediates.[93]

It is difficult to prove definitively whether the haemangioblast, haemogenic endothelium or a combination of the two theories leads to haematopoietic and vascular development. However, evidence supporting similarities between these two processes cannot be disputed, at least in the embryo. Future research will determine whether similar differentiation pathways lead to blood and EC production in the adult.

1.3.3.8 Signalling in ECs

Coordinated cell signalling is essential for proper cell development, differentiation and function. Among other proteins, Janus kinase 2 (JAK2) is known to be important in regulating proper development and function of ECs. JAK2 is a non-receptor tyrosine

kinase, which requires association with a receptor to elicit signalling.[94] Typically, ligand-bound receptors activate associated JAK2 proteins, resulting in their activation and phosphorylation of downstream signalling molecules. Hyperactive JAK2 signalling was shown to contribute to hypertension and vascular-associated diabetic pathology.[95,96] In contrast, JAK2 deficiency led to impaired vasodilation, angiogenesis and perfusion in an inducible JAK2 knockout mouse model.[97] These findings suggest that functional JAK2 signalling is important in maintaining homeostatic EC properties.

1.4 Thrombohaemorrhagic Diseases

Haemostasis and thrombosis are dynamic physiological processes. However, because they are quite complex any disruption between pro- and anti-thrombotic properties can have a negative impact on patient health. Due to the systemic nature of haemostasis and thrombosis, adverse events can affect any area of the body. Conversely, systemic disease may disrupt haemostatic and thrombotic balances (Figure 1.9).

1.4.1 Arterial and venous thrombosis

Arterial thrombosis mainly occurs in vessels of high shear stress, as in atherosclerosis or in vessels of low shear stress, as in cardioembolism. Atherosclerosis is a chronic disease caused by lipid deposition in the vessel wall and inflammatory exacerbation.[98] The atherosclerotic plaque consists of inflammatory cells and mediators, many of which can initiate thrombosis. When concealed under a fibrous cap, these components are hidden from circulating blood; however, rupture of the plaque releases its components and exposes the subendothelial layer as in vessel injury. These events stimulate thrombus formation and are often followed by adverse cardiac events such as stroke or myocardial infarction. Cardioembolic disease often results from cardiac arrhythmias, when stasis leads to thrombus development.[5] These thrombi are particularly dangerous; as they form in a heart

chamber they are often large. If a cardioembolism dislodges, patients may suffer from infarction or stroke.

VTE is manifested as DVT and PE.[99] DVT occurs in deep veins, mainly in the legs, and is exacerbated when patients are inactive for prolonged periods of time. PE refers to a venous thrombus which has become lodged in the pulmonary circulation.

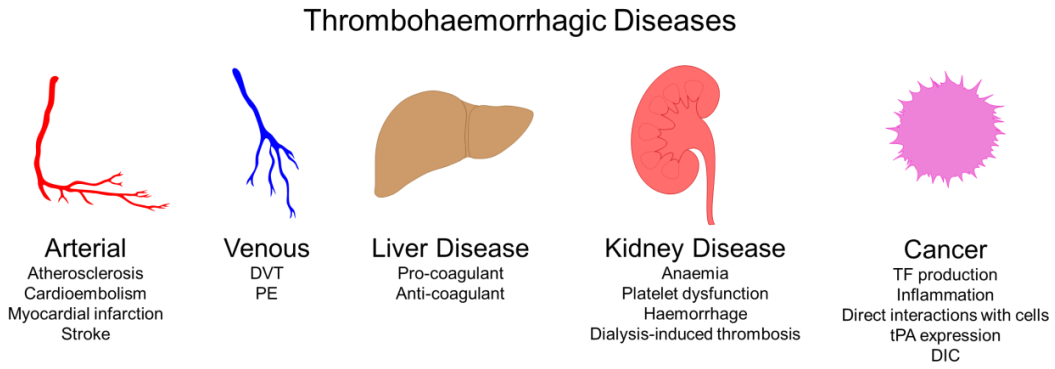

Figure 1.9 Thrombohaemorrhagic diseases
Diseases involving thrombosis and haemorrhage are common in arterial and venous systems, but are also common co-morbidities of other diseases. In particular, liver and kidney diseases often cause haemostasis complications due to their physiological roles in producing coagulation factors and filtering blood, respectively. In cancer, tumour cells promote inflammation to facilitate their survival, however this often causes haemostatic complications as well.

In contrast to arterial thrombi, venous thrombi occur in low shear stress environments; therefore, blood stasis is a main contributor to thrombosis in these vessels.

1.4.2 Aberrant haemostasis in liver and renal diseases

Diseases of the liver and kidney have also led to patient complications with haemostasis and thrombosis. The liver is the site of production of many haemostatic factors and blood production cytokines.[100] When liver functions begin deteriorating, haemostatic balance is sometimes maintained as both pro- and anti-coagulant factors are affected by the disease. However, as disease progresses, patients often exhibit either clotting or bleeding complications, depending on how the haemostatic balance is affected in individual patients. Patients with renal disease are particularly susceptible to haemorrhage, although thrombosis can also occur.[101] Defects in primary haemostasis are common and these defects have been attributed to anaemia and platelet dysfunction, which can be exacerbated by dialysis treatment.[102] Conversely, dialysis treatment can also cause blood to become hypercoagulable, a feature of Virchow's triad, promoting thrombosis. The risks for thrombosis and bleeding need to be assessed thoroughly in order to best treat patients with chronic liver and kidney disease.

1.4.2 Thrombosis in cancer

Malignancies are inherently lethal, but complications associated with bleeding and thrombosis make them even more deadly. Tumour cells have the ability to directly alter the balance of haemostatic factors.[103] They themselves can produce potent activators of coagulation, such as TF, or they can induce monocytes and ECs to express TF. ECs and monocytes are sensitive to the array of inflammatory cytokines produced by tumour cells, often resulting in a shift from an anti- to pro-thrombotic phenotype. Further, direct interactions among tumour, ECs and monocytes promote adhesion to the EC surface.[104] In contrast, tumour cells can induce fibrinolysis by expressing UK or tPA.[105] Additionally, widespread induction of pro-thrombotic phenotypes in ECs and monocytes by tumour cells can result in consumption of functional platelets in disseminated intravascular coagulation (DIC).[106] DIC results in minute thrombus formation throughout the body which paradoxically induces bleeding in patients when haemostatic factors and cells are consumed in the thrombi.

Patients suffering from these complications require haemostasis/thrombosis treatment in addition to their chemotherapy.

Haematological malignancies are among the cancers that give rise to haemostasis and thrombosis complications. In particular, myeloproliferative neoplasms (MPNs) are most commonly associated with complications related to these processes. Often, patients are diagnosed with MPNs when they present to the clinic with a clotting or bleeding episode. Details of MPNs and the associated clotting and bleeding abnormalities are discussed in the following section.

1.5 Myeloproliferative Neoplasms (MPNs)

The term "myeloproliferative disorders" was first used to describe a group of diseases characterised by excessive myeloid cell production by William Dameshek in 1951.[107] Previously, diseases resulting in erythrocytosis, thrombocytosis, leucocytosis and myelofibrosis were considered separate entities of unknown origin. Dameshek recognised the similarities between these disease states, their clinical pathologies, disease progression and ultimately patient outcome and treatment and suggested that they be considered as related disorders. Dameshek's observations were advanced for his time, but nearly five decades would pass before the shared molecular underpinnings among myeloproliferative disorders would be discovered.

The myeloproliferative disorders are now referred to as myeloproliferative neoplasms (MPNs) according to the most recent World Health Organization classification in 2008.[108] The purpose of this new classification was to highlight the aggressive cellular proliferation that is characteristic of these diseases. The classical MPNs include chronic myelogenous leukaemia (CML), chronic neutrophilic leukaemia (CNL), polycythaemia vera (PV), essential thrombocythaemia (ET), primary myelofibrosis (PMF), chronic eosinophilic leukaemia (CEL) and mastocytosis. These diseases are broadly classified as MPNs because they all exhibit excessive myeloproliferation in the bone marrow leading to increased levels of mature myeloid cells in the peripheral blood.

1.5.1 Haematopoiesis

Similar to haemostasis and thrombosis, haematopoiesis is an essential physiological process that begins in the developing embryo and continues through adulthood.

Primitive haematopoiesis begins in the yolk sac alongside primitive angiogenesis, both of which occur in regions called "blood islands."[109] The first haematopoietic cells are myeloid cells, mainly primitive erythrocytes which provide the growing embryo with oxygen and nutrients. Later, dHSCs arise in the AGM region of the embryo.[110] dHSCs self-renew and differentiate to both myeloid and lymphoid progenitors, which further differentiate to give rise to all the mature blood cell types in circulation (Figure 1.10). Cells isolated from the AGM region are able to reconstitute irradiated mice, showing that among these cells is a cell-type which has stem-properties.[111] Haematopoiesis is re-located to the foetal liver and eventually to the bone marrow where it remains an essential function throughout adulthood.

HSC differentiation is regulated by both intrinsic transcriptional regulation and extrinsic cytokine signalling. Moreover, differences in haematopoietic niches influence blood cell production; each haematopoietic organ has its own niche and even within organs areas are separated according to function. Vascular and osteoblastic niches within bone marrow vary considerably in their own function and in the factors they express and secrete. Therefore, HSCs which localise to these different regions are influenced by the microenvironment in which they reside.[112] We know that localisation of haematopoietic cells changes throughout embryonic development, from the primitive erythrocytes produced in the yolk sac to dHSC homing to the bone marrow where haematopoiesis is maintained. In adults localisation is equally important; for example, in the thymus T cell maturation is directly linked to its progression through different zones of the thymus.[113] Therefore, compartmentalisation of cells is important for both primitive and definitive haematopoietic development.

The way cells respond to these environmental cues causes distinct intracellular signalling and transcriptional regulation, resulting in differentiation of myeloid and lymphoid progenitors to all of the mature blood cell types. In lymphoid development, IL-7/IL-7R is an indispensable cytokine-receptor pair.[114]Deficiencies in a key component of the IL-7R result in mice which lack T or B cells.[115] Transcription factors PU.1 and GATA-3 favour lymphoid differentiation and GATA-1 and GATA-2 expression favour myeloid differentiation. Common myeloid progenitors further differentiate to granulocyte progenitors and megakaryocyte/erythroid progenitors (MEPs). Megakaryocytes and erythrocytes share lineage-restriction transcription factor patterns, at least in the beginning. GATA-1, FOG and NF-E2 are all expressed

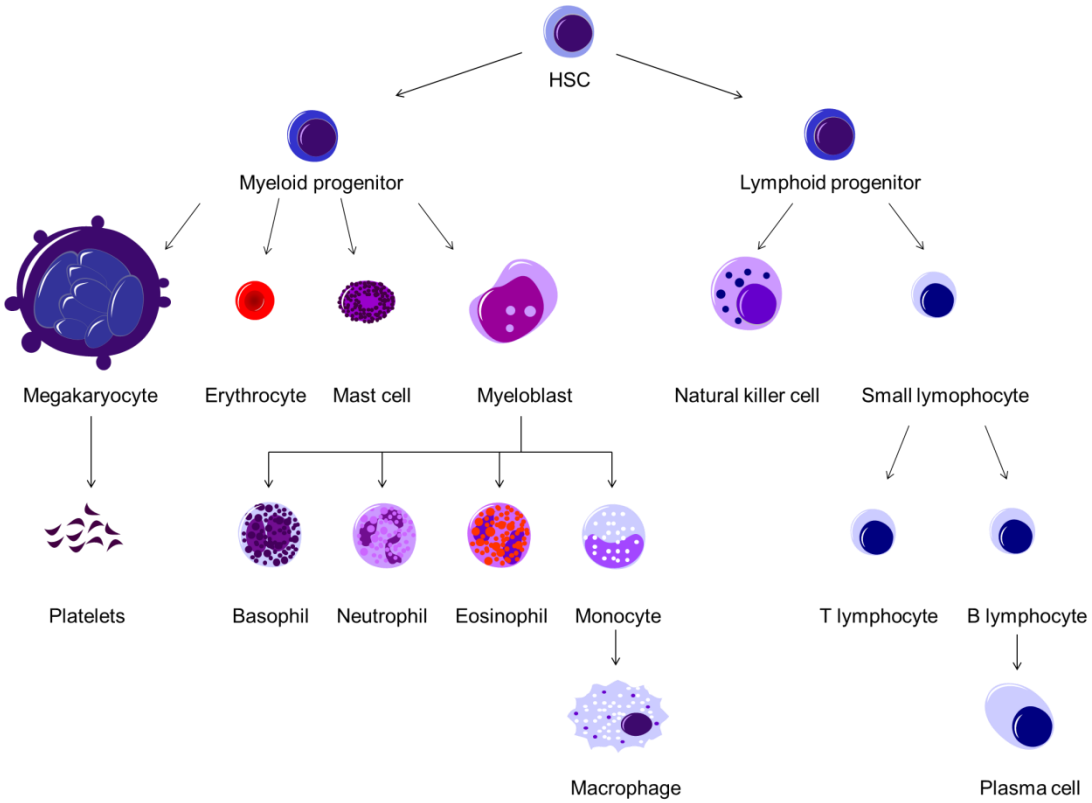

Figure 1.10 Haematopoiesis
Haematopoiesis is the process by which an HSC differentiates into all the mature myeloid and lymphoid cells in peripheral blood. It is highly regulated and the coordination of cytokine signalling and transcriptional regulation results in adequate production of each cell type. Myeloid and lymphoid restriction occurs early on in the process.

in MEPs, but further cytokine/transcription factor expression differences begin to restrict MEPs to either the megakaryocyte or erythroid lineages.[116] For example, GATA-2 expression in MEPs has been shown to favour megakaryocyte differentiation *in vitro*.[117] Expression of thrombopoietin (TPO) and its receptor, c-mpl, supports HSC maintenance and differentiation to the megakaryocyte lineage.[116] Erythroid differentiation is favoured by expression of erythropoietin (EPO) and its receptor, EPOR. c-mpl and EPOR are type I cytokine receptors, which lack intrinsic kinase activity. They associate with non-receptor tyrosine kinases such as JAK2 to transduce signalling.[118] The signalling and transcriptional networks described here provide an overview and are by no means comprehensive. Each stage of haematopoietic cell differentiation is controlled by a combination of factors, which result in maintenance of stem/progenitor pools and differentiation to mature cells. The few mechanisms discussed here demonstrate the complexity of haematopoiesis and suggest that haematopoietic deregulation may affect one or several lineages of haematopoietic cells.

1.5.3 Philadelphia (Ph) chromosome-negative MPNs

In 1960, a pivotal discovery in MPN research was made when the chromosomal translocation leading to the break point cluster-Abelson tyrosine kinase (BCR-ABL) fusion protein was discovered to be the cause of CML.[119] BCR-ABL, alternatively named the Philadelphia chromosome, leads to constitutive ABL kinase activity resulting in myeloproliferation. This discovery has led to the development of the BCR-ABL tyrosine kinase inhibitor, imatinib, possibly the most successful targeted anti-cancer treatment in history.[120]

Ph chromosome-negative MPNs include PV, ET and PMF (Figure 1.11). In general, PV, ET and PMF are characterised by an increase in red blood cells, platelets and megakaryocytes, respectively. MPNs are rare diseases; the latest epidemiological study estimates incidence rates of 0.86, 1.03 and 0.46 per 100,000 people in Europe for PV, ET and PMF, respectively.[121] MPNs are generally diseases of the elderly, with most patients being diagnosed at an age greater than 65. However, these conditions can, in rare occasions, occur in children and young adults.[122] PV and PMF have slightly higher incidences in males and ET is slightly more common in females.[123]

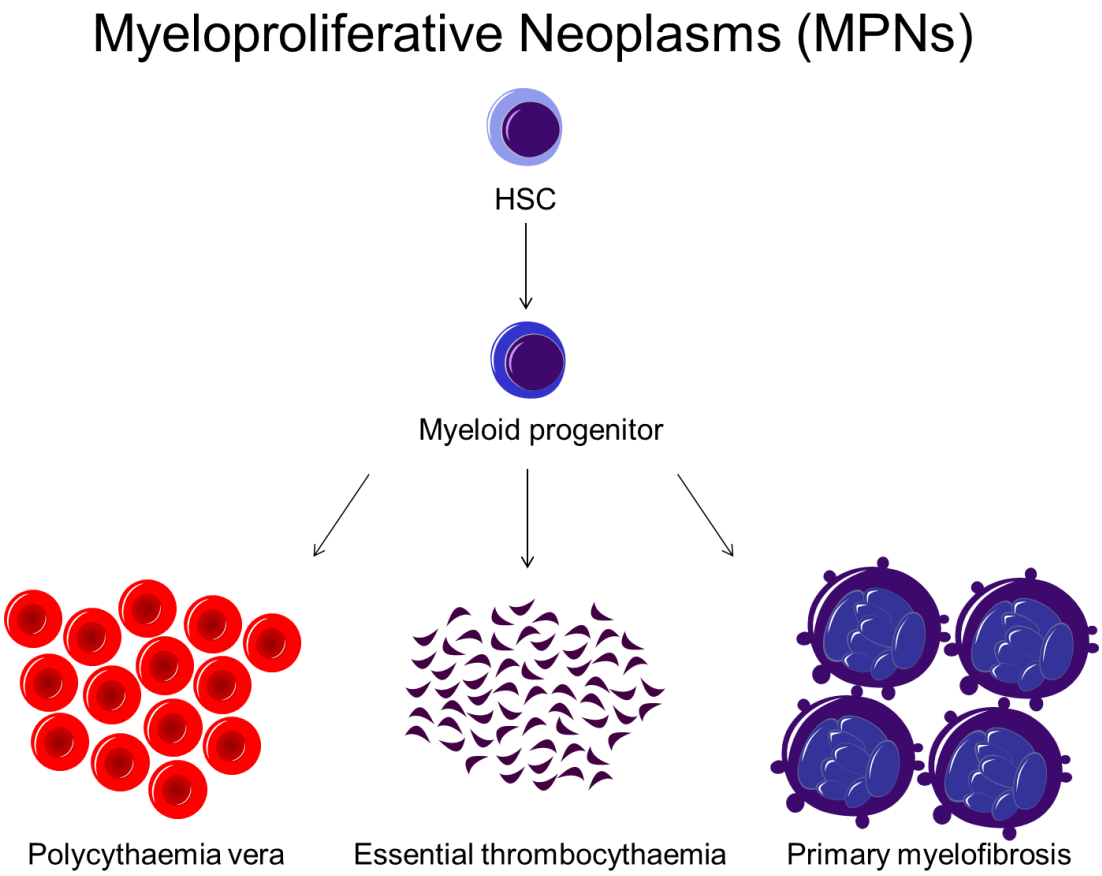

Figure 1.11 Myeloproliferative neoplasms (MPNs)
The classical Ph- MPNs include 3 diseases: PV, ET and PMF. PV and ET are characterised by an increase in red blood cells and platelets in circulation, respectively. PMF is characterised by an increase in megakaryopoiesis in the bone marrow which leads to excessive production of extracellular matrix proteins and scarring of the bone marrow. Patients with PMF often succumb to aplastic anaemia.

1.5.4 Thrombosis and haemostasis in MPNs

Signs and symptoms of MPNs in patients are non-specific; they include fatigue, weight loss, fever, night sweats, pruritus, splenomegaly and bone pain.[124] Patients report these symptoms to have a negative impact on their quality of life; however the life-threatening consequences of MPNs are most commonly caused by complications associated with haemostasis and thrombosis.[125] These events include arterial thrombosis (stroke, myocardial infarction), venous thrombosis (DVT, PE) and bleeding diathesis (particularly in the central nervous system, gastrointestinal tract and in deep tissue). In particular, patients with MPNs are at risk for splanchnic venous thromboses, which are commonly associated with the clinical manifestation of Budd Chiari Syndrome (BCS).[126] Patients with BCS are often discovered to have an underlying MPN.

Thrombosis in patients with MPNs has been attributed to changes in blood viscosity, platelets and underlying risk factors which predispose MPN patients towards these complications. Elevated haematocrit levels, as in many PV patients, is associated with changes in blood viscosity which favour thrombosis.[127] This increase in viscosity appears to be more complex than simply being the result of an increase in cell count. A study on cerebral blood flow identified changes in oxygen transport and perfusion to be the main culprit of changes in viscosity.[128] In either case, the increase in viscosity of blood leads to increased endothelial-blood cell interactions, resulting in a greater chance of thrombus formation. One treatment for patients with PV has been phlebotomy, with the aim of lowering haematocrit levels to decrease risk of thrombosis.[129]

Defects in platelet function have also been noted in patients with MPNs. Platelets normally produce TxA2 when activated, however patients with ET and PV have been reported to have basal TxA2 generation in platelets. [130,131] One treatment for this potential complication is low-dose aspirin therapy. Aspirin inhibits the enzyme cyclooxygenase, which converts prostaglandins to TxA2 in platelets. Platelets and ECs were shown to express markers of activation through detection of P- and E-selectin molecules in plasma of patients with MPNs.[132] Separately, granulocytes in PV and ET patients were shown to express markers of activation alongside elevated levels of plasma haemostasis factors.[133] Together, there is evidence to support that MPN

development in some patients affects two components of Virchow's triad: stasis and hypercoagulability.

Conversely, patients with MPNs can also suffer bleeding complications. In patients with bleeding diathesis, platelets have been shown to harbour defects in production and/or storage of dense and α-granule components.[134,135] Many of the components stored in platelet dense and α-granules promote platelet activation, therefore platelets deficient for these components are unable to promote platelet activation. Further, platelet aggregation studies have shown that platelets from MPN patients with bleeding complications exhibit defects in aggregation.[136] Aggregation defects have been attributed to lack of response to agonists such as ADP, thrombin and collagen and to a decrease in expression of receptors which are important in platelet activation.[137] Platelets also failed to agglutinate in the presence of ristocetin, indicative of a defect in vWF-induced platelet adhesion.[9] Patients with thrombocytosis have been reported to exhibit acquired von Willebrand Disease (AvWD). In AvWD, elevated platelet levels result in decreased levels of functional ulta-large molecular weight vWF multimers in plasma. This decrease in functional vWF is most likely due to increased proteolytic processing by the protease ADAMTS13.[138,139] Finally, patients on low-dose aspirin therapy to prevent thrombotic episodes sometimes experience adverse bleeding events as a side-effect of their treatment.

1.5.6 Treatment

Treatments for patients with MPNs are limited. Phlebotomy, for patients with elevated haematocrit levels is effective at lowering haematocrit levels, restoring normal blood viscosity and decreasing thrombosis risk.[140] However, it is cumbersome and often uncomfortable for the patient. Alternatively, low-dose aspirin therapy can be used to reduce thrombosis; however this may increase the risk of bleeding diathesis.[141] Patients at "high risk" for disease complications may be prescribed cytoreductive therapy, typically hydroxycarbamide. It is clear from MPN patient treatments that the main strategy is to prevent haemostasis and thrombosis complications in these patients. In theory, this should be the goal as patients with MPNs often succumb to these complications instead of their primary disease. However in practice, this strategy is difficult to execute effectively due to the complex balance of factors involved in

haemostasis and thrombosis. Attempting to alter components of these systems may inadvertently put patients at risk for other complications.

1.5.5 Mutations in Ph- MPNs

In contrast to CML, the molecular underpinnings of Ph- MPNs cannot be attributed to a single genetic aberration. However, a variety of mutations have been identified across these diseases, many of which have a role in the (Janus kinase-signal transducers and activators of transcription (JAK-STAT) pathway.[142] Even the most recently discovered mutation in calreticulin (CALR), which on the outset appeared to be unrelated to JAK-STAT, was shown to increase activation of STAT5.[143,144] It was later demonstrated that CALR binding the type I cytokine receptor, mpl, is required for haematopoietic disease.[145] Several mutations have been identified in mpl itself, in a region which may be important in reducing spontaneous receptor activation.[146] Mutations in regulatory proteins, such as the adaptor protein, LNK (SH2B3), or members of the suppressor of cytokine signalling (SOCS) family have been identified in patients as well.[142] However, mutations that are most common among Ph- MPNs are in JAK2 itself. JAK2 exon 12 mutations were identified in a subset of patients with PV, however these mutations are rare and not much is known about the mechanism of JAK2 exon 12 mutation-driven MPNs.[147,148] In contrast, the point mutation $JAK2^{V617F}$ is the most common mutation among Ph- MPNs and since its discovery in 2005 MPN research has largely focused on the mechanisms of $JAK2^{V617F}$-driven disease.[149-152]

1.6 Janus Kinase 2 (JAK2)

JAKs are non-receptor tyrosine kinases and include JAK1, JAK2 JAK3 and TYK2. Evidence supports the essential role of JAK1 in immune function; JAK1 deficient mice have impaired immune cell development and inflammatory responses.[153] JAK2 is essential for myeloid development and is required for signalling through EPOR, mpl, IL-3R and interferon (IFN)-γ.[118] Mutations in patients with severe combined immune deficiency confirmed the importance of JAK3 in T and B cell development.[154,155] Tyk2 is important in mediating IL-12 and IFN-α responses; Tyk2 deficient mice develop lymphoid cells, however T cell response is impaired.[156] Together, the JAK family transmits cytokine signals through receptors which lack intrinsic kinase activity and mutations identified in humans and mouse knockout models have confirmed the importance these proteins have on haematopoietic cell

development and function. Given the importance of JAKs in regulating haematopoietic development, activating mutations in JAKs may contribute to hyper-proliferation in these cell types. Indeed, the point mutation $JAK2^{V617F}$ increases myeloproliferation resulting in elevated levels of myeloid cells in peripheral blood. Here, the function of $JAK2^{WT}$ and $JAK2^{V617F}$ are discussed in more detail.

1.6.1 JAK2 structure

JAK2 consists of seven JAK homology (JH) domains, labelled accordingly as JH1-JH7.[157] JH3-JH7 are the N-terminus of JAK2 and contain a 4.1/ezrin/radixin/moesin (FERM) domain and SH2 (Src homology 2) domain. The former regulates JAK2 association with type I and type II cytokine receptors via box 1 and box 2 motifs.[158] On JAK2 activation, phosphorylation of the FERM domain results in receptor dissociation of JAK2 and subsequent degradation, implicating a role for FERM in regulating JAK2 kinase activity.[159] The JH1 and JH2 domains are the kinase and pseudokinase domains, respectively, and they are located at the C-terminus.[157] The kinase domain is enzymatically active and responds to ligand binding to its associated receptor. Activation of JAK2 requires phosphorylation of the "activation loop" within the JH1 domain, which is likely a result of trans-autophosphorylation of neighbouring JAK2 molecules.[160] The pseudokinase domain, originally speculated to be catalytically inactive, has been shown to have a regulatory role for JH1 kinase activity.[161] Recently, structural modelling suggests that direct interactions between JH1 and JH2 are responsible for this auto-regulation.[162] Interestingly, this structural work revealed that JH2 has serine/tyrosine kinase activity and phosphorylates residues within the JH2 domain. These phosphorylation events were shown to be critical in regulating JH1 kinase activity; mutations which disrupted autophosphorylation of JH2 resulted in increased JH1 kinase activity.

1.6.2 JAK2 signalling

JAK2 associates with a number of type I cytokine receptors; therefore, research into the binding and activation of JAK2 in one receptor is often translated to how it might bind and signal in other receptors. In growth hormone (GH) receptor activation, GH binding to the receptor induces a conformational change in the intracellular domain of the receptor, resulting in disruption of the JH1-JH2 inhibitory interaction.[94] This results in trans-autophosphorylation of neighbouring JAK2 subunits. Individual JAK2

molecules associate with receptor monomers, however in signal transmission ligand binds to homo- or hetero-dimeric receptors, which brings neighbouring JAK2 molecules into closer proximity. Evidence for both constitutive receptor dimerization and ligand-induced receptor dimerization exists. Crystallography studies have shown that EPOR exists as pre-formed dimers on the cell surface, however ligand binding induces a rotational shift intracellularly that allows progression of signalling.[163] Evidence suggests that the receptor MPL exists in monomer-dimer equilibrium and ligand binding favours dimerization of receptor monomers.[164] However, more recent unpublished data shows that receptors exist as monomers on the surface and require ligand binding to induce dimerization (Dr. Ian Hitchcock, personal contact). This was shown using total internal reflection fluorescence (TIRF) microscopy where receptor monomers were tracked and monitored for interactions over a period of time. Clearly, dimerization of receptor monomers is a key step in cytokine receptor responses; without dimerization, JAK2 molecules would not be able to perform the necessary trans-autophosphorylation required to activate neighbouring JH1 kinase domains.

A primary result of JAK2 activation is phosphorylation of downstream signal transducers and activators of transcription (STAT) proteins (Figure 1.12). There are seven STAT family members, STAT1, STAT2, STAT3, STAT4, STAT5a, STAT5b and STAT6.[165] Activated STATs can then homo- or hetero-dimerize and translocate to the nucleus where they act as transcription factors. JAK-STAT signalling is in part regulated by specific JAK and STAT activation pathways, or a combination of active JAK-STAT proteins. Although traditionally individual cytokines have been associated with activating specific STAT molecules, signalling is likely to be more complex and involve qualitative and quantitative changes in active STAT molecules to induce changes in cell behaviour.

STAT3 and STAT5 have been studied the most extensively in the context of haematopoietic development. Recently, dHSCs from the AGM region of the embryo were shown express higher levels of STAT3 compared to other STATs.[166] Alternatively, upregulation of specific genes suggested STAT5 might be involved in dHSC development. STAT5 involvement in HSC maintenance and differentiation is supported by effects of STAT5 over-expression in primary cord blood-derived HSCs.[167,168] In addition to HSC development, data has shown that STAT1 is important

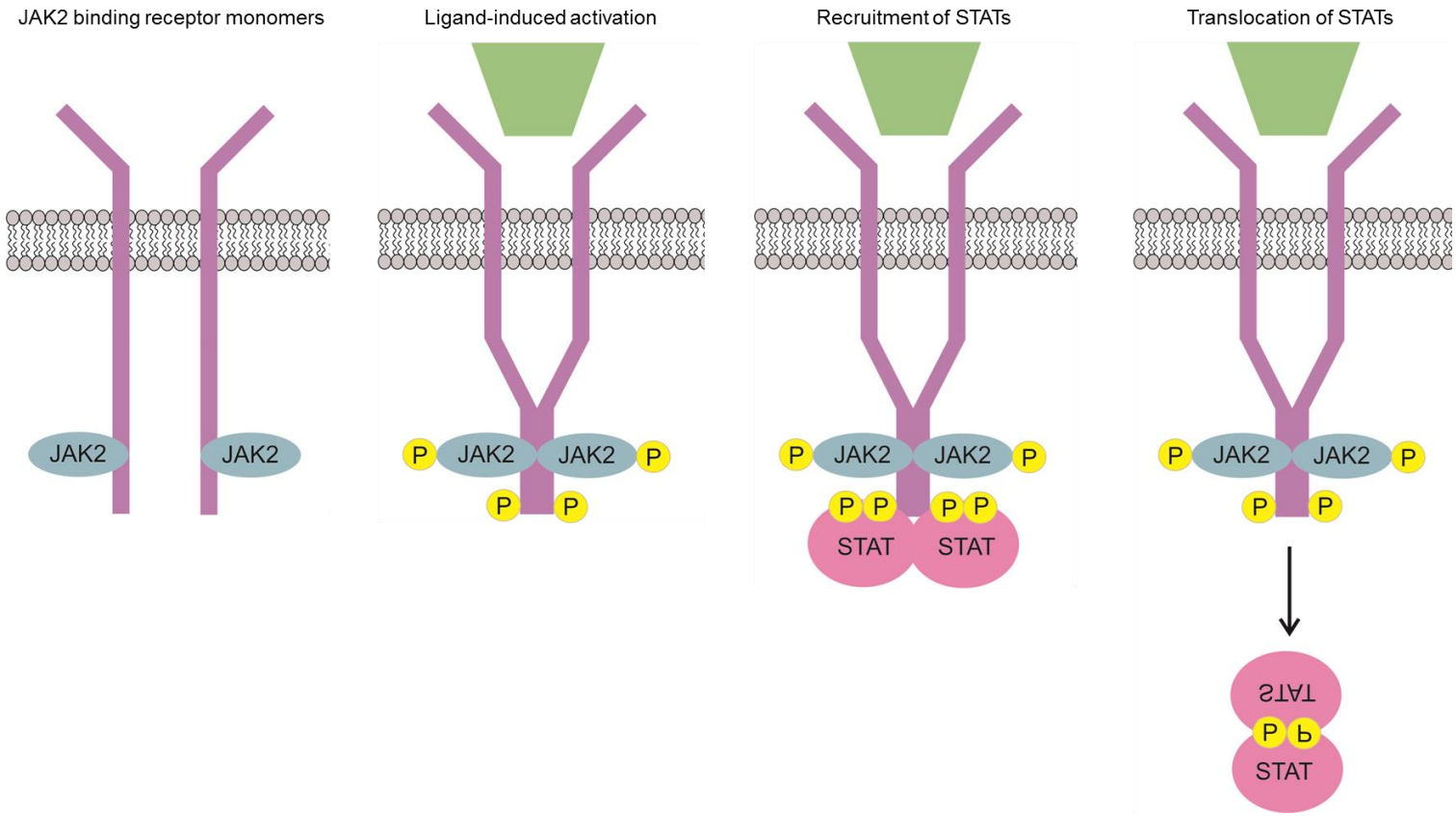

Figure 1.12 JAK2 signalling

JAK2, a nonreceptor tyrosine kinase associates with receptors which lack intrinsic kinase activity. When ligand binds, receptors undergo a conformational change whereby the JAK2 subunits can trans-autophosphorylate each other, activating JAK2 kinase activity. The phosphorylated residues allow STAT recruitment and JAK2 subsequently phosphorylates STAT proteins. STATs can then dimerise and translocate to the nucleus where they regulate gene transcription directly.

in megakaryocyte lineage restriction.[169] STAT1 activation is primarily driven by IFN-γ mediated JAK2 activation, which is involved in inflammation.[170] Together, evidence supports the roles of STAT1, STAT3 and STAT5 in particular in haematopoiesis.

In ECs, STAT1 and STAT3 appear to have roles in vascular maintenance and remodelling. In one study, angiotensin II and endothelin-1induced activation of both STAT1 and STAT3 caused vascular complications in a rat model for diabetes.[96] Another study demonstrated that vascular injury induced activation of JAK2 and STAT3, which were otherwise not activated or expressed in intact vessels.[171] In an oxidative stress injury model, JAK2 and STAT3 were shown to be important in EC protection.[172] These data implicate JAK/STAT, in particular JAK2, STAT1 and STAT3 in mediating physiological and potentially pathological vascular responses.

1.6.3 Regulation of JAK2 signalling

JAK2 activity is in part regulated by its own structural domains and interactions with neighbouring JAK2 molecules. However, there are also extrinsic mechanisms of JAK2 regulation mediated by interactions with other proteins. As JAK2 is activated by trans-autophosphorylation, one mechanism of JAK2 regulation is by phosphatase activity. Src homology region 2 domain-containing phosphatase (SHP)-1 and SHP-2 are two such phosphatases important in JAK2 regulation.[173] SHP-1 directly associates with JAK2 and evidence from SHP-1/JAK1 structural data suggests that SHP-1 is involved in de-phosphorylation of the activation loop.[174] Additionally, SHP-1 expression is restricted mainly to haematopoietic cells, suggesting it is important for regulating haematopoietic development.[175] SHP-2 is expressed globally and is important in regulating IFN-γ induced signalling.[176] Another phosphatase, protein-tyrosine phosphatase 1B (PTP1B) targets JAK2 for de-phosphorylation.[173] Similar to SHP-2, the effects of PTP1B appear to be related to IFN-γ signalling. Protein tyrosine phosphatase, receptor type C; (PTPRC ,CD45), a receptor tyrosine phosphatase, regulates JAK2 activity in response to IL-3 and EPO.[177]

SOCS1 and SOCS3 regulate JAK2 activity via their E3 ubiquitin ligase activity.[173] Both SOCS contain SH2 domains and kinase inhibitory regions that facilitate binding to receptor-JAK2 complexes.[178] SOCS1 binds directly to JAK2 on the activation loop; SOCS3 binds instead to activated receptors. Once bound, SOCS ubiquitylates and targets JAK2 and its associated receptor for degradation. The “SOCS

box" domain recruits E2 ligase and together, the SOCS complex elicits E3 ubiqutin ligase activity.[179] Therefore, regulation by SOCS proteins consists of 2 mechanisms: direct inhibition of JAK2 catalytic activity and degradation of receptors. LNK is an adaptor protein which contains both Src homology (SH) 2 and pleckstrin homology (PH) domains.[173] Mice deficient for LNK show increased haematopoiesis, related to increased cytokine signalling.[180] The mechanism of LNK regulation of JAK2 however, is not known.

1.6.4 JAK2^{V617F}

The field of Ph- MPN research changed significantly when four separate groups reported findings of a single point mutation in JAK2 among a subset of patients with MPNs.[149-152] Cytogenetic studies identified chromosome 9p as a region of interest for genes involved in MPN pathogenesis.[181,182] More specifically, regions that were subject to loss of heterozygosity (LOH) at 9p were compared among PV patients and this led to the identification of JAK2 as a possible kinase involved in PV progression.[149] In another study, PV progenitor cells were treated with inhibitors for JAK2, PI3K or Src, which impaired endogenous erythroid colony formation, a function of cells isolated from PV patients.[151] Treatment of PV cells with siRNA for JAK2 confirmed the importance of this particular kinase in PV cell maintenance and proliferation. Separately, global genomic kinase screens were conducted to identify potential mutations because kinase involvement in other malignancies was well documented in literature.[150,152] Together, the data published from these findings all identified the point mutation JAK2^{V617F} to be common among Ph- MPNs.

*JAK2*Exon14^{G1849T} is a point mutation resulting in a guanine to thymine transversion at nucleotide 1849 in exon 14 of JAK2. This causes an amino acid substitution from valine to phenylalanine at position 617 in the pseudokinase domain. JAK2^{V617F} is a somatic, clonal mutation detected in cells of the myeloid lineage but is absent in other cell types and tissues and is therefore acquired in a myeloid progenitor cell. It was initially reported to promote proliferation and survival in the IL-3-dependent cell line Ba/F3 and TPO-dependent cell line UT7 through cytokine hypersensitivity.[149,151] Increased expression of phosphorylated JAK2 and STAT5 confirmed the activation of this pathway in transformed cell lines and the induced transcriptional profile confirmed the role of STAT5 in proliferation. Patients were

found to harbour one, two or zero copies of the JAK2^{V617F} allele. Clinical data suggests that homozygous patients have a longer disease course and are at higher risk for disease complications, including thrombosis, haemorrhage and fibrosis, when compared to heterozygous or JAK2^{V617F}-negative patients.[149-152] This suggests that after the mutation is acquired, a LOH event may confer a proliferative advantage in the malignant clone making the disease more aggressive. Indeed, three of the four studies reported that LOH is likely to be caused by mitotic recombination, resulting in JAK2^{V617F} duplication.[149,151,152] Further support for the ability of JAK2^{V617F} to transform haematopoietic cells was shown by the observed erythrocytosis in murine bone marrow chimeras that received JAK2^{V617F}-transduced bone marrow cells.[151] Although common among Ph- MPNs, greater than 99% of PV patients express JAK2^{V617F} and approximately 50% of ET and PMF patients express JAK2^{V617F}.[150]

1.6.5 Structural analysis of the JAK2^{V617F} mutation

The location of JAK2^{V617F} in the pseudokinase domain suggests that the mutation disrupts the autoinhibition of JH1 by JH2; however the mechanism by which this disruption occurs is still not well described (Figure 1.13). Structural biologists have made recent advancements in this field which suggest that the JH1 domain of one JAK2 is inhibited by the JH2 domain of a neighbouring JAK2, and JAK2^{V617F} stabilises JH1/JH2 interactions that favour trans-phosphorylation, thus alleviating the auto-inhibition.[183] Structural simulations indicate that JAK2^{V617F} mutation location is at the JH1/JH2 interface, corroborating the evidence which suggests that autoinhibition is driven by direct pseudokinase/kinase domain interaction.[184]

Whilst JAK2^{V617F} causes aberrant kinase activity of the JH1 domain, it also impairs the catalytic activity of the JH2 domain.[185] Ser523 and Tyr570 are residues that are phosphorylated by JH2 and negatively regulate JAK2 kinase activity.[162] Phosphorylation at Tyr570 was found to be decreased in JAK2^{V617F}-positive patient cells, identifying a second possible mechanism for JAK2^{V617F}-induced increased kinase activity.[185] The linker region of JH2 has also been identified as an important region that undergoes a conformational change when activated.[186] This region of JH2 is encoded by exon 12 and although unrelated to JAK2^{V617F}, mutations in exon 12 have also been identified in patients with PV.[147]

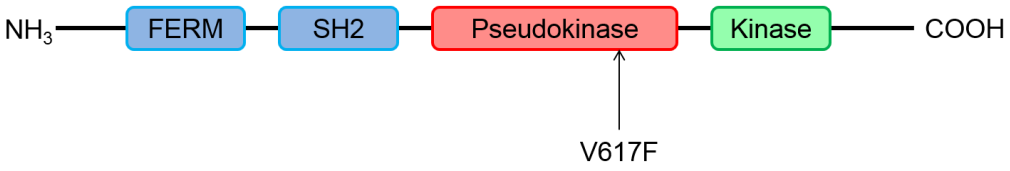

Figure 1.13 JAK2 domain diagram
JAK2 contains seven JAK homology (JH) domains (JH1-7). The JH1 domain at the C-terminus contains JAK2 kinase activity; the JH2 domain, also known as the pseudokinase domain is auto-inhibitory and is the location of the point mutation which causes $JAK2^{V617F}$. JAK2 also contains an SH2 domain and a FERM domain, which allows it to bind to cytokine receptors.

1.6.6 Allelic burden of JAK2^{V617F}

When JAK2^{V617F} was originally discovered in 2005, all four founding groups identified patients with homozygous and heterozygous expression of the mutant allele.[149-152] The majority of patients with MPNs were heterozygous for the mutation, but a subpopulation was homozygous suggesting that a second genetic event may cause transition to homozygosity at that genetic locus. JAK2 was initially investigated because LOH had occurred at the locus where JAK2 was located, in patients with MPNs.[149] This LOH resulted in duplication of the mutant allele, instead of deletion of the WT allele; further supporting that homozygous patients may have originally possessed only one copy of the allele.

The effects of JAK2^{V617F}-mutant copy number remain an important area of MPN research today. Early investigations into clinical cohort mutational status identified that most patients which harboured two copies of the allele had PV; about 25-30% of patients with PV and about 2-4% of patients with ET were homozygous for JAK2^{V617F}.[184] Homozygosity was associated with higher haemoglobin levels, higher leukocyte counts, lower platelets and increased risk of transition to a fibrotic stage of disease, all clinical manifestations of PV.[184,187] Disease prognosis of homozygous patients is poor compared to heterozygous patients, as exhibited by an increased risk for haemostatic complications and the need for cytoreductive therapy. Lastly, transformation to acute myeloid leukaemia (AML), perhaps the most aggressive consequence of MPN pathogenesis, is also associated with homozygous JAK2^{V617F}-mutational status. Further, MPN transformation to AML may result in the loss of JAK2 mutant expression altogether, which suggests that MPNs are diseases of genomic instability. However, in AML patients which harbour JAK2^{V617F}, homozygosity was preferred as was a pre-fibrotic stage characteristic of myelofibrosis.[188]

To determine whether JAK2^{V617F}-copy number has a role in directing disease phenotype, Tiedt and colleagues developed an inducible transgenic mouse model.[189] In this model, JAK2^{V617F} expression levels corresponded to disease phenotype in mice; higher expression of the mutation lead to a PV-like phenotype and lower expression lead to an ET-like phenotype. This supports patient data, which showed that

homozygosity was more commonly expressed in PV patients compared to ET patients.[184]

JAK2^{V617F}-homozygosity may drive an "erythroid" phenotype in patients with MPNs, however clonal analysis of JAK2^{V617F}-mutational status in patients with PV and ET suggests there may be other factors which contribute towards disease outcome. Colonies from patients with both disease types showed evidence of homozygous clones; however only in PV patients could this clone expand and become the dominant clone.[190] This suggests that JAK2^{V617F}-positive cells in both PV and ET have the ability to undergo LOH and become homozygous; however alternative factors influence the expansion of those cells. Factors which cause expansion of the homozygous clone in PV, whether they are cell-intrinsic, extracellular or a combined effort, remain to be determined.

1.6.7 Additional hypotheses for the clinical manifestation of three diseases

One topic that has been consistently of interest in MPN research is the mechanism driving JAK2^{V617F}-disease into three disparate phenotypes. JAK2^{V617}-allelic burden is one hypothesis, however a subset of patients with PV are heterozygous and a subset of patients with ET are homozygous for JAK2^{V617F}. Further, clonal analysis suggests homozygosity may be an effect, not a cause of disease phenotype.[190] These findings suggest that other factors may cause, or at least contribute to disease differentiation in JAK2^{V617F}-positive MPNs.

One factor which may contribute to disease differentiation is individual patient predisposition to one phenotype over another. The role of STAT1 in megakaryopoiesis was discovered when a Gata-1 deficient mouse model had both defective platelet production and decreased expression of STAT1.[169] Expression of STAT1 in knockout mice and cultured knockout megakaryocytes restored some function of megakaryopoiesis. The effects of STAT1 signalling illustrated in the Gata-1 deficient models show that STAT1 influences differentiation towards the megakaryocyte lineage over other myeloid lineages. In the context of JAK2^{V617F}, STAT1 expression drives an ET-phenotype, where decreased expression of STAT1 drives a PV-pehnotype.[191,192] These data suggest that patients with a predisposition for megakaryocyte differentiation, potentially though expression of STAT1, are more likely to develop ET should an MPN develop.

In section 1.5.5, mutations in addition to JAK2^{V617F} were discussed. Although these mutations were in proteins related to JAK-STAT signalling, mutations in MPNs are not limited to this signalling pathway. In particular, mutations in tet methylcytosine dioxygenase 2 (TET2) were identified in patients with MPNs.[193] TET2 is a tumour suppressor gene; mutations in TET2 were found among patients with MPNs and other myeloid cancers.[194] Further investigation into TET2 mutations in MPNs showed support for both pre-JAK2^{V617F} and post- JAK2^{V617F} acquisition of mutations in TET2 in different samples.[195] Evidence of additional mutations, including mutations involving TET2, suggest that MPNs may be the result of genomic instability.[196] It is currently not known whether the primary insult is acquisition of JAK2^{V617F} and additional mutations are further acquired, or if primary mutations exist and their effects on myeloproliferation are enhanced once JAK2^{V617F} is acquired.

1.6.8 Insights into JAK2^{V617F} mechanism by *in vivo* murine models

Mouse models are invaluable tools for investigating human diseases and many groups have applied this technology to the study of MPNs. Xenotransplants of JAK2^{V617F}-positive human haematopoietic progenitor cells (CD34+) into NOD/SCID mice showed disparate results. In one study, CD34+ cells isolated from the spleen of PMF patients engrafted more aggressively than did cells isolated from peripheral blood.[197] Contrastingly, another study was unable to show that JAK2^{V617F}-mutational status provided a competitive advantage over control patient cell engraftment.[198] The disparity in results may be a reflection of differences in individual patient cell generation, or the limitations implicit in xenotransplants due to species-specific differences.

Syngeneic models such as those produced in retroviral bone marrow transplants, bypass some of the limitations of xenotransplants. In these experiments, bone marrow cells were harvested from mice, retrovirally-transduced with JAK2^{WT} or JAK2^{V617F}-expressing viruses and re-introduced into irradiated mice of the same genetic background. On three separate occasions, this method produced diseased mice with clinical features similar to those observed in PV patients, when JAK2^{V617F}-cells successfully engrafted.[199-201] In one study, disease progressed from PV-like symptoms marked by erythrocytosis, to PMF-like symptoms marked by anaemia, splenomegaly and bone marrow fibrosis, a progression that can occur in humans.[199] Separately, serial

transplantation experiments, whereby HSCs from one transplant chimera were used in a subsequent transplant, did not recapitulate disease phenotype suggesting that JAK2^{V617F} may contribute towards HSC exhaustion.[200]

JAK2^{V617F} knock-in or transgenic mouse models have also been engineered. Two separate models showed that homozygous expression of JAK2^{V617F} resulted in PV-like disease and heterozygous expression of JAK2^{V617F} resulted in ET-like disease.[189,202] These results corroborate patient data which suggests that homozygosity is more common in PV patients than in ET patients.[184] Mouse models have also proved to be useful for investigating the effects of JAK2^{V617F} in different cell types. In one model, expression of JAK2^{V617F} in erythroid progenitors caused PV-like disease in mice; however this effect was not transplantable.[203] Similarly, another study found that serial transplantation of HSCs, but not erythroid progenitors which expressed JAK2^{V617F} could cause disease in chimeric mice.[204] Further examination of this model showed that when JAK2^{V617F} expression was induced at the HSC stage, the disease phenotype was more aggressive and eventually transformed to myelofibrosis, compared to a more mild disease phenotype observed when JAK2^{V617F} expression was induced in a later progenitor.[205] Although the effects of JAK2^{V617F} expression in the HSC on disease initiation cannot be discounted, other studies suggest that mutation expression leads to impaired self-renewal capacity and stem cell exhaustion. Stem cells showed evidence of DNA damage and impaired cell cycling, ultimately leading to the inability to transmit disease through transplantation.[206] HSCs expressing JAK2^{V617F} were shown to divide into two differentiated cells, further support for the impact of JAK2^{V617F} on self-renewal dysfunction.[207] These studies demonstrate that JAK2^{V617F} expression in the HSC drives disease initiation through promoting differentiation and proliferation but may also lead to cell-intrinsic changes that result in HSC exhaustion.

MPN mouse models are particularly useful because they recapitulate the symptoms of human disease quite accurately. However, like all models there are limitations. As discussed in a previous section, JAK2^{V617F} is typically one mutation of many in patients with MPNs. Models which express JAK2^{V617F} lack expression of mutations in other genes and it is likely that MPN initiation and progression are more complex than these models.[196] Moreover, JAK2^{V617F} is an acquired mutation, which differs from most mouse models which have congenital mutations.

1.6.9 JAK2^{V617F} and the clinic: impact on diagnosis and treatment

Definitive diagnosis of MPNs has historically been challenging. Many of the clinical features of MPNs overlap with each other and subsequently, one disease phenotype may progress to another. Further, characteristic symptoms of MPNs such as erythrocytosis and thrombocytosis may actually be effects of unrelated diseases. Since Dameshek's classification of myeloproliferative disorders in 1951, diagnosis of MPNs has evolved, becoming more distinctive as knowledge of disease cause and progression has improved.

In 1967, the Polycythemia Vera Study Group (PVSG) was formed with the intention of organising such criteria. This group established blood cell counts above which patients could be diagnosed with an MPN and excluded a diagnosis of MPN in patients which may have another underlying disease causing their myeloproliferation. A major flaw in this classification was the absence of incorporating other diagnostic tests, mainly bone marrow histology, into the diagnostic criteria.[208] In 2001, the WHO further defined diagnostic criteria for haematological malignancies by categorising the myeloproliferative disorders and including bone marrow histological findings of hypercellularity in the diagnosis. It was at this time the WHO recognised the importance of cytogenetic analysis of cells, suggesting that diagnostic criteria would be further defined as mutations and genetic abnormalities were discovered to be specific to certain diseases. In 2001, the known role of the Philadelphia chromosome in CML made identification of this translocation an essential part of CML diagnosis.

In 2008, the WHO released an update on the classification and diagnostic criteria for MPNs. After the pivotal discovery of JAK2^{V617F}, detection of this mutation was incorporated into the diagnostic procedure of patients with MPNs, a positive detection confirming MPN diagnosis.[208] However, incorporating JAK2^{V617F} analysis into diagnosis is slightly precarious as only half of ET and PMF patients carry the mutation. Therefore, negative detection does not necessarily rule out MPN diagnosis. JAK2^{V617F}-negative patients are further analysed for other known mutations in JAK2 exon 12 or the receptor mpl, and these cytogenetic results are combined with analyses of peripheral blood cell counts and bone marrow histology to either confirm or dismiss an MPN diagnosis.

Targeting JAK2^{V617F} in MPN patients would likely be an effective therapy. Unfortunately, no such inhibitors which target mutant JAK2 specifically exist. Ruxolitinib, a JAK1/JAK2 inhibitor is used in severe cases of myelofibrosis.[209] The broad specificity of ruxolitinib renders it ineffective towards eradicating the mutant clone or decreasing JAK2^{V617F} allelic burden.[210] Instead, its success as a treatment for myelofibrosis is based on its effects of reducing splenomegaly and improving patient quality of life.

1.7 JAK2^{V617F} in the Endothelium

JAK2^{V617F} causes myeloproliferation, leading to hypercellularity of the bone marrow and increased circulation of mature myeloid cells. As cells of the bone marrow rely heavily on their microenvironment for support, hyper-proliferation of HSCs in MPN patients is likely to have an effect on other cell types. In other neoplastic malignancies, re-organisation of stromal compartments and neo-angiogenesis to provide a vascular network is required to support expansion of the rapidly proliferating cells.[211]

In particular, PMF is characterised by extensive changes in the bone marrow architecture. Some patients with MPNs were shown to have increased microvessel density; patients with myelofibrosis had the greatest increase in angiogenesis, which correlated with bone marrow hypercellularity.[212] In a separate study, spleen microvessel density was increased in patients with myelofibrosis compared to control patients, suggesting that neo-angiogenesis contributes towards a microenvironment conducive for extramedullary haematopoiesis.[213] In both reports, increased microvessel density corresponded to disease aggressiveness; in the bone marrow, patients with higher microvessel density had poorer disease prognosis and in the spleen, patients with higher microvessel density had increased extramedullary haematopoiesis. Whether new vessel growth occurred in response to failing haematopoiesis in the bone marrow, attempting to promote blood cell production elsewhere or whether it was being harnessed by neoplastic cells to promote malignant transformation is currently unknown. However, it is a process which appears to coincide with MPN disease progression.

In general, haematological malignancies are associated with cytogenetic abnormalities which occur in stem and/or progenitor cells that drive proliferation. The importance of neo-angiogenesis in these diseases, combined with the possibility that

a postnatal haemangioblast-type cell exists prompted investigation into whether the same mutations/chromosomal aberrations that exist in haematopoietic cells also exist in ECs. In patients with Philadelphia chromosome-positive CML, the *BCR/ABL* fusion gene was identified in ECs generated *in vitro* from bone marrow cells and in the endothelium of the myocardium in 1 patient.[214] In multiple myeloma patients, circulating ECs contained the 13q14 deletion detected in plasma cells and in B-cell lymphoma patients, microvascular ECs contained the same cytogenetic abnormality as the tumour cells.[215,216] These studies suggest, but do not prove, that genetic insults responsible for haematological malignancies are acquired in a primitive cell type, giving rise to both haematopoietic and ECs with characteristic genetic changes (Figure 1.14).

To date there have been three reports of endothelial $JAK2^{V617F}$ expression in patients with MPNs. In the first report, liver ECs from patients with Budd-Chiari syndrome with associated PV were isolated by laser capture microdissection.[217] Homozygous endothelial- $JAK2^{V617F}$expression was identified in 2 of 3 patients, the third patient had only $JAK2^{WT}$ expression in ECs but heterozygous $JAK2^{V617F}$ in peripheral granulocytes. The second report identified circulating EPCs with $JAK2^{V617F}$ expression in patients of all 3 MPN subtypes and this was found to correlate with increased risk of thrombosis.[218] In the most recent report, ECs were isolated from spleens of patients with MPNs by laser capture microdissection, cell sorting and *in vitro* culture of mature ECs and EPCs.[219] In this study, $JAK2^{V617F}$ expression was identified in mature ECs from both microvessels and veins, but was not present in progenitor cells expanded *in vitro*. The contrasting results between the latter two reports may be indicative of patient sample heterogeneity, or they may demonstrate differences in disease progression between patients. These observations may lend insight to the clonal hierarchy of haematopoiesis, where the mutation is acquired and how this mutation is propagated in multiple cell types.

Following the identification of $JAK2^{V617F}$ ECs in BCS, Sozer and colleagues isolated $CD34^{+}$ cells from patients with MPNs and cord blood and transplanted them into immunodeficient mice to determine the ability of these cells to colonise vessels.[220] On isolation of liver and lung tissues from these mice, human cells expressing endothelial markers were identified, confirming the ability of $CD34^{+}$ cells to

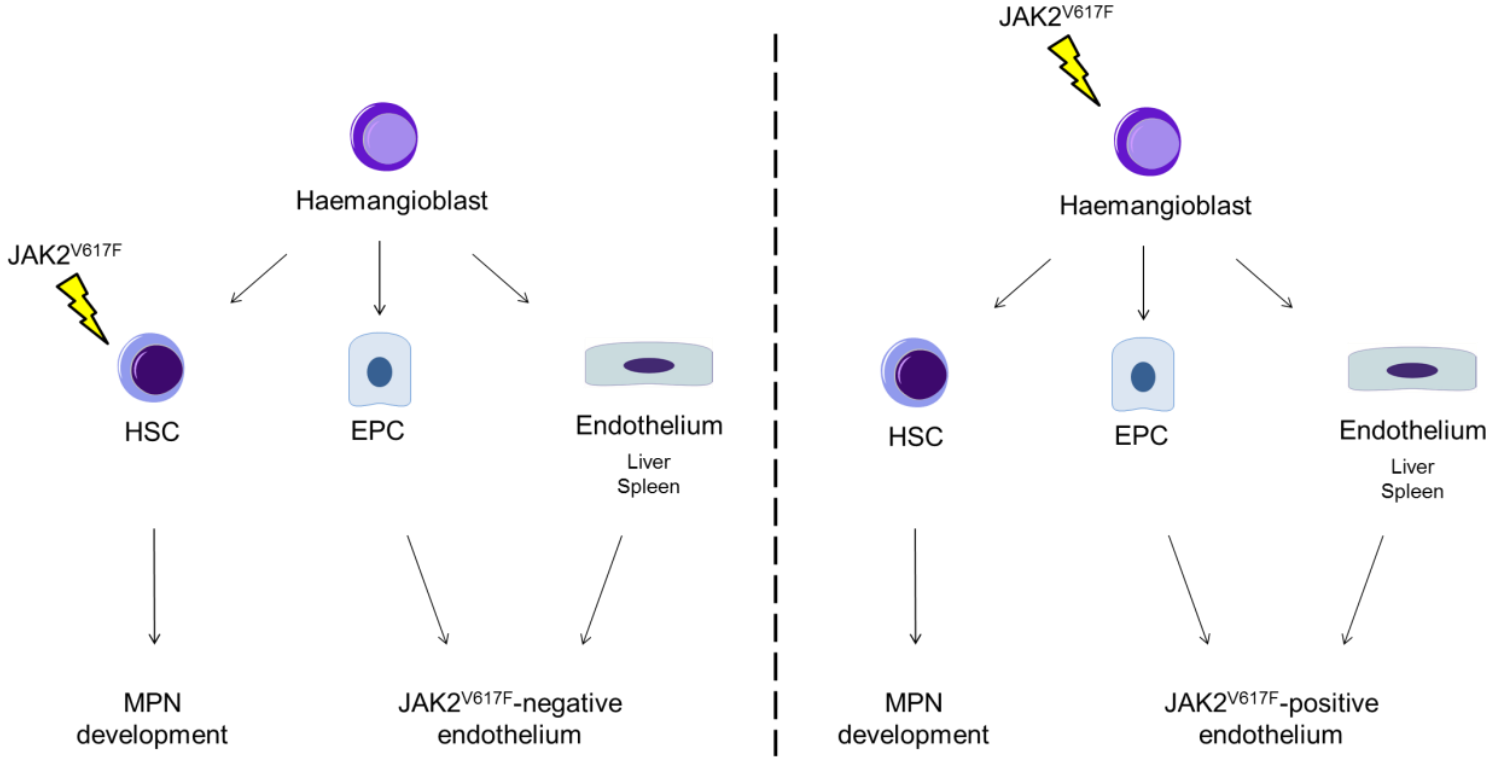

Figure 1.14 Acquisition of JAK2^{V617F}

JAK2^{V617F} is the most common acquired mutation in MPNs. The mutation is known to be acquired in the HSC, leading to hyperproliferation of myeloid cells manifested in MPNs (left). However more recently, JAK2^{V617F} was also identified in ECs, suggesting that the mutation is acquired in a more primitive cell type, such as the haemangioblast (right).

differentiate into endothelial-like cells. Furthermore, $CD34^{+}$ cells derived from patients with MPNs gave rise to endothelial-like cells which expressed $JAK2^{V617F}$. These results confirm experimentally that mutant haematopoietic cells can contribute to mutant endothelial-like cells, corroborating results which identify mutant ECs in patients with MPNs.

$JAK2^{V617F}$ expression in ECs may have broad implications. ECs are known to be important in malignant processes through neo-angiogenesis but also may contribute towards thrombohaemorrhagic complications seen in patients. In particular, complications experienced by patients with MPNs are mainly the result of clotting or bleeding events; therefore, it is likely that mutant ECs contribute towards these events given the dynamic role of ECs in haemostasis. The effects of $JAK2^{V617F}$-ECs on haemostasis and the mechanisms of $JAK2^{V617F}$ activation in ECs are not known. Current MPN treatments are limited and are mainly focused on preventing thrombosis; however equally dangerous are bleeding diathesis. Therefore it is important to understand the mechanisms behind thrombosis and bleeding in patients with MPNs so patient-specific therapies can be developed and life-threatening complications can be avoided. Further research into $JAK2^{V617F}$-EC effects and mechanisms will help us achieve this goal.

1.8 Primary Aims

Patients with MPNs commonly experience complications caused by dysfunctional haemostasis and thrombosis. Patient treatment is limited and aimed at preventing these adverse events, typically by low-dose aspirin therapy. However, a subset of patients experience increased risk of bleeding diatheses and these patients are at an even greater risk for experiencing complications if they are treated with low-dose aspirin. Currently, there are no methods for stratifying MPN patients to distinguish those who are at risk for thrombosis or bleeding. In order to improve MPN patient treatment, a better understanding of the mechanisms behind haemostasis and thrombosis complications is required. The following specific aims were investigated to advance our understanding of this important field.

- Determine the effects on haemostasis and thrombosis in a mouse model of MPNs using *in vivo* thrombosis assays

- Elucidate the mechanisms driving $JAK2^{V617F}$-activation in ECs using an *in vitro* model of $JAK2^{V617F}$-endothelial expression

- Determine allelic burden of $JAK2^{V617F}$ in ECs generated from patient samples and the effects of $JAK2^{V617F}$ expression on EC phenotype

CHAPTER 2 GENERAL MATERIALS AND METHODS

2.1 Cell Culture

2.1.1 Cell culture plasticware and reagents

Tissue culture flasks were purchased from BD Biosciences, plates and serological pipettes were purchased from Cellstar or Sarstedt. Dulbecco's Modified Eagle Medium (DMEM), Dulbecco's Phosphate-Buffered Saline (DPBS), penicillin-streptomycin (PS, 10,000 U/mL), L-glutamine (G, 200mM) and trypsin-EDTA (0.05%) were purchased from Life Technologies. Heat-inactivated Fetal Bovine Serum (FBS) was purchased from GE Healthcare HyClone and Endothelial Cell Growth Medium MV2 and supplement were purchased from Promocell. Endothelial cell growth medium BulletKit (EGM-2 MV) was purchased from Lonza.

2.1.2 Cell lines and culture conditions

Human Embryonic Kidney (HEK)293T cells were received from Dr. Dimitris Lagos and cultured in DMEM supplemented with 10% (v/v) FBS and 1% (v/v) PSG in 10cm tissue culture dishes. Primary human umbilical vein endothelial cells (HUVECs) were purchased from Promocell and Life Technologies and human aortic endothelial cells (HAECs) were purchased from Life Technologies. Both primary cell types were cultured in supplemented Endothelial Cell Growth Medium MV2 (Promocell) in $25cm^2$ flasks and 10cm dishes. Primary blood outgrowth endothelial cells (BOECs) generated were cultured in EGM-2MV (Lonza). Cells were grown to ~75-90% confluency and were then subcultured. Cells were washed once in DPBS and incubated with trypsin at room temperature to detach cells. Trypsin was neutralized with FBS-containing medium and cells were re-plated in their respective cell culture media. Cells were incubated at 37^oC and 5% (v/v) CO_2.

2.2 Western Blot Analysis

2.2.1 Protein lysate generation

Cultured cells were washed 3 times with ice-cold DPBS to thoroughly remove media and its components and lysed in protein lysis buffer (1% [v/v] Triton X-100, 150mM NaCl, 50mM Tris, pH7.4) containing protease inhibitor cocktail (AEBSF, Aprotinin, Bestatin, E-64, Leupeptin and Pepstain A, Sigma) and phosphatase inhibitors (1mM Na_3VO_4, 10mM NaF). Lysis buffer was added directly to the cells on the tissue culture dish and samples were incubated on ice for 10mins. Lysed cells were scraped from the plate, collected into Eppendorf tubes and centrifuged at 20,500*g* at 4^{o}C for 15mins to remove cell debris. The supernatant containing the protein lysate was collected into new Eppendorf tubes and stored at -20^{o}C.

2.2.2 Protein assay

Protein concentration was quantified using the Bio-Rad DC Protein Assay in a 96-well flat bottom plate. This assay uses protein chemistry with alkaline copper tartrate and Folin to produce a colour change in solution that can be detected by measuring absorbance of light. Protein forms a complex with cupric ions in an alkaline/tartrate solution producing a light blue colour change and this complex then reduces Folin to produce a more pronounced blue colour that can be detected by absorbance. Standard samples containing bovine serum albumin (BSA) were prepared at concentrations of 0, 0.25, 0.5, 1, 2 and 4 µg/µL in PBS and used in triplicate and protein samples of unknown concentration were used in duplicate for each assay. Working reagent A, containing the alkaline copper tartrate solution, was freshly prepared each time by mixing 1mL of reagent A with 25µL of reagent S and 20µL of this solution was added to each standard/unknown protein sample. Then, 200µL of Reagent B containing Folin was added to each sample and the plate was left to incubate at room temperature for ten minutes. The plate was then analysed using the Bio-Rad iMark microplate absorbance reader at 655nm.

2.2.3 Sodium dodecyl sulfate (SDS)-polyacrylamide gel electrophoresis (PAGE) and protein transfer

Polyacrylamide gel electrophoresis was performed using the Novex NuPAGE SDS-PAGE Gel System (Life Technologies). Protein samples were prepared using lysis

buffer, 4X NuPAGE SDS sample buffer (106mM tris HCl, 141mM tris Base, 2% [w/v] LDS, 10% [v/v] glycerol, 0.51mM EDTA, 0.22mM SERVA Blue G250, 0.175mM phenol red, pH8.5), 2.5% (v/v) 2-mercaptoethanol (β-ME) and 10µg of protein. Samples were boiled at 100^{o}C for 5mins and centrifuged at 17,000*g* for 1min to collect evaporated residue. NuPAGE Bis-Tris gels (4-12% gradient, Life Technologies) were used to resolve the protein samples by molecular weight and were run at 200V for 50mins using 1X NuPAGE MOPS (2.5mM MOPS, 2.5mM Tris base, 0.005% [w/v] SDS, 50µM EDTA, pH7.7).

Protein was transferred to polyvinylidene difluoride (PVDF) membrane (Bio-Rad) using the Bio-Rad Mini-Protean II Cell wet transfer system. The PVDF membrane was activated with methanol for 30secs with gentle shaking and washed with distilled water and transfer buffer (24mM Tris base, 150mM glycine, 20% [v/v] methanol). The transfer was set up as follows: sponge, Whatman paper, membrane, gel, Whatman paper, sponge on the clear surface of the transfer cassette. The cassette was then inserted into the transfer apparatus, with the black surface facing the black side of the apparatus. Transfer was conducted at 110V for 1hr using an ice block and magnetic stir bar to keep the apparatus cool.

2.2.4 Immunoblotting

After protein transfer was completed, the membrane was rinsed briefly in Tris-buffered saline, 0.1% (v/v) Tween-20 (TBST) and blocked in either 4% (w/v) milk/TBST or 4% (w/v) BSA/TBST for 1hr at room temperature. Primary antibody was prepared in either 4% (w/v) milk/TBST or 4% (w/v) BSA/TBST according to the specific antibody dilution ranging from 1:1000-1:500,000 and incubated overnight at 4^{o}C with gentle shaking on the Stovall Belly Dancer (Greensboro, NC, USA).

On day 2, the PVDF membrane was washed with TBST, 1X 15mins, 3X 5mins, and incubated with secondary antibody, conjugated to horseradish peroxidase (HRP), diluted in 4% (w/v) milk/TBST for 1hr at room temperature. After incubation, membranes were washed of unbound secondary antibody with TBST, 1X 15mins and 3X 5mins, and the membrane was exposed to Amersham Enhanced Chemiluminescent (ECL) Prime western blotting detection reagent (GE Healthcare Life Sciences) for 5mins. Luminescence was detected by exposing the membrane to HyBlot CL autoradiography film (Denville Scientific). Exposure times varied from 1sec to

10mins depending on strength of antibody detection of protein. A list of primary and secondary antibodies and their corresponding dilutions and buffers is provided (Table 2.1).

2.2.5 Membrane stripping

Stripping buffer (62mM Tris base, 70mM SDS, pH 6.8) was prepared with 0.5% (v/v) β-ME and heated to 60^{o}C. The membrane was incubated in these conditions for 10mins with gentle shaking every 2mins. The membrane was rinsed thoroughly with TBST and re-blocked in either 4% (w/v) milk/TBST or 4% (w/v) BSA/TBST for 1hr at room temperature. Antibody incubation and protein detection was completed as described in section 2.2.4.

2.3 Genomic DNA Isolation

DNA was prepared according to the Gentra Puregene Handbook (Qiagen). Cells were lysed in Cell Lysis Solution (Qiagen) and vortexed for 10sec. 100µL of protein precipitation solution was added to the lysate, and the mixture was vortexed for an additional 20sec. The solution was then incubated on ice for 5mins to ensure precipitation of proteins. Samples were then centrifuged at 16,000*g* for 1min and the supernatant was carefully poured into new Eppendorf tubes containing 300µL isopropanol and the protein pellet was discarded. The supernatant-isopropanol mixture was inverted 50 times and centrifuged at 16,000*g* for 1min. The supernatant was discarded in an alcohol-waste container and the resulting DNA pellet was washed 1 time with 300µL of 70% (v/v) ethanol. The samples were centrifuged again at 16,000*g* for 1min and the DNA pellet was dried for 5mins, inverted. DNA was hydrated in 100µL of DNA Hydrating solution (Qiagen) and quantified using the NanoDrop2000 (Thermo Scientific).

2.3.1 DNA sequencing

Sequencing was completed by Eurofins Genomics. Samples were prepared by mixing 15µL of DNA template (50-100ng/µL of plasmid DNA, 5ng/µL of purified polymerase chain reaction (PCR) products 300-100bp) with 2µL of primer (10pmol/µL). Sequences were analysed using Sequence Scanner v1.0 (Applied Biosystems Software).

Table 2.1 Primary and Secondary Antibodies Used for Immunoblotting

Antibody	Company	Catalog Number	Dilution	Buffer
ADAMTS-13	Santa Cruz	sc-25584	1:1,000	4%milk/TBST
TFPI (G-5)	Santa Cruz	sc-365920	1:1,000	4%BSA/TBST
CD39	BioLegend	135702	1:1,000	4%milk/TBST
pJAK2	Cell Signaling	3776S	1:2,000	4%BSA/TBST
JAK2	Cell Signaling	3230L	1:10,000	4%milk/TBST
GFP	Santa Cruz	sc-8334	1:1,000	4%milk/TBST
4G10 pY-biotin	Millipore	16-452	1:20,000	4%BSA/TBST
pSTAT3	Cell Signaling	9145S	1:2,000	4%BSA/TBST
STAT3	Cell Signaling	9132S	1:5,000	4%BSA/TBST
pSTAT1	Cell Signaling	9167S	1:5,000	4%BSA/TBST
STAT1	Cell Signaling	9172P	1:5,000	4%milk/TBST
V5-HRP	Invitrogen	R961-25	1:10,000	4%milk/TBST
actin-HRP	Sigma	A3854	1:1million	4%milk/TBST
rabbit-HRP	Cell Signaling	7074S	1:2,000	4%milk/TBST
mouse-HRP	Cell Signaling	7076S	1:5,000	4%milk/TBST
streptavidin-HRP	Cell Signaling	3999S	1:10,000	4%milk/TBST

2.4 Total RNA Isolation

RNA was isolated using the RNeasy mini kit (Qiagen). Cells were lysed in buffer RLT + 10µL/mL β-ME, vortexed thoroughly and stored in -80ºC until RNA could be isolated.

To isolate RNA, 1 volume of 70% (v/v) ethanol was added to thawed cell lysate and the samples were mixed. Samples were pipetted onto RNeasy spin columns and centrifuged for 15sec at 8,000*g*. RNA bound to the membrane in the spin column was then digested with DNase I in Buffer RDD (Qiagen) for 15mins at room temperature. Samples were then washed with buffer RW1 and buffer was removed by centrifugation for 15sec at 8,000*g*. Samples were washed twice with buffer RPE and after the final wash samples were centrifuged for 2mins at 8,000*g* to completely dry the membranes. RNA was eluted from the membrane by RNase-free water and the samples were centrifuged for 1min at 8,000*g* to collect the RNA. RNA was quantified using NanoDrop2000 (Thermo Scientific).

2.5 cDNA Synthesis from Total RNA

cDNA was synthesized from RNA template using the SuperScript First-Strand Synthesis System for RT-PCR (Invitrogen). First, RNA (50-500ng), 10mM dNTP mix and 0.5µg/µL oligo(dT) primer mix were combined and incubated at 65ºC for 5mins. This reaction was cooled at 4ºC for at least 1min, while reagents were being prepared for the next step. 10X RT buffer, 25mM $MgCl_2$, 0.1M DTT and 40U/µL RNaseOUT were combined separately and this was added to the first reaction. The final concentrations of each component were as follows: 1mM dNTP, 0.025µg/µL primers, 1X RT buffer, 5mM $MgCl_2$, 0.01M DTT, 2U/µL RNaseOUT. The combined solution was mixed gently, collected by centrifugation and incubated at 42ºC for 2mins. The final component, SuperScript II RT was then added to each sample for a final concentration of 2.5U/µL. DEPC-treated water was added to each Minus RT control instead of RT. The reactions were incubated at 42ºC for 50mins after which the reaction was terminated at 70ºC for 15mins. Samples were cooled to 4ºC, collected by brief centrifugation and 1µL of RNase H (2U/µL) was added to each sample. Samples were incubated at 37ºC for 20minsand were then transferred to 1.5mL Eppendorf tubes and stored at -20ºC.

2.6 Quantitative Polymerase Chain Reaction (qPCR)

qPCR assays were performed using TaqMan PCR probes and reagents (ThermoFisher). Gene expression assay, reference assay, master mix and RNase free water were combined 1:1:10:4, respectively. Gene expression assays included: JAK2 (Hs01078117_m1), TJP2 (Hs00910543_m1), CDCP1 (Hs01080405_m1) and CCL2 (Hs00234140_m1), which were all conjugated to FAM dye. The reference assay used was eukaryotic 18S rRNA (4310893E), which was conjugated to VIC/TAMRA dye. Gene expression master mix (4369016) was used for all reactions. 4µL of cDNA and 16µL of the combined gene expression, reference assay, master mix and water were added to each well of a MicroAmp Fast 96-well reaction plate (Applied Biosystems) and the plate was covered with an Optical Adhesive Cover (Applied Biosystems). Samples were centrifuged briefly and run on either the StepOnePlus Real Time PCR System (Applied Biosystems) or the QuantStudio 3 (Applied Biosystems). Data was exported and analysed using Microsoft Excel.

2.7 Flow Cytometry

Mouse blood was collected by retro-orbital bleed and 100µL of this sample was added to 900µL of PBS. Diluted blood was then mixed with 9mL of ammonium chloride solution (15.5mM NH_4Cl, 1.2mM $NaHCO_3$, 0.01mM EDTA) and incubated at 4^oC for 3mins to lyse red blood cells. The remaining cells were collected by centrifugation at 300g for 5mins and the cell pellet was washed 2 times with PBS. The cell pellet was then resuspended in 50µL of flow cytometry buffer (PBS+1% (w/v) BSA) and 1µL each of CD45.1 and CD45.2 mouse antibodies were added to each sample (Table 2.2). The samples were mixed and incubated at room temperature for 15mins in the dark. An additional 300µL of flow cytometry buffer was added to each sample just before analysis.

Samples of HUVECs and BOECs (~$1x10^5$ cells) were collected and re-suspended in 50µL of Cell Staining Buffer (BioLegend). Antibodies for human FITC-CD45, FITC-CD31 or AlexaFluor 488-CD309 (VEGFR2) were incubated with each BOEC sample for 30mins at 4^oC (Table 2.2). These samples were washed 1 time with buffer and re-suspended in 300µL of buffer for analysis. HUVECs were

Table 2.2 Antibodies Used for Flow Cytometry and FACS

Antibody	Company	Catalog Number	Dilution
PE mouse CD45.1	BD Biosciences	553776	1:50
AlexaFluor 488 mouse CD45.2	BioLegend	109816	1:50
FITC human CD31	eBioscience	11-0319-42	1:200
FITC human CD45	BD Biosciences	555482	1:100
AlexaFluor 488 human CD309 (VEGFR2)	BioLegend	359913	1:50
Brilliant Violet 510 human CD45	BioLegend	304035	1:50
APC human CD34	BioLegend	343607	1:50
PE human CD133	Miltenyi Biotec	130-098-826	1:50
Brilliant Violet 421 human CD146	BioLegend	361003	1:50

unstained, but were analysed for expression of green fluorescent protein (GFP). All samples were analysed by the Accuri C6 Flow Cytometry (BD Biosciences).

2.8 Fluorescence Activated Cell Sorting (FACS)

PBMCs were re-suspended in 50µL of Cell Staining Buffer (BioLegend) and incubated with human antibodies to AlexaFluor 488-CD309 (VEGFR2), Brilliant Violet 510-CD45, APC-CD34, PE-CD133 and Brilliant Violet 421-CD146 and with 1µL of viability stain eFluor 780 (eBioscience) for 30mins at 4^{o}C (Table 2.2). Stained cells were washed 1 time with buffer and then resuspended in 500µL-1mL of buffer for cell sorting. HUVECs were resuspended at a concentration of 1x10^{6}cells/mL in PBS+1% (w/v) BSA. Cells were sorted based on GFP expression. Both sample types were sorted by the MoFlo Astrios cell sorter (Beckman Coulter) with help from the Imaging and Cytometry facility and staff at the University of York.

2.9 Immunofluorescence (IF)

Megakaryocyte samples were blocked in 5% (v/v) goat serum, 0.3% (v/v) triton X-100 in PBS for 1hr at room temperature. Primary antibody was prepared in 1% (w/v) BSA, 0.3% (v/v) triton X-100 in PBS at a dilution of 1:100 for VWF (Dako) and 1:10 for P-selectin (BD Pharmingen). BOEC samples were permeabilised in 0.5% (v/v) triton X-100/PBS for 10mins, washed 3 times in PBS 5mins each and then blocked in 5% (v/v) goat serum for 1hr at room temperature. Primary antibody vWF (Dako) was diluted 1:100 in blocking buffer and added to the samples. All samples were incubated in primary antibody overnight at 4^{o}C. On day 2, samples were washed 3 times, 5mins each with PBS and incubated in secondary antibody for 1hr at room temperature. Alexa Fluor® 488-anti-rat (Molecular Probes) was used to detect P-selectin, Alexa Fluor® 647-anti-rabbit (Molecular Probes) was used to detect vWF, and rhodamine-phalloidin (Molecular Probes) were all used at a 1:500 concentration, diluted in blocking buffer. Samples were then washed 3 times, 5mins each with PBS and mounted with medium containing DAPI stain (Vector Laboratories). Samples were imaged with the Zeiss LSM 880 confocal microscope in the Technology Facility at the University of York.

2.10 Statistical Analysis

Data was analysed using GraphPad Prism 5 and R software. Experiments with 2 independent groups were analysed by t tests and experiments with greater than 2 independent groups and 1 explanatory variable were analysed by one-way analysis of variance (ANOVA). Experiments with 2 independent groups and 2 explanatory variables were analysed by two-way ANOVA. Linear regression analyses of proliferation were first analysed using GraphPad Prism 5 software. Subsequent comparison between linear and quadratic regression models were analysed by R software. Asterisks indicate the following, **$p<0.01$, ***$p<0.001$, ****$p<0.0001$.

CHAPTER 3 JAK2^{V617F} EXPRESSION IN ENDOTHELIAL CELLS CONTRIBUTES TO DYSFUNCTIONAL HAEMOSTASIS

3.1 Experimental Rationale

Thrombosis and haemostasis complications remain to be the most common causes of morbidity in patients with MPNs. These processes involve various proteins and cell types, including both haematopoietic and ECs. The presence of JAK2^{V617F} in both of these cell types raises the question of how the mutation affects the normal function of these cells in thrombus formation and haemorrhage. In this chapter, the effects of haematopoietic and endothelial expression of JAK2^{V617F} on thrombosis and haemostasis are investigated using a transgenic mouse model and *in vivo* vessel injury assays.

3.1.1 *Tie2-Cre/FF1* mouse model

The *Flip Flop 1* (*FF1*) mouse model was generated by Raked Skoda (Basel, Switzerland) for use in conditional JAK2^{V617F} expression in mice.[189] The transgene consists of the human JAK2 promoter and exons 1-25 with part of the construct flanked by mutant *loxP* sites. *Lox66* was inserted in exon 12 and *lox71* was inserted after the polyadenylation signal following exon 25. *Lox66* and *lox71* mutant *loxP* sites were previously described variations of the WT *loxP* which could be used to generate conditional mouse models.[221] Normally, *Cre*-recombinase expression results in excision of neighbouring *loxP* sites, but inversion of a sequence located between two *loxP* sites oriented head-to-head. The transgene is continuously inverted for the duration of *Cre*-recombinase expression. However, inversion of a sequence located between *lox66* and *lox71* results in the generation of one WT *loxP* site and one double mutant *lox66/lox71* site, the latter of which has reduced affinity for *Cre*-recombinase. Expression of *Cre* results in transgene inversion, but not excision, when the transgene is flanked by *lox66* and *lox71*. The *FF1* transgenic line was determined to contain 9

copies of the transgene integrated at chromosome 8, band A1, a site that does not contain any known genes.[189] In *FF1*, *Cre* expression results in transgene inversion and excision until the final copy is inverted and flanked by *loxP*^{WT} and *lox66/lox71*, leaving only one copy in the correct orientation for expression.

The *Tie2-Cre* transgenic mouse was first developed to investigate transgene expression in endothelial cells.[222] Tunica intima endothelial kinase 2 (*Tie2*) is a receptor tyrosine kinase which binds angiopoietin 1 and 2. The *Tie2-Cre* transgene contains the mouse *Tie2* promoter, *Cre* cDNA, *metallothionein 1* (*MT-1*) polyadenylation sequence and the *Tie2* intron 1 enhancer. Reporter mice containing *lacZ* transgene expression on *Cre* recombination were used to detect the location of *Tie2-Cre* expression. *LacZ* expression was detected in endothelial cells in the aorta, umbilical arteries, veins and smaller blood vessels in mouse embryos when reporter mice were crossed with *Tie2-Cre* mice. Later, *Tie2-Cre* activity was described in haematopoietic cells in addition to endothelial cells using *Rosa26R-EYFP* reporter mice.[223] EYFP expression was detected in all subsets of haematopoietic cells in adult bone marrow and spleen samples and in embryonic yolk sac haematopoietic cells, when the reporter was recombined with *Tie2-Cre*. Together, these data support the use of *Tie2-Cre* transgenic mice in conditional expression of *loxP* flanked transgenes in endothelial and haematopoietic cells.

To study JAK2^{V617F} expression in endothelial and haematopoietic cells, *FF1* and *Tie2-Cre* transgenic mice were crossed to generate *Tie2-Cre/FF1* mice (Figure 3.1).[224] Expression of JAK2^{V617F} in both cell types was confirmed by quantitative PCR of human and mouse *JAK2* in bone marrow neutrophils, megakaryocytes and endothelial cells. *Tie2-Cre/FF1* mice exhibited signs of disease development beginning at 8 weeks of age when platelet and neutrophil counts started to increase. Spleens harvested at 16 weeks from transgenic mice showed splenomegaly compared to WT age-matched spleens. These symptoms confirmed MPN development in *Tie2-Cre/FF1* mice.

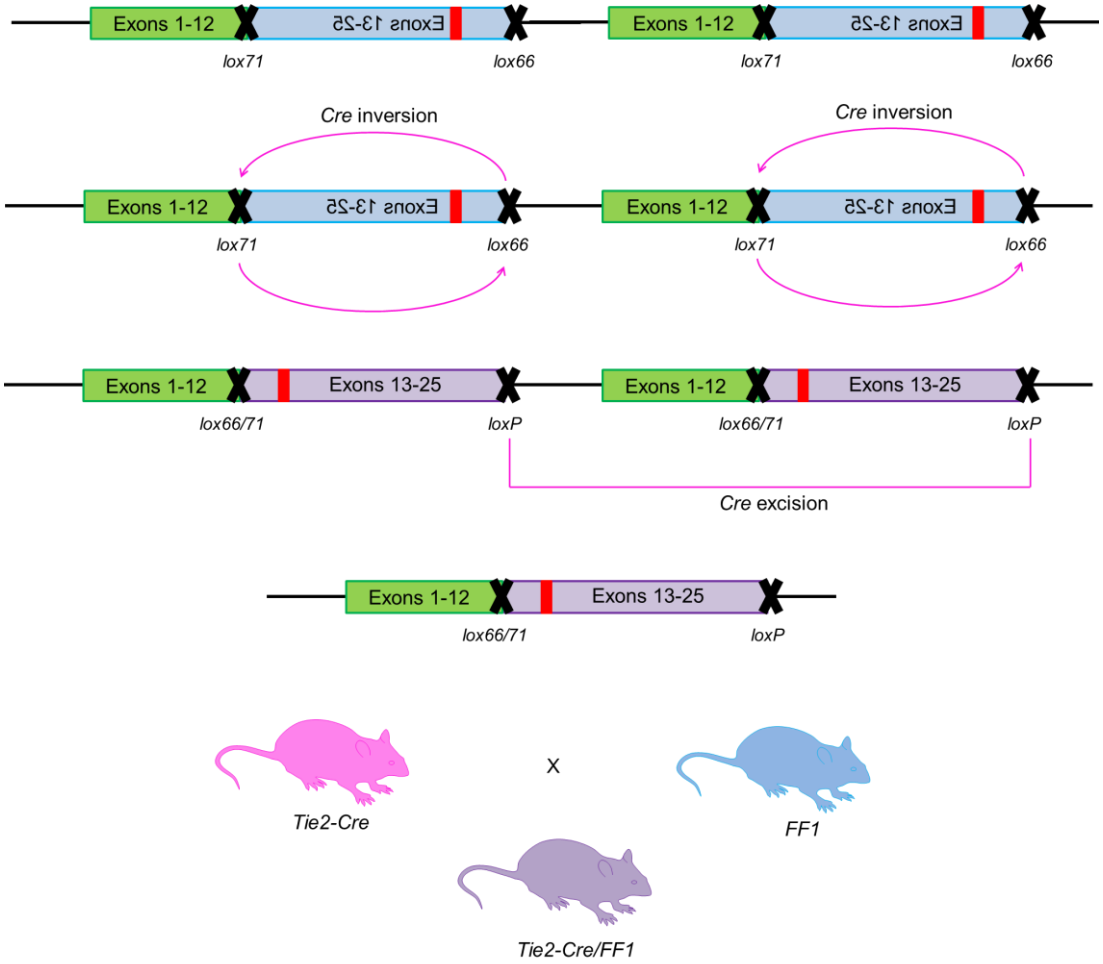

Figure 3.1 Schematic of *Tie2-Cre/FF1* transgenic mouse generation
FF1 mice contain a human *JAK2* transgene, with exons 13-25 in the inverse orientation, flanked by mutant *loxP* sites, *lox66* and *lox71*. On expression of *Cre*-recombinase, the transgene is inverted into the correct orientation and multiple copies are excised until one copy is left, flanked by one WT *loxP* site and one double mutant *lox66/lox71* site. In our model, we used *Tie2-Cre* recombinase to express the transgene in endothelial and haematopoietic lineages. The $JAK2^{V617F}$ mutation is located in exon 14 (indicated by the red bar).

3.1.2 *Pf4-Cre/FF1* mouse model

The *Pf4-Cre* transgenic mouse was generated to investigate conditional transgene expression in megakaryocytes and platelets.[225] This transgenic construct consists of the mouse *Pf4* promoter and gene, with *Cre* cDNA replacing exon 1 of the *Pf4* gene. Reporter mice confirmed expression of *Pf4-Cre* transgene recombination in megakaryocytes and platelets.

To determine the effects of megakaryocyte lineage-restricted expression of $JAK2^{V617F}$, *FF1* and *Pf4-Cre* transgenic mice were crossed to generate *Pf4-Cre/FF1* mice. Transgene expression was confirmed in megakaryocytes by quantitative PCR of human and mouse *JAK2*. Unlike the *Tie2-Cre/FF1* mice, the *Pf4-Cre/FF1* mice did not display evidence of MPN development. Platelet, neutrophil, red blood cell and lymphocyte counts did not differ between *Pf4-Cre/FF1* and WT mice at all time points measured. Therefore, *Tie2-Cre/FF1* model was the main focus in future experiments because this model displayed bona fide MPN manifestation.

3.1.3 Platelet function in *Tie2-Cre/FF1* and *Pf4-Cre/FF1* mice

As $JAK2^{V617F}$ expression was confirmed in the megakaryocyte lineage in both *Tie2-Cre/FF1* and *Pf4-Cre/FF1* mouse models, investigation of the effects of mutant JAK2 on platelet function became feasible.[224] *Tie2-Cre/FF1* whole blood aggregometry showed an increase in aggregation response to epinephrine (10μM), ADP (20μM) or collagen (10μg/mL) compared to both *Pf4-Cre/FF1* and WT whole blood. However, when platelet count was equalised between the three groups in washed platelet aggregometry, there was no significant difference in aggregation responses. Further, platelet expression of integrin β_{III}, α_{IIb}, β_{I} and α_{II} were not significantly different between the three groups, nor was expression of P-selectin or activated $\alpha_{IIb}\beta_{III}$ different, confirming that platelet activity was unchanged. Future experiments will focus on the effects of $JAK2^{V617F}$ expression on haemostasis *in vivo*, where the function and contribution of all cell types and protein factors is preserved and effects of mutant JAK2 on the system as a whole can be determined.

3.2 Materials and Methods

3.2.1 Transgenic mice

All mice were bred and housed in accordance with regulations established by the Division of Laboratory Animal Resources (DLAR) at Stony Brook University. Animal experiments were conducted under approval from the Institutional Animal Care and Use Committee (IACUC) and animal health was monitored post-procedure for potential side-effects caused by the experiment. Animals that exhibited signs of distress such as weight loss, unkempt appearance and fight wounds were euthanized by carbon dioxide inhalation.

3.2.2 Blood collection, complete blood counts and plasma isolation

Blood was collected from mice by submandibular bleed into EDTA-coated tubes (BD Biosciences). Mice were anesthetized with 2.5% isoflurane by mask and a small puncture was made in the submandibular vein using a 4mm animal lancet (Goldenrod, MEDIpoint). Approximately 100µL of blood was collected per sample and analysed for complete blood counts by the Hemavet 950FS (Drew Scientific Group, Erba Diagnostics, Inc.). Whole mouse blood was centrifuged at 14,000*g* for 10mins and the plasma fraction was collected.

3.2.3 Carotid artery occlusion assay

The carotid artery occlusion assay was used to determine haemostasis response to vessel injury *in vivo*. Mice were anesthetized with 70mg/kg pentobarbital prior to isolation of the right common carotid artery. The artery was rested in a 0.5mm Nanoprobe, blood flow was measured using a multichannel perivascular flow module (Transonic Systems Inc.) and analysed using LabChart Pro software (AD Instruments). After baseline blood flow rate was recorded, injury was induced upstream of the probe by applying filter paper (1.2mm x 1.2mm) soaked in 7.5% (w/v) ferric chloride to the surface of the vessel. The filter paper was removed after 2mins and the injured area was flushed with PBS to remove excess ferric chloride. Blood flow was monitored for 30mins post-injury, after which the assay was terminated and the vessel was removed for histology.

3.2.4 Histology

Carotid arteries were fixed in 70% (v/v) ethanol/acetate for 10mins and in formalin for an additional 20mins. The arteries were further processed by the Histology Core Facility at Stony Brook University. After processing, the arteries were embedded in paraffin wax and 5µm-thick sections were obtained using the microtome. Carotid artery sections were stained using the Carstairs' method.[226] Slides were baked at 60ºC for 1hr, deparaffinised in xylene, rehydrated in a series of alcohol gradients from 100% (v/v) ethanol to 70% (v/v) ethanol and hydrated in distilled water. The slides were then incubated in a series of histological stains: ferric ammonium sulfate (5%, w/v) for 5mins, Mayer's hematoxylin for 5mins, picric acid-orange G solution for 30mins, ponceau fuschin solution for 5mins, phosphotungstic acid (1%, w/v) for 5mins and aniline blue solution for 30mins. Each staining step proceeded with a washing step with distilled water. Slides were dehydrated in a gradient of alcohols, cleared in xylene and mounted using Histomount (ThermoFisher Scientific).

3.2.5 Tail bleed assay

Mice were anesthetised with 2.5% (v/v) isoflurane by mask and positioned prone above a collection tube filled with saline. The tail measuring 2mm from the distal end was removed and the remaining tail was placed in saline (37ºC). Bleeding time was recorded until occlusion or end-of-assay at 10mins post-injury. Mice which failed to occlude after 10mins were cauterised at the injured site to cease bleeding.

3.2.6 Murine bone marrow transplants

The *Tie2-Cre/FF1* mouse model contains $JAK2^{V617F}$ expression in both haematopoietic and endothelial cells.[224] To restrict $JAK2^{V617F}$ expression to either haematopoietic or endothelial cells, chimeric mice were generated using bone marrow transplantation. Recipient mice were irradiated with one dose of 9Gy using the Stony Brook University DLAR caesium source. Donor mice were euthanized by carbon dioxide asphyxiation, femurs and tibias were removed and flushed with cell culture media and the cell suspension was washed with PBS and filtered through a 100µm filter. Recipient mice were anesthetised with isoflurane and 5-10 million bone marrow cells were injected retro-orbitally. Mice were treated with antibiotic water (400mg/L sulfamethoxazole and 80mg/L trimethoprim) 2 days prior to irradiation and until

chimerism was confirmed by flow cytometry detection of chimeric B cell antigens. At 4 weeks post-transplant a blood sample was collected to monitor donor cell engraftment.

To distinguish donor and recipient bone marrow cells, B6.SJL-*Ptprc*^{a} *Pepc*^{b}/BoyJ mice were used in transplant experiments (Jackson Laboratory). The B6.SJL-*Ptprc*^{a} *Pepc*^{b}/BoyJ mouse, alternatively known as CD45.1 or Ly5.1 expresses the leukocyte antigen *Ptprc*^{a}, which differs from WT and *Tie2-Cre/FF1* mice which express *Ptprc*^{b}, alternatively known as CD45.2 or Ly5.2. Antibodies specific for CD45.1 or CD45.2 (BioLegend) were used to characterise blood cells post-transplant to determine the successful engraftment of donor cells.

3.2.7 vWF multimer analysis

To resolve vWF multimer components, a 0.1% (w/v) SDS-1% (w/v) agarose gel was prepared using specialised Seakem gold agarose (Cambrex Bio Science Rockland Inc.). The gel consisted of two layers: the agarose layer (50mM tris, 384mM glycine, 0.1% [w/v] SDS, 30% [v/v] glycerin, 1% [w/v] agarose) for vWF resolution and an acrylamide plug (12% [v/v] acrylamide, 0.5M Tris [pH 9.3], 10% [v/v] glycerin, 0.15% [v/v] TEMED, 0.025% [w/v] ammonium persulfate) beneath the SDS-agarose layer. Plasma samples were prepared in sample buffer (25mM Tris [pH 6.7], 3M urea, 5mM EDTA [pH 8], 1% [w/v] SDS, 0.015% [w/v] bromophenol blue) and heated at 60^{o}C for 20mins. Samples were loaded into the wells and the gel was run at 2mA overnight (24-48hrs) at 4^{o}C in running buffer (50mM Tris, 284mM glycine, 0.1% [w/v] SDS). When the running dye met the acrylamide plug, the gel was removed from the apparatus and transferred to a methanol-activated PVDF membrane at 180mA for 1hr and 15mins in transfer buffer (249mM Tris, 1.92M glycine) using a semi-dry transfer apparatus (Bio-rad). The membrane was blocked in 5% (w/v) milk in TBS for 1hr at room temperature and probed with rabbit anti-human vWF-HRP (Dako) at a dilution of 1:1000 in blocking buffer for 2hrs at room temperature. The membrane was washed twice with water and three times with TBST, each for 5mins after which Amersham ECL was applied to the membrane for 5mins. The membrane was visualised using the Protein Simple FluorChem imager.

3.2.8 Ristocetin-induced platelet agglutination assay

Mice were euthanized by carbon dioxide asphyxiation and whole blood was removed by cardiac puncture. Whole blood was diluted 1:1 in pre-warmed Ringer's solution (123mM sodium chloride, 1.5mM calcium chloride, 4.96mM potassium chloride) and the sample was equilibrated to temperature for an additional 5mins. Calcium chloride (2mM) was added to the sample and 10secs later the agonist Ristocetin (2mg/mL) was added. Platelet agglutination was measured by electrode impedance, with an increase in agglutination causing an increase in resistance detected by the electrode. Sample incubation and resistance detection were performed at 37^{o}C whilst mixing, using a two-channel aggregometer (Chronolog).

3.2.9 Megakaryocyte isolation

Bone marrow cells were harvested, washed, filtered and plated in Opti-MEM medium treated with penicillin/streptomycin/glutamate (1% [v/v] PSG) and supplemented with 3% (v/v) IL-3 and TPO. The cells were incubated in 5% carbon dioxide at 37^{o}C for 3 days, when megakaryocytes were visibly present in the culture under the microscope. Megakaryocytes were isolated from culture over a discontinuous BSA gradient and collected by centrifugation. To generate protein lysate, megakaryocytes were lysed in radioimmunoprecipitation assay (RIPA) buffer (50mM Tris [pH 7.5], 150mM NaCl, 0.2% [w/v] SDS, 0.5% [w/v] sodium deoxycholate, 1% [v/v] triton X-100) supplemented with protease cocktail inhibitor (Sigma) and phosphatase inhibitors (1mM Na_3VO_4, 10mM NaF). To prepare microscope slides, megakaryocytes were fixed in 4% (w/v) paraformaldehyde for 5mins at room temperature and cytospun at 18*g* for 5mins at a cell concentration of $1x10^5$cells/mL in 1% (w/v) BSA/PBS.

3.2.10 Platelet isolation

Mice were euthanized by carbon dioxide asphyxiation and whole blood was collected by cardiac puncture. Blood was diluted 1:1 in wash buffer (150mM sodium chloride, 20mM PIPES, pH 6.5), mixed gently and centrifuged at 200*g* for 10mins with brakes off. Platelet rich plasma (PRP) was collected from the top fraction and 1uM prostaglandin E1 and 0.02U/mL apyrase were added to the PRP to prevent activation of platelets. Platelets were then washed and lysed in nonidet P-40 (NP-40) lysis buffer (1% [v/v] NP-40, 50mM Tris, 150mM sodium chloride, pH 8).

3.2.11 EC isolation

Mice were euthanized by carbon dioxide asphyxiation and perfused with sterile cold citrated saline (136.9mM sodium chloride, 2.68mM potassium chloride, 54.7mM citric acid monohydrate, pH 7). Lungs were extracted and transferred to a tissue culture dish containing 10% (v/v) FBS/RPMI media. Lungs were minced manually with dissection scissors, transferred to a collagenase solution (1mg/mL type IV collagenase [Collagenase A, Roche], 4250 U DNase [D4513, Sigma]) and incubated in a shaking incubator at 37^{o}C for 45 minutes. The mixture was further dissociated by filtering through a needle (18G) and syringe twenty times, after which the mixture was passed through a 70µm filter to remove large, undissociated pieces. The cell suspension was collected by centrifugation at 400*g* for 5mins, red blood cells were lysed in ammonium chloride solution (15.5mM ammonium chloride, 1.2mM sodium bicarbonate, 0.01mM EDTA) and the sample was washed in PBS. ECs were isolated by CD45 depletion, CD31 collection using magnetic beads and magnetic activated cell sorting (MACS, Miltenyi Biotec). MACS was carried out in MACS buffer (0.5% [w/v] BSA, 2mM EDTA [pH 8] in PBS) and $CD45^{-}CD31^{+}$ cells were lysed in RIPA buffer (with protease and phosphatase inhibitors).

3.3 Results

3.3.1 *Tie2-Cre/FF1* mice exhibit dysfunctional haemostasis in response to vessel injury

To investigate the effects of $JAK2^{V617F}$ expression in haematopoietic and ECs on haemostasis, two *in vivo* haemostasis assays were used: carotid artery occlusion assay and tail bleed assay. Prior to carotid artery occlusion assay, a sample of blood was taken from all WT and *Tie2-Cre/FF1* experimental mice to confirm normal and elevated platelet/neutrophil counts, respectively (Figure 3.2A-B). Red blood cell counts were not significantly different between the two groups of experimental mice (Figure 3.2C).

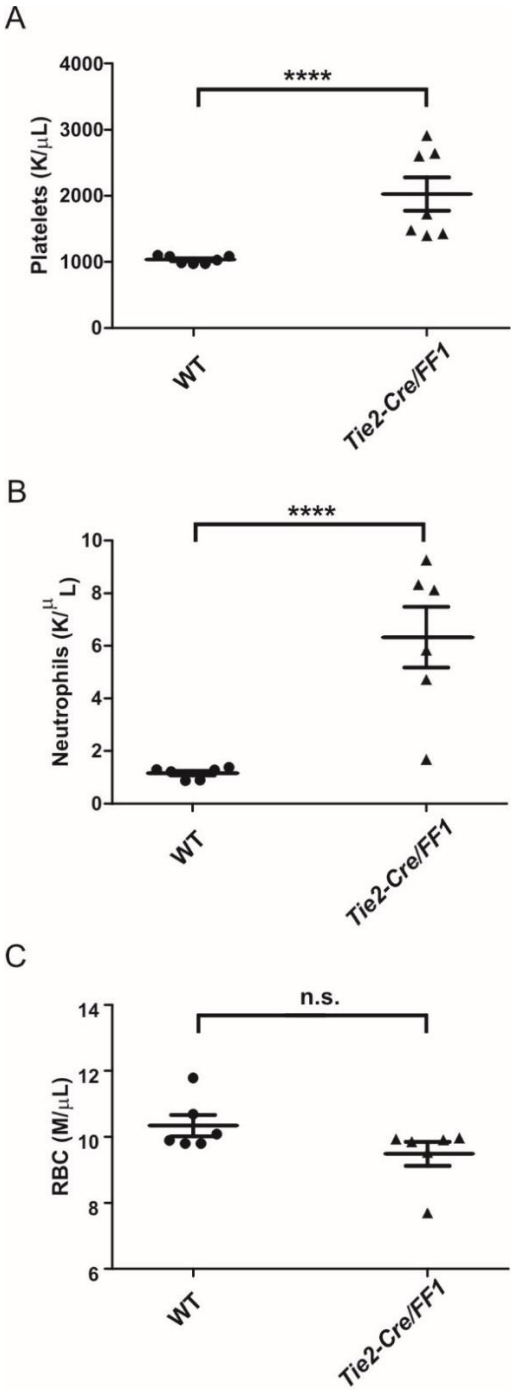

Figure 3.2 Complete blood counts (CBCs) prior to carotid artery occlusion assay

Five days before carotid artery occlusion assay, blood counts were re-examined to confirm disease phenotype. (A) Platelets and (B) neutrophils remained elevated in *Tie2-Cre/FF1* mice and (C) red blood cell counts were comparable between *Tie2-Cre/FF1* and WT mice and were within normal limits. (One point equals one animal, one-way ANOVA, ****$p<0.0001$)

Baseline flow rate in wild-type (WT) and *Tie2-Cre/FF1* mice was approximately 600µL/min. On ferric chloride injury, WT mice formed an occlusive thrombus, indicated by a drop in flow rate to just above 0µL/min. Time to occlusion for WT mice was 7.4min ± 0.4. In contrast, *Tie2-Cre/FF1* mice maintained blood flow at a rate similar to baseline flow rate for the duration of the assay (Figure 3.3A). Time to occlusion for *Tie2-Cre/FF1* mice was recorded at 30mins, the assay end-point and differences in occlusion time between WT and *Tie2-Cre/FF1* mice were quantified and found to be statistically significant (Figure 3.3B). Carstairs' staining of carotid artery sections showed distinct morphological changes between WT and *Tie2-Cre/FF1* injured sites. In the uninjured section, the vessel was filled with red blood cells and platelets (Figure 3.4A). In WT injured sections, the vessel was filled with an occlusive platelet-rich thrombus and displayed areas of fibrin deposition (Figure 3.4B). In contrast, the injured section of the *Tie2-Cre/FF1* artery showed an area of platelet plug formation but never showed occlusive fibrin-rich thrombus propagation (Figure 3.4C). These results corroborated the results of the blood flow traces; *Tie2-Cre/FF1* mice fail to form an occlusive thrombus in response to carotid vessel injury. To investigate haemostasis in smaller vessels, mouse tails were injured. *Tie2-Cre/FF1* mice had a prolonged time to occlusion (397.9secs ± 67.42) compared to WT (167.6secs ± 13.19) (Figure 3.5). Together, the results from the carotid artery occlusion assay and tail bleed assay suggest that murine expression of $JAK2^{V617F}$ in haematopoietic and endothelial cells leads to a dysfunctional response to vessel injury.

3.3.2 Endothelial $JAK2^{V617F}$ expression causes unstable clot formation in response to vessel injury

To dissect the distinct role of $JAK2^{V617F}$ in haematopoietic cells and endothelial cells, bone marrow transplant chimeric mice were generated to express $JAK2^{V617F}$ in either haematopoietic or endothelial cells. Four transplant mice were generated: (1) WT transplant control, (2) *Tie2-Cre/FF1* bone marrow into WT recipient ($JAK2^{V617F}$ haematopoietic-only mice), (3) WT bone marrow into *Tie2-Cre/FF1* recipient ($JAK2^{V617F}$ endothelial-only mice) and (4) *Tie2-Cre/FF1* transplant control (Figure 3.6). Chimerism was confirmed four weeks post-transplant by tracking CD45.1/CD45.2 expression by flow cytometry (Figure 3.7). Chimerism was also confirmed by complete blood counts; platelets and neutrophils of mice which received

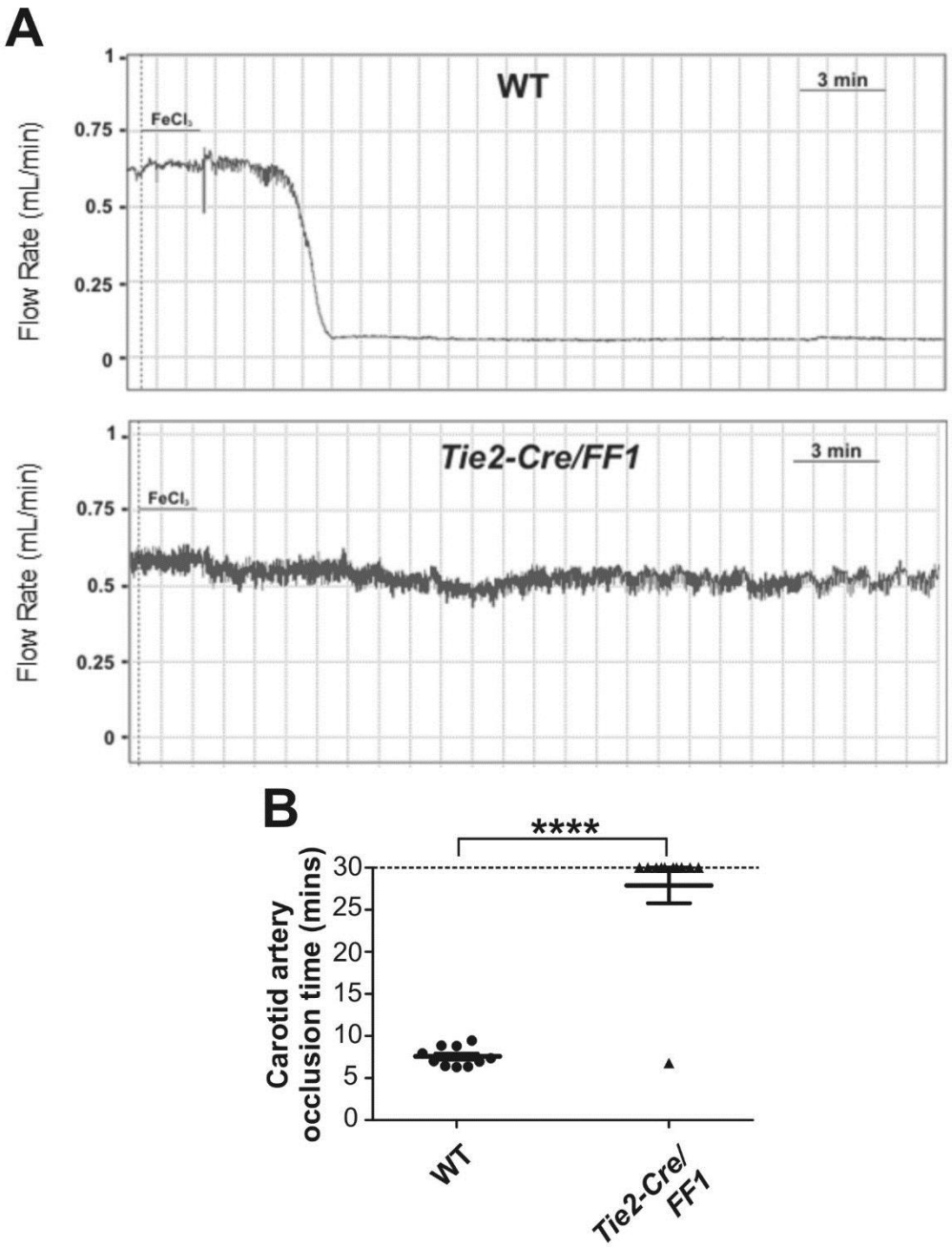

Figure 3.3 Carotid artery occlusion assay reveals dysfunctional haemostasis phenotype in Tie2-Cre/FF1 mice

(A) Doppler flow probe traces show that WT mice respond to ferric chloride injury by forming a completely occlusive thrombus 7.4min ± 0.4minutes post-injury. This is indicated by a flow rate that is approximately 0mL/min. In contrast, *Tie2-Cre/FF1* mice fail to respond to ferric chloride injury as demonstrated by flow rate that is maintained throughout the assay. (B) Quantification of time to occlusion, 30 minutes indicating that occlusion did not occur throughout the duration of the assay (t test, ****$p<0.0001$).

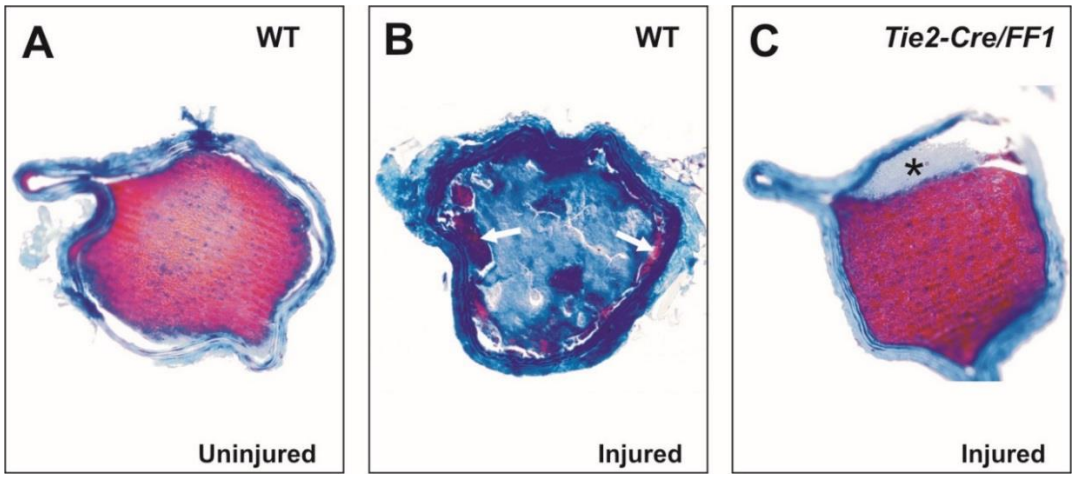

Figure 3.4 Carstairs' staining of carotid artery sections post-injury
(A) Uninjured arteries appear to be filled with blood in the vessel lumen, displayed by red-yellow red blood cells and blue platelets. (B) Injured vessels from WT mice formed occlusive thrombi demonstrated by the blue fibrin-rich clot (arrows indicate regions of dark red/purple, areas of fibrin deposition). (C) Injured vessels from *Tie2-Cre/FF1* mice form a platelet plug (*) but are unable to propagate an occlusive thrombus throughout the lumen.

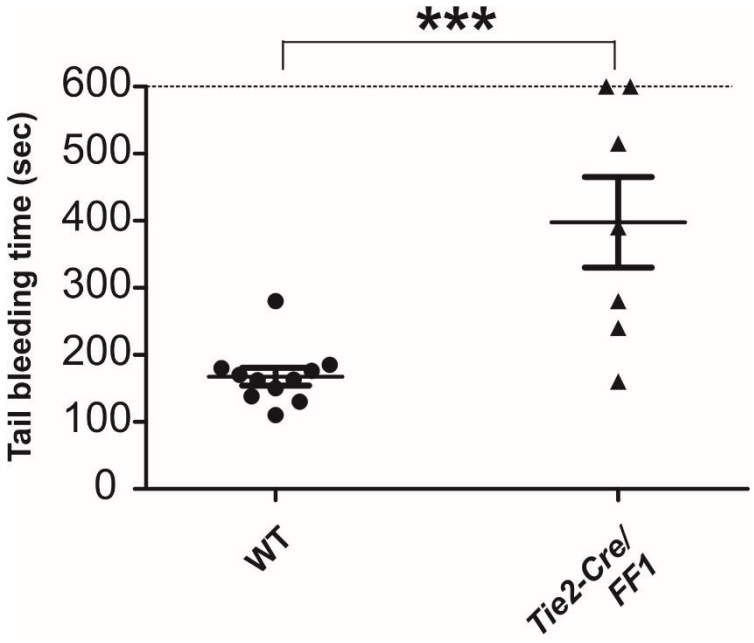

Figure 3.5 Tail bleeding assay corroborates dysfunctional haemostasis observed in Tie2-Cre/FF1 mice

Tail injury was induced by severing 2mm distal from the tip of the mouse tail. The tail was submerged in warm (37°C) saline and bleeding time was recorded until an occlusive thrombus formed and bleeding ceased. *Tie2-Cre/FF1* mice had prolonged bleeding times in response to tail injury, compared to WT mice. Two mice continued to bleed at assay time point (600secs, 10mins) and were cauterised to prevent excessive blood flow (t test, ***$p<0.001$).

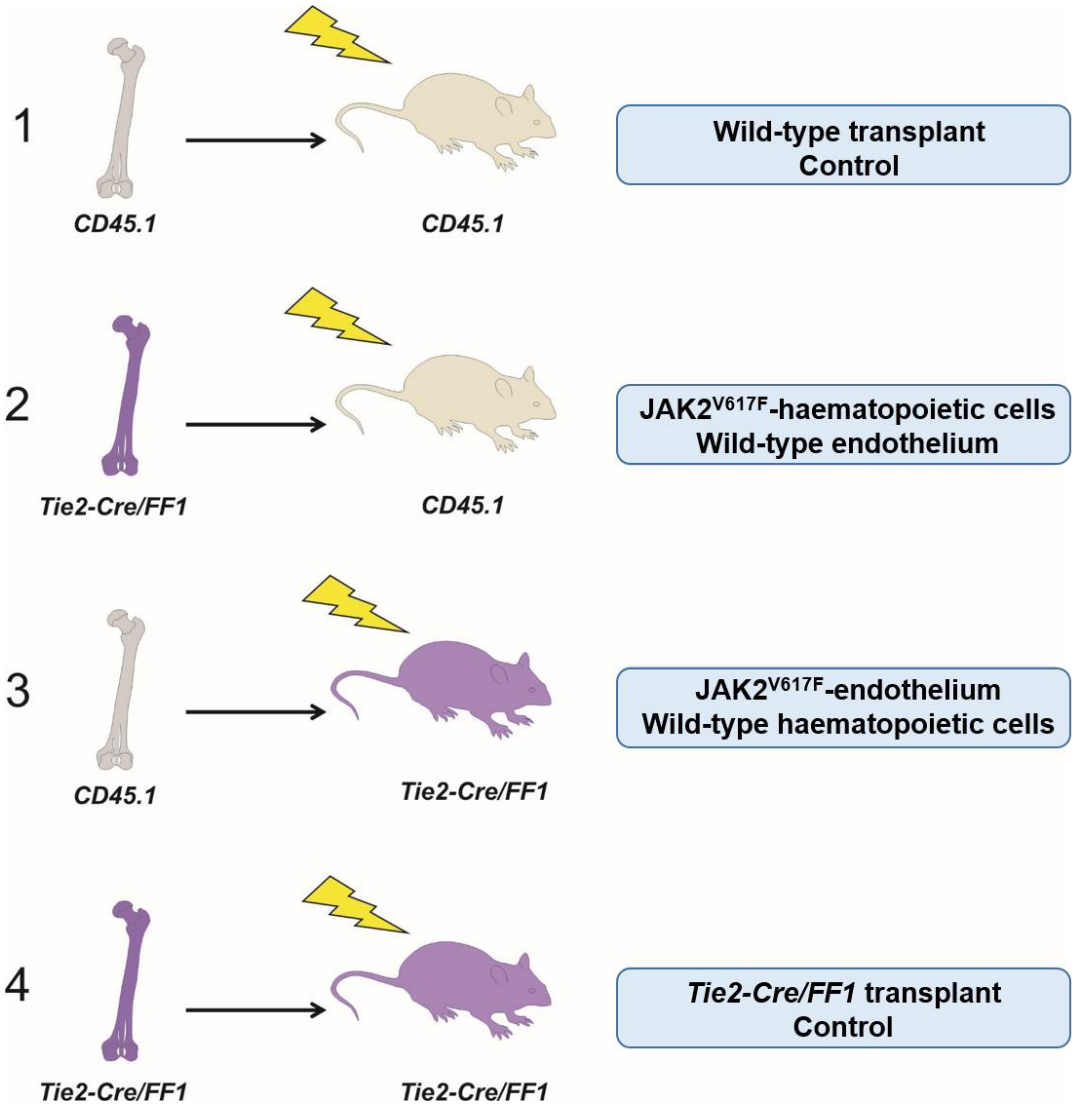

Figure 3.6 Schematic of generation of bone marrow transplant mice
Marrow from *Tie2-Cre/FF1* mice was harvested and injected retro-orbitally into irradiated WT mice to generate $JAK2^{V617F}$ haematopoietic-only mice (2). In contrast, bone marrow from WT mice was harvested and injected retro-orbitally into irradiated *Tie2-Cre/FF1* mice to generate $JAK2^{V617F}$ endothelial-only mice (3). WT control (1) and *Tie2-Cre/FF1* control (4) transplants were also generated. WT mice with differential B cell antigen CD45.1 were used to monitor chimerism.

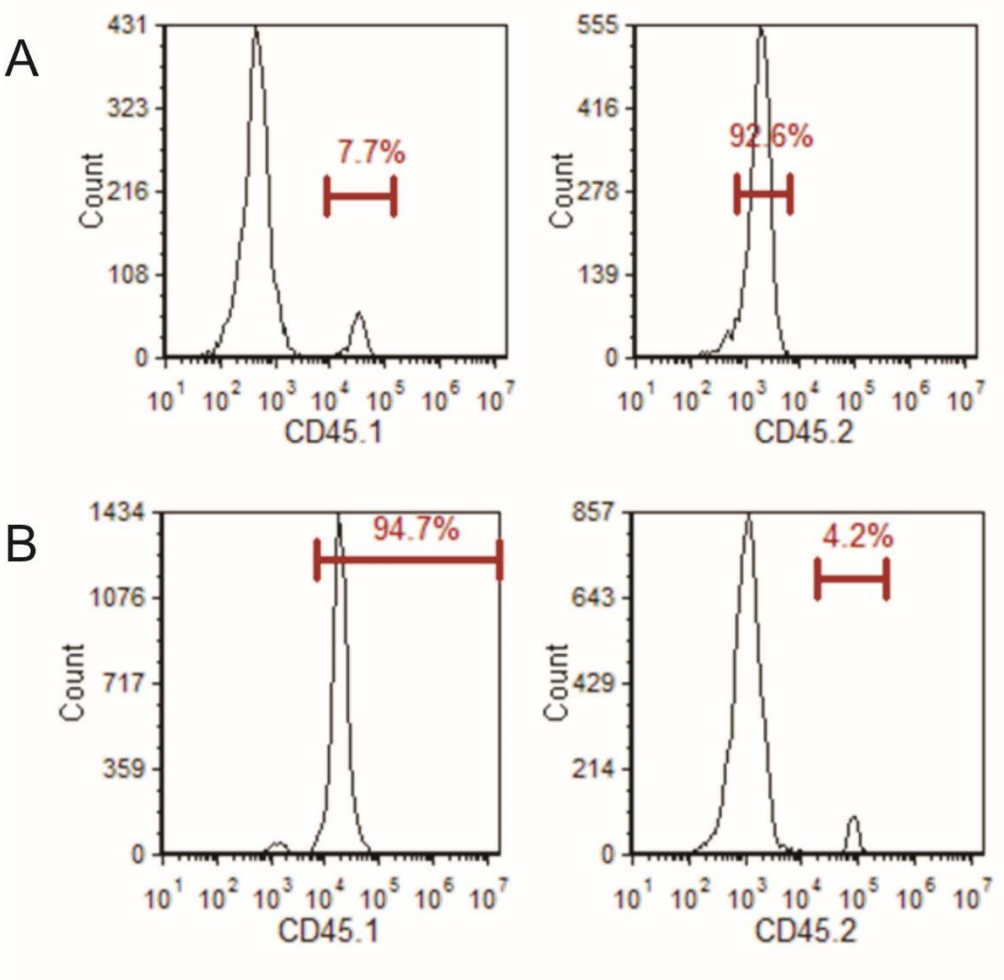

Figure 3.7 Representative flow cytometry analyses of bone marrow transplant chimeras

Expression of $JAK2^{V617F}$ in mice was restricted to either the haematopoietic or endothelial lineages by using bone marrow transplants to generate chimeric mice. To track chimerism, WT mice expressing the differential B cell antigen CD45.1 were used. *Tie2-Cre/FF1* mice expressed the differential B cell antigen CD45.2. These antigens could be distinguished by antibodies specific for each antigen; therefore, chimerism could be traced by collecting a small sample of blood and staining with antibodies for CD45.1/CD45.2 antigens. (A) *Tie2Cre/FF1* bone marrow (CD45.2) reconstituted WT (CD45.1) mice, generating $JAK2^{V617F}$-haematopoietic only mice. (B) WT bone marrow (CD45.1) reconstituted *Tie2-Cre/FF1* (CD45.2) mice, generating $JAK2^{V617F}$-endothelial only mice. Blood samples were collected and investigated for CD45.1/CD45.2 expression 4 weeks post-transplant.

marrow from *Tie2-Cre/FF1* donors exhibited elevated cell counts and mice which received marrow from WT donors exhibited normal cell counts (Figure 3.8).

In response to ferric chloride-induced carotid injury, transplant control mice responded similarly to WT and *Tie2-Cre/FF1* congenital mice (WT transplant control, 9.3mins ± 2.2; *Tie2-Cre/FF1* transplant control, 28.5mins ±2.6). $JAK2^{V617F}$ haematopoietic-only mice formed occlusive thrombi similar to WT mice (8.9mins ±1.3). In contrast, $JAK2^{V617F}$ endothelial-only mice displayed a phenotype unique to both WT and *Tie2-Cre/FF1* congenital mice with a time to occlusion averaging between the two congenital mouse strains (18.7mins ± 8.9) (Figure 3.9A-B). This average is the result of some mice forming occlusive thrombi and some mice with sustained blood flow after 30mins. Histological analysis of the arteries show platelet plug formation in $JAK2^{V617F}$-endothelial only mice similar to *Tie2-Cre/FF1* congenital mice, compared to occlusive thrombi which formed in both WT control and $JAK2^{V617F}$ haematopoietic-only mice (Figure 3.10A-C). In contrast, time to occlusion on tail injury did not differ significantly between $JAK2^{V617F}$ haematopoietic-only (64.8secs±12.9) and $JAK2^{V617F}$ endothelial-only (80.7secs±37.5) mice (Figure 3.11). This time to occlusion is not significantly different to the occlusion time of WT control mice (70secs±13), indicating that cell-specific $JAK2^{V617F}$ expression does not have a significant effect on response to tail injury.

3.3.3 Functional vWF expression is altered in *Tie2-Cre/FF1* mice and in $JAK2^{V617F}$-endothelial only mice

Plasma collected from congenital WT and *Tie2-Cre/FF1* mice revealed a multimer pattern shift from ultra-large molecular weight multimers to low molecular weight multimers in *Tie2-Cre/FF1* mice (Figure 3.12A). The absence of ultra-large molecular weight multimers in *Tie2-Cre/FF1* mice suggests that platelet agglutination might be impaired in these mice. Indeed, ristocetin-induced platelet agglutination assay shows that platelet agglutination in whole blood is impaired in *Tie2-Cre/FF1* samples compared to WT samples (Figure 3.13A-B). Plasma samples collected from transplant mice show no difference in multimer pattern between $JAK2^{V617F}$ haematopoietic-only and $JAK2^{V617F}$ endothelial-only mice (Figure 3.12B). However, vWF function is impaired in $JAK2^{V617F}$ endothelial-only mice, as shown by an inability to respond to

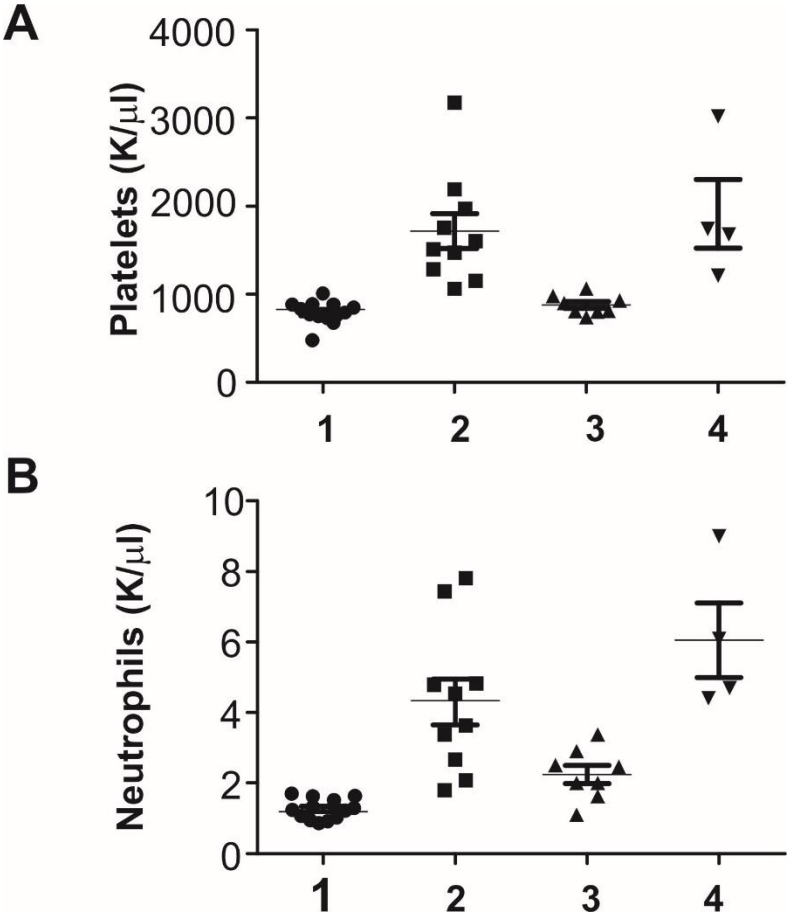

Figure 3.8 Platelet and neutrophil counts in transplant mice
Chimeric mice display expected (A) platelet and (B) neutrophil counts after chimerism. Mice with $JAK2^{V617F}$ expression in their haematopoietic cells (2 and 4) exhibit increased platelet and neutrophil counts and mice with WT haematopoietic cells (1 and 3) exhibit platelet and neutrophil counts within the normal range. (1) WT transplant control mice, (2) $JAK2^{V617F}$-haematopoietic only mice, (3) $JAK2^{V617F}$-endothelial only mice, (4) *Tie2-Cre/FF1* transplant control mice

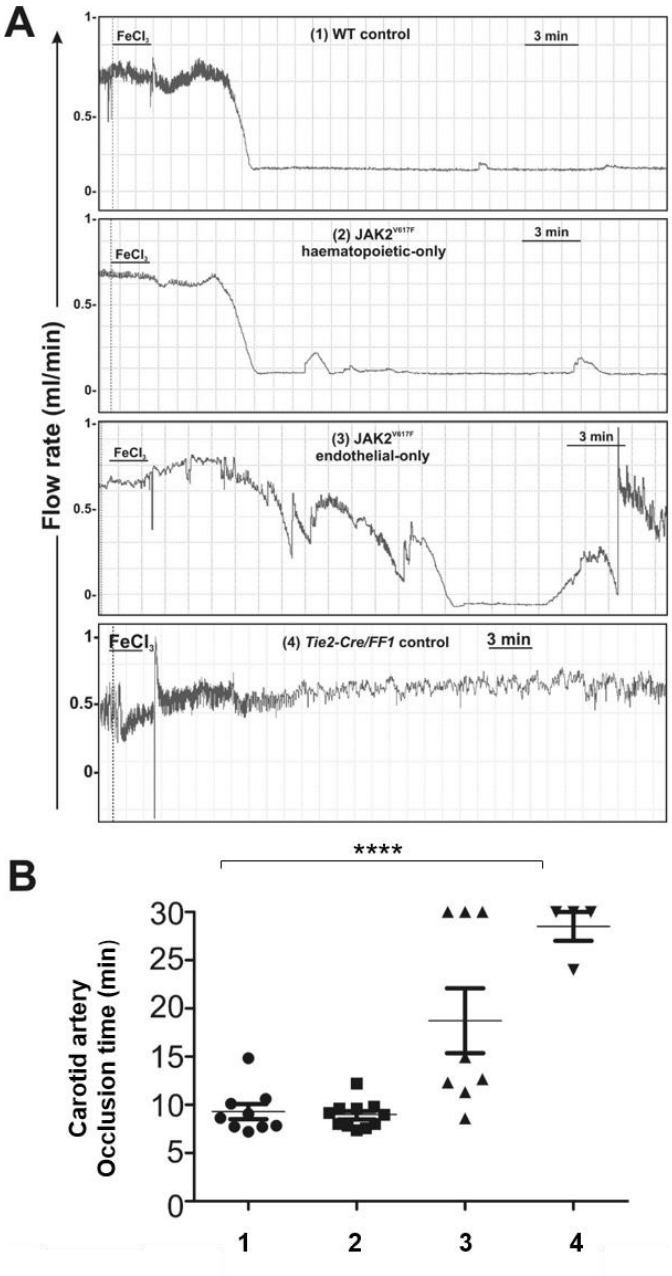

Figure 3.9 Carotid artery occlusion assay on transplant chimeras
(A) Representative Doppler flow traces from transplant chimeras and (B) quantification of time to occlusion. JAK2^{V617F}-endothelial only mice show a unique phenotype: half the cohort form occlusive thrombi and half the cohort form unstable thrombi. (One-way ANOVA, ****p<0.0001)

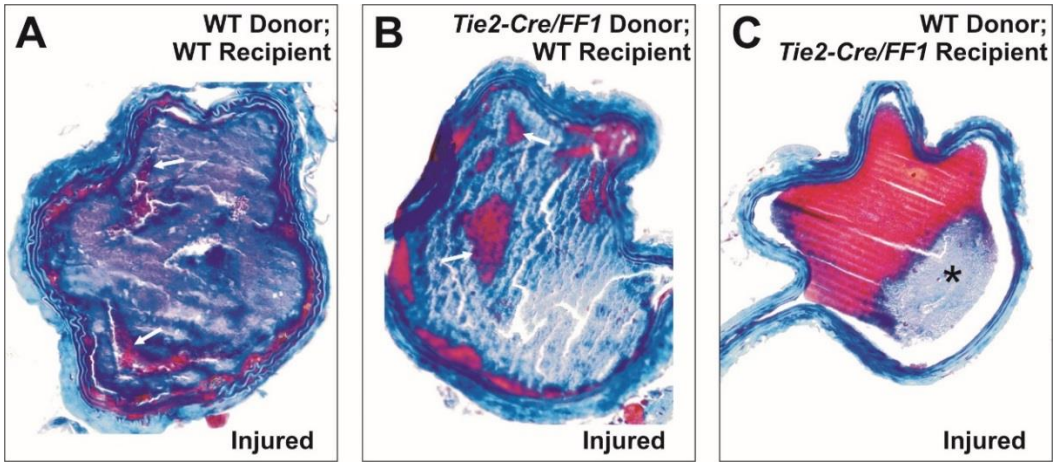

Figure 3.10 Carstairs' staining of carotid artery sections post-injury of chimeric mice

(A)WT control mice and (B) $JAK2^{V617F}$-haematopoietic only mice form occlusive thrombi post-ferric chloride injury. (C) $JAK2^{V617F}$-endothelial only mice form a platelet plug (*), but do not form an occlusive thrombus, similar to *Tie2-Cre/FF1* transgenic mice.

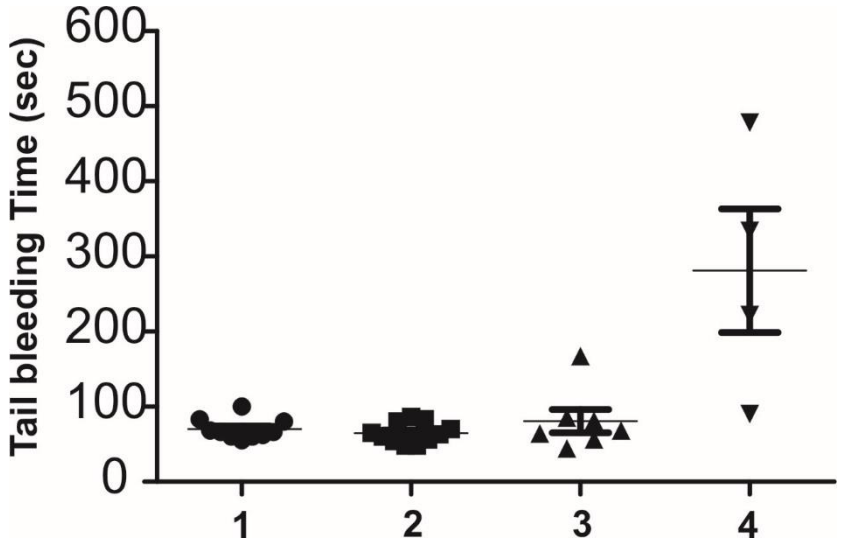

Figure 3.11 Tail bleed assay on transplant chimeras
In contrast to the carotid artery occlusion assay, JAK2^{V617F}-endothelial only mice display normal bleeding times. (1) WT control mice, (2) JAK2^{V617F} hameatopoietic -only mice, (3) JAK2^{V617F} endothelial-only mice, (4) *Tie2-Cre/FF1* control mice.

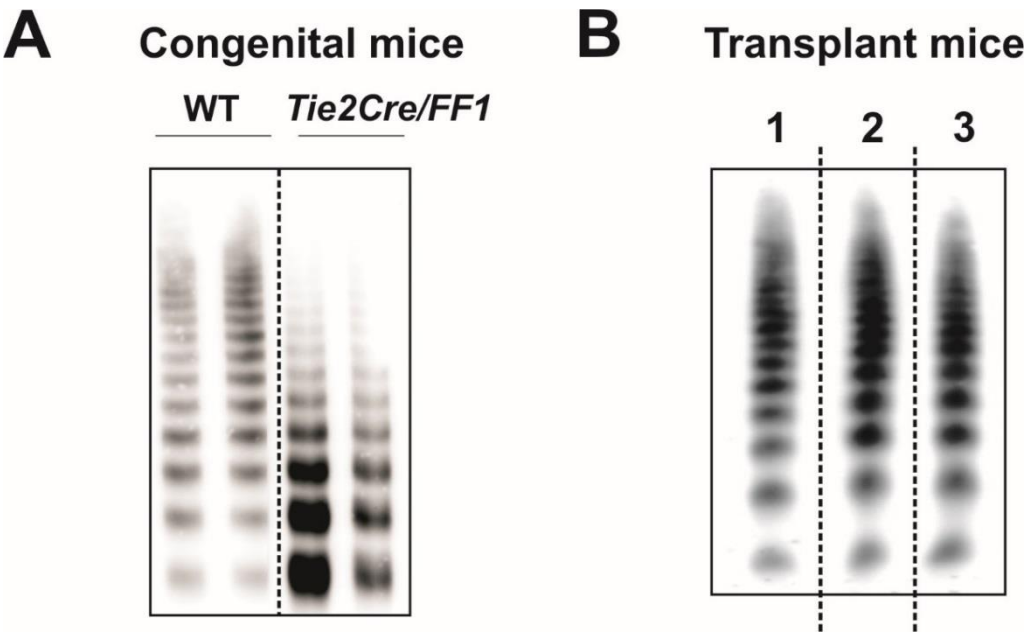

Figure 3.12 vWF multimer analysis
(A) Plasma from *Tie2-Cre/FF1* mice show an increase in low molecular weight multimers and an absence of ultra large molecular weight multimers. Plasma from WT mice show an equal distribution of multimers of all sizes. (B) Plasma from transplant mice show no difference in multimer pattern. (1) WT control, (2) $JAK2^{V617F}$ haematopoietic-only, (3) $JAK2^{V617F}$ endothelial-only

ristocetin (Figure 3.13C-D). These data suggest the vWF is one component affected by JAK2^{V617F} expression and this effect is more robust in endothelial cells.

Protein lysate from endothelial cells, platelets and megakaryocytes from WT and *Tie2-Cre/FF1* mice were analysed for vWF multimer pattern. Although vWF is mainly produced in endothelial cells, megakaryocytes also synthesise vWF and store vWF in α-granules where it remains in circulating platelets.[18] In EC lysate, low molecular weight multimers appear to be more abundant in both WT and *Tie2-Cre/FF1* lysates, however they appear to be increased in *Tie2-Cre/FF1* lysates (Figure 3.14A). In WT megakaryocyte and platelet lysate, it appears that vWF multimer pattern shifts from low molecular weight multimers in megakaryocytes to high molecular weight multimers in platelets and megakaryocyte lysate generated from *Tie2-Cre/FF1* mice display an increase in low molecular weight multimers (Figure 3.14B). Protein from endothelial cells, megakaryocytes and platelets was quantified using the Bio-Rad DC Protein Assay and 10µg of protein was loaded per sample. A suitable loading control for these gels was not available in the range of vWF multimer sizes (250kDa - 20,000kDa).

To investigate the possibility that megakaryocyte vWF contributes to the increase in low molecular weight vWF multimers in plasma, megakaryocytes were stained at different stages of maturation to visualise vWF localisation. It appears that in early stages of maturation, vWF is localised in the cytoplasm of megakaryocytes, but as megakaryocytes mature vWF becomes localised to the cell surface (Figure 3.15A). When vWF staining is combined with P-selectin staining, we do not see co-localisation of vWF and P-selectin at the cell surface during this later stage of maturation (Figure 3.15B). vWF and P-selectin are both stored in α-granules in platelets, however this data suggests that during megakaryocyte development these two proteins localise separately.

ADAMTS13 has a role in regulating vWF multimer size in plasma. To determine if ADAMTS13 expression contributes towards the change in multimer pattern seen in *Tie2-Cre/FF1* mice, ADAMTS13 protein expression was analysed in EC lysates. Expression of ADAMTS13 appears to be slightly reduced in *Tie2-Cre/FF1* EC lysates, compared to WT EC lysates (Figure 3.16). Further research into

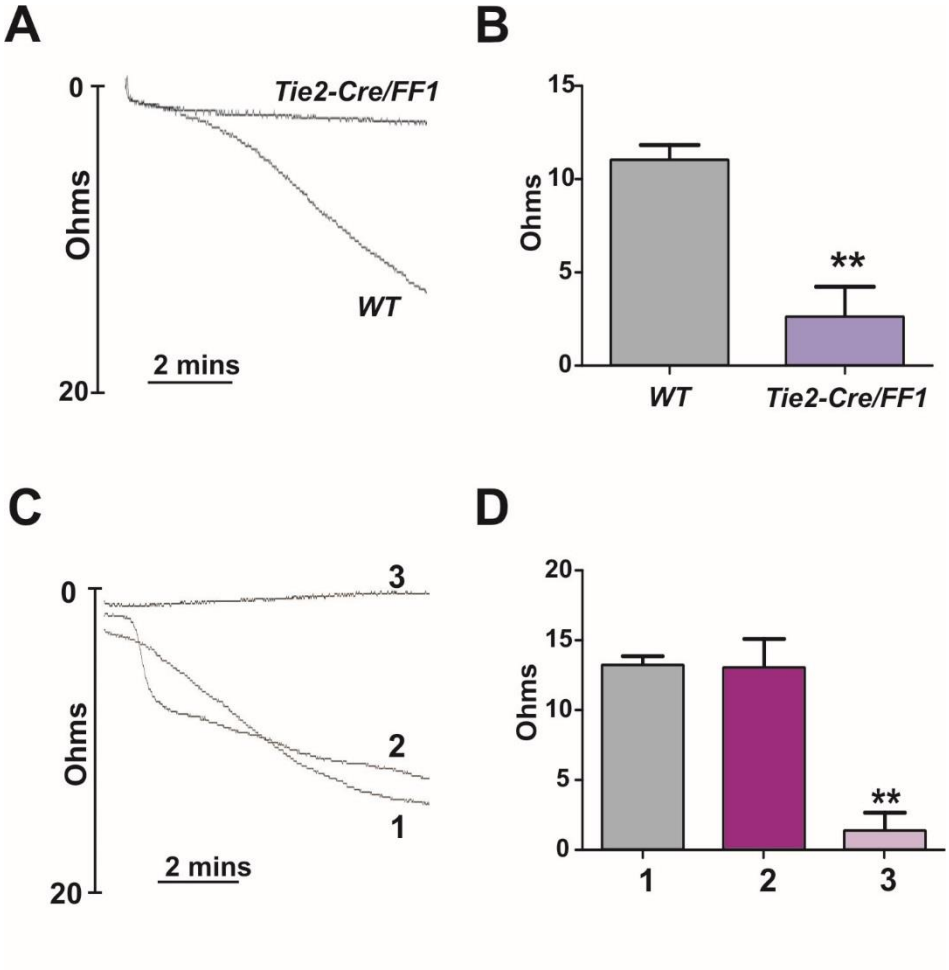

Figure 3.13 vWF functional analysis by ristocetin-induced platelet agglutination

(A) WT whole blood agglutinates in response to ristocetin, however *Tie2-Cre/FF1* whole blood does not respond to agonist. (B) Quantification of ristocetin-induced platelet agglutination in congenital whole blood (t test, **p=0.0018) (C) Whole blood from WT control and $JAK2^{V617F}$ haematopoietic-only mice agglutinate in response to ristocetin, however $JAK2^{V617F}$ endothelial-only mice fail to respond to agonist. (D) Quantification of ristocetin-induced platelet agglutination in transplant whole blood (One-way ANOVA, **p=0.0010). Transplant mice, (1) WT control, (2) $JAK2^{V617F}$ haematopoietic-only, (3) $JAK2^{V617F}$ endothelial-only.

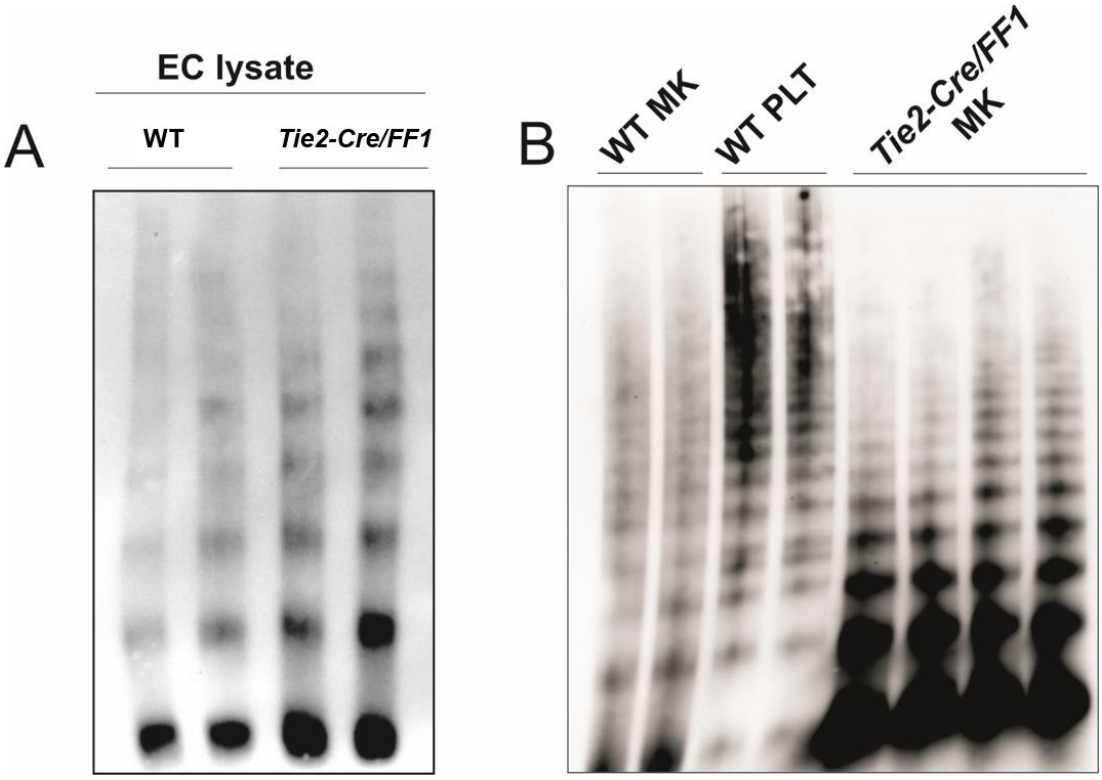

Figure 3.14 Multimer analysis of cell lysates which express vWF
(A) JAK2^{V617F}-endothelium shows an increase in expression of low molecular weight multimers compared to WT endothelium. (B) WT megakaryocyte (MK) and platelet (PLT) lysates indicate a shift in multimer patter between these two cell types with platelets containing the functional ultra-large multimers. *Tie2-Cre/FF1* megakaryocytes contain increased amounts of low molecular weight multimers.

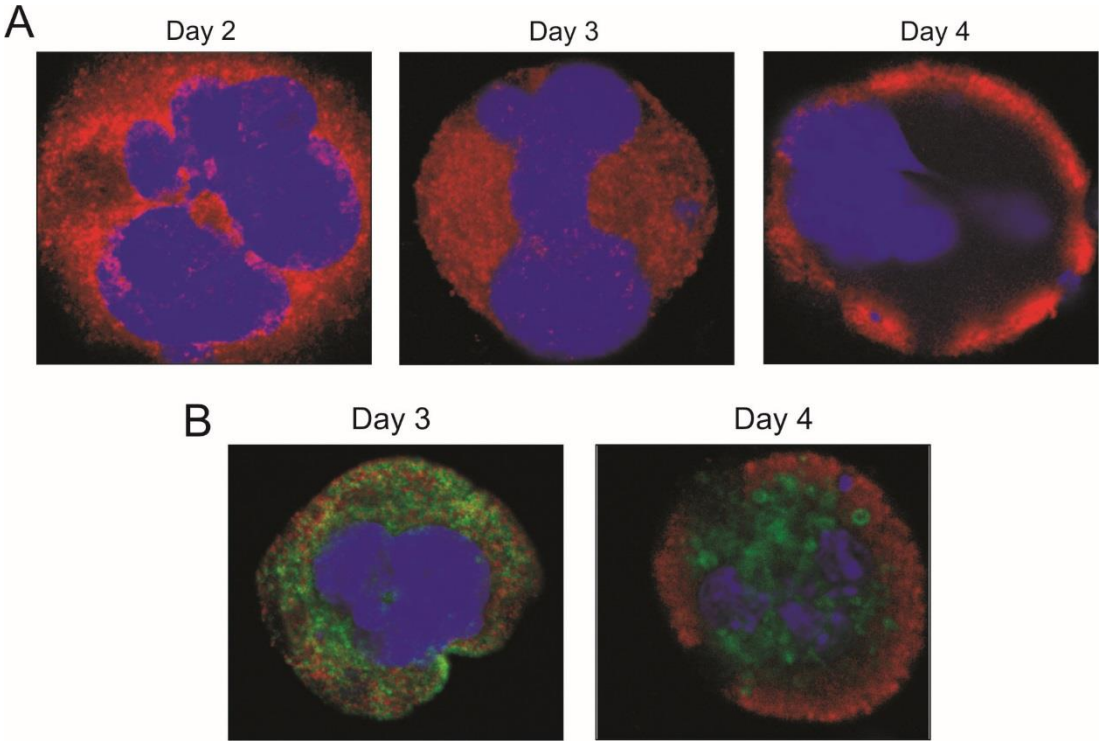

Figure 3.15 vWF localisation in megakaryocytes throughout maturation
(A) Immunofluorescence of megakaryocytes at different stages of maturation shows that vWF (red) localises to the cell surface as megakaryocytes mature. (B) Additional staining for P-selectin (green) shows that these two proteins localise differently in maturing megakaryocytes. vWF localises to the cell surface at day 4 and P-selectin remains in the cytosol. Blue, DAPI nuclear stain.

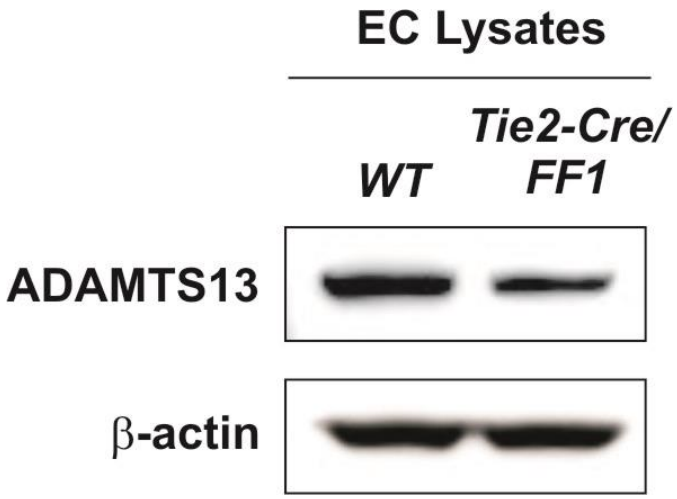

Figure 3.16 ADAMTS13 expression in endothelial cell lysates
EC lysates were collected from WT and *Tie2-Cre/FF1* mouse lungs. ECs were pooled from 3 mice of each genotype. ADAMTS13 expression was slightly reduced in *Tie2-Cre/FF1* EC lysates.

ADAMTS13 function in Tie2-Cre/FF1 mice is needed to determine the role of ADAMTS13 in the multimer pattern observed in this mouse model.

3.3.4 JAK2^{V617F}-positive endothelial cells have increased expression of TFPI and CD39

Endothelial cells produce, express and secrete numerous factors that affect haemostasis. TFPI binds to and inactivates factor Xa and TF:Factor VIIa complexes, both of which promote clot formation in the coagulation cascade. CD39 cleaves ADP, a potent platelet agonist. TFPI and CD39 both contribute to maintaining proper haemostasis by inhibiting aberrant clotting. In EC lysate, we observe an increase in protein expression of both TFPI and CD39 in *Tie2-Cre/FF1* samples, compared to WT samples (Figure 3.17).

3.4 Discussion

Patients with MPNs commonly experience complications due to clotting and bleeding. Often patients are diagnosed with an MPN after an adverse event caused by a clot or bleed brings them to the clinic for treatment. Recent evidence of MPN mutation in both haematopoietic and ECs of some patients raises many interesting questions concerning disease initiation, progression and effects on overall patient health. The combined efforts of both haematopoietic and ECs towards maintaining normal haemostasis are well known, however it is unknown how expression of the MPN mutation JAK2^{V617F} affects the normal functions of these cells in haemostasis.

Previously, the lab developed a mouse model for MPNs by breeding the transgenic mouse *FF1*, which contains the inactive JAK2^{V617F} construct, with a *Cre-recombinase* mouse *Tie2-Cre*. The result of this breeding strategy was progeny expressing JAK2^{V617F} in both haematopoietic and ECs. This congenital expression of JAK2^{V617F} differs from the human disease which results from acquisition of the mutation in adult patients. However, despite the difference in temporal expression of JAK2^{V617F}, the mouse model mimics the human disease by exhibiting thrombocytosis, neutrophilia and splenomegaly.

Given the role of platelets in clot formation and the high percentage of patients with MPNs and clotting complications, the initial discovery of a defect in occlusive thrombus formation in the mouse model was a bit surprising. Despite high platelet

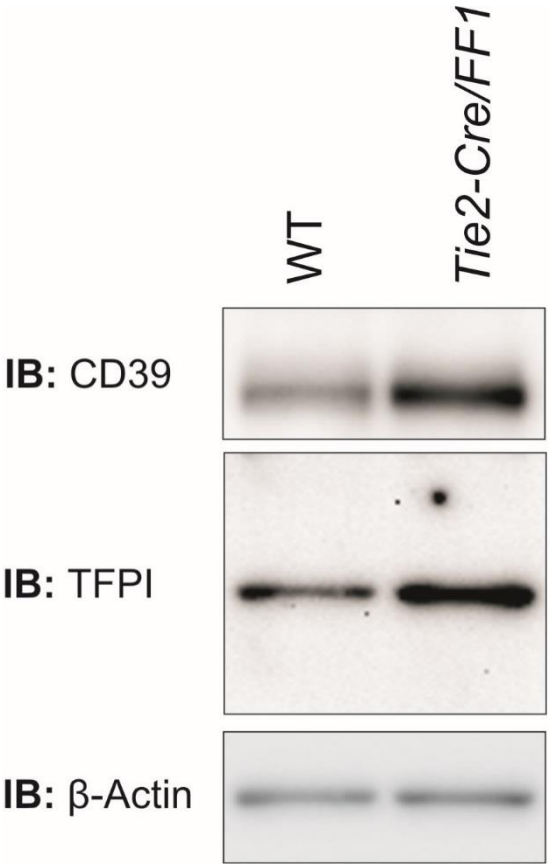

Figure 3.17 Endothelial cell lysate expression of CD39 and TFPI
EC lysates were collected from WT and *Tie2-Cre/FF1* mouse lungs. ECs were pooled from 3 mice of each genotype. Expression of CD39 and TFPI was increased in endothelial cells of *Tie2-Cre/FF1* mice compared to WT.

counts, JAK2^{V617F} congenital mice failed to form occlusive thrombi in response to ferric chloride-induced arterial injury and tail vessel injury. Histology of injured vessels revealed that JAK2^{V617F} congenital mice formed unstable thrombi, shown by initial platelet plug formation but absence of clot propagation. Similar results were obtained in a PV mouse model; unstable clot formation occurred in response to both ferric chloride and tail injury.[227] Investigation into platelet function in this mouse model revealed decreased expression of platelet glycoprotein VI and FcRγ chain and a decreased activation of platelets in response to stimulation. In contrast, investigation into platelet function in the *Tie2-Cre/FF1* mouse model, investigated by another member of the lab, revealed JAK2^{V617F} platelet function to be normal.[224] In both models, JAK2^{V617F} expression in platelets was insufficient to be the sole cause of thrombus instability.

Endothelial-restricted JAK2^{V617F} expression exhibited similar, albeit less severe, clot instability compared to congenital mice. In contrast, haematopoietic-restricted JAK2^{V617F} mice formed stable thrombi in response to injury. Together, these data suggest endothelial JAK2^{V617F} expression contributes significantly towards dysfunctional haemostasis; however the combined expression of JAK2^{V617F} in both haematopoietic and ECs results in a more striking phenotype. Undoubtedly, these results highlight the importance of both cell types in haemostasis, confirming that blood and endothelium work collectively to maintain proper haemostasis. The differences in response to ferric chloride injury compared to tail vessel injury exhibited in endothelial-specific JAK2^{V617F} mice may be attributed to effects of vessel and vascular bed specific endothelial phenotypes. ECs line all blood vessels, including large arteries, small capillaries, veins and venules, in all organs and regions of the body. EC functions are vast and differ depending on the vessel type and region in which they reside.[50,51] For example, vWF and TFPI are particularly important in venule and capillary haemostasis, respectively. In this context, the differences observed between large vessel injury (ferric chloride carotid artery injury) and microvessel injury (tail vessel injury) suggests that JAK2^{V617F} affects these vessels differently. ECs were subsequently isolated from lungs of WT and *Tie2-Cre/FF1* mice and an increase in TFPI, CD39 and low molecular weight vWF expression in ECs expressing JAK2^{V617F} was observed. Further investigation is needed to determine if these changes are systemic or specific to the microvascular endothelium of the lung.

Moreover, vessel and vascular specific effects of JAK2^{V617F} on ECs need to be determined to define the mechanism behind the differences in arterial and microvascular responses to vessel injury in the *Tie2-Cre/FF1* mouse model.

Changes in vWF multimer pattern and function were investigated more extensively using mouse plasma, endothelial, megakaryocyte and platelet lysate. In patients, bleeding diathesis is most commonly seen in ET and these effects have been attributed to AvWD.[9,228] In AvWD, ultra-large molecular weight vWF multimers are proteolysed or removed from circulation when platelet levels are exceedingly high. Indeed, when plasma samples from transgenic and control mice were resolved, there was an observed a shift in multimer pattern in transgenic mice resulting in a loss of the functional ultra-large molecular weight vWF multimers. These results were corroborated with the ristocetin-induced platelet agglutination assay, which demonstrated an absence of functional vWF in plasma of transgenic mice when whole blood failed to agglutinate in response to the agonist ristocetin. Multimer patterns in both transplant mouse models remained normal, however whole blood from endothelial specific JAK2^{V617F} mice failed to agglutinate in the ristocetin-induced platelet agglutination assay. These results suggest that a mechanism more complex than simply platelet removal of ultra-large molecular weight vWF may be occurring in mice expressing JAK2^{V617F}. Perhaps in ECs, JAK2^{V617F} affects production of functional vWF, a process that is inherently complex.

In EC lysates, there was an increase in expression of low molecular weight multimers in ECs expressing JAK2^{V617F}. It is still unclear whether this increased expression led directly to a similar increase in low molecular weight multimers in plasma, or if post-translational processing in JAK2^{V617F}-ECs was perturbed, leading to release of low molecular weight multimers due to the absence of ultra large molecular weight multimers. Similarly, in JAK2^{V617F}-positive megakaryocytes we observed an increase in low molecular weight multimers. It is currently not known whether megakaryocytes contribute to vWF release themselves or if all vWF produced in megakaryocytes is processed into α-granules in platelets for subsequent release into circulation. Immunofluorescence staining of two α-granule components, vWF and P-selectin, showed that at one stage of megakaryocyte maturation, these two components were localised separately. Specifically, at day 4 of megakaryocyte maturation *in vitro* vWF is localised at the cell surface and P-selectin remains in the cytosol. Although

this does not prove that megakaryocytes directly secrete vWF, the localisation of vWF to the cell surface suggests this may be possible. Further work is needed to determine megakaryocyte-specific release of haemostasis factors.

Production and secretion of vWF are complex processes, beginning with protein post-translational modification in the endoplasmic reticulum and golgi and ending with either constitutive secretion or packaging of mature molecules into Weibel-Palade bodies. NO, a product of eNOS, is anti-inflammatory and inhibits the release of Weibel-Palade bodies from ECs.[229] An inducible JAK2 knockout mouse model demonstrated that loss of JAK2 resulted in abnormal EC function related to impaired response to vasodilators.[97] Further investigation indicated that eNOS expression was decreased in this model, a consequence of altered transcriptional regulation. JAK2 deficiency in this system resulted in altered Raf-1/MEK1 signalling as opposed to canonical STAT signalling. A separate study investigating inducible NOS (iNOS) demonstrated that ECs from iNOS-/- mice were depleted of Weibel-Palade bodies, due to exocytosis.[230] Results from both studies indicate a role for NO in anti-inflammation, preventing the release of inflammatory components contained in Weibel-Palade bodies within ECs. In the *Tie2-Cre/FF1* mouse model JAK2 activity is enhanced, therefore it is postulated that eNOS expression is increased, leading to an increase in NO expression and exocytosis of Weibel-Palade bodies. To investigate this, NG-nitro-L-arginine methyl ester (L-NAME), an inhibitor of NOS can be used to attempt to ameliorate the consequences of enhanced eNOS activity.[231]

Altogether, EC expression of $JAK2^{V617F}$ was determined to affect haemostasis by disrupting stable thrombus formation. Moreover, three factors, TFPI, CD39 and vWF were identified as factors affected by $JAK2^{V617F}$ expression in ECs, with expression of TFPI and CD39 increased and functional vWF decreased in $JAK2^{V617F}$-ECs. How these effects work together to produce the dysfunctional haemostasis phenotype observed in the *Tie2-Cre/FF1* mouse model is unknown and it is possible there are additional factors affected by $JAK2^{V617F}$ expression which also contribute towards this phenotype. Future experiments will aim to define the mechanism of $JAK2^{V617F}$ activation in ECs and how the effects of $JAK2^{V617F}$-endothelim in mice relate to the effects of $JAK2^{V617F}$-endothelium in patients with MPNs.

CHAPTER 4 ELUCIDATING THE MECHANISM OF JAK2^{V617F} ACTIVATION IN ENDOTHELIAL CELLS *IN VITRO*

4.2 Experimental Rationale

In the previous chapter, endothelial expression of JAK2^{V617F} was identified to be important in the dysfunctional haemostasis response to ferric chloride-induced carotid artery injury in mice. Here, we aim to investigate the signalling and gene expression changes in JAK2^{V617F}-positive endothelial cells, compared to ECs which express only JAK2^{WT}. An *in vitro* model of endothelial JAK2^{V617F} expression was established using HUVECs and HAECs. This system was then used to determine changes in JAK2 signalling protein expression and activation and changes in gene expression.

4.2 Materials and Methods

4.2.1 Transient transfection

HUVECs were seeded at 1.5x10^5 cells per well in 6-well plates and incubated overnight at 37ºC and 5% CO_2. DNA from *pEF1/HisA-V5-JAK2^{WT}* and *pEF1/HisA-V5-JAK2^{V617F}* (Figure 4.1) constructs was diluted into RPMI or Opti-MEM media without serum. Plus^{TM} reagent (ThermoFisher) was added to the diluted DNA and the mixture was incubated at room temperature for 5mins. Lipfectamine LTX (ThermoFisher) was then added and the combined mixture was incubated at room temperature for 25mins. Per well, 1μg of DNA and 3μL of lipofectamine were used for transfection of empty vector and JAK2^{V617F} constructs. For the WT construct, 0.5μg of DNA and 3μL of lipofectamine were used. These values were determined by empirical testing of varying DNA amounts and evaluating the resulting JAK2 expression in endothelial cells. The volume of Plus^{TM} reagent used was dependent on the volume of DNA.

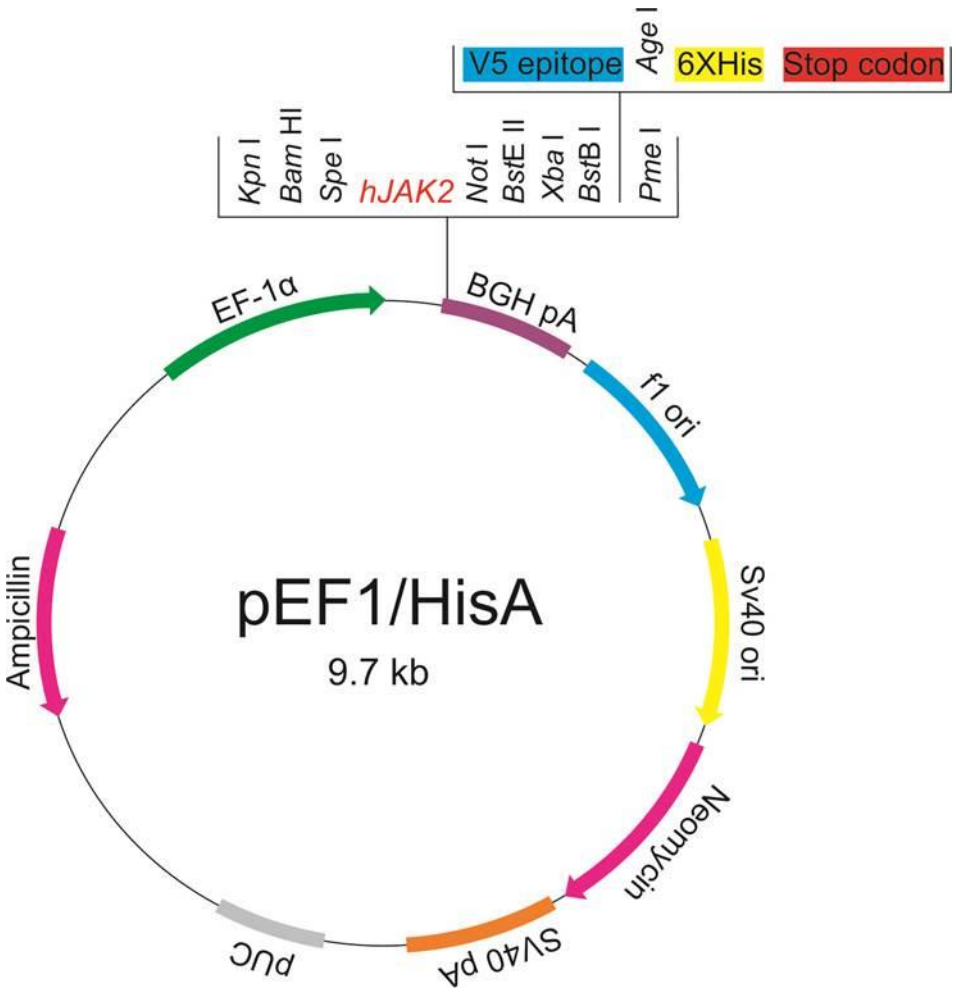

Figure 4.1 *pEF1/HisA* vector with *JAK2* insert
pEF1/HisA vector contains a multiple cloning site (MCS) where JAK2 has been inserted between *Spe*I and *Not*I restriction sites. Towards the 3' end of the MCS is a sequence for a V5-His tag that can be used to identify the cloned insert. *V5-JAK2* is transcribed through the *EF-1α* promoter region and ampicillin resistance is used to screen for transformed *E.coli*.

During complex incubation, HUVECs were washed 3 times with 1XPBS to remove all serum/media. HUVECs and DNA/lipid complexes were incubated for 4hrs at 37^{o}C and 5% CO_2 after which they were removed and replaced with complete HUVEC media. 24hrs later, cells were washed three times with 1XPBS and lysed using 1% (v/v) Triton X-100 protein lysis buffer (with protease and phosphatase inhibitors).

4.2.2 Mutagenesis

The lentiviral plasmid pWPI containing human *JAK2*^{WT} was kindly provided by Dr. Gregor Hoermann (Medical University of Vienna) (Figure 4.2). Plasmid identity was confirmed by diagnostic digest using restriction enzymes *Spe*I and *Pac*I (New England Biolabs), incubating the reaction at 37^{o}C for 1hr and resolving the digested products on a 0.8% (w/v) agarose gel/tris-acetate-EDTA (TAE) buffer (Figure 4.3A). The *JAK2*^{WT} sequence was confirmed using five forward and four reverse sequencing primers (Table 4.1 and Figure 4.4) using external sequencing services (Eurofins Scientific) (Figure 4.3B). Mutagenesis reagents from the QuikChange XL kit (Agilent Technologies) and a modified PCR protocol were used to induce the point mutation causing JAK2^{V617F}. Taguchi PCR allows for the testing of different PCR parameters in one assay, resulting in a more efficient PCR optimisation. The parameters tested, the primers used and the cycling conditions programmed in our mutagenesis reaction are provided (Table 4.2 and 4.3). The total reaction volume was 25µL.

Following PCR amplification, 5µL aliquots of each reaction were removed and resolved in a 0.8% (w/v) agarose/TAE gel. Reactions which showed products were then digested with *Dpn*I restriction enzyme for 1hr at 37^{o}C and transformed into XL10 Gold Ultracompetent cells (Agilent Technologies) according to section 4.2.3. Colonies were screened for the *JAK2* construct by colony PCR using the primers and cycling parameters provided (Table 4.4). Of the 24 colonies screened, 19 were positive for *JAK2* (Figure 4.5A) and 3 of the 4 colonies sequenced were positive for the JAK2^{V617F} mutation (Figure 4.5B).

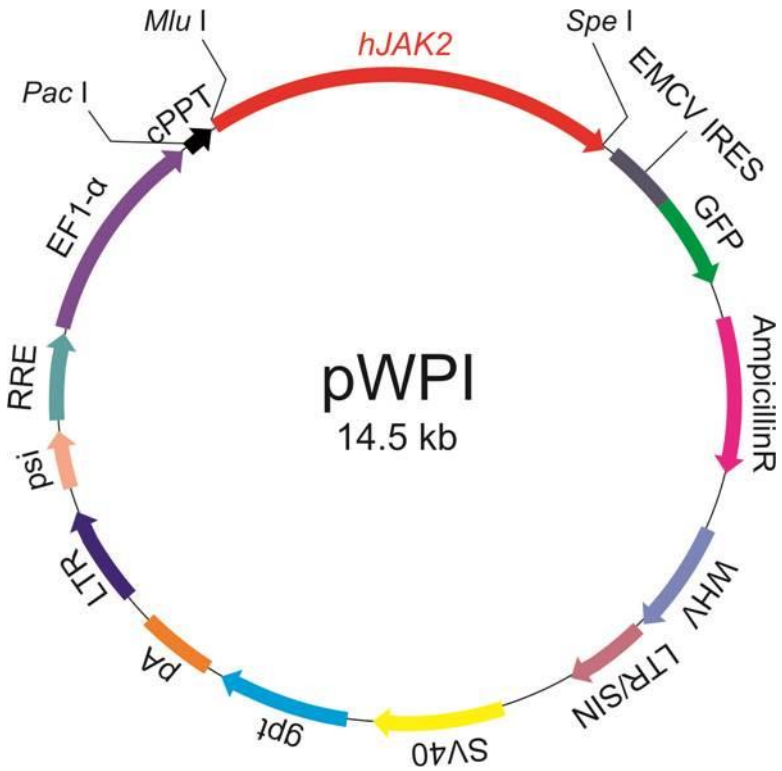

Figure 4.2 pWPI lentiviral vector with JAK2 insert
pWPI vector is a lentiviral vector containing an *EGFP* tag to facilitate identification of transduced cells. The *JAK2* insert was cloned between *Mlu*I and *Spe*I and transcription of the construct is under the *EF-1α* promoter. Ampicillin resistance is used to screen for transformed *E.coli* colonies.

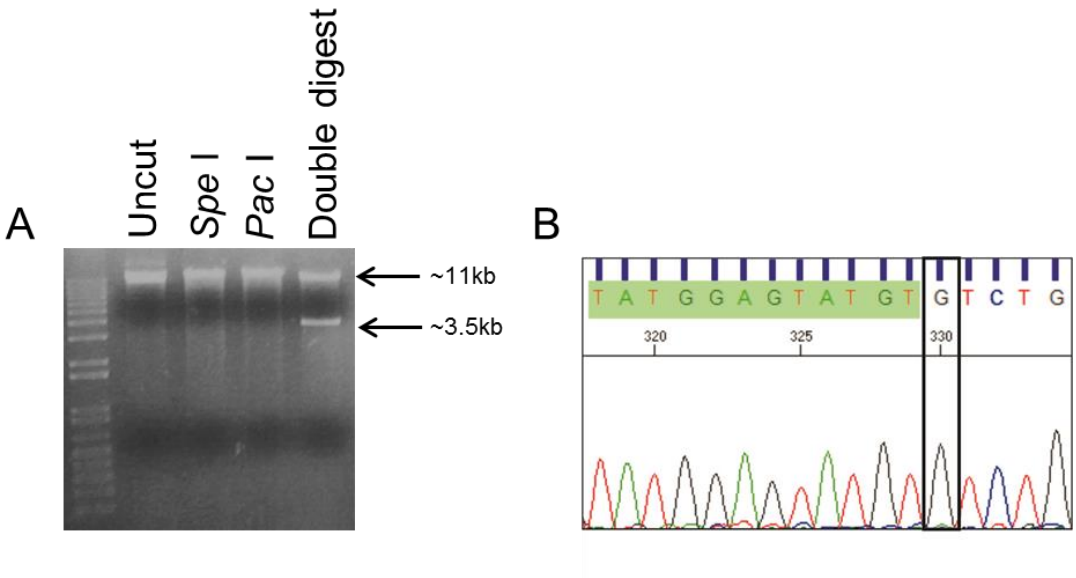

Figure 4.3 *pWPI-JAK2WT* plasmid validation
(A) Diagnostic digest of *pWPI-JAK2* plasmid. Double digest with *Spe*I and *Pac*I reveals two bands at ~11kb and ~3.5kb. (B) Sequencing of *pWPI-JAK2* reveals the correct $JAK2^{WT}$ sequence.

Table 4.1 hJAK2 Sequencing Primers

Primer	Sequence
Forward 1	5'-CAACAGAGCCTATCGGCATGG-3'
Forward 2	5'-ACCTCCAGCCGTGCTTGAAA-3'
Forward 3	5'-TGTCCCCCAAAGCCAAAAGA-3'
Forward 4	5'-CCATGGGTACCACCTGAATGC-3'
Forward 5	5'-CACAGGGATCTGGCAACGAG-3'
Reverse 1	5'-CTGGCAGTGGCTTTGCATTG-3'
Reverse 2	5'-CTCGTCTCCACAGACACATACTCCA-3'
Reverse 3	5'-CCGGTCTTCAAAGGCACCAG-3'
Reverse 4	5'-TCATCGTAAGGCAGGCC-3'

5'ATGGGAATGGCCTGCCTTACGATGACAGAAATGGAGGGAACATCCACCTCTTCTATATATCAGA
ATGGTGATATTTCTGGAAATGCCAATTCTATGAAGCAAATAGATCCAGTTCTTCAGGTGTATCTTT
ACCATTCCCTTGGGAAATCTGAGGCAGATTATCTGACCTTTCCATCTGGGGAGTATGTTGCAGAA
GAAATCTGTATTGCTGCTTCTAAAGCTTGTGGTATCACACCTGTGTATCATAATATGTTTGCTTTAA
TGAGTGAAACAGAAAGGATCTGGTATCCACCCAACCATGTCTTCCATATAGATGAGTCAACCAGG
CATAATGTACTCTACAGAATAAGATTTTACTTTCCTCGTTGGTATTGCAGTGGCAGCAACAGAGCC
TATCGGCATGGAATATCTCGAGGTGCTGAAGCTCCTCTTCTTGATGACTTTGTCATGTCTTACCTC
TTTGCTCAGTGGCGGCATGATTTTGTGCACGGATGGATAAAAGTACCTGTGACTCATGAAACACA
GGAAGAATGTCTTGGGATGGCAGTGTTAGATATGATGAGAATAGCCAAAGAAAACGATCAAACCC
CACTGGCCATCTATAACTCTATCAGCTACAAGACATTCTTACCAAAATGTATTCGAGCAAAGATCC
AAGACTATCATATTTTGACAAGGAAGCGAATAAGGTACAGATTTCGCAGATTTATTCAGCAATTCA
GCCAATGCAAAGCCACTGCCAGAAACTTGAAACTTAAGTATCTTATAAATCTGGAAACTCTGCAG
TCTGCCTTCTACACAGAGAAATTTGAAGTAAAAGAACCTGGAAGTGGTCCTTCAGGTGAGGAGAT
TTTTGCAACCATTATAATAACTGGAAACGGTGGAATTCAGTGGTCAAGAGGGAAACATAAAGAAA
GTGAGACACTGACAGAACAGGATTTACAGTTATATTGCGATTTTCCTAATATTATTGATGTCAGTA
TTAAGCAAGCAAACCAAGAGGGTTCAAATGAAAGCCGAGTTGTAACTATCCATAAGCAAGATGGT
AAAAATCTGGAAATTGAACTTAGCTCATTAAGGGAAGCTTTGTCTTTCGTGTCATTAATTGATGGA
TATTATAGATTAACTGCAGATGCACATCATTACCTCTGTAAAGAAGTAGCACCTCCAGCCGTGCTT
GAAAATATACAAAGCAACTGTCATGGCCCAATTTCGATGGATTTTGCCATTAGTAAACTGAAGAAA
GCAGGTAATCAGACTGGACTGTATGTACTTCGATGCAGTCCTAAGGACTTTAATAAATATTTTTTG
ACTTTTGCTGTCGAGCGAGAAAATGTCATTGAATATAAACACTGTTTGATTACAAAAAATGAGAAT
GAAGAGTACAACCTCAGTGGGACAAAGAAGAACTTCAGCAGTCTTAAAGATCTTTTGAATTGTTA
CCAGATGGAAACTGTTCGCTCAGACAATATAATTTTCCAGTTTACTAAATGCTGTCCCCCAAAGCC
AAAAGATAAATCAAACCTTCTAGTCTTCAGAACGAATGGTGTTTCTGATGTACCAACCTCACCAAC
ATTACAGAGGCCTACTCATATGAACCAAATGGTGTTTCACAAAATCAGAAATGAAGATTTGATATT
TAATGAAAGCCTTGGCCAAGGCACTTTTACAAAGATTTTTAAAGGCGTACGAAGAGAAGTAGGAG
ACTACGGTCAACTGCATGAAACAGAAGTTCTTTTAAAAGTTCTGGATAAAGCACACAGAAACTATT
CAGAGTCTTTCTTTGAAGCAGCAAGTATGATGAGCAAGCTTTCTCACAAGCATTTGGTTTTAAATT
ATGGAGTATGTGTCTGTGGAGACGAGAATATTCTGGTTCAGGAGTTTGTAAAATTTGGATCACTA
GATACATATCTGAAAAAGAATAAAAATTGTATAAATATATTATGGAAACTTGAAGTTGCTAAACAGT
TGGCATGGGCCATGCATTTTCTAGAAGAAAACACCCTTATTCATGGGAATGTATGTGCCAAAAAT
ATTCTGCTTATCAGAGAAGAAGACAGGAAGACAGGAAATCCTCCTTTCATCAAACTTAGTGATCC
TGGCATTAGTATTACAGTTTTGCCAAAGGACATTCTTCAGGAGAGAATACCATGGGTACCACCTG
AATGCATTGAAAATCCTAAAAATTTAAATTTGGCAACAGACAAATGGAGTTTTGGTACCACTTTGT
GGGAAATCTGCAGTGGAGGAGATAAACCTCTAAGTGCTCTGGATTCTCAAAGAAAGCTACAATTT
TATGAAGATAGGCATCAGCTTCCTGCACCAAAGTGGGCAGAATTAGCAAACCTTATAAATAATTG
TATGGATTATGAACCAGATTTCAGGCCTTCTTTCAGAGCCATCATACGAGATCTTAACAGTTTGTT
TACTCCAGATTATGAACTATTAACAGAAAATGACATGTTACCAAATATGAGGATAGGTGCCCTGG
GGTTTTCTGGTGCCTTTGAAGACCGGGATCCTACACAGTTTGAAGAGAGACATTTGAAATTTCTA
CAGCAACTTGGCAAGGGTAATTTTGGGAGTGTGGAGATGTGCCGGTATGACCCTCTACAGGACA
ACACTGGGGAGGTGGTCGCTGTAAAAAAGCTTCAGCATAGTACTGAAGAGCACCTAAGAGACTT
TGAAAGGGAAATTGAAATCCTGAAATCCCTACAGCATGACAACATTGTAAAGTACAAGGGAGTGT
GCTACAGTGCTGGTCGGCGTAATCTAAAATTAATTATGGAATATTTACCATATGGAAGTTTACGAG
ACTATCTTCAAAAACATAAAGAACGGATAGATCACATAAAACTTCTGCAGTACACATCTCAGATAT
GCAAGGGTATGGAGTATCTTGGTACAAAAAGGTATATCCACAGGGATCTGGCAACGAGAAATATA
TTGGTGGAGAACGAGAACAGAGTTAAAATTGGAGATTTTGGGTTAACCAAAGTCTTGCCACAAGA
CAAAGAATACTATAAAGTAAAAGAACCTGGTGAAAGTCCCATATTCTGGTATGCTCCAGAATCACT
GACAGAGAGCAAGTTTTCTGTGGCCTCAGATGTTTGGAGCTTTGGAGTGGTTCTGTATGAACTTT
TCACATACATTGAGAAGAGTAAAAGTCCACCAGCGGAATTTATGCGTATGATTGGCAATGACAAA
CAAGGACAGATGATCGTGTTCCATTTGATAGAACTTTTGAAGAATAATGGAAGATTACCAAGACC
AGATGGATGCCCAGATGAGATCTATATGATCATGACAGAATGCTGGAACAATAATGTAAATCAAC
GCCCCTCCTTTAGGGATCTAGCTCTTCGAGTGGATCAAATAAGGGATAACATGGCTGGATGA3'

Figure 4.4 hJAK2 cDNA sequence

Human *JAK2* cDNA sequence used to validate sequencing data of $JAK2^{WT}$ and $JAK2^{V617F}$ constructs. This sequence is referenced in NCBI (NM_004972.3). Binding sites for forward primers (green) and reverse primers (pink) are indicated.

Table 4.2 Taguchi PCR Parameters

Sample	dH20 (µL)	10X buffer	$MgCl_2$ (µL)	dNTPs (µL)	DNA (µL)	Primers x2 (µL)	DMSO (µL)	Polymerase (µL)
1	15.5	2.5	0	0.5	0.5	1.5	2.5	0.5
2	10.5	2.5	3 (7.5mM)	2	1	1.5	2.5	0.5
3	5.5	2.5	5 (15mM)	4	2	1.5	2.5	0.5
4	6	2.5	3 (7.5mM)	4	0.5	3	2.5	0.5
5	7	2.5	5 (15mM)	0.5	1	3	2.5	0.5
6	9.5	2.5	0	2	2	3	2.5	0.5
7	0	2.5	5 (15mM)	2	0.5	6	2.5	0.5
8	2.5	2.5	0	4	1	6	2.5	0.5
9	2	2.5	3 (7.5mM)	0.5	2	6	2.5	0.5
10	16	2.5	0	0.5	0	1.5	2.5	0.5
MgCl2	Prepared 7.5mM and 15mM working concentrations from 25mM stock solution							
dNTPs	Prepared 2.5mM working concentration from 10mM stock solution							
DNA	Used DNA at a concentration of 300ng/µL							
Primers	Prepared 1µM working concentrations from 10µM stock solutions							

Table 4.3 JAK2V617F Mutagenesis Primers and Cycling Parameters

Vector	Primers	Tm (°C)	Annealing Temperature (°C)	Mutation
pWPI	F-5'-AGCATTTGGTTTTAAATTATGGAGTATGTTTCTGTGGAGACGAGA-3'	63.4	50	V617F
	R-3'-TCTCGTCTCCACAGAAACATACTCCATAATTTAAAACCAAATGCT-3'			

Segment	Cycles	Temperature (°C)	Time
1	1	95	30 seconds
2	12	95	30 seconds
		50	1 minute
		68	2 minutes/kb (30 minutes)
3	1	68	10 minutes

Table 4.4 JAK2 Colony PCR Primers and Cycling Parameters

Gene	Primers	Tm (°C)	Annealing Temperature (°C)	Amplicon (bp)
hJAK2	F-5'-GAAGAACTTCAGCAGTCTTAAAGATC-3'	53.8	48	574
	R-5'-CCATGCCAACTGTTTAGCAACTTC-3'	56.9		

Segment	Cycles	Temperature (° C)	Time
1	1	95	15 minutes
2	30	94	1 minute
		48	1 minute
		72	1 minute
3	1	72	10 minutes

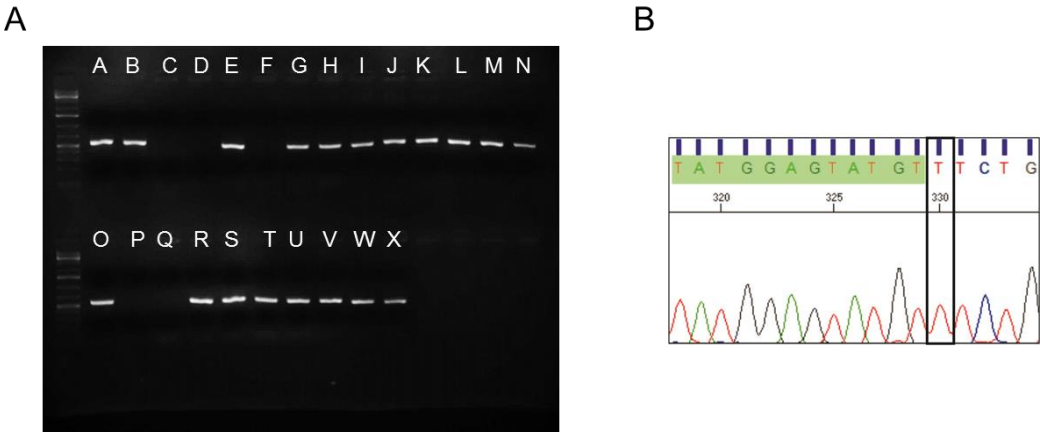

Figure 4.5 Generation of pWPI-JAK2V617F plasmid
(A) Colony PCR screen for *hJAK2*. *JAK2* was amplified in 19 of the 24 colonies screened. (B) Sequencing result of plasmid which contains the point mutation $JAK2^{G1849T}$ which results in $JAK2^{V617F}$.

4.2.3 Bacterial transformation

XL10 Gold Ultracompetent cells (XL10, Agilent Technologies) or Stellar Competent cells (Clontech) were thawed on ice and aliquoted into 50µL aliquots for use in 1 transformation reaction. 2µL of β-mercaptoethanol (Agilent Technologies) was added to XL10 cells, the combination was mixed by gentle swirling with the pipette tip and the cells were incubated on ice for an additional 10mins, swirling every 2mins. 2µL and 2.5µL of the mutagenesis and infusion cloning mixtures were added to XL10 and Stellar cells, respectively and the cells were incubated on ice for 30mins. XL10 and Stellar cell mixtures were then heat shocked at 42°C for 30secs and 45secs, respectively and incubated on ice for an additional 2mins. 500µL of pre-warmed Lysogeny Broth (LB) media (Millipore) or Super Optimal broth with Catabolite (S.O.C.) repression (Clontech) was added to XL10 and Stellar cells, respectively and the mixtures were incubated at 37°C, shaking at 225rpm for 1hr. The mixture was then plated on LB agar plates containing 100µg/mL of ampicillin (Melford) and incubated overnight at 37°C. Plates were analysed for colony growth the following morning.

4.2.4 Lentivirus generation

Lentiviruses were generated using HEK293T cells, a highly transfectable cell line which contains the SV40 large T-antigen conducive for virus generation. HEK293T cells were passaged the day before transfection to ensure cell growth was in the exponential phase. To generate lentivirus, 3 plasmids were co-transfected into HEK293T cells according to the lipid transfection methods described in 4.2.1. Transfections were carried out in 10cm petri dishes and reagents were scaled accordingly. A total of 15µg of DNA was used to co-transfect the cells, 4.5µg of both p8.91 and pMDG and 6µg of the respective pWPI plasmid (empty vector, $JAK2^{WT}$ or $JAK2^{V617F}$). The plasmids p8.91 and pMDG are the lentiviral packaging plasmid and vsv-g envelope plasmid, respectively, both of which are required for successful generation of human lentivirus particles. The p8.91 and pMDG plasmids used to generate lentiviruses described here were provided by Dr. Dimitris Lagos (University of York). Lipid/DNA complexes were incubated with HEK293T cells for 5hrs, after which they were removed and replaced with 10% (v/v) FBS/DMEM cell culture media.

Conditioned media containing the lentirvirus particles was collected and filtered through a 0.45µm syringe filter 48hrs post-transfection. The conditioned media was stored in autoclaved screw-cap Eppendorf tubes at -80^{o}C until use in transduction experiments. All reagents and cells used in lentivirus production were decontaminated with 10% (w/v) virkon solution.

4.2.5 Transduction of human primary cells

HUVECs and HAECs were seeded at 8x10^{4} cells per well in 6-well plates 24hrs before transduction. Viral supernatant aliquots were thawed in a 37^{o}C water bath and cells were prepared for transduction with 2 washes with 1XPBS and adding 10% (v/v) FBS/DMEM for a final volume of 2mL per well. The viral supernatant was then added to the cells and they were incubated at 37^{o}C/5% CO_2 for 6hrs. Viral supernatant volumes were varied to determine optimal transduction efficiency. Equal JAK2 protein expression was determined by western blot for volumes of 250µL of JAK2^{WT} virus and 2mL of JAK2^{V617F} virus. These volumes were used to generate protein lysate samples for the final JAK2 signalling analysis and RNA samples for RNA sequencing. Virus was removed after the 6hr incubation period and replaced with endothelial cell media. The cells were analysed for transduction efficiency 3 days post-transduction.

4.2.6 Spinfection of human primary cells

Cells were prepared according to a similar protocol described in 4.2.4, however just after the viral particles were added to the cells, the plates were centrifuged at 800*g* for 20mins at room temperature. The cells were then incubated at 37^{o}C/5%CO_2 for 6hrs, after which viruses were removed and the media was replaced with endothelial cell media. Cells were analysed for transduction efficiency 3 days post-transduction.

4.2.7 *In vitro* permeability assay

HUVECs were transduced with JAK2^{WT} and JAK2^{V617F} lentivirus as described in section 4.2.5. Cells were then plated on 12mm Transwell plates with 0.4µm pore polyester membrane inserts (Scientific Laboratory Supplies, Nottingham, UK) at a concentration of 5x10^{5} cells per well. Cells were incubated at 37^{o}C and 5%CO_2 for 3 days, to allow stable cell junctions to form. FITC-dextran (molecular weight of 10,000, Sigma) was prepared at 1mg/mL in HUVEC media (without phenol red). For the transwell, FITC-dextran media was prepared either with no treatment, or with

thrombin at 1U/mL (Enzyme Research Laboratories, IN, USA). Separately, HUVEC media (without phenol red and without FITC-dextran) was prepared with no treatment or with thrombin for the bottom well. Media was aspirated from the bottom well first, then transwell and treatment was added to the transwell first and then to the bottom well, to prevent disruption of the monolayer. 50µL samples were removed from the bottom well after 5 and 15mins of treatment and analysed using the BMG Polarstar Optima fluorescent plate reader (BMG Labtech). Serial dilutions of FITC-dextran alone were used as standard solutions. Blank values were subtracted from fluorescent measurements and each measurement was normalised to a 1:32 dilution of FITC-dextran standard solution (prepared on day of assay). These values were then converted to percent fluorescence. Each well was washed 1 time with 1XPBS and stained with cresyl violet solution (Sigma) for 10mins at room temperature. Stain was removed, transwells were washed 1 time with 1XPBS and images of the transwells were captured immediately using the Olympus CKX41 microscope and digital camera. An identical plating and treatment procedure was followed for plating out cells on tissue culture plastic. These cells were imaged to compare monolayers of cells on plastic to cells on the transwell membrane.

4.2.8 Infusion cloning

Lentiviral plasmids containing V5-tagged JAK2 constructs were generated using the In-Fusion HD Cloning kit (Clontech). Linearized vector of pWPI was generated by restriction enzyme digest using *Mlu*I and *Spe*I. The insert was amplified from the pEF1/HisA plasmid using primers designed by the online Primer Design Tool (Clontech, Table 4.5). Digested vector and insert amplicons were resolved on 0.6% (w/v) agarose/TAE gels stained with SYBR Safe DNA gel stain (Invitrogen). Fragments of the correct size (~11kb for vector and ~3.5kb for insert) were excised and gel purified using the QIAquick gel extraction kit (Qiagen). In-Fusion reaction mixtures were prepared (Table 4.5) and incubated at 50^{o}C for 15mins. The newly generated constructs were transformed into Stellar competent cells according to the manufacturer's protocol (Clontech, Figure 4.6). Colonies were screened by colony PCR and sequencing as described previously.

Table 4.5 Infusion Cloning: Primers, PCR Reaction Setup,* Cycling Parameters* and Infusion Reaction.*

*Adapted from Clontech

Insert	Vector	Primers	Tm (°C)	Annealing Temperature (° C)	Amplicon (kb)
pEF1/HisA	pWPI	F-5'-TGGATCCATCACGCGATGGGAATGGCCTGCCTT-3'	69.7	55	~3.5
		R-5'-CCCGTAGTTTACTAGTCAATGGTGATGGTGATGAT-3'	61.7		

Reagent	Volume (µL)	Final Conentration
HiFi PCR Premic	12.5	1X
FOR Primer	1	0.2µM
REV Primer	1	0.2µM
Template	1	80ng
dH2O	9.5	
	25µL total	
Primers	5µM working concentration	
DNA	80ng/µL	

Cycle number	Temperature (° C)	Time
35	98	10 seconds
	55	15 seconds
	72	15 seconds

Component	Final amount	WT volume (µL)	V617F Volume (µL)
5X In-Fusion HD Enzyme Premix	1X	2	2
Linearized Vector	50ng	3.7	3.7
Purified PCR Amplicon	200ng	2.6	3.4
dH2O		1.7	0.9
		10µL total	10µL total
pWPI linearized vector	13.6ng/µL		
V5 WT JAK2 insert	78.2ng/µL		
V5 V617F JAK2 insert	59ng/µL		

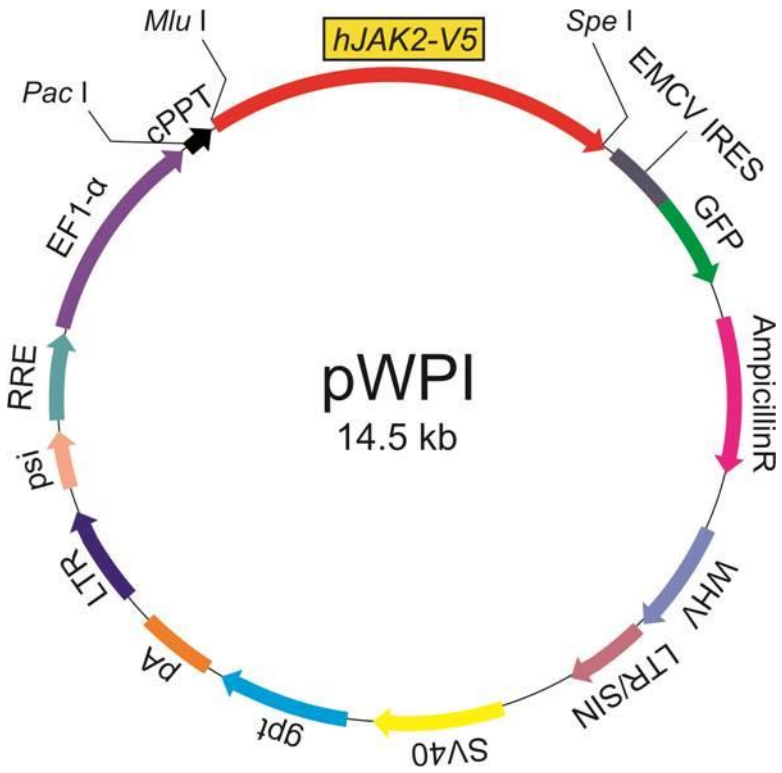

Figure 4.6 pWPI vector with V5-JAK2 insert
Lentiviral plasmid containing V5-tagged *JAK2* constructs. *JAK2^{WT}-V5* and *JAK2^{V617F}-V5* were amplified from *pEF1/HisA* vectors and inserted into *pWPI* using Infusion cloning.

4.2.9 Co-immunoprecipitation

Two methods of immunoprecipitation were tested: V5-antibody (Invitrogen)/agarose A beads (Millipore) and V5-tagged beads (QED Bioscience). Protein lysates were generated (as described in section 2.2.1) from HUVECs transduced with V5-tagged JAK2 constructs and biotinylation of cell surface proteins was performed in half the samples to aid in identification of these proteins after IP. Lysates were aliquoted into 100μg aliquots, the amount used in each IP experiment. Lysates were pre-cleared with goat IgG antibody (Sigma) for 30mins and with agarose A beads for an additional hour. Pre-cleared lysate was collected and samples that required antibody incubation were incubated with 2μg of V5-antibody overnight. The following day, these samples were collected and incubated with agarose A beads for an additional 3hrs. Simultaneously, pre-cleared lysate was added directly to V5-tagged beads and incubated in the same manner. All incubation steps were carried out by end-to-end rotation at 4^{o}C. Samples were then collected, washed 4 times with 1% (v/v) Triton X-100 and eluted using 30μL 1X SDS loading buffer (50mMM tris-HCl pH 6.8, 2% [w/v] SDS, 11.5% [v/v] glycerol, 25mM EDTA pH 8) for 10mins at 37^{o}C. A 4μL aliquot of each eluted sample was used to detect V5 expression in eluted sample by western blot, 26μL was resolved by NuPAGE and stained with either Sypro Ruby or Coomassie gel stains.

4.2.10 Sypro Ruby gel staining

NuPAGE gels were fixed for 30mins in a solution of 10% (v/v) methanol/7% (v/v) acetic acid. Sypro Ruby stain was then added to the gel and incubated on an orbital shaker for 3hrs, protected from light (Molecular Probes). The gel was transferred to a clean dish and washed in 10% (v/v) methanol/7% (v/v) acetic acid for an additional 30mins. The stained gel was visualised using ultraviolet light (Syngene Bio Imaging System).

4.2.11 Coomassie gel staining

The NuPAGE gel was washed briefly with distilled water and then incubated with coomassie stain for 1hr at room temperature (Bio-Rad). The gel was then de-stained by 2 quick distilled water washes and then overnight in distilled water with gentle

rocking. Samples were excised from the gel and sent to the Proteomics Core Facility (University of York) for further processing.

4.2.12 Liquid chromatography-mass spectrometry (LC-MS)

Lysates generated for LC-MS were crosslinked with dithiobis (succinimidylpropionate) (DSP) crosslinking reagent for 30mins at room termperature on a platform rocker. The cells were washed 3 times with 1XPBS and lysed as described previously. V5-tagged $JAK2^{WT}$ and V5-empty vector HUVEC samples were immunoprecipitated, resolved on a NuPAGE gel, visualised by Coomassie staining and excised as described in 4.2.10. LC-MS was then performed on these samples by Adam Dowle of the Proteomics Core Facility (University of York). Spectra generated from these samples were compared against the human subset of the UniProt database and matches were filtered using Mascot Percolator to minimise false positives.

4.2.13 RNA sequencing

RNA was generated using the RNeasy kit according to the protocol described by the manufacturer (Qiagen). Purification of RNA by $PolyA^+$ enrichment and library preparation were completed by Dr. Sally James of the Genomic Core Facility (University of York). The samples were sequenced by the HiSeq 3000 machine (University of Leeds).

Raw data was collated and analysed by Dr. Sandy Macdonald of Bioinformatics (University of York). Briefly, STAR splice-aware read mapper (https://github.com/alexdobin/STAR) was used to map sequencing reads to GRCh38 Gencode 24 version of the human genome (STAR). Reads were mapped using the following options: "—outSAMstrandField intronMotif", "—ourFilterType BySJout", "—outFilterIntronMotifs RemoveNoncanonical" and "—outSAMtype BAM SortedByCoordinate". Quantification and differential expression analysis were completed using Cufflinks software (http://cole-trapnell-lab.github.io/cufflinks/).

4.3 Results

4.3.1 Transient expression of JAK2^{V617F} in endothelial cells results in sustained JAK2 activation

Effects of JAK2^{V617F} expression in endothelial cells were first investigated by transient overexpression of the mutant and WT constructs in HUVECs. Transfecting HUVECs with equal amounts of either JAK2^{WT} or JAK2^{V617F} DNA resulted in different levels of JAK2 overexpression; it appeared that the JAK2^{WT} expression was increased compared to JAK2^{V617F} expression. After empirical testing of various DNA concentrations, transfection efficiencies were equalised by transfecting HUVECs with WT and mutant constructs in a 1:2 ratio. These results were confirmed by western blot detection of the V5 tag (Figure 4.7). The membrane was then re-probed for pJAK2, which was detected only in JAK2^{V617F} expressing cells (Figure 4.7). These results established that JAK2 can be overexpressed in endothelial primary cells and that mutant JAK2 expression results in sustained JAK2 activation.

4.3.2 Lentiviral transduction of JAK2^{V617F} in endothelial cells is less efficient compared to transduction of JAK2^{WT} in endothelial cells

Expression of V5-JAK2 in lipid-transfected HUVECs was short-lasting; V5 was detected at 24hrs post-transfection but lost after 48hrs. To generate stable expression of JAK2 in HUVECS, lentiviruses were produced to transduce HUVECs and HAECs. Cells were analysed for GFP expression 3 days post-transduction by flow cytometry (Figure 4.8). Empty vector lentivirus particles were highly efficient at transduction even at low volumes. WT lentivirus particles exhibited a steady increase in transduction efficiency with increase in viral supernatant and mutant lentivirus particles were the least effective in transducing HUVECs, showing little improvement in transduction efficiency even at high volumes (Figure 4.9). RNA and protein expression analyses confirmed the flow cytometry results (Figure 10A-B). RNA expression of JAK2 was high in all WT transduced samples and low in all JAK2^{V617F} transduced samples (Figure 4.10A). Similarly, JAK2 protein expression increased according to increases in viral volume used in transduction of WT samples but remained low in JAK2^{V617F} samples at all viral volumes (Figure 4.10B).

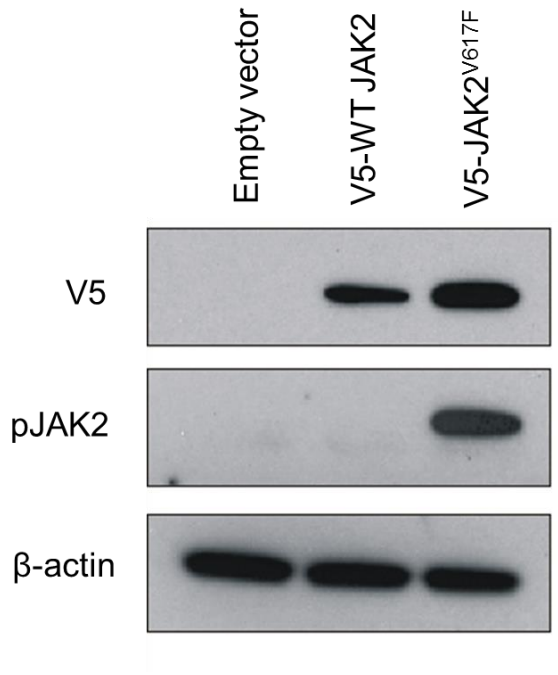

Figure 4.7 Transient overexpression of V5-tagged JAK2 constructs
HUVECs at passage 4 were transfected with V5-tagged JAK2 constructs using Lipofectamine LTX. Protein lysate was collected 24 hours post-transfection and analysed by western blot. V5 expression was equalised between $JAK2^{WT}$ and $JAK2^{V617F}$ samples using a 1:2 ratio of DNA during transfection. pJAK2 was sustained in the $JAK2^{V617F}$ sample, but was not detected in the $JAK2^{WT}$ sample.

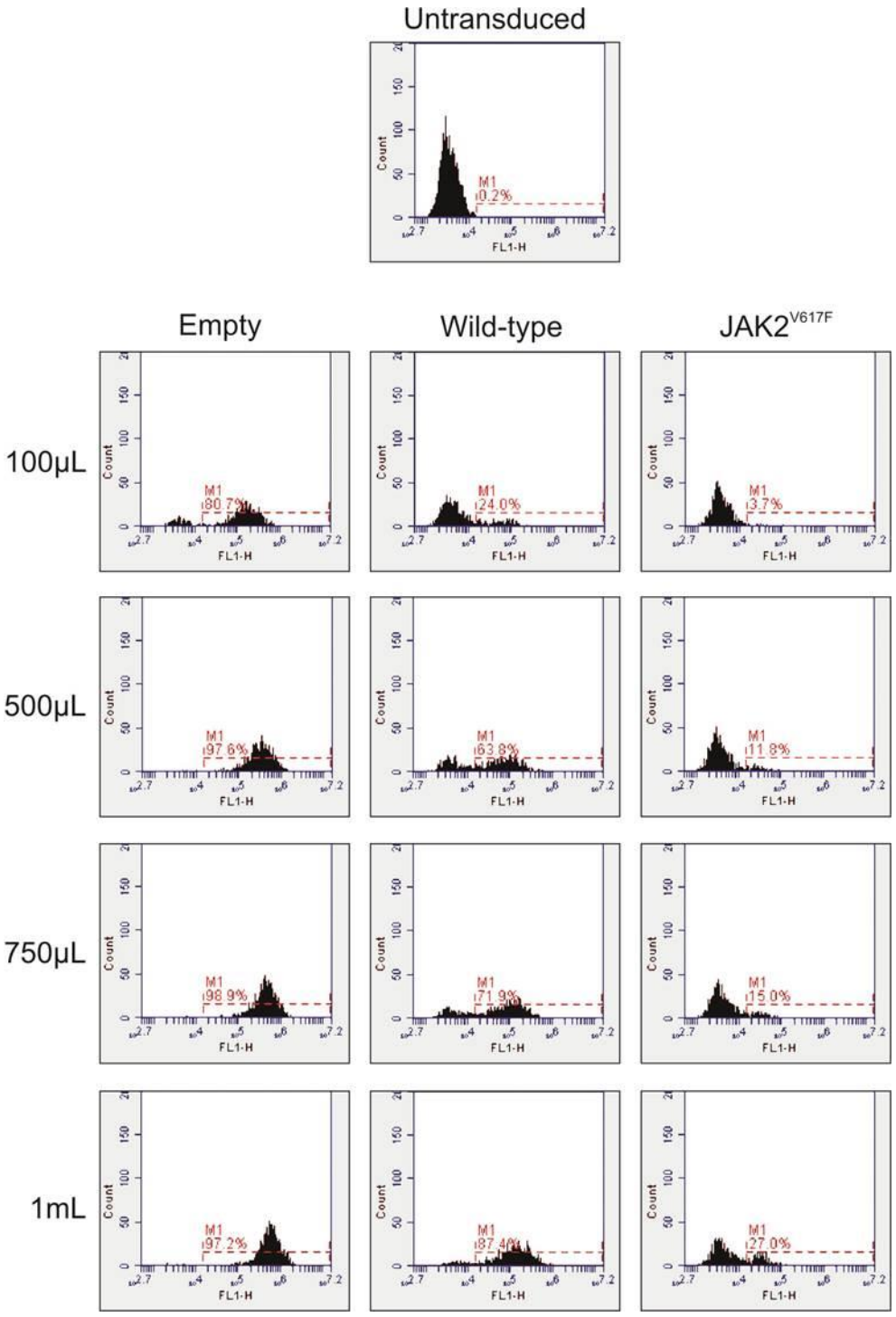

Figure 4.8 Flow cytometry analysis of GFP expression in lenti-transduced cells
HUVECs were transduced with different volumes of viral supernatant and were analysed for GFP expression 3 days post-transduction. Transduction with empty virus showed high GFP expression at all volumes. Transduction with $JAK2^{WT}$ virus increased with increasing volumes of virus. Transduction with $JAK2^{V617F}$ lentivirus also increased with increasing volumes of virus, however transduction efficiency was lower in each sample, compared to corresponding $JAK2^{WT}$ volumes.

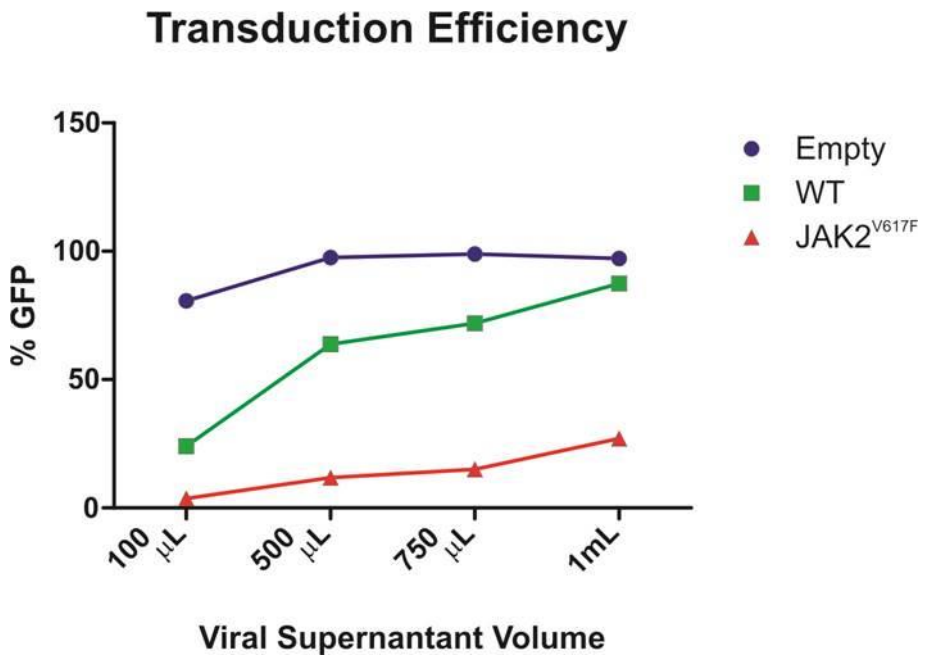

Figure 4.9 Transduction efficiency of JAK2-lentiviruses in HUVECs
Graphical representation of the differences in transduction efficiency of empty vector, $JAK2^{WT}$ and $JAK2^{V617F}$ lentiviruses. At all volumes tested, empty vector lentivirus samples had consistently high transduction efficiencies. Both $JAK2^{WT}$ and $JAK2^{V617F}$ viruses increased in transduction efficiencies with increasing volumes; $JAK2^{WT}$ had consistently higher transduction efficiencies at all viral volumes compared to $JAK2^{V617F}$ (n=1 for each sample).

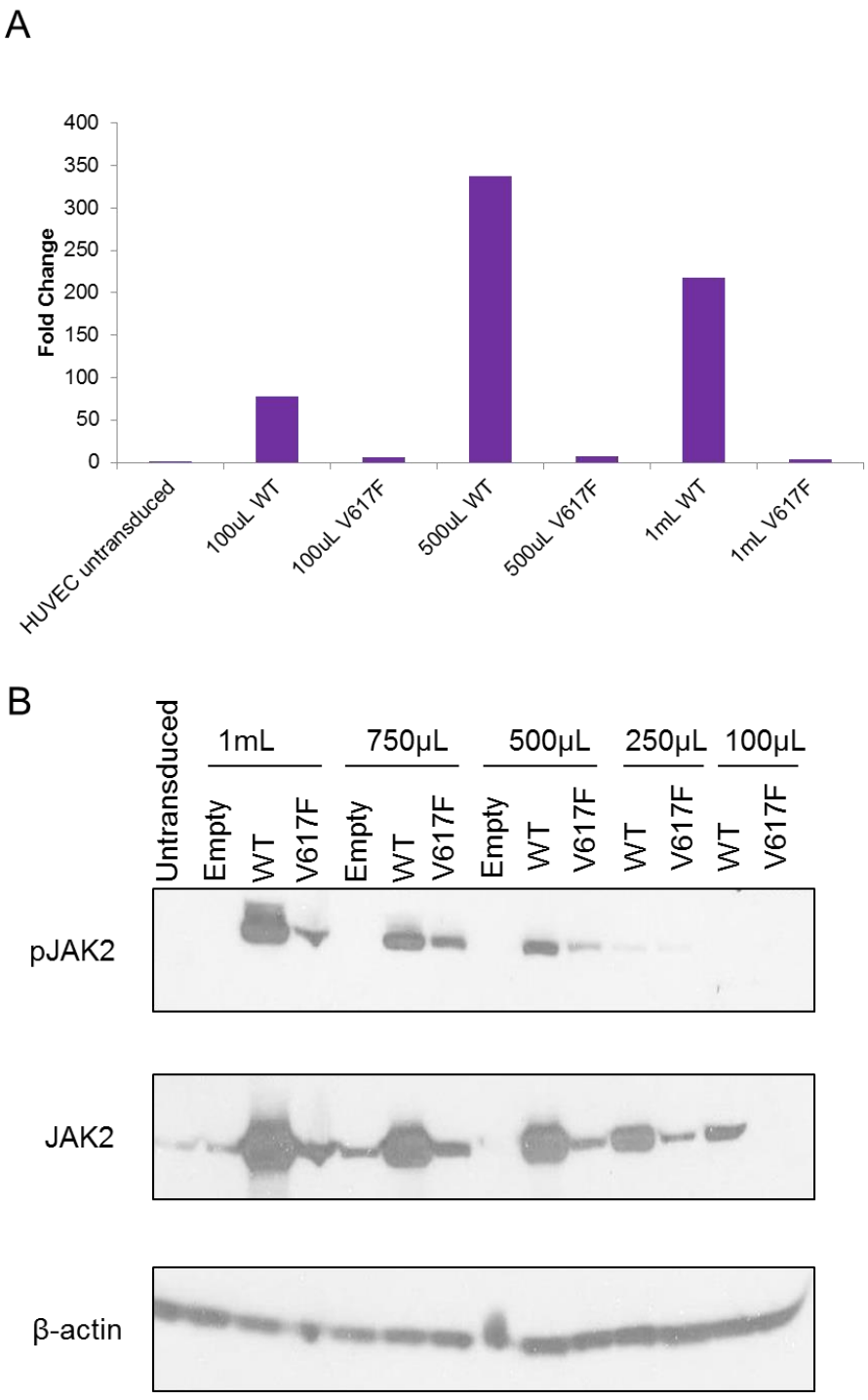

Figure 4.10 JAK2WT lentivirus has higher transduction efficiency in HUVECs when compared to JAK2V617F lentivirus

(A) RNA expression of JAK2 in $JAK2^{WT}$ and $JAK2^{V617F}$ transduced HUVECs, measured by qPCR. RNA expression of JAK2 is higher in $JAK2^{WT}$ samples compared to $JAK2^{V617F}$ samples at each volume tested. (B) Protein expression of pJAK2 and JAK2 in empty vector, $JAK2^{WT}$ and $JAK2^{V617F}$ transduced HUVECs, measured by western blot. Similar to RNA expression, protein expression of JAK2 is higher in $JAK2^{WT}$ samples compared to $JAK2^{V617F}$ samples at each volume (n=1 for each sample).

Spinfection did not appear to have any effect on transduction efficiency according to flow cytometry and western blot analyses (Figure 4.11A-B).

To overcome disparities between WT and mutant JAK2 transduction efficiencies, transduced HUVECs were sorted according to different levels of GFP expression. FACS was used to sort GFP-, GFP+low and GFP+high cell populations; collected protein from these sorted samples and expression of JAK2 and GFP were analysed by western blot (Figure 4.12). In WT transduced cells it appears that high GFP expression corresponds to high JAK2 expression and in both WT and mutant transduced cells a median GFP expression corresponds to a similar expression of JAK2 protein. Expression of GFP and corresponding JAK2 was seen in the GFP- population of empty, WT and mutant transduced cells. The reasons for this are unclear, but may be attributed to inefficient cell sorting. Importantly, it appears that despite $JAK2^{V617F}$ transduced cells having low GFP expression, as shown by flow cytometry and the GFP western blot, these cells still express JAK2 at a level that is comparable to their GFP expression by western.

4.3.3 Stable expression of $JAK2^{V617F}$ in endothelial cells results in sustained activation of JAK2 and STAT3 and increased expression of STAT1 *in vitro*

After employing several different strategies to improve transduction efficiency of mutant viral particles, viral volume optimisation was used to generate cells with equal JAK2 expression. Using this strategy, protein lysates of starved and unstarved transduced WT and mutant HUVECs were generated. General phospho-tyrosine immunoblotting suggested there may be an increase in activated signalling proteins in $JAK2^{V617F}$ cells that were not starved (Figure 4.13). To obtain a more clear understanding of signalling in these cells, starved WT and mutant HUVECs and HAECs were lysed for protein and analysed for activated JAK2 and STAT3 expression. In both primary cell types, active JAK2 and STAT3 was increased in $JAK2^{V617F}$ cells compared to $JAK2^{WT}$ cells whilst total JAK2 and STAT3 expression remained equal between samples (Figure 4.14). These results confirmed equalised JAK2 overexpression in $JAK2^{WT}$ and $JAK2^{V617F}$ samples and revealed that $JAK2^{V617F}$ expression results in sustained JAK2 signalling despite cell-starving conditions. Similar to JAK2 and STAT3, STAT1 activation was also sustained in

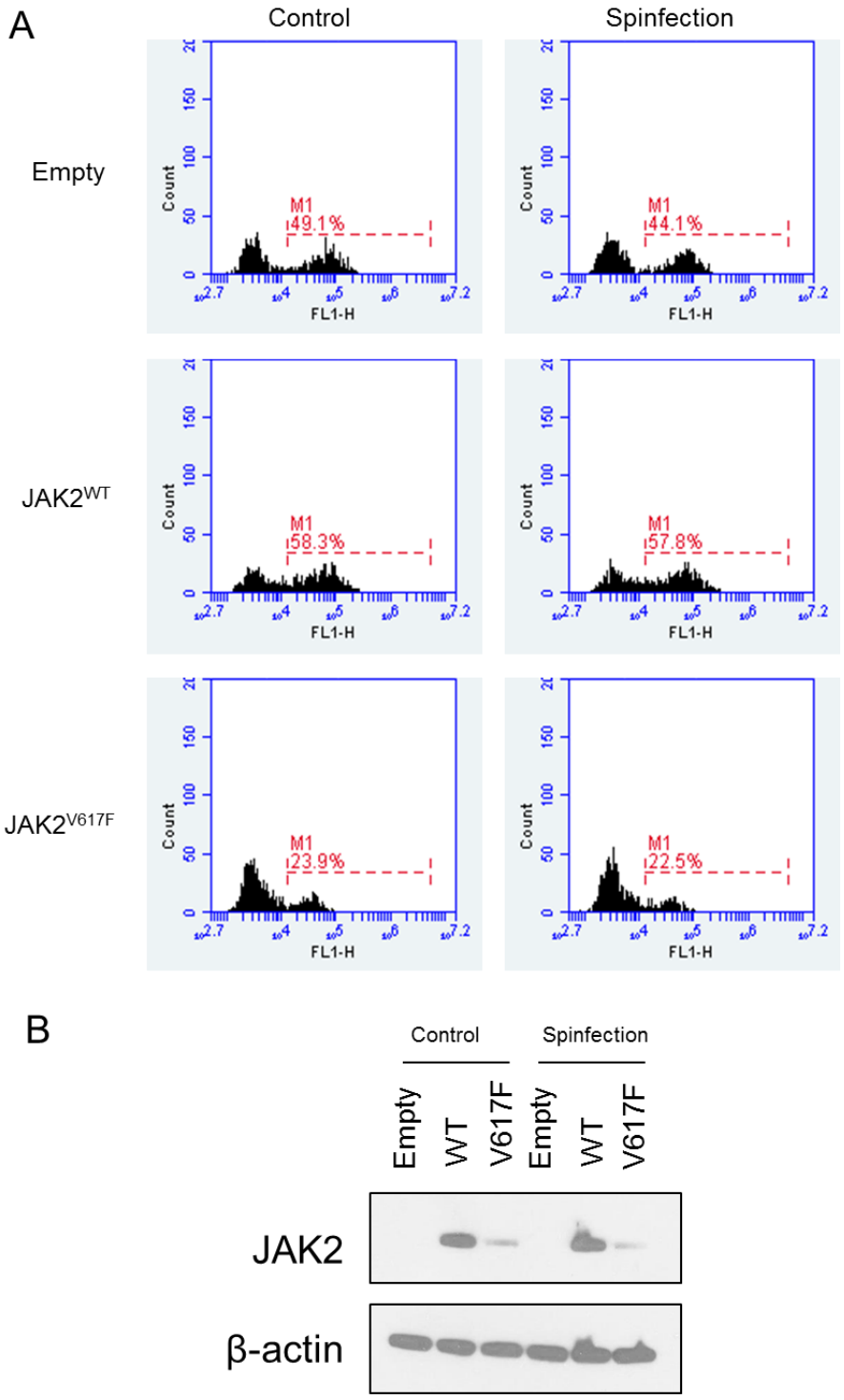

Figure 4.11 Spinfection of HUVECS with JAK2 lentiviruses
(A) Flow cytometry analysis of GFP expression 3 days post-transduction. Spinfection does not affect lentivirus transduction in empty vector, $JAK2^{WT}$ or $JAK2^{V617F}$ samples. (B) Western blot analysis of JAK2 expression 3 days post-transduction. Spinfection does not affect protein expression of JAK2 in $JAK2^{WT}$ or $JAK2^{V617F}$ samples (n=1 for each sample).

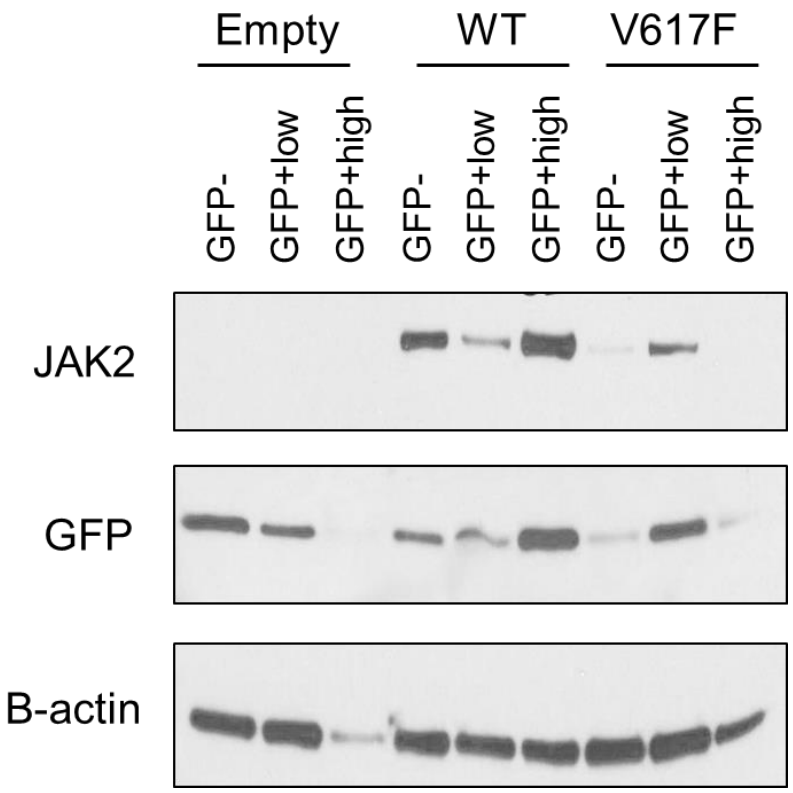

Figure 4.12 GFP expression and JAK2 expression analysis by western blot post-FACS

Transduced HUVECs were cell sorted by FACS according to level of GFP expression. GFP and JAK2 expression were analysed by western blot to determine if protein levels of these two proteins were similar in each sample. It does appear that an increase in GFP expression corresponds to an increase in JAK2 expression in $JAK2^{WT}$ samples. However, GFP expression in GFP- samples was present in empty vector, $JAK2^{WT}$ and $JAK2^{V617F}$ samples. It is unknown whether expression of GFP in these samples is caused by non-specific binding of GFP antibody or inefficient cell sort (n=1 for each sample).

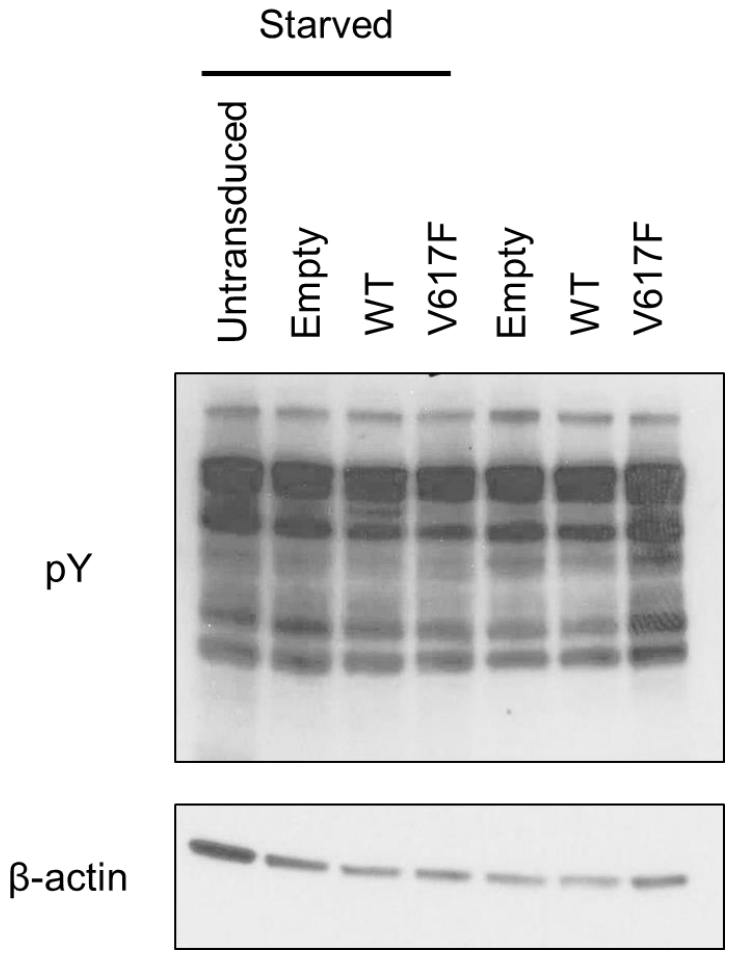

Figure 4.13 Phospho-tyrosine expression in transduced HUVECs
HUVEC lysates were generated from unstarved and starved cells transduced with empty vector, $JAK2^{WT}$ or $JAK2^{V617F}$. General phospho-tyrosine (pY) immunoblotting showed a slight increase in pY expression in $JAK2^{V617F}$-HUVECs which were unstarved.

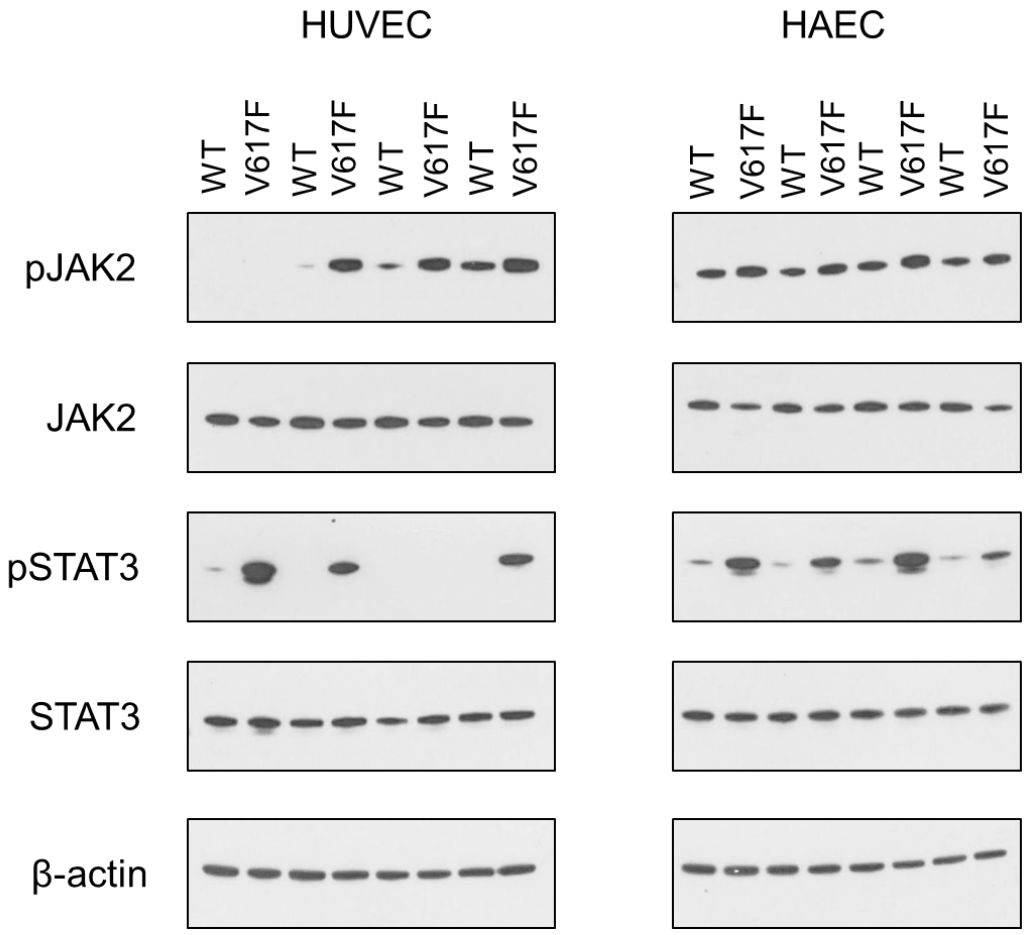

Figure 4.14 Western blot analysis of JAK/STAT signalling in transduced cells
HUVEC (left) and HAEC (right) lysates were generated from $JAK2^{WT}$ and $JAK2^{V617F}$ transduced cells. Cells were starved for 16hrs before protein was collected. JAK2 and STAT3 activation and expression were detected by immunoblotting for the phosphorylated and total proteins, respectively. It appears that activation of JAK2 and STAT3 are sustained in $JAK2^{V617F}$ samples, compared to $JAK2^{WT}$ samples despite total JAK2 and STAT3 expression remaining equal.

$JAK2^{V617F}$-expressing HUVECs (Figure 4.15A). However in contrast, total STAT1 was also increased in mutant cells compared to WT cells. These changes were quantified by densitometry and found to be significant (p=0.0003, Figure 4.15B).

4.3.4 $JAK2^{V617F}$ expression increases vascular permeability

Data show that $JAK2^{V617F}$ expression increases permeability of HUVECs in response to stimulation with thrombin at both 5 and 15min time points (Figure 4.16). At 5mins, mean (±SD) percent fluorescence values were 2.749 (±1.436) for $JAK2^{WT}$, 5.038 (±1.147) for $JAK2^{WT}$ + thrombin, 3.932 (±1.672) for $JAK2^{V617F}$ and 8.138 (±2.570) for $JAK2^{V617F}$ + thrombin. At 15mins, mean (±SD) percent fluorescent values were 3.779 (±1.364) for $JAK2^{WT}$, 6.909 (±1.748) for $JAK2^{WT}$ +thrombin, 6.425 (±3.013) for $JAK2^{V617F}$ and 13.83 (±5.747) for $JAK2^{V617F}$ + thrombin. Two-way ANOVA shows that both genotype and thrombin treatment significantly affect permeability in HUVECs.

Images of stained transwell monolayers post-treatment showed that permeability in both $JAK2^{WT}$ and $JAK2^{V617F}$ is increased in response to thrombin (Figure 4.17A). This increase appears to be greater in $JAK2^{V617F}$ HUVEC monolayers. Permeability was assessed by visualising gaps between cells clusters; however Monolayers were difficult to observe on the transwells. Cells plated and treated on plastic in parallel were also analysed (Figure 4.17B). In this figure, $JAK2^{WT}$ cells appear to have a cobblestone morphology which re-aligns in response to thrombin to introduce some gaps. $JAK2^{V617F}$ cells appear to be less uniform even before treatment. In response to treatment, $JAK2^{V617F}$ cells become more porous.

4.3.5 JAK2 immunoprecipitation (IP) is confirmed in V5-tagged $JAK2^{WT}$ samples, however binding partners remain unknown

JAK2 is known to bind to cytokine receptors which lack intrinsic kinase activity. However, it is not known which receptor JAK2 is binding in ECs, causing the signalling and gene expression changes described here. To identify potential binding partners, V5-tagged $JAK2^{WT}$ or $JAK2^{V617F}$ lentiviruses were used to transduce HUVECs and expression of V5-JAK2 was confirmed by western blot (Figure 4.18). Moreover, despite low levels of total JAK2 expression in $JAK2^{V617F}$ cells, pJAK2 is sustained in these samples (Figure 4.18). Similarly, pSTAT3

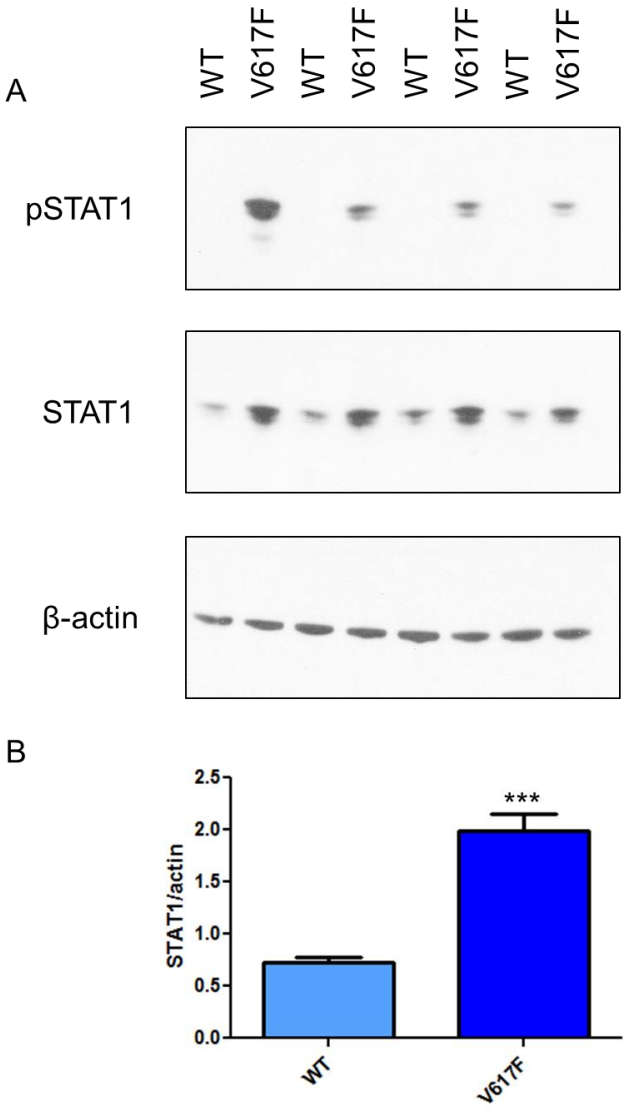

Figure 4.15 Activation and expression of STAT1 detected by western blot
(A) Both phosphorylated STAT1 and total STAT1 are increased in JAK2^{V617F}-transduced cells compared to JAK2^{WT}. (B) Quantification of total STAT1 normalised to actin confirms that STAT1 is increased in JAK2^{V617F} HUVECs (n=4, t test, ***p=0.0003).

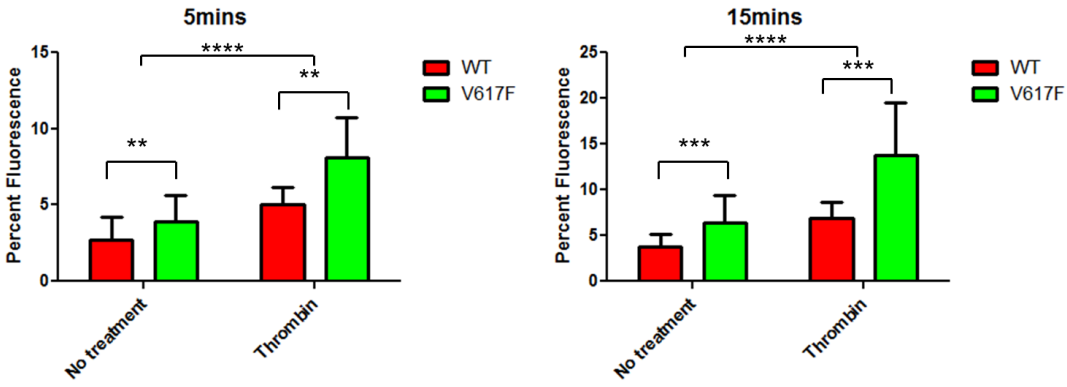

Figure 4.16 Vascular permeability is increased in JAK2V617F-HUVECs
Permeability was measured by percent fluorescence of the media underneath the transwell at 5 and 15mins post-thrombin stimulation. Thrombin increases permeability of both $JAK2^{WT}$ and $JAK2^{V617F}$ HUVECs, but permeability in $JAK2^{V617F}$ HUVECs is significantly greater compared to $JAK2^{WT}$ HUVECs in response to thrombin (Two-way ANOVA, **p<0.01, ***p<0.001, ****p<0.0001). Data were obtained from 3 separate experiments, with each sample type performed in triplicate during each experiment.

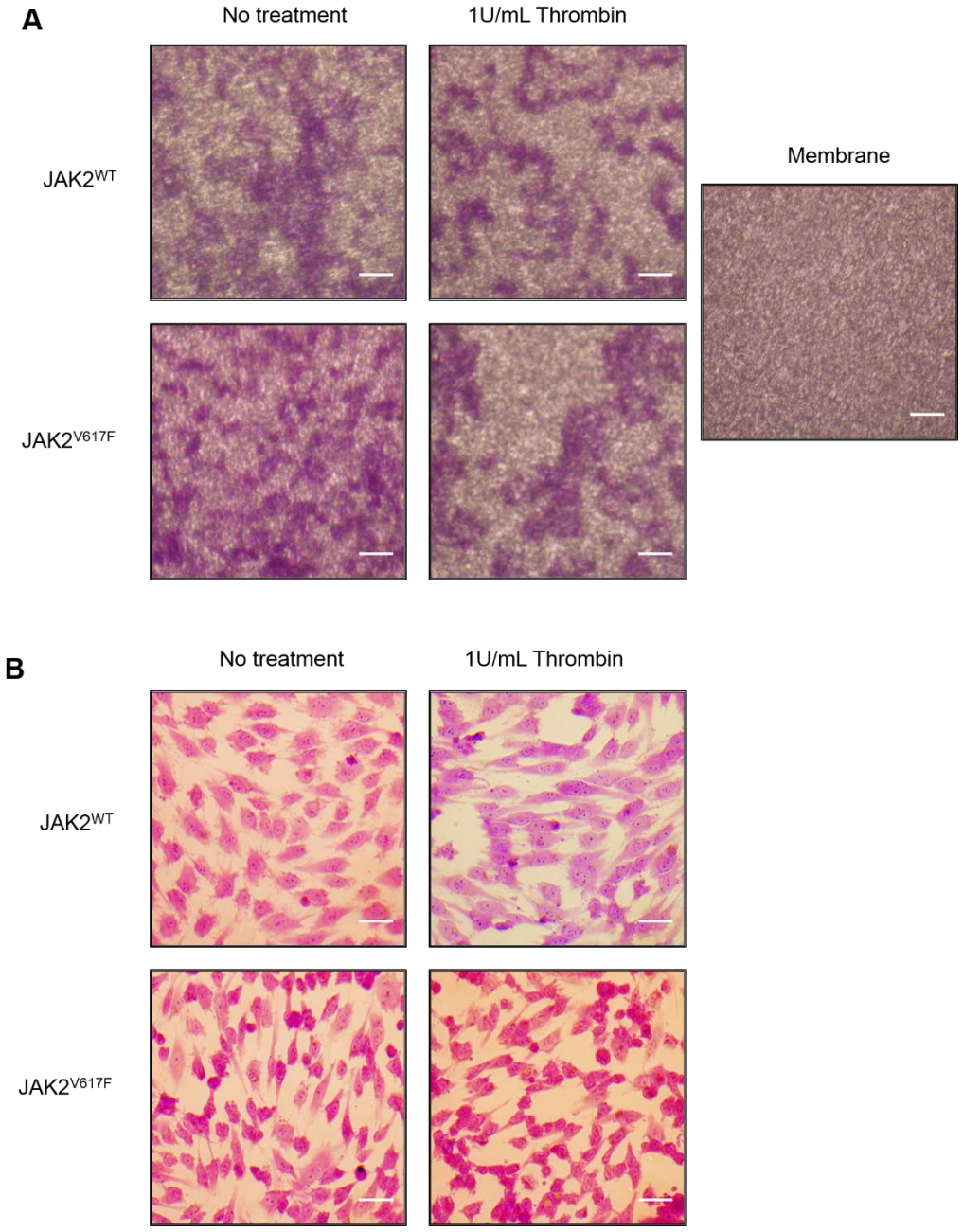

Figure 4.17 Analysis of permeability by cresyl violet staining and microscopy

(A) Cresyl violet staining of transwell membranes showed an increase in permeability of HUVECs in response to thrombin. JAK2^{V617F} expression enhanced permeability in response to thrombin. An image of a stained transwell membrane without cultured cells is shown for comparison. (B) Cresyl violet staining of HUVEC monolayers on tissue culture plastic showed realignment of cells in response to thrombin, introducing pores in the samples. JAK2^{V617F}-HUVECs appeared to have increased permeability in response to thrombin. Thrombin-treated samples were treated for 15mins prior to staining, n=1, 20X objective lens, scale bar=40µm.

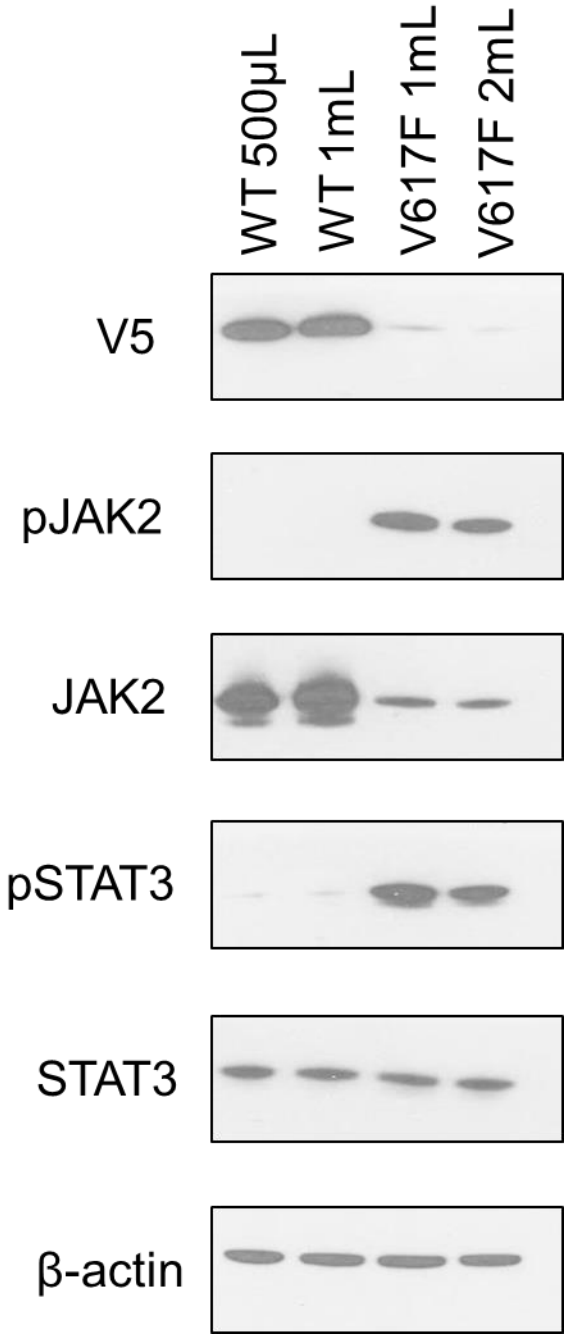

Figure 4.18 Western blot analysis of signalling differences between JAK2WT and JAK2V617F HUVECs transduced with V5-tagged JAK2 lentiviruses
Expression of V5 and JAK2 is increased in $JAK2^{WT}$ samples, compared to $JAK2^{V617F}$ samples at both virus volumes, however activated JAK2 and STAT3 is increased in $JAK2^{V617F}$. Total STAT3 remained unchanged in all samples (n=1 for each sample type).

expression is sustained in mutant JAK2 samples whilst total STAT3 remained equal between $JAK2^{WT}$ and $JAK2^{V617F}$ samples (Figure 4.18). These results corroborate the signalling observed in HUVECS transduced with the original untagged lentiviruses.

Both methods of IP successfully precipitated V5-JAK2; however precipitation with V5 beads eliminated elution of antibody heavy and light chains (Figure 4.19). Therefore, IP with V5 beads was determined to be optimal. Little JAK2 precipitated from $JAK2^{V617F}$ samples and it is unclear if this was due to poor transduction efficiency or poor immunoprecipitation, although western blot data does suggest that some $JAK2^{V617F}$ was precipitated. IP conditions were optimised and fresh, DSP-crosslinked protein was harvested from $JAK2^{WT}$ samples and immediately precipitated to minimise potential protein-protein interaction dissociation. Coomassie staining of IP samples confirmed protein precipitation in the WT sample (Figure 4.20A). Western blot analysis confirmed V5 pull down (Figure 4.20B). JAK2 precipitation was again confirmed by the LC-MS spectra which identified JAK2 in our V5- $JAK2^{WT}$ sample, but not in our control sample (Table 4.6). Unfortunately, JAK2 binding partners were not identified.

4.3.6 $JAK2^{V617F}$ expression leads to increased expression of chemokine ligand 2 (CCL2), CUB domain containing protein 1 (CDCP1) and tight junction protein 2 (TJP2)

To further investigate signalling and gene expression changes in mutant endothelial cells, RNA samples from HUVECs expressing $JAK2^{WT}$ and HUVECs expressing $JAK2^{V617F}$ were prepared for RNA sequencing. In total, 127 genes were significantly differentially expressed between the two groups (Figure 4.21). Functional interactions among these genes were investigated through the computer programme "String" (Figure 4.22). String shows that several genes are directly linked to JAK2 and several other genes are directly related to STAT1. Additionally, there is a cluster of type I interferon response-related genes in the centre. Increased RNA expression of CCL2 and TJP2, which are directly linked to JAK2 and STAT1, respectively and CDCP1 were confirmed by qPCR (Figure 4.23). These genes were selected for validation because all three genes have been reported to influence EC permeability.

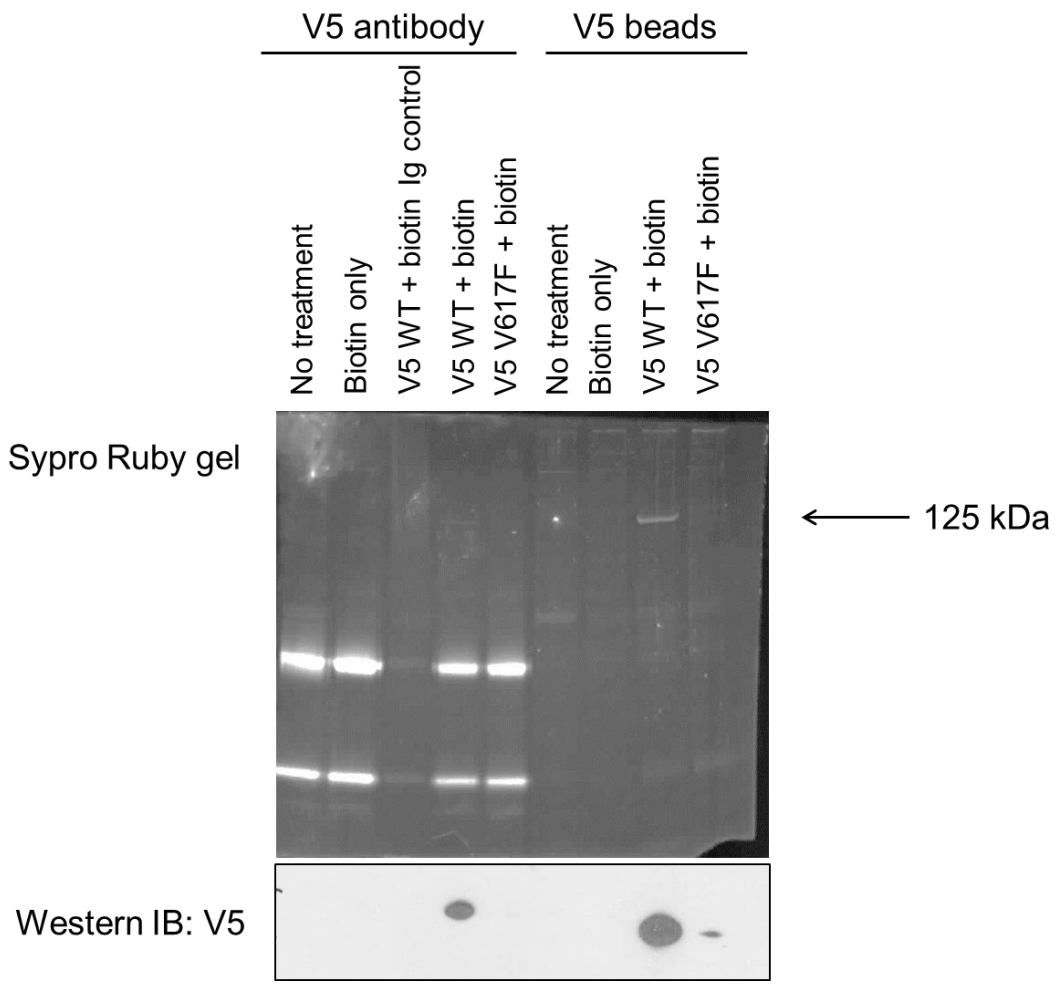

Figure 4.19 Immunoprecipitation optimisation of V5-tagged proteins
Sypro ruby stained gel (top) identifies a protein around 125kDa in the $JAK2^{WT}$ sample precipitated with V5-beads. Western blot (bottom) confirms pull down of V5-tagged JAK2 in $JAK2^{WT}$ and $JAK2^{V617F}$ samples precipitated with V5-beads and in $JAK2^{WT}$ precipitated with V5 antibody/agarose beads (n=1).

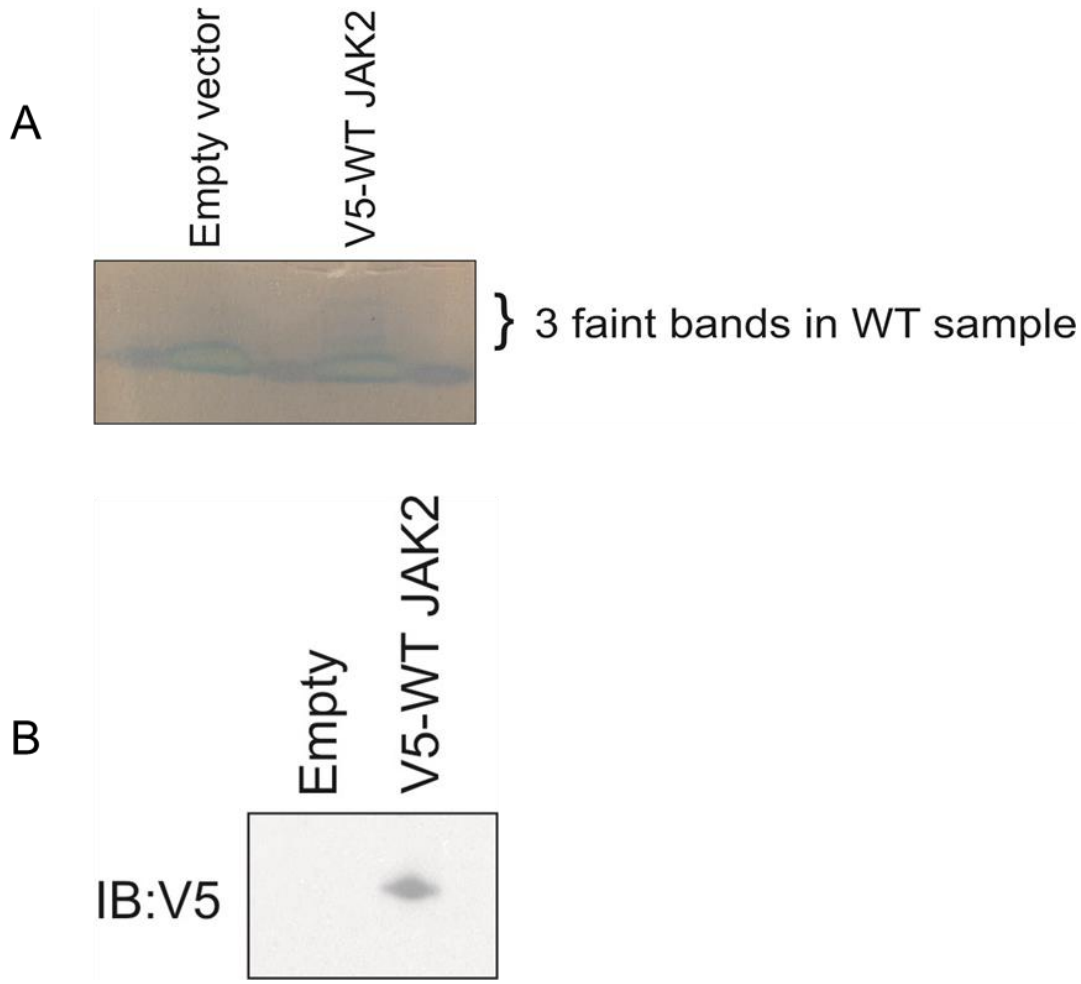

Figure 4.20 Immunoprecipitation of V5-tagged JAK2 for LC-MS
(A) Coomassie stained gel showing three faint protein bands in the V5-JAK2^{WT} sample that are absent in the control sample. (B) Western blot confirming V5 precipiation.

Table 4.6 LC-MS results

Protein	Control - Sequences	V5_WT Sequences	Control - Spectra	V5_WT - Spectra	Control DSP Mod	V5_WT DSP mod
Keratin, type II cytoskeletal 1 OS=Homo sapiens GN=KRT1 PE=1 SV=6 - P04264	9	12	16	16	0	0
Keratin, type I cytoskeletal 9 OS=Homo sapiens GN=KRT9 PE=1 SV=3 - P35527	8	11	10	11	0	0
Keratin, type II cytoskeletal 2 epidermal OS=Homo sapiens GN=KRT2 PE=1 SV=2 - P35908	8	11	10	12	0	0
Keratin, type I cytoskeletal 10 OS=Homo sapiens GN=KRT10 PE=1 SV=6 - P13645	11	10	13	12	0	0
Tyrosine-protein kinase JAK2 OS=Homo sapiens GN=JAK2 PE=1 SV=2 - O60674		9		11		2
Keratin, type I cytoskeletal 14 OS=Homo sapiens GN=KRT14 PE=1 SV=4 - P02533	7	4	7	4	0	0
Keratin, type II cytoskeletal 5 OS=Homo sapiens GN=KRT5 PE=1 SV=3 - P13647	4	4	5	4	0	0
Keratin, type II cytoskeletal 6B OS=Homo sapiens GN=KRT6B PE=1 SV=5 - P04259		4		4		0
Keratin, type I cytoskeletal 16 OS=Homo sapiens GN=KRT16 PE=1 SV=4 - P08779	4	3	4	3	0	0
Keratin, type II cytoskeletal 6A OS=Homo sapiens GN=KRT6A PE=1 SV=3 - P02538	4	3	5	3	0	0
Keratin, type I cytoskeletal 13 OS=Homo sapiens GN=KRT13 PE=1 SV=4 - P13646		2		2		0
Keratin, type II cytoskeletal 4 OS=Homo sapiens GN=KRT4 PE=1 SV=4 - P19013		2		3		0

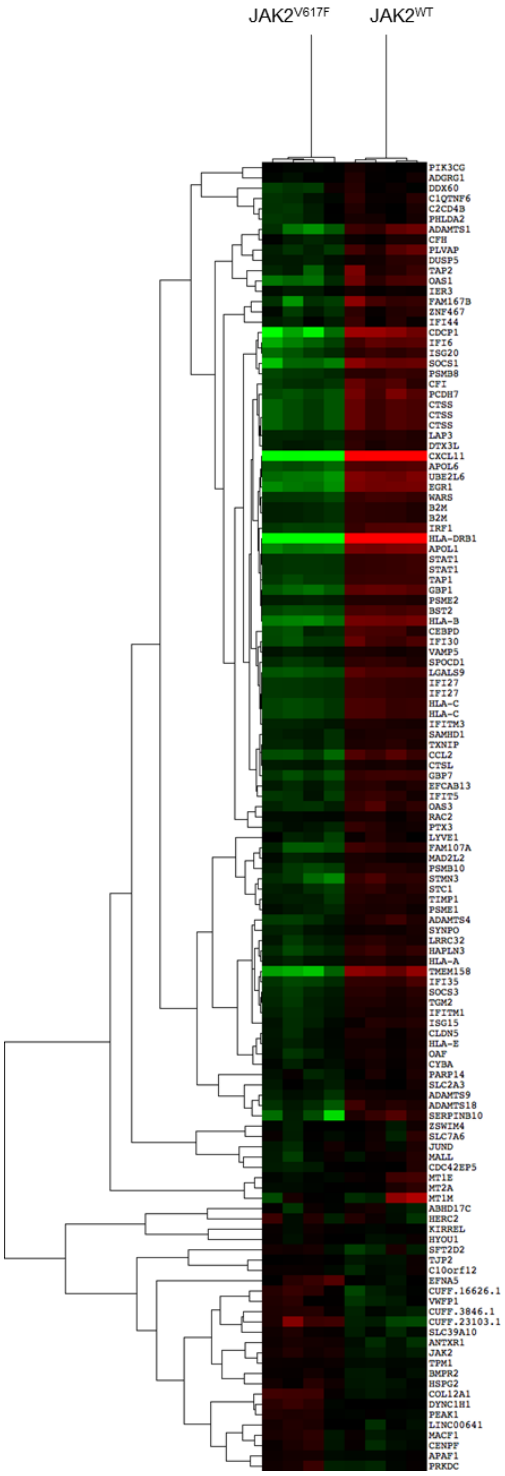

Figure 4.21 Transcriptional landscape of HUVECs expressing JAK2WT and JAK2V617F

Hierarchical clustering of genes which are co-regulated between $JAK2^{WT}$ and $JAK2^{V617F}$ HUVECs, where green represents gene upregulation and red represents gene downregulation. A total of 127 genes were significantly differentially expressed between $JAK2^{WT}$ and $JAK2^{V617F}$ samples.

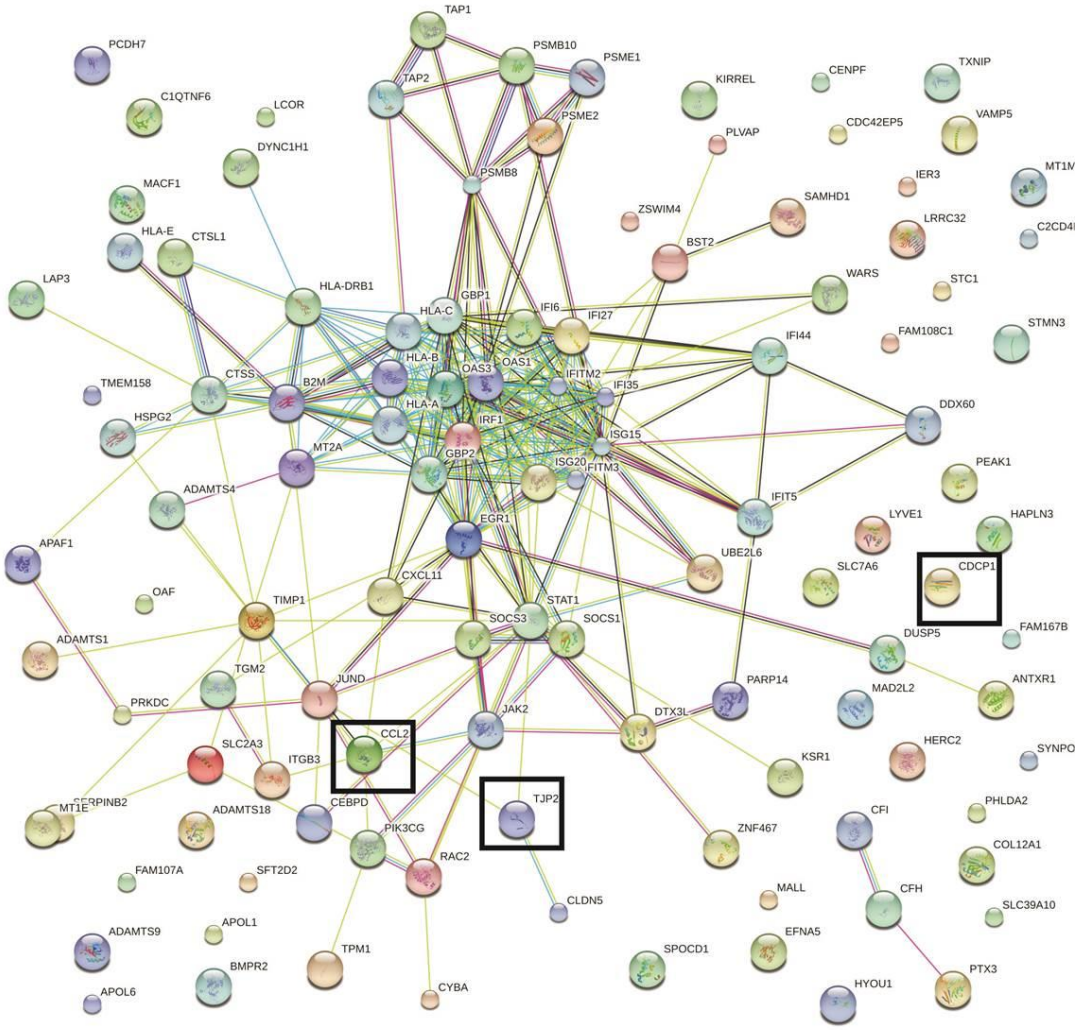

Figure 4.22 String diagram of genes that are significantly differentially expressed between JAK2WT and JAK2V617F HUVEC samples

String diagram showing functional relationships between target genes in RNA sequencing, where connecting lines between genes represents a known interaction or gene relation. There is a cluster of genes centred in the middle of the diagram, which all appear to be related to IFN-signalling. CCL2, TJP2 and CDCP1 were chosen for validation (boxed). CCL2 is related to both JAK2 and STAT1, TJP2 is related to STAT1 and CDCP1 is unrelated to JAK2 and STAT1.

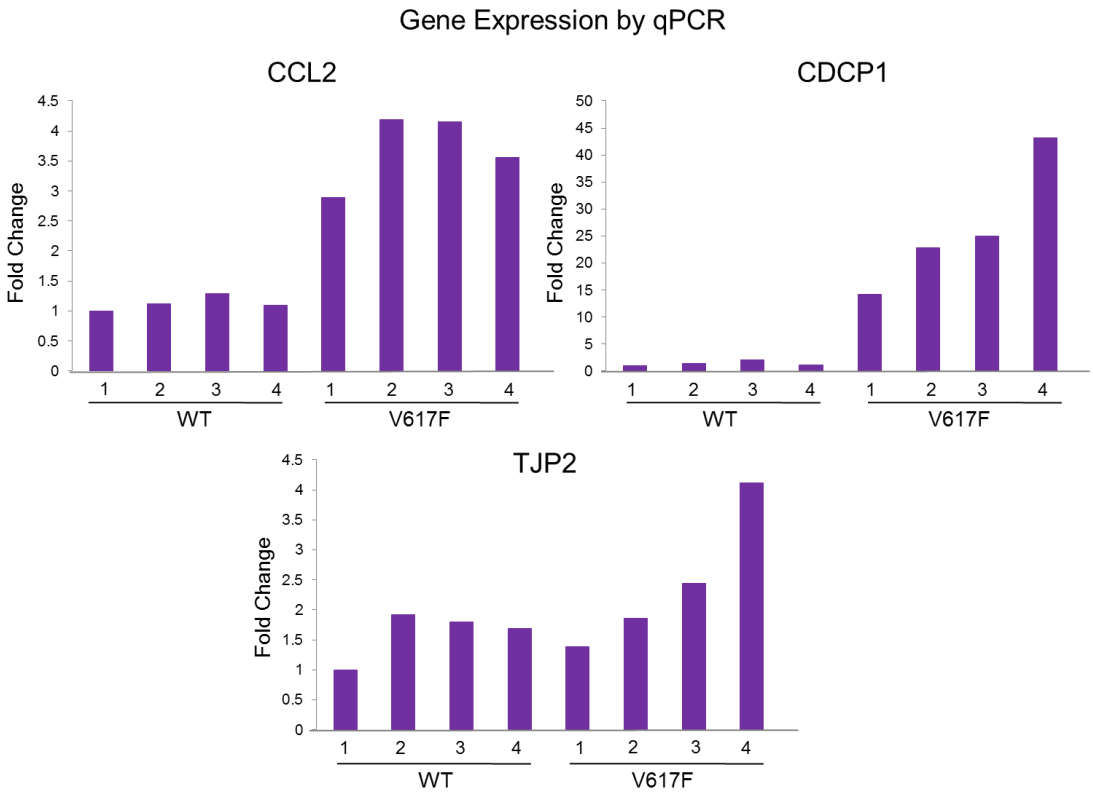

Figure 4.23 qPCR validation of RNA sequencing targets
CCL2, CDCP1 and TJP2 were chosen to validate RNA sequencing results. All three genes are upregulated in JAK2^{V617F}-HUVECs compared to JAK2^{WT}-HUVECs.

4.4 Discussion

The role of JAK2 in the development of the haematopoietic system has been studied extensively and it is known that JAK2 is indispensable for haematopoiesis. Equally, hyperactive JAK2 in MPNs is responsible for disease development in the majority of patients. Endothelial JAK2 has not been studied as extensively, but evidence suggests its role in this cell type is equally important, promoting proper endothelial cell function. Previous data from the lab has shown that $JAK2^{V617F}$ in ECs causes a dysfunctional response to vessel injur, however it is unclear what is causing these defects. Here, an *in vitro* system for studying $JAK2^{WT}$ and $JAK2^{V617F}$ in primary human endothelial cells was established, with the aim of deciphering mechanisms for $JAK2^{V617F}$-endothelial dysfunction.

Generating $JAK2^{V617F}$ expression in ECs was challenging compared to overexpression of the WT construct. During initial transient JAK2 overexpression experiments in HUVECs it appeared that $JAK2^{WT}$ expression was greater than $JAK2^{V617F}$ expression using similar DNA amounts in transfection. Similar observations were made using lentivirus to overexpress JAK2 stably. In both systems, different plasmids and different techniques were used, yet the same difficulty of equalising total JAK2 expression among $JAK2^{WT}$ and $JAK2^{V617F}$ samples existed. Again, when the V5-tagged $JAK2^{WT}$ and $JAK2^{V617F}$ constructs were cloned into the lentiviral vector pWPI, viruses produced showed disparate transduction efficiencies. Data suggests that low expression of $JAK2^{V617F}$ compared to $JAK2^{WT}$ is not attributed to protein turnover in the mutant samples because RNA expression is also low in $JAK2^{V617F}$ samples compared to $JAK2^{WT}$. Copy number integration was not determined, however previous reports suggest that copy number can be related to transduction efficiency, with an integration of one vector copy corresponding to ~30% transduction efficiency.[232] Once transduction conditions had been optimised, transduction experiments were performed using 250μL of $JAK2^{WT}$ and 2mL of $JAK2^{V617F}$ lentivirus. These volumes result in ~30% transduction efficiency, suggesting that copy number integration in these cells is around 1. Importantly, protein expression of JAK2 in both samples produced using these virus volumes was equal, yet activation of JAK2 and the downstream signalling molecule STAT3 were sustained in $JAK2^{V617F}$ samples in starving conditions. These results suggest that

JAK2 is hyperactive in cells expressing $JAK2^{V617F}$ compared to cells expressing $JAK2^{WT}$, similar to the signalling effects of $JAK2^{V617F}$ in haematopoietic cells.

Another signalling difference worth noting is the effect of $JAK2^{V617F}$ on STAT1 expression. In addition to sustained STAT1 activation, total STAT1 protein and RNA expression was increased in $JAK2^{V617F}$ samples compared to $JAK2^{WT}$. STAT proteins are known to homo and heterodimerise with each other, translocate to the nucleus and exert changes in gene expression. It is unclear at the present time how this increase in total STAT1 expression in $JAK2^{V617F}$ ECs affects the downstream gene expression patterns. There are certainly STAT-specific roles in gene expression and STAT1 in particular has been associated with the interferon response in immune reactions and pro-apoptotic response in tumour cells.[233,234] JAK2-STAT1 signalling may also have a role in inflammation in general and one consequence of inflammation in ECs is increased permeability. *In vitro*, permeability of HUVECs was increased in response to the agonist thrombin and this increase was enhanced in cells which express $JAK2^{V617F}$. Increased permeability is a necessary effect during the first stage of wound healing, however if this permeability is increased or sustained other functions of ECs may be impaired. Further investigations into the roles of mutant JAK2 and STAT1 expression in ECs will elucidate the extent to which these proteins cause the increase in permeability seen in HUVECs and may define additional effects for these proteins in ECs.

Ideally, identifying the receptor mutant JAK2 is associating with in ECs would further help determine signalling and gene expression changes in this cell type. Although attempts at identifying this receptor were unsuccessful, there are many plausible candidate receptors. Several involve a co-receptor, gp130, which is known to bind JAK2 and elicit JAK/STAT signalling. In ECs, soluble IL6/IL6R can bind to gp130 and cause transignalling.[235,236] Gp130 also acts as a co-receptor for other signalling molecules including leukaemia inhibitory factor receptor (LIFR), oncostatin M receptor (OSMR), and interleukin-27 receptor (WSX1). Separately, G-protein coupled receptors can also use JAK2 signalling to elicit changes in gene expression.[237] These candidates are all possible binding partners for mutant JAK2 and further research is needed to determine which receptor should be the primary target in this context, perhaps a receptor which signals mainly through STAT1.

The interferon response in endothelial cells is another signalling system that requires investigation. In the RNA sequence analysis, genes related to IFN-α/β signalling appeared in the cluster centred in the middle of the String diagram. These results were initially puzzling, because IFN-α/β are known to elicit their effects through JAK1 and TYK2, whereas IFN-γ responses are through JAK2. However, it has been documented that IFN-α/β and IFN-γ can crosstalk through the regulation of downstream signalling proteins.[238] It is not clear whether similar crosstalk signalling is occurring in this system, however it is clear that genes related to interferon signalling and inflammation are universally upregulated in $JAK2^{V617F}$ samples compared to $JAK2^{WT}$, which suggests a pro-inflammatory phenotype in $JAK2^{V617F}$-endothelial cells.

Inflammation and haemostasis are unique but related processes; mechanisms contributing towards inflammation affect the haemostatic balance and similarly, haemostatic factors influence the inflammatory response. IFN-γ stimulates EC expression of VCAM-1 and ICAM-1, which facilitates leukocyte and platelet adhesion to the EC surface.[239] Mouse models for atherosclerosis demonstrate that IFN-γ treatment increases the size of atherosclerotic lesions through enhanced recruitment and incorporation of lymphocytes.[240] Atherosclerosis and underlying endothelial dysfunction is also associated with the autoimmune disease systemic lupus erythematosus (SLE). Moreover, patients with SLE had fewer EPCs in circulation and differentiation of EPCs to mature ECs in culture was reduced. IFN-α was shown to promote EPC dysfunction by inhibiting angiogenesis and inducing apoptosis.[241] The EPC phenotype observed in patients with SLE could be reversed when the type I interferon response was neutralised. These findings support the role of the interferon response in promoting thrombosis and endothelial dysfunction.

Chronic inflammation in patients with MPNs is a current research theme. The role of inflammation in atherosclerosis development is widely accepted and more recently the effects of inflammation on MPN clonal development is beginning to be appreciated. The inflammatory cytokine lipocalin-2 (LCN2) has a role in ROS production and DNA damage.[242] Treatment of mesenchymal stem cells with LCN2 promoted the generation of osteoblasts, matrix proteins and angiogenesis, resembling the manifestation of myelofibrosis. TNF-α production was increased in $JAK2^{V617F}$-positive cells, which promoted the clonal evolution of MPN disease progression by

selecting for malignant cells that were resistant to TNF-α.[243] This study alludes to the importance of inflammatory mediators in both disease initiation and clonal evolution. LCN-2 and TNF-α have both been reported to be elevated in patients with MPNs.[120,242]

CCR2/JAK2 signalling in endothelial cells was reported to mediate vascular permeability in the context of tumour cell extravasation.[244] The role of EC permeability in mediating the first stages of wound healing was an attractive area to investigate, given the dysfunctional wound healing phenotype in MPN mouse model described in Chapter 3. A more recent study identified STAT3 activation in response to CCL2 signalling in cancer fibroblasts leading to an inflammatory phenotype.[245] The link between JAK2/STAT3 signalling and CCL2 signalling was interesting because of the importance of chemokine signalling in vascular permeability and inflammation. The physiological role of CCL2 is monocyte recruitment to injured vessels and this recruitment has also been reported during the development of atherosclerotic lesions.[246] Moreover, CCL2 stimulated the release of tissue factor from smooth muscle cells, contributing to the thrombotic complications manifested in atherosclerotic disease.[247] These data implicate CCL2 in endothelial biology, atherosclerosis pathology and thrombotic disease. On receipt of the RNA sequencing data, two chemokine ligands were upregulated in JAK2^{V617F} and one was CCL2. Increased expression of CCL2 was then confirmed in JAK2^{V617F} HUVEC RNA samples by qPCR.

TJP2 and CDCP1 were targets that first identified as having a potential role in JAK2^{V617F}-endothelial phenotype through the RNA sequencing analysis. TJP2 became immediately attractive as a target because of its known role in endothelial permeability and cell-cell interactions.[248] TJP2 function may go beyond the endothelial cell and function in vascular biology as a whole: in vascular smooth muscle, STAT1, through TJP2, regulates gene transcription promoting proliferation of vascular smooth muscle cells.[248] A study of vascular inflammation in the central nervous system revealed an upregulation of TJP2 in response to CCL2, linking inflammation to permeability in the blood brain barrier.[249] CDCP1 as a target is a bit more obscure as it does not seem to relate to any of the other gene targets on the String diagram although it has been reported to have a role in mediating cell adhesion.[250]. Unlike CCL2 and TJP2 the connection between CDCP1 and JAK2 is not well defined. It instead signals through Src kinase, however similar to CCL2/CCR2, CDCP1 is implicated in promoting

metastasis of tumour cells.[251] CDCP1 is expressed at low levels in endothelial cells endogenously, however when JAK2^{V617F} is expressed in HUVECs there is an increase in expression of CDCP1 which equates to a large fold change. CDCP1 has been reported to induce cell detachment, facilitating metastatic disease.[252] Although JAK2^{V617F}-HUVECs did not appear to detach *in vitro*, it is possible detachment would have been observed if the culture period was extended. It is also possible that cell detachment affected the increased permeability observed in JAK2^{V617F}-HUVECs. The specific effects of this increase in CDCP1 expression in JAK2^{V617F} endothelial cells are not known, however given that JAK2^{V617F} ECs in the MPN mouse model respond abnormally to vessel injury, it may be worth investigating proteins which are expressed at low levels normally but at high levels with mutant JAK2 expression.

Increased expression of CCL2, TJP2 and CDCP1 was identified in RNA sequencing and validated with qPCR. Future experiments are needed to determine the biological relevance of these genes. Using small interfering RNA (siRNA), expression of each gene can be repressed and effects on phenotype and signalling can be tested using permeability assays and western blot. Inflammation can be induced or suppressed by treating HUVECs with inflammatory and anti-inflammatory cytokines, respectively and effects of treatment can be compared to cells which express mutant JAK2. It is predicted that inflammation will contribute to endothelial dysfunction when combined with JAK2^{V617F} expression.

CHAPTER 5 DISSECTING THE ROLE OF JAK2^{V617F} IN ENDOTHELIUM OF PATIENTS WITH POLYCYTHAEMIA VERA

5.1 Experimental Rationale

JAK2^{V617F} expression has been identified in patient endothelial cells by 3 separate groups: liver endothelial cells of patients with BCS[217], splenic endothelial cells of patients with myelofibrosis[219] and endothelial colony forming cells isolated from whole blood of patients with different MPNs.[218] Patients with PV are venesected when haematocrit levels are greater than 54% and this blood is discarded.[253] Here, we aim to isolate endothelial cells from these samples, identify JAK2^{V617F} allelic burden and determine the effects of JAK2^{V617F} on the function of these cells.

5.2 Materials and Methods

5.2.1 Human samples

Access to patient samples was made possible through the York Tissue Bank (University of York, approved by the Health Research Authority [National Research Ethics Service] Leeds East Research Ethics Committee, ref: 15/YH/0016). Blood samples were drawn at York Hospital and transported to the University for processing. Patient consent was obtained before the first sample was collected.

5.2.2 Peripheral blood mononuclear cell (PBMC) isolation

PBMCs were isolated by Ficoll density gradient centrifugation (GE Healthcare). Peripheral blood was carefully layered onto Ficoll and centrifuged at 400*g* for 35mins at room temperature with the centrifuge brake off. The buffy coat layer was collected and diluted 1:1 in 1XPBS. Cells were centrifuged at 300*g* for 20mins at room temperature with the centrifuge brake on for collection.

5.2.3 CFU-Hill assay

PBMCs were isolated as described in 5.2.2 and plated in duplicate at $5x10^6$ cells/well in 6-well plates coated with 25µg/mL fibronectin (Sigma). Cells were cultured in CFU-Hill medium (STEMCELL Technologies Inc.) for 2 days at 37ºC and 5% (v/v) carbon dioxide. On day 2, nonadherent cells were collected by pipetting, a cell count was obtained and cells were re-plated in duplicate at $1x10^6$ cells/well in 24-well fibronectin-coated plates. CFU-Hill medium was added as needed for a total volume of 1mL per well. Cells were incubated for an additional 5 days. On day 7, nonadherent cells were removed and wells were washed once with 1XPBS. Cultures were fixed with absolute methanol for 5mins at room temperature and stained with Giemsa staining solution (VWR) for 5mins at room temperature. Wells were rinsed with tap water once and plates were stored at room temperature for scoring at a later date. Colonies were enumerated using a standard light microscope (Olympus CKX41).

5.2.4 Generation of blood outgrowth endothelial cells (BOECs)

PBMCs were isolated as described in 5.2.2, resuspended in BOEC generation medium (EGM-2V, Bulletkit, Lonza) and plated in a single, collagen-coated T75 flask.[79] Flasks were coated with 50µg/mL of Type I collagen (BD Biosciences) diluted in 0.02M acetic acid (Sigma) for 1hr prior to cell plating. The flasks were washed 2 times with 1XPBS to remove collagen and acetic acid prior to plating. Medium was changed every 2 days until colonies emerged, between 1-3 weeks post-plating. Colonies consisting of 1000-2000 cells by microscopy were re-plated in new T75 collagen-coated flasks.

5.2.5 Allele-specific competitive blocker (ACB) PCR

The ACB PCR assay allows for amplification of the mutant JAK2 allele specifically (Figure 5.1).[254] Amplification of the WT allele is inhibited by a "blocking" primer, which contains a phosphate group at the 3' end, blocking extension of the amplicon. PCR reactions consisted of 1X PCR buffer (Qiagen), 2mM magnesium chloride (Qiagen), 200µM dNTP mix (Thermo Scientific), 0.4µM of forward and reverse mutant primers (IDT), 0.2µM of WT forward primer (blocking primer, IDT) and 0.5U HotStar Taq polymerase (Qiagen). DNA was isolated using the Gentra Puregene DNA isolation kit (Qiagen), quantified by nanodrop (Thermo

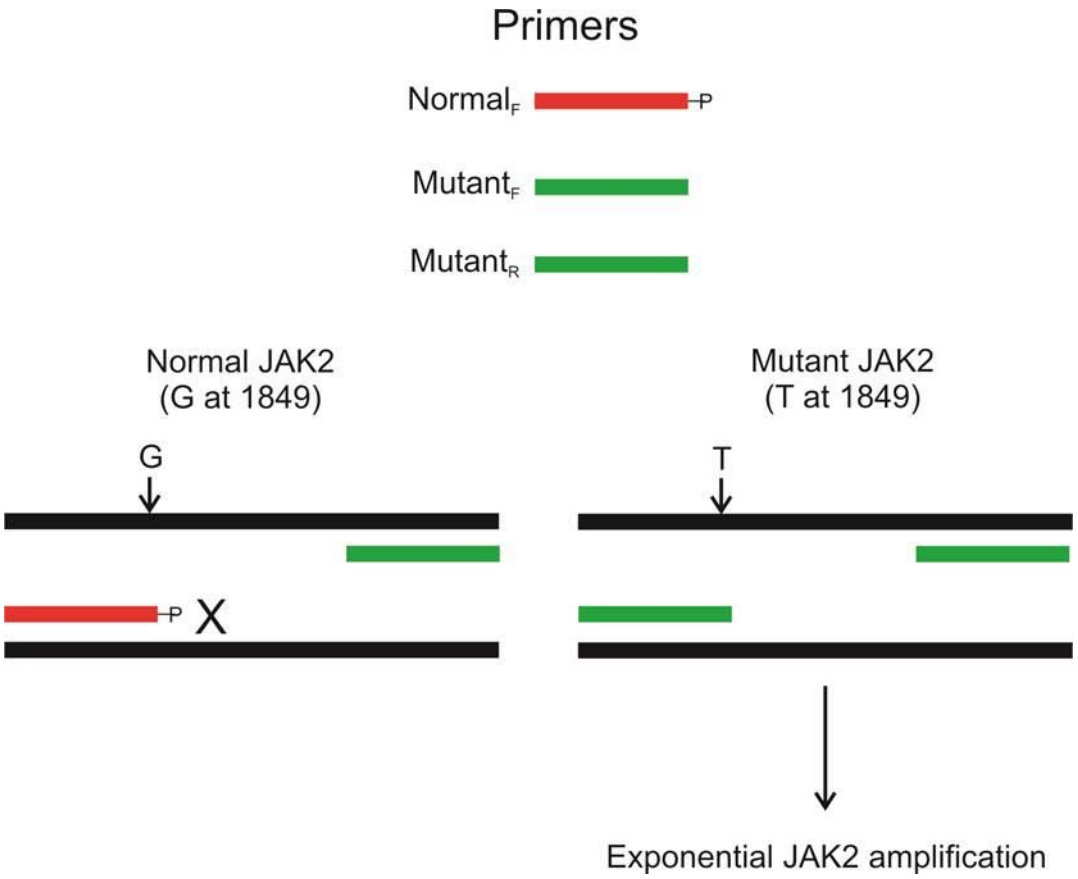

Figure 5.1 Schematic of ACB PCR assay
The ACB assay was used to determine the presence of the mutation which causes JAK2^{V617F} by specifically amplifying this allele. The first forward primer is complementary to the mutant region, with the final residue matching the mutant residue (Mutant$_F$). The second forward primer is complementary to the same region; however the final residue matches the WT allele (Normal$_F$). The Normal$_F$ primer contains a phosphate modification which prevents extension by the polymerase. The last primer is the reverse primer, which allows amplification when the Mutant$_F$ primer binds.

Scientific) and 100ng of DNA was added to each reaction. ACB reactions were carried out in triplicate to minimise false-negative or false-positive results. A control reaction was run alongside the ACB reaction to assess DNA quality, to rule-out false negative results obtained with poor quality DNA. Primers and cycling conditions for ACB and control reactions are provided (Table 5.1). Reactions were analysed on 1.5% (w/v) agarose/TAE gels stained with 5mg/mL ethidium bromide (Severn Biotec Ltd.).

5.2.6 Quantitative allele-specific amplification (QuASA) assay

The QuASA assay was purchased and performed according to the manufacturer's protocol (Genesig). QuASA is an allele-specific quantitative PCR that occurs in 2 stages, modified such that the assay is particularly sensitive to allelic differences. In the first stage, primers bind specifically to mutant or WT alleles at the 3' end and at the 5' end a tag is added that is then incorporated into the amplicons. These primers have a very low Tm, minimising non-specific binding and this stage is therefore carried out at a low annealing temperature (50^{o}C). In the second stage, primers are designed to the 5'tagged regions of the amplicon and annealing temperature is increased (60^{o}C). These modifications increase the specificity and accuracy of allele-specific qPCR.

5.2.7 X-chromosome inactivation pattern (XCIP) assay

The XCIP assay for clonality is frequently used to test for clonal derivation of cell populations in haematological malignancies.[255] It is based on the principle of random X-chromosome inactivation by methylation in females during embryonic development, which is subsequently passed on to daughter cells in cell division. In polyclonal cell populations, cells will express either the maternal or paternal X-chromosome in equal proportions. However, as cells become clonal this proportion is skewed to show maternal/paternal chromosome expression in unequal proportions and in completely clonal populations, only 1 chromosome will be expressed. The restriction enzyme *Hpa*II digests unmethylated DNA, leaving only the methylated chromosomes intact. Therefore, comparing gene expression before and after *HpaII* digestion can distinguish between polyclonal and monoclonal cell samples in female patients. Here, gene expression of the HUMARA gene was used to test clonality in BOEC samples from female patients. This gene was previously determined to be

Table 5.1 ACB Assay Primers and Cycling Parameters

Primer	Sequence	Tm (°C)	Annealing Temperature (°C)	Amplicon (bp)
ACB WT "blocking"	5'-GCATTTGGTTTTAAATTATGGAGTATGTG/3Phos/-3'	53.8	64	139
ACB Mutant Forward	5'-GCATTTGGTTTTAAATTATGGAGTATGAT-3'	53.1		
ACB Mutant Reverse	5'-ACTGACACCTAGCTGTGATCCTG-3'	58.2		
Control Forward	5'-TTCCTTAGTCTTTCTTTGAAGCAG-3'	53.1	64	191
Control Reverse	5'-ACTGACACCTAGCTGTGATCCTG-3'	58.2		

Segment	Cycles	Temperature (°C)	Time
1	1	95	15 minutes
2	45	94	30 seconds
		64	30 seconds
		72	30 seconds
3	1	72	10 minutes

useful in clonality assays due to 90% of females being polymorphic for the hypervariable CAG short tandem repeat in exon 1 of this gene.[256] One male patient was used as a control.

DNA was digested with *Hpa*II (New England Biolabs) overnight at 37ºC. DNA was then diluted to a concentration of 20ng/μL with distilled water and used in PCR amplification of the human androgen receptor gene (HUMARA). Primers and cycling conditions are provided (Table 5.2). Amplicons were resolved on 4% (w/v) agarose/TAE gels stained with ethidium bromide for analysis.

5.2.8 Quantitative phase microscopy

Ptychography is a novel algorithm used to produce high quality, quantitative images from diffraction patterns caused by the phase shift that occurs when light passes through a sample.[257] Here, the inverted VL21 microscope (Phasefocus, Sheffield, UK) was used to image the samples, which were contained in a Solent Scientific environmental chamber (Solent Scientific Limited, UK) to maintain cell culture conditions at 37ºC and 5% (v/v) CO_2.[258] Images were generated every 10mins per sample and these images were reconstructed using Ptychographic Iterative Engine (ePIP) algorithm (Phasefocus Virtual Lens, Phasefocus, Sheffield, UK). ImageJ and CAT software (Phasefocus, Sheffield, UK) were used for cell segmentation and generation of images.

Cells were plated at $5x10^4$cells/well in glass-bottom 6-well plates coated with 50μg/mL Type I collagen as described in 5.2.4. The cells were then imaged using the quantitative phase focus microscope for 72 hours. After imaging, cells were fixed in paraformaldehyde for 10mins and stored in PBS/azide for IF. Segmentation and analysis of cell morphology and movement were completed by Dr. Rakesh Suman (Phasefocus, Sheffield, UK).

Table 5.2 Primers and Cycling Parameters Used in XCIP Clonality Assay

Primer	Sequence	Tm (°C)	Annealing Temperature (°C)
AR For	5'-GCTGTGAAGGTTGCTGTTCCTCAT-3'	59.7	54
AR Rev	5'-TCCAGAATCTGTTCCAGAGCGTGC-3'	61	

Segment	Cycles	Temperature (°C)	Time
1	1	95	15 minutes
2	36	95	30 seconds
		54	30 seconds
		72	45 seconds
3	1	72	5 minutes

5.3 Results

5.3.1 PV patient subjects vary in age, gender, blood cell counts and disease progression

All patients included in this study were being treated for PV at York Hospital. Patients varied in age, gender, haemoglobin levels, packed cell volume, white cell counts, ferritin levels, disease duration and treatment (Table 5.3). In general, patients either had high haemoglobin, packed cell volume and white cell counts or high platelets. Patients with high haemoglobin or white cell counts tended to have lower ferritin levels. Ferritin is a measure of iron storage; as patients with PV are far from being iron deficient, ferritin levels are often low. All patients received venesection when haematocrit levels were elevated, however 4 patients also received hydroxycarbamide therapy. Blood panel data received were generated at initial patient diagnosis or when care was transferred to York Hospital. Patient disease duration was 40months on average, ranging from 6 months to 125months. Patients were between the ages of 46 and 85, with an average age of 65, and the cohort included 3 females and 6 males.

5.3.2 Endothelial progenitor and mature cells are difficult to isolate from PV patient blood samples by FACS

Ficoll density centrifugation separated whole blood into plasma, PBMCs and red blood cells/granulocytes (Figure 5.2). Most samples processed had red cell contamination in the Ficoll layer, presumably due to high red blood cell counts in these patients. PBMCs were cell sorted for endothelial progenitor cells ($CD45^{-/Dim}$, $CD34^{+}$, $CD133^{+/-}$, $VEGFR2^{+/-}$) and mature endothelial cells ($CD45^{-/Dim}$, $CD146^{+}$, $CD34^{+/-}$, $VEGFR2^{+/-}$) (Figure 5.3).[75] Together, endothelial progenitor cells and endothelial cells constitute 0.01%-0.0001% of PBMCs.[259] Sorting cells of this frequency proved to be challenging; events sorted ranged between 100-5000 cells. Sorted cells were split into 2 groups, 1 group to isolate RNA to analyse gene expression of endothelial-specific genes and the other to isolate DNA to determine the presence of $JAK2^{V617F}$. Both tasks proved difficult due to the amount of RNA and DNA isolated from the small population of sorted cells. Gene expression by conventional PCR of cDNA (Table 5.4) showed expression of both CD34 and VWF

Table 5.3 Patient Clinical Parameters

*Patients were transferred to York Hospital

Purple indicates values above and blue indicates values below the reference range

	Patient	Gender	Age	Haemoglobin (g/L)	Packed Cell Volume (L/L)	Platelets ($x10^9$/L)	White Cell Count ($x10^9$/L)	Ferritin (ng/mL)	Diagnosis Date	Months since Diagnosis	Treatment
	20150807-1	M	56	202	0.605	356	11.3	21	Nov-13	31	
	20150807-2	F	65	136	0.401	712	11.3	77	Jul-12	47	
	20152708-1	M	53	208	0.602	368	7.7	19	Dec-13	30	
	20160120-1	F	85	148	0.445	107	4.6		Dec-14	18	
*	20151023-1	M	75	147	0.396	194	6.4				Hydroxycarbamide
	20151023-2	F	46	191	0.548	383	9	29	Apr-13	38	
*	20151202-1	M	64	148	0.465	404	11.2	8	Jan-05	125	Hydroxycarbamide
	20160120-2	M	70	175	0.527	739	12.5	126	Dec-15	6	Hydroxycarbamide
	20150806-1	M	69	211	0.586	245	13.3	301	Apr-14	26	Hydroxycarbamide

Reference Ranges		
	Male	Female
Haemoglobin	135-180	115-160
Packed Cell Volume	0.40-0.52	0.37-0.47
Platelets	150-400	150-400
White Cell Count	4.0-11.0	4.0-11.0
Ferritin	25-350	10-300

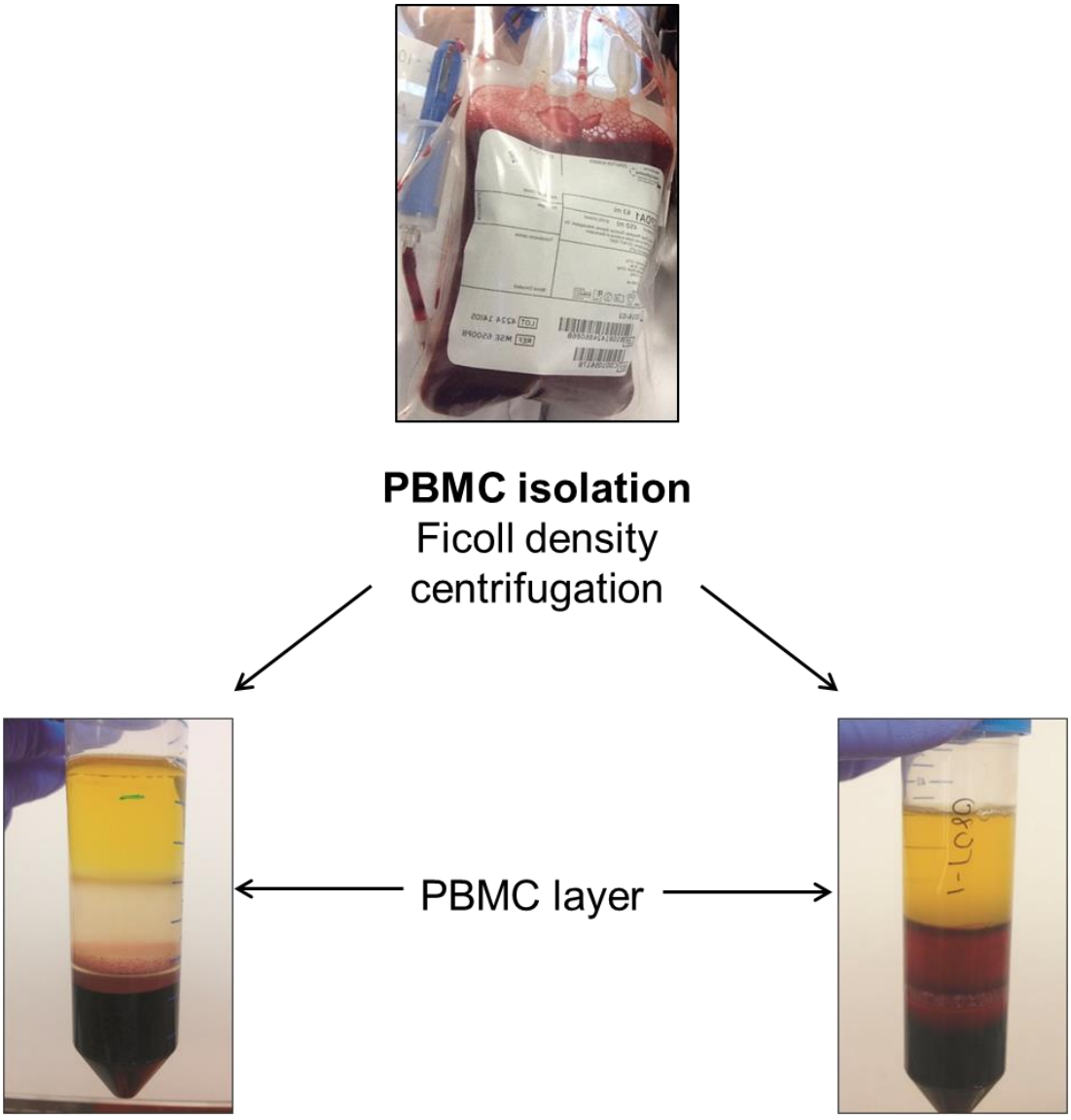

Figure 5.2 Schematic of whole blood collection and processing
Whole blood was collected into citrate-anticoagulant coated blood bags and blood components were separated by Ficoll-density centrifugation. The PBMC layer indicated was collected. Red cell contamination in the Ficoll layer (right sample) was common, as these samples came from patients with elevated haematocrit levels. Collection of red cells with PBMCs could not always be avoided, however this did not seem to affect generation of ECs.

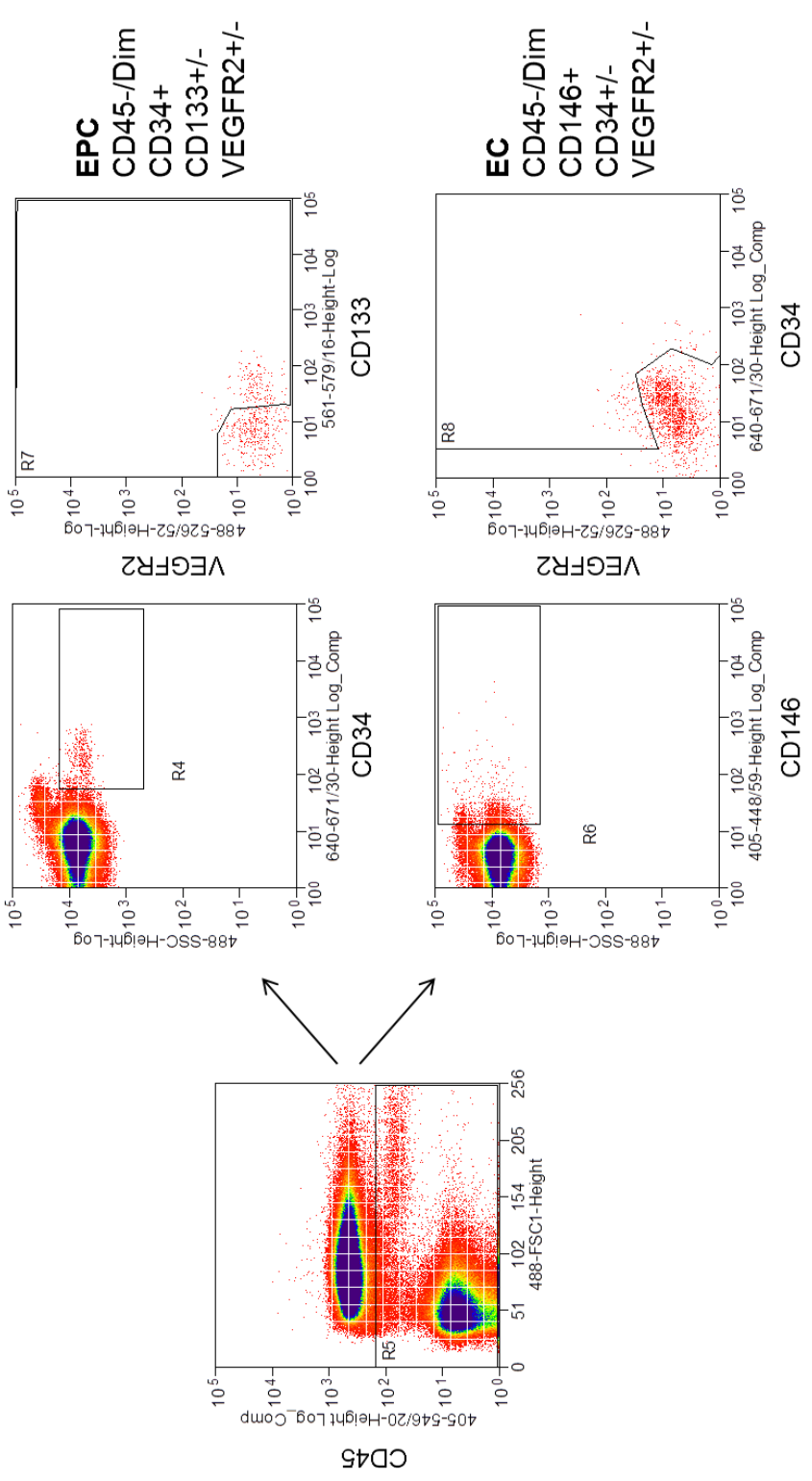

Figure 5.3 FACS of PBMCs to isolate EPCs and mature ECs
FACS was used to separate EPCs and circulating ECs from PBMCs. PBMCs were stained with APC-CD34, PE-CD133, AlexaFluor488-CD309, BV510-CD45, BV421-CD146 and viability dye eFluor 780. The first gate was set up to include CD45-/Dim cells. These cells were then separated into 2 populations: CD34+CD133+/-VEGFR2+/- to isolate EPCs and CD146+CD34+/-VEGFR2+/- to isolate mature ECs.

Table 5.4 Primers for Detection of EC Markers CD34 and vWF

Primer	Sequence	Tm (°C)	Annealing Temperature (°C)	Amplicon (bp)
hCD34 For	5'-TGAAGCCTAGCCTGTCACCT-3'	58.2	53	199
hCD34 Rev	5'-CGCACAGCTGGAGGTCTTAT-3'	57.1		
hVWF For	5'-TAAGTCTGAAGTAGAGGTGG-3'	50.4	50	108
hVWF Rev	5'-AGAGCAGCAGGAGCACTGGT-3'	61.3		

in EPCs and ECs (Figure 5.4). Unfortunately, ACB PCR was unreliable for the detection of $JAK2^{V617F}$ in these samples.

5.3.3 Blood outgrowth endothelial cells (BOECs) can be generated from PV patient blood samples

To overcome the shortcomings of EPC and EC isolation by FACS, BOECs were generated by culturing PBMCs for 1-3 weeks. BOECs appeared first as small colonies, which grew to confluent monolayers with characteristic endothelial cell cobblestone morphology (Figure 5.5). BOECs were further characterised by expression of VEGFR2 and PECAM, two endothelial cell markers and negative expression for CD45, the leukocyte common antigen (Figure 5.6). In culture, BOECs displayed varying growth rates and morphological differences which helped shape future experimental planning. DNA, RNA and protein samples were collected from proliferating BOECs.

5.3.4 PV patients express $JAK2^{V617F}$ in BOECs at varying levels

DNA isolated from BOEC samples was first analysed for $JAK2^{V617F}$ mutation status by ACB PCR. Human erythroleukaemia cells (HEL) were used a positive control, as these cells are known to express $JAK2^{V617F}$.[260] Untransduced HUVECs were used as the negative control. Of the 9 patient samples generated, only 2 patient samples appeared to definitively express $JAK2^{V617F}$ according to the ACB PCR assay (Figure 5.7). Other samples appeared to be either negative for the mutation or could not be properly analysed due to nonspecific band amplification. Control reactions were positive for all patient BOEC samples, indicating quality DNA was isolated. Next, exon 14 was amplified from each BOEC sample and sent for direct sequencing of the mutation (Table 5.5). All samples were reported to contain the WT nucleotide guanine, however on examination of the individual sequencing peaks it appeared that in one patient BOEC sample there was overlap between guanine and thymidine nucleotides at the mutation position (Figure 5.8). This patient corresponded to one of the "definitive" $JAK2^{V617F}$ BOEC samples analysed by ACB PCR assay. Lastly, QuASA was used to quantify percent $JAK2^{V617F}$ allelic burden by amplification of both WT and mutant alleles and comparing levels of $JAK2^{V617F}$ to $JAK2^{WT}$. Patient BOEC samples varied in $JAK2^{V617F}$ allelic burden from 0% to 59.8% and interestingly, the patient sample with 59.8% $JAK2^{V617F}$ allelic burden corresponded

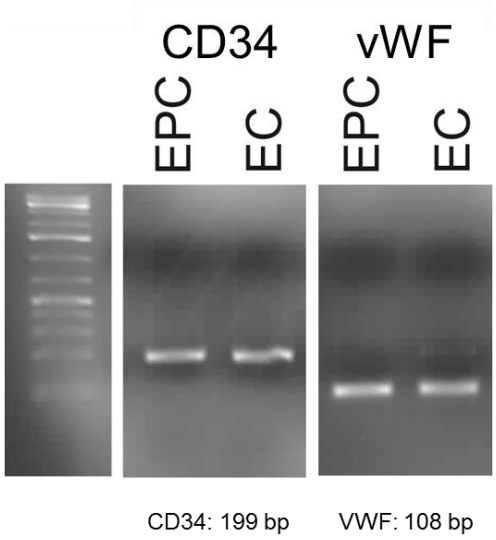

Figure 5.4 Detection of EC markers in sorted samples by PCR
RNA was collected from FACS sorted EPC and EC populations. RNA was converted to cDNA and expression for CD34 and vWF was detected by conventional PCR. Both EPC and EC populations were positive for CD34 and vWF (n=1).

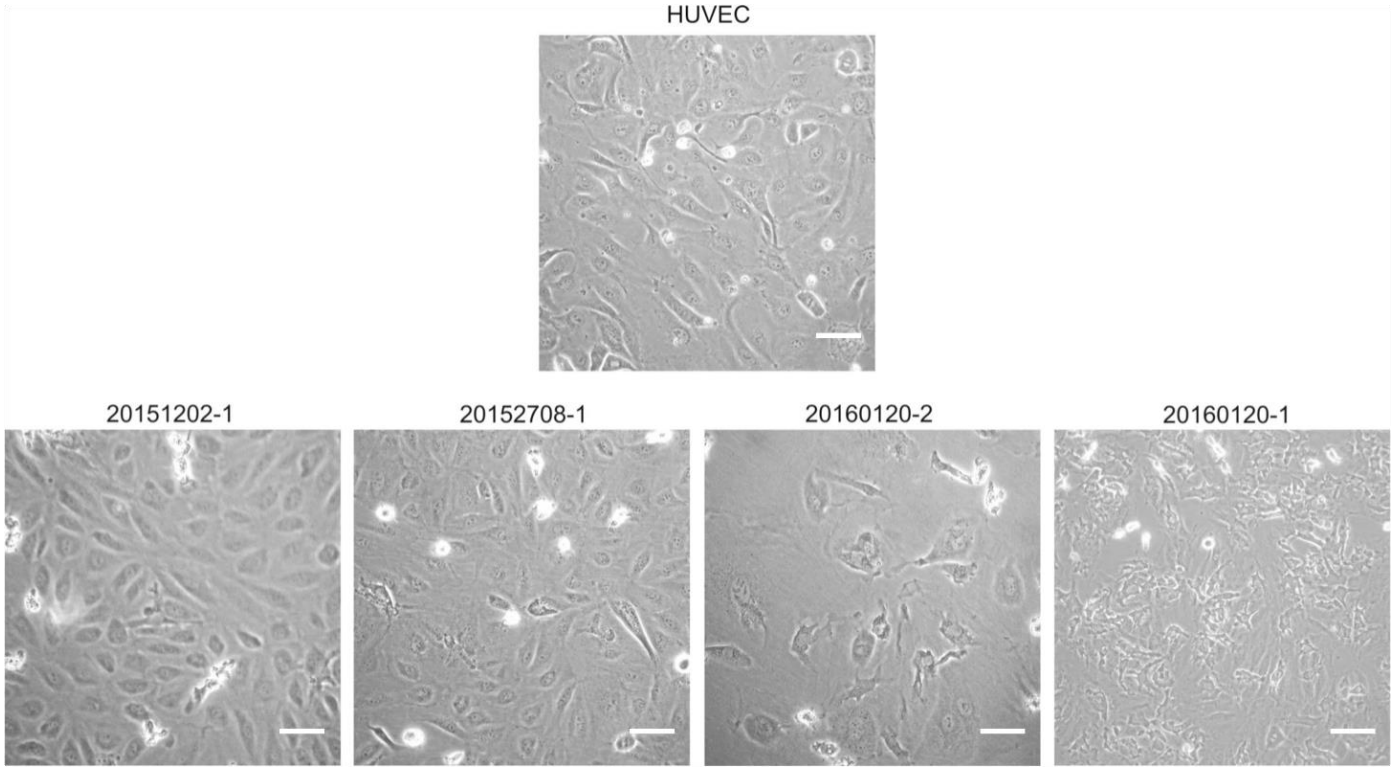

Figure 5.5 Morphology of BOECs generated by bright field microscopy

Morphology of BOECs was first observed using bright field microscopy (Olympus CKX41). BOECs have a cobblestone morphology which resembles HUVECs in many cases. Samples 20151202-1 and 20152708-1 are most similar to HUVECs, with visibly smooth cell-cell junctions forming. However samples 20160120-2 and 20160120-1 have a different morphology with disrupted cell-cell junctions, or junctions with jagged edges (20X objective, n=4, scale bar=40μm).

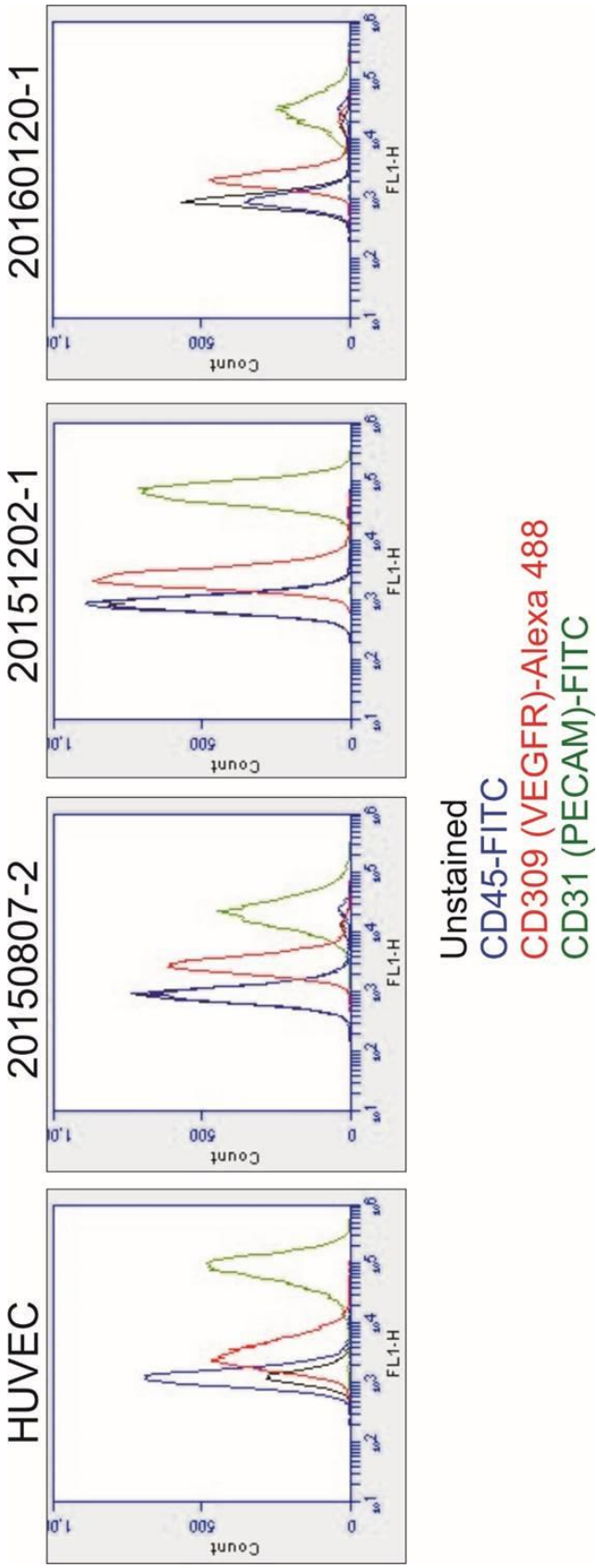

Figure 5.6 Characterisation of BOECs by flow cytometry
BOECs were stained with FITC-CD45 (BD Pharmingen), AlexaFluor488-CD309 (BioLegend) and FITC-CD31(eBioscience) and analysed by flow cytometry. Similar to HUVECs, BOECs are negative for CD45, the haematopoietic marker and positive for CD309 and CD31, both of which are endothelial markers. This assay was repeated on 3 different samples generated on separate dates.

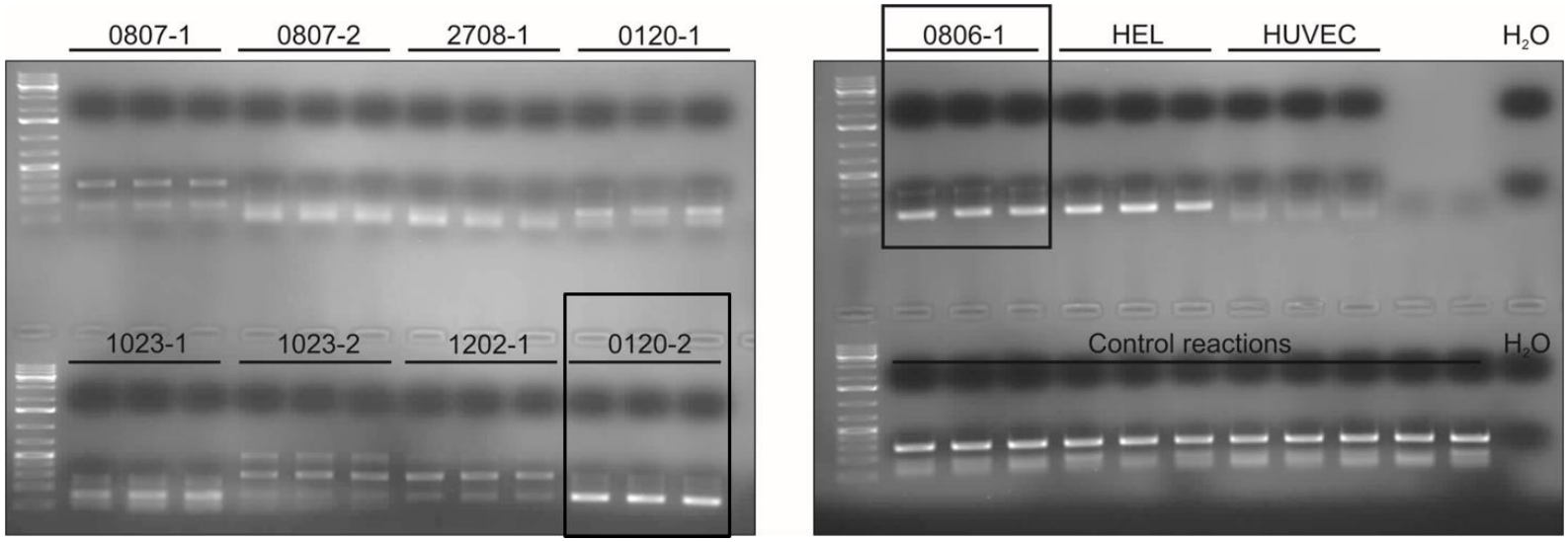

Figure 5.7 Determining JAK2V617F mutation status by ACB assay

ACB assay was used to detect $JAK2^{V617F}$ expression in BOEC samples. Amplification of the mutant allele occurred in sample 0806-1 and 0120-2, which matches amplification in the positive control (HEL). Samples 0807-2 and 2708-1 did not show amplification and this matched the negative control (HUVEC). It was not clear in any other sample whether the mutant allele was present or whether the blocking primer was inefficient at blocking amplification of the WT allele (n=3).

Table 5.5 Primers for JAK2 Exon 14 Amplification and Sequencing

Primer	Sequence	Tm (°C)	Annealing Temperature (°C)	Amplicon (bp)
hJAK2 exon 14 For	5'-GCTGAAAGTAGGAGAAAGTGCATC-3'	55.8	54	288
hJAK2 exon 14 Rev	5'-CTGACACCTAGCTGTGATCCTG-3'	56.9		
hJAK2 exon 14 Sequencing	5'-GGCAGAGAGAATTTTCTGAACT-3'	52.8		

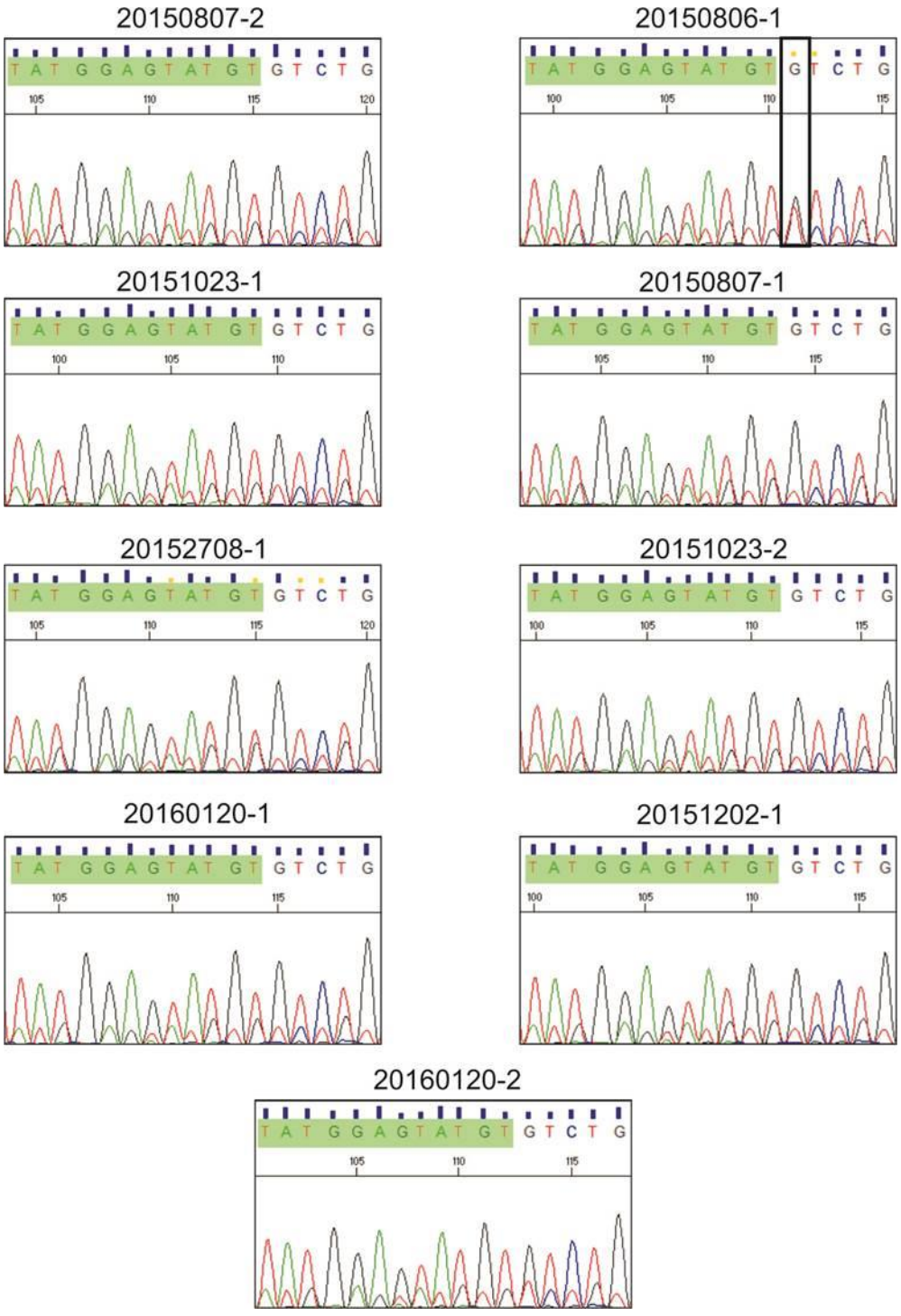

Figure 5.8 Determining JAK2V617F mutation status by sequencing
JAK2 exon 14 was amplified from each BOEC sample and sequenced for the $JAK2^{V617F}$ mutation. Although all samples were determined to be $JAK2^{WT}$, sample 20150806-1 showed overlapping G/T peaks at the mutational position, suggesting this sample may be heterozygous for the mutation (n=3).

to the sample that showed overlap in guanine/thymidine residues at mutation position by sequencing and to 1 of the samples that was positive for $JAK2^{V617F}$ by ACB PCR (Figure 5.9). Together, these results identify $JAK2^{V617F}$ in BOECs and show this mutation to be present at varying levels in PV patient endothelial cells.

5.3.5 $JAK2^{V617F}$ allelic burden correlates with CFU-Hill colony formation and gene expression

CFU-Hill colonies were identified by a core of circular-shaped cells with elongated cells radiating from the central core (Figure 5.10A). Colonies were enumerated from patient samples which generated BOECs and CFU-Hill quantity was analysed compared to patient age and percent $JAK2^{V617F}$ allelic burden as determined by QuASA. Age does not appear to have an effect on CFU-Hill colony generation (Figure 5.10B); however $JAK2^{V617F}$ allelic burden correlates negatively with CFU-Hill colony quantity (Figure 5.10C). Median values for enumerated colonies ranged from 0 to 56 and fewer colonies were enumerated in samples which had a higher $JAK2^{V617F}$ allelic burden.

RNA samples collected from patient BOECs were used in qPCR analysis for the 3 genes validated in HUVEC RNA sequencing, CCL2, TJP2 and CDCP1 (Figure 5.11). Although no clear pattern was detected, patients with 30% $JAK2^{V617F}$ allelic burden exhibited the highest fold change in these genes (Figure 5.12). Patient 0120-1 had increased expression of TJP2 and CDCP1 and patient 0120-2 had increased expression of CCL1. BOECs from patient 0806-2, with the highest $JAK2^{V617F}$ allelic burden (59.8%) failed to proliferate sufficiently for RNA harvest.

Blood parameters and patient information received from York Hospital were analysed a second time to compare each value with $JAK2^{V617F}$ allelic burden in BOECs (Figure 5.13). Age, haemoglobin, packed cell volume and white cell counts all appeared to correlate positively with percent $JAK2^{V617F}$ allelic burden and disease duration and platelet counts appeared to correlate negatively with percent $JAK2^{V617F}$ allelic burden. However, differences were not statistically significant. The only significant correlation was between ferritin levels and percent $JAK2^{V617F}$ allelic burden, although a larger patient cohort is needed to confirm this finding.

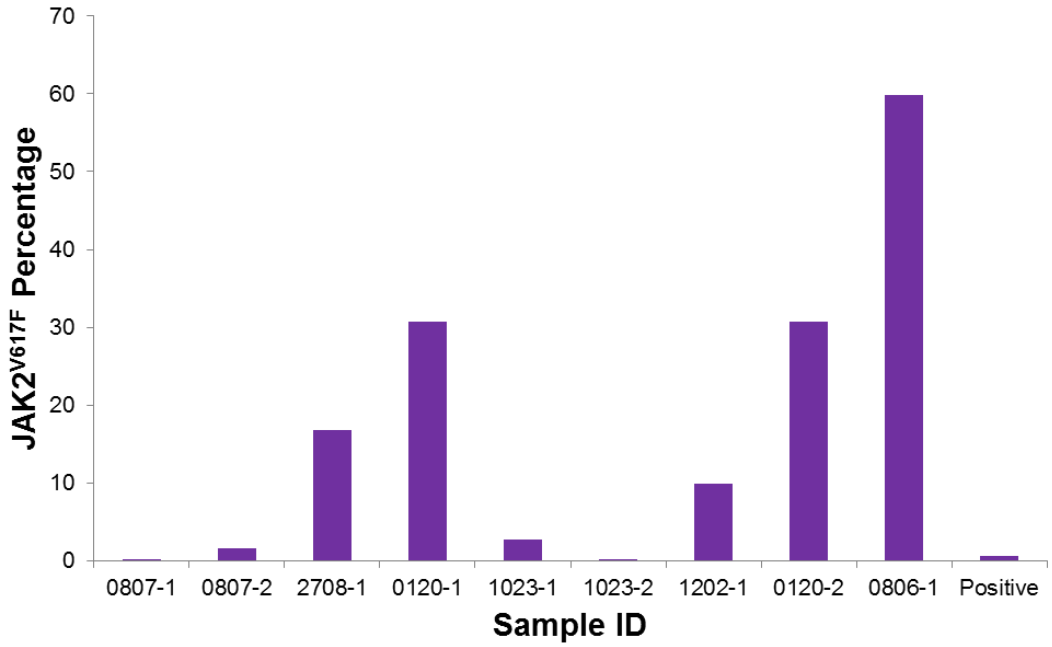

Figure 5.9 Determining JAK2V617F mutation status by QuASA
$JAK2^{V617F}$ and $JAK2^{WT}$ alleles were amplified in a commercially available real time qPCR assay called QuASA. In this assay, percent mutation burden in each patient is determined by comparing amplification of the mutant allele to amplification of the WT allele. Sample 0806-1 expressed the highest percent allelic burden of $JAK2^{V617F}$ (59.8%), which was determined to be positive for the $JAK2^{V617F}$ mutation using ACB assay and sequencing. Percent $JAK2^{V617F}$ allelic burden was variable among BOEC samples. The positive control contains 1% $JAK2^{V617F}$ mutant DNA (n=1).

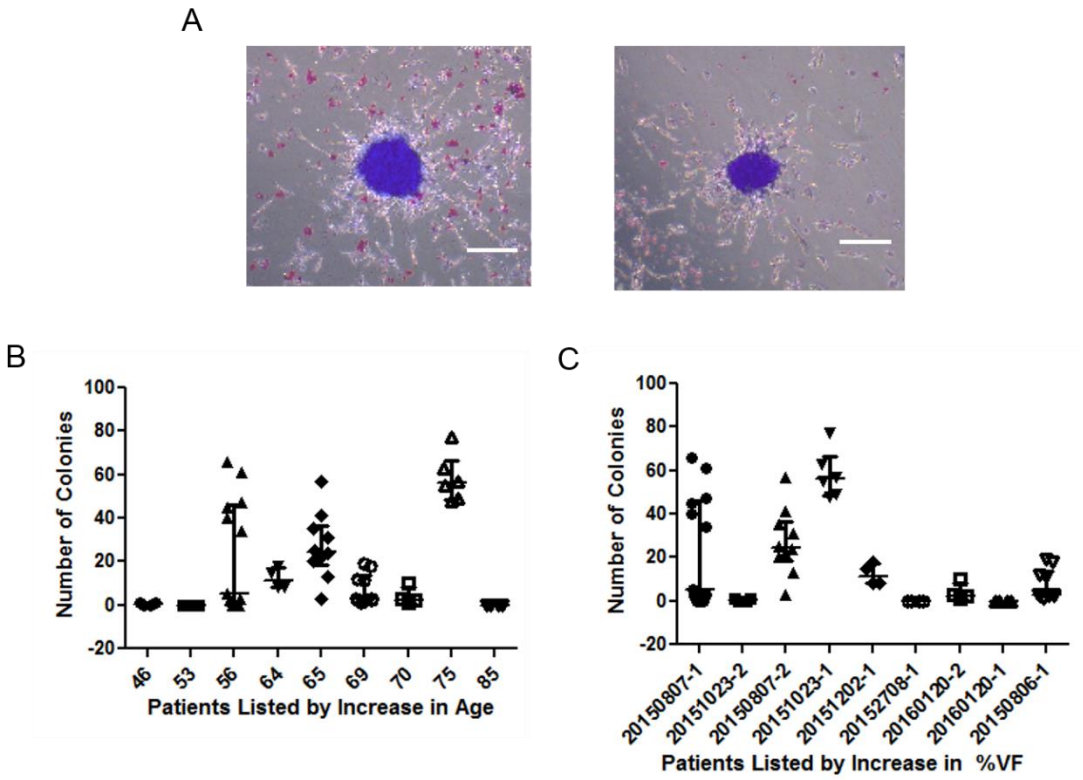

Figure 5.10 CFU-Hill colony generation and enumeration
(A) CFU-Hill colonies were generated as described in section 5.2.3. CFU-Hill colonies contain a cluster of round cells in the centre with radiating spindle-shaped cells from the cluster. Colony enumeration was compared to both (B) patient age and (C) allelic burden of $JAK2^{V617F}$. Data suggest that colony generation is not dependent on patient age, but may decrease as mutant allelic burden increases (20X objective, scale bar=200µm).

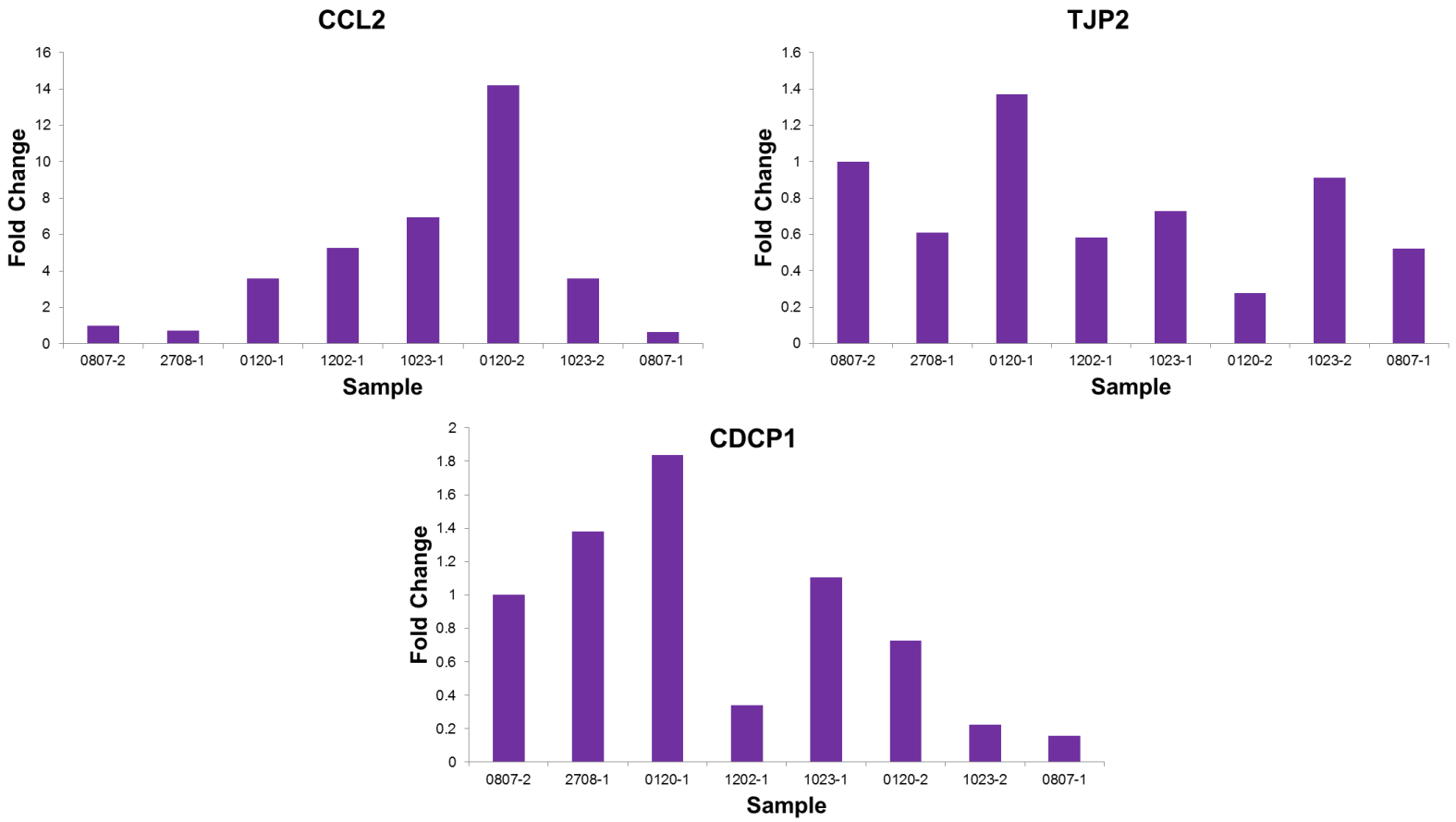

Figure 5.11 Gene expression analyses of CCL2, TJP2 and CDCP1 in BOEC samples

Real time qPCR was used to determine expression of CCL2, TJP2 and CDCP1 in BOEC samples. All 3 genes showed variation in expression among the different samples (n=1).

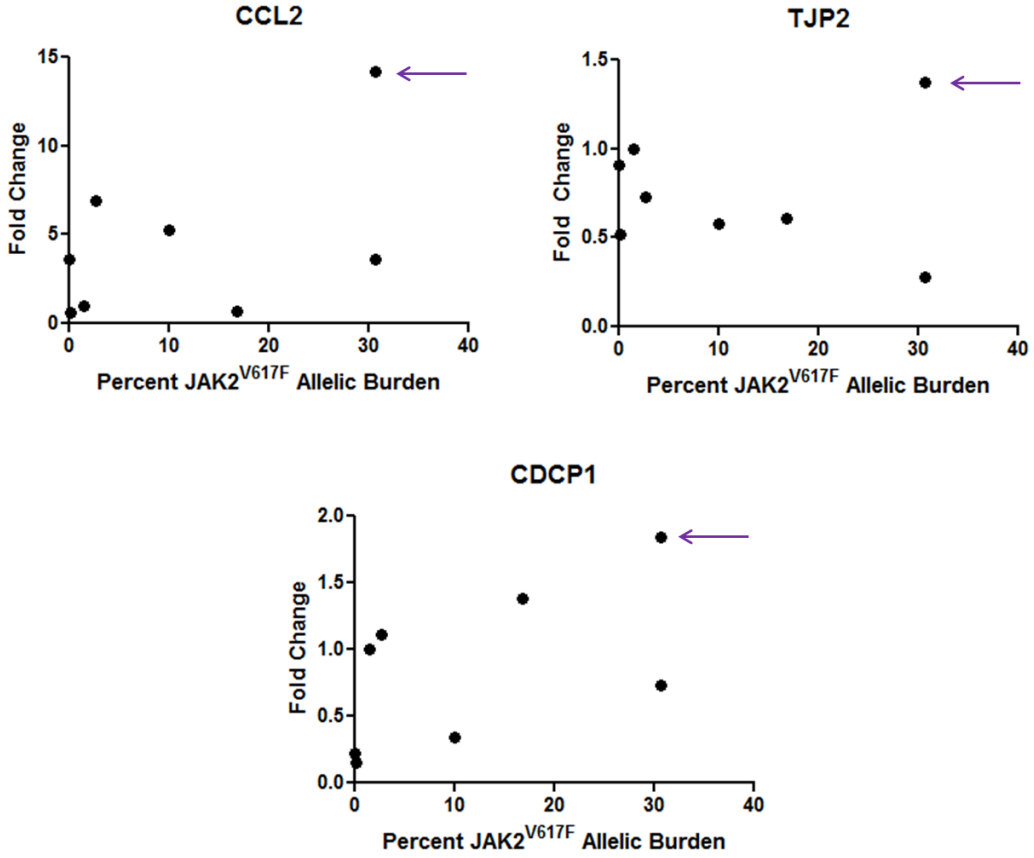

Figure 5.12 Gene expression of CCL2, TJP2 and CDCP1 compared to JAK2V617F allelic burden
Although gene expression of CCL2, TJP2 and CDCP1 is variable among patients, samples which have 30% JAK2 ^{V617F} allelic burden have the highest fold change in each gene (n=1).

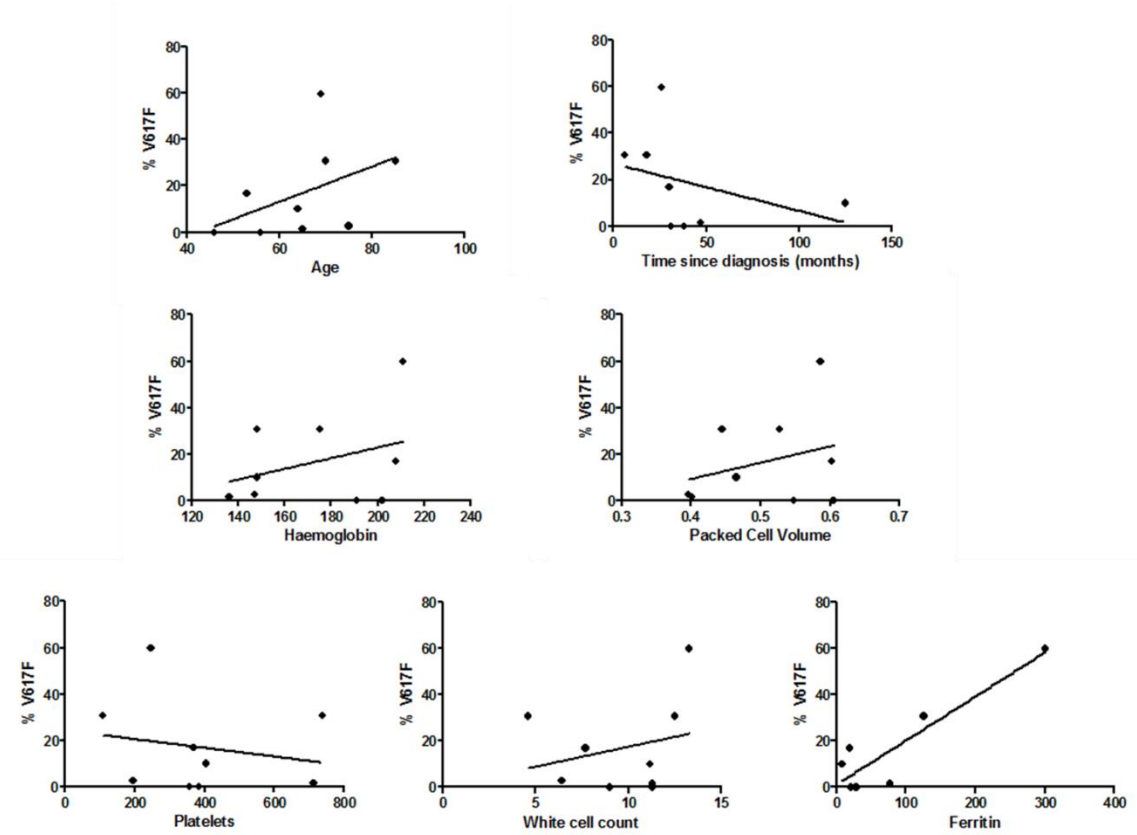

Figure 5.13 Percent JAK2V617F allelic burden compared to patient clinical parameters

$JAK2^{V617F}$ allelic burden was found to correlate positively with patient age, haemoglobin, packed cell volume, white cell counts and ferritin and negatively with disease duration and platelet counts. The only significant correlation was found to be ferritin levels and $JAK2^{V617F}$ allelic burden (linear regression, p=0.005); however additional samples are needed to validate this finding.

5.3.5 Female patients show evidence of endothelial cell clonality

XCIP of HUMARA in female patients suggests that endothelial cells are becoming clonal during BOEC generation (Figure 5.14). In all 3 female patients, undigested samples show amplification of more than 1 band, confirming they are heterozygous for this gene. In *Hpa*II digested samples, band proportion is skewed in 0807-2 and 0120-1 samples and in 1023-2, only 1 band is present. The male control patient shows 1 band in the undigested sample and 0 bands in the digested sample, confirming that *Hpa*II digestion is complete and PCR amplification is specific.

5.3.6 $JAK2^{V617F}$ allelic burden correlates with endothelial cell phenotype

Initial observations of BOECs in culture suggested that BOEC generation and expansion was highly variable among patients. To further explore differences in BOEC samples generated from different patients and to quantify these changes, each patient sample was imaged for 48hrs using phase focus microscopy (Phasefocus, Sheffield, UK). Images were recorded every 10mins to create a time-lapse video of cells in culture, which was then used to segment individual cells for tracking over time. Images captured at 0hr, 24hrs and 48hrs showed differences in cell morphology and growth capacity between patient samples (Figure 5.15). Specifically, samples 1023-2 and 0807-2 grew to confluency after 48hrs in culture and all other samples remained sub-confluent at varying levels. Immunoblotting showed that these same 2 samples, 1023-2 and 0807-2, had increased pJAK2 expression compared to all other patient samples, whilst total JAK2 expression remained equal amongst all samples (Figure 5.16). Expression of pSTAT1 and STAT1 varied among samples (Figure 5.16).

Segmentation and tracking of individual cells made quantification of cell morphology and motility over time feasible. Patient samples varied in both cell area and dry mass. Cell area ranged from 1415μm^2 (±558.3) to 5104μm^2(±2872) and cells with larger cell areas tended to also have higher allelic burden of $JAK2^{V617F}$(Figure 5.17A). Cell dry mass ranged from 217.5pg(±121.9) to 820.7pg(± 610.8) and cells with larger masses also had higher allelic burden of $JAK2^{V617F}$(Figure 5.17B). Visually, cells which had higher $JAK2^{V617F}$ allelic burden appeared larger and more round and flat in shape. Cells which had low levels of $JAK2^{V617F}$ expression appeared smaller and more elongated in shape.

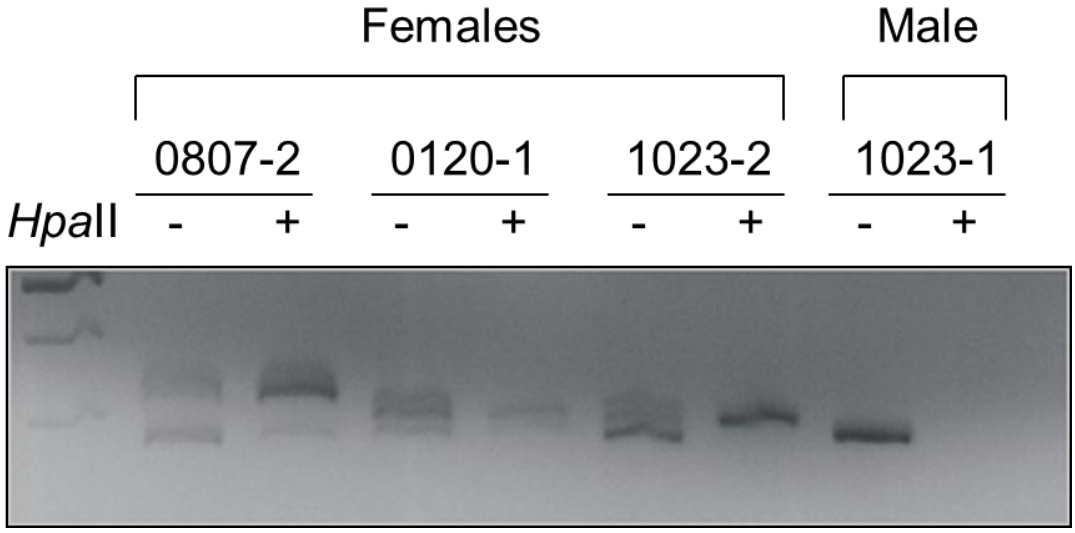

Figure 5.14 XCIP assay for clonality
Female patient BOEC samples were tested for clonality using HUMARA XCIP. Samples 0807-2 and 0120-1 showed evidence for becoming clonal, as *Hpa*II digestion resulted in unequal band distribution. Data showed sample 1023-2 to be clonal, as only 1 band was present after *Hpa*II digestion. The male sample showed only 1 band in the undigested sample, which disappeared in the digested sample, confirming that *Hpa*II digestion and amplification were complete (n=3).

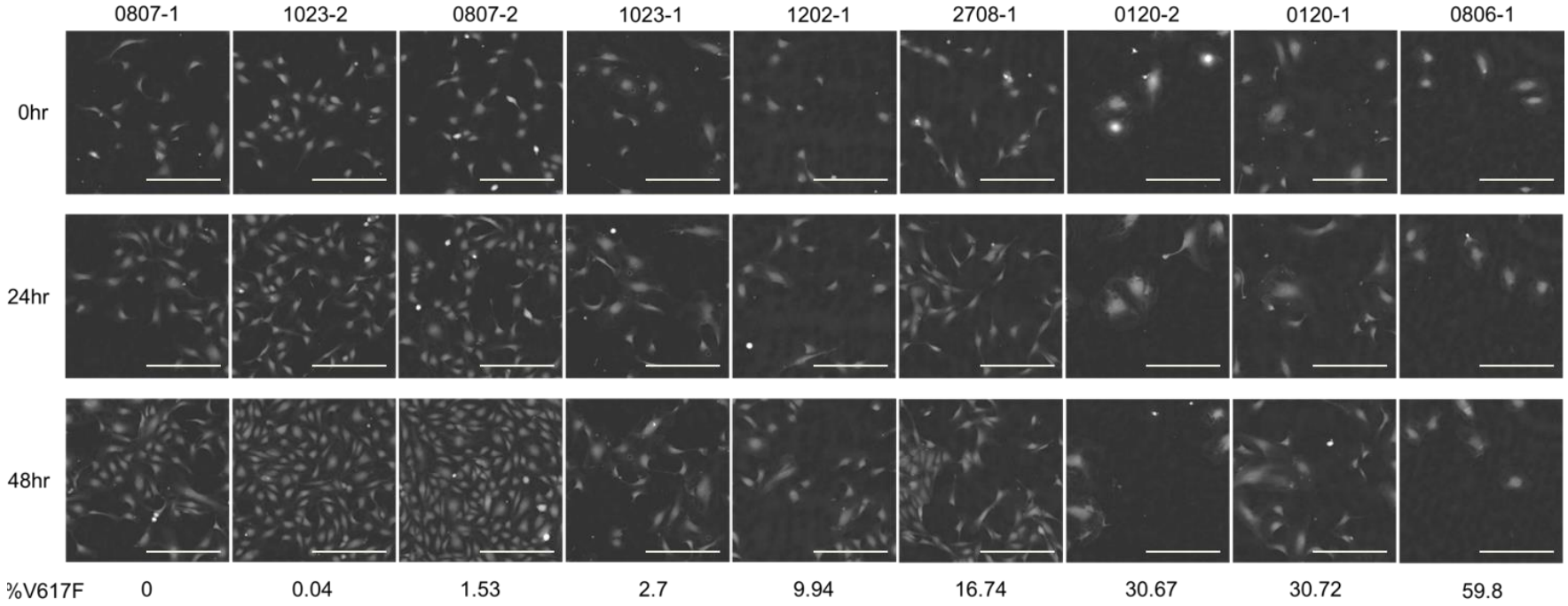

Figure 5.15 Phase focus microscopy images of BOEC samples

Each BOEC sample was imaged continuously for 48 hours using phase focus microscopy. Snapshots of each sample are shown for 0hr, 24hrs and 48hrs. Samples 1023-2 and 0807-2 were 100% confluent at 48 hours and all other samples remained sub-confluent. Samples 0120-2 and 0806-1 did not proliferate during the 48hr period and these samples have 30.67% and 59.8% $JAK2^{V617F}$ allelic burden, respectively (20X objective, n=1, scale bar=500μm).

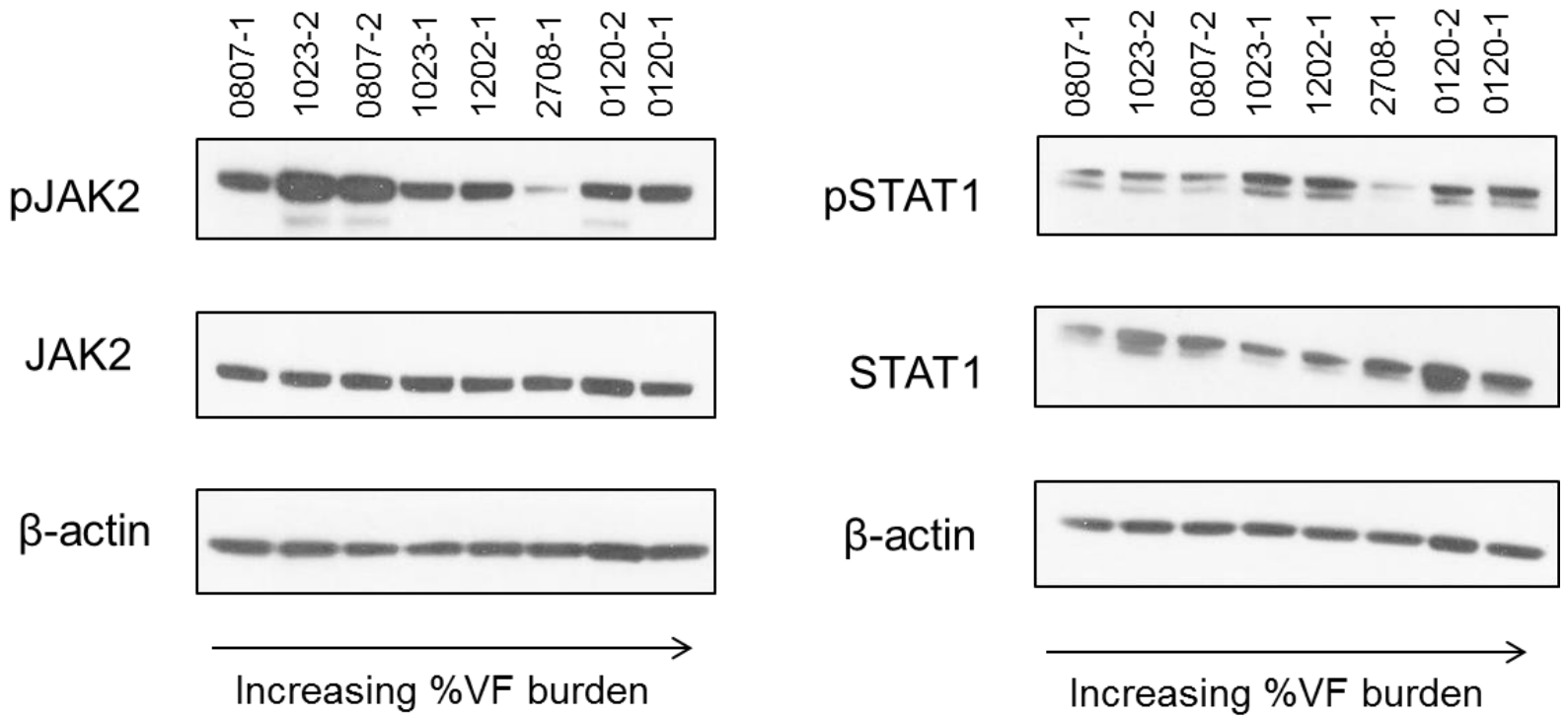

Figure 5.16 BOEC western blot analysis

Protein lysate was collected from BOEC samples that were not starved and expression of pJAK2, JAK2, pSTAT1 and STAT1 were detected by western blot. Data shows that pJAK2 was increased in samples 1023-2 and 0807-2, whilst total JAK2 remained equal among samples. Expression of pSTAT1 and STAT1 varied among BOEC samples (n=1).

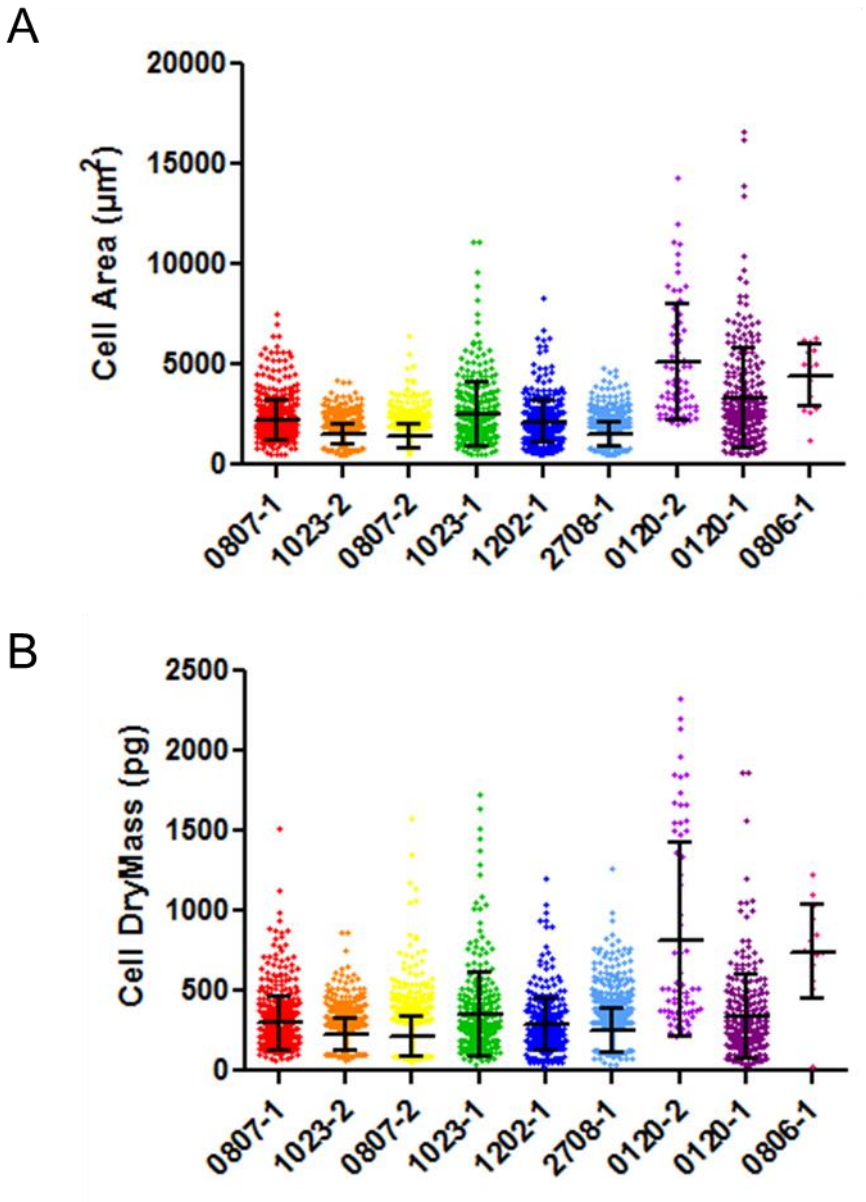

Figure 5.17 Analysis of BOEC morphology by phase focus microscopy
Quantitative phase focus microscopy and cell segmentation were used to quantify (A) cell area and (B) cell dry mass of BOEC samples. Data shows that both parameters are increased in samples which express a higher percent burden of $JAK2^{V617F}$ (bars represent mean ± SEM, n=1).

Samples also appeared to vary in cell motility. Instantaneous cell speed ranged from 0.003555μm/sec(±0.002340) to 0.009829μm/sec(±0.004234), with slower cells having a higher allelic burden of $JAK2^{V617F}$ (Figure 5.18A). Histogram graphical display of percent relative frequency versus instantaneous cell speed shows that cells in sample 0806-1 move at low speed and at low frequency, compared to the other samples (Figure 5.18B). Cells from sample 0807-2 appear to move the most frequently, one of the two samples which reached confluency at 48hrs. Meandering indices were measured to determine the degree to which cell paths deviated from a straight line. Meandering indices ranged from 0.2763a.u.(±0.2655) to 0.4638a.u.(±0.2644) and cells which have higher motility also had greater meandering indices (Figure 5.18C). Cells from sample 0806-1, which migrated the least and at the slowest rate, also had the lowest meandering index. All morphology and motility values reported are mean±standard deviation.

Cultures used for phase focus imaging were then fixed and stained for vWF, actin and DAPI nuclear stain (Figure 5.19). The most striking observation appears in samples 0120-2 and 0806-1, the same 2 samples that did not proliferate. In these samples, cells were visibly larger and they appeared to be multinucleated. These samples also appeared to have a more extensive cytoskeletal network. In particular, sample 0806-1 appears to have 2 centrosomes distributed at opposite ends of the cell, with spindle apparatus radiating towards the centre of the cell. Altogether, the presence of multiple nuclei, polarisation of centrosomes, formation of spindle apparatus and lack of proliferation suggest these 2 samples are not completing the cell cycle.

5.3.7 $JAK2^{V617F}$ allelic burden has a negative impact on proliferation potential

Proliferation was quantified by enumerating cells at each time point and normalising cell counts to the number of cells at time point 0hr. Similar to morphology and motility parameters, BOECs had varying proliferation rates between patient samples (Figure 5.20A). Samples 0807-2, 2708-1 and 1023-2 proliferated nearly 4-fold during the 48hr period and samples 0120-2 and 0806-1 did not proliferate at all. All but 1 sample (0120-2) had significantly non-zero slopes; linear regression analysis showed positive slope values for all samples apart from 0806-1, which suggests that

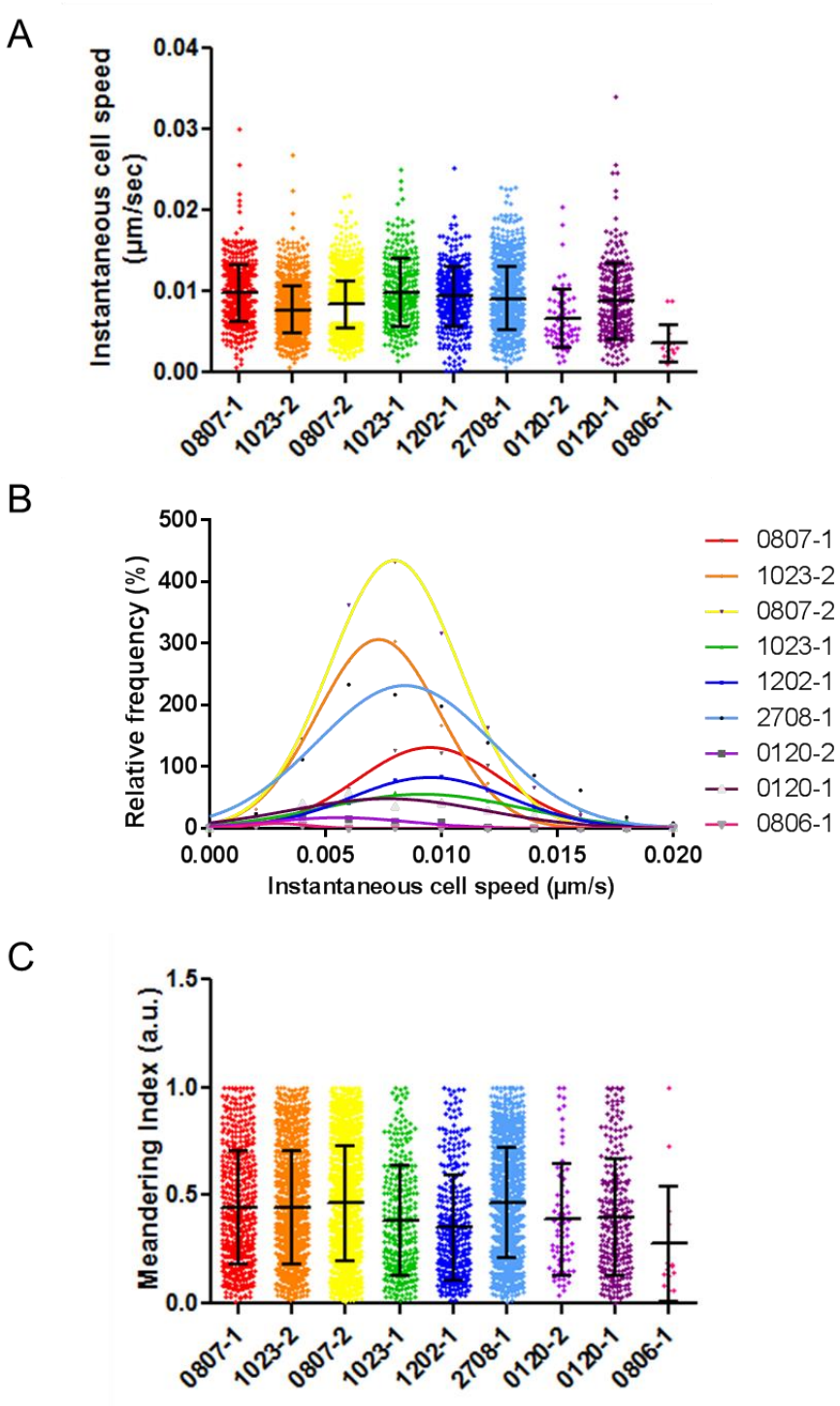

Figure 5.18 Analysis of BOEC motility by phase focus microscopy
Quantitative phase focus microscopy and cell segmentation were used to quantify (A) instantaneous cell speed, which was then converted to (B) relative frequency versus instantaneous cell speed, and (C) meandering index. Data shows that cell speed and meandering index are decreased in samples which express a higher percent burden of $JAK2^{V617F}$ (bars represent mean ± SEM, n=1).

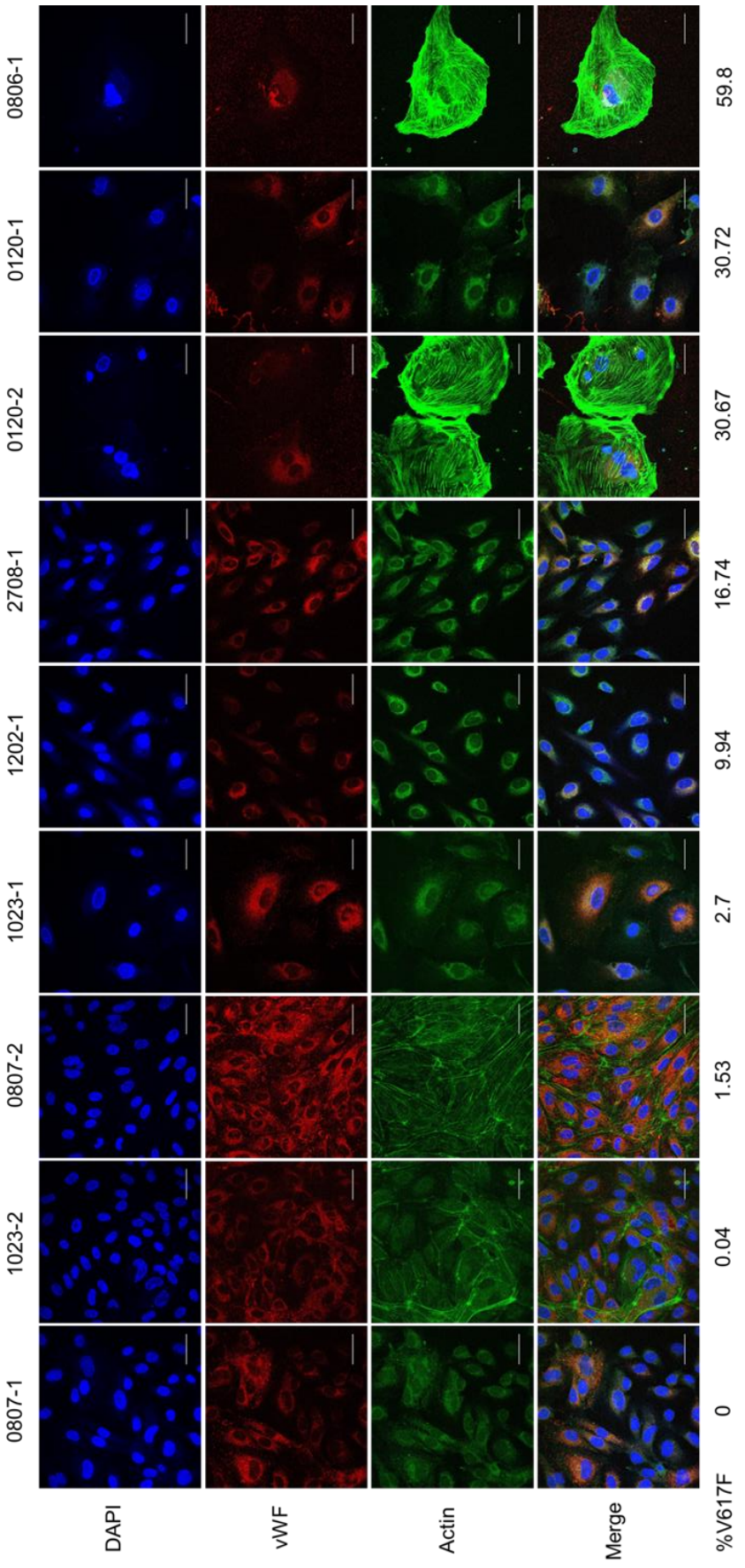

Figure 5.19 IF of BOECs cultured for phase focus microscopy
Post-phase focus imaging, BOECs were fixed and stained for vWF (red), actin (green) and DAPI nuclear stain (blue). Cells from samples 0120-2 and 0806-1 are larger, multi-nucleated and have extensive cytoskeletal networks compared to the other samples. These 2 samples also have higher allelic burden of $JAK2^{V617F}$ compared to the other samples (20X objective, scale bar=40µm).

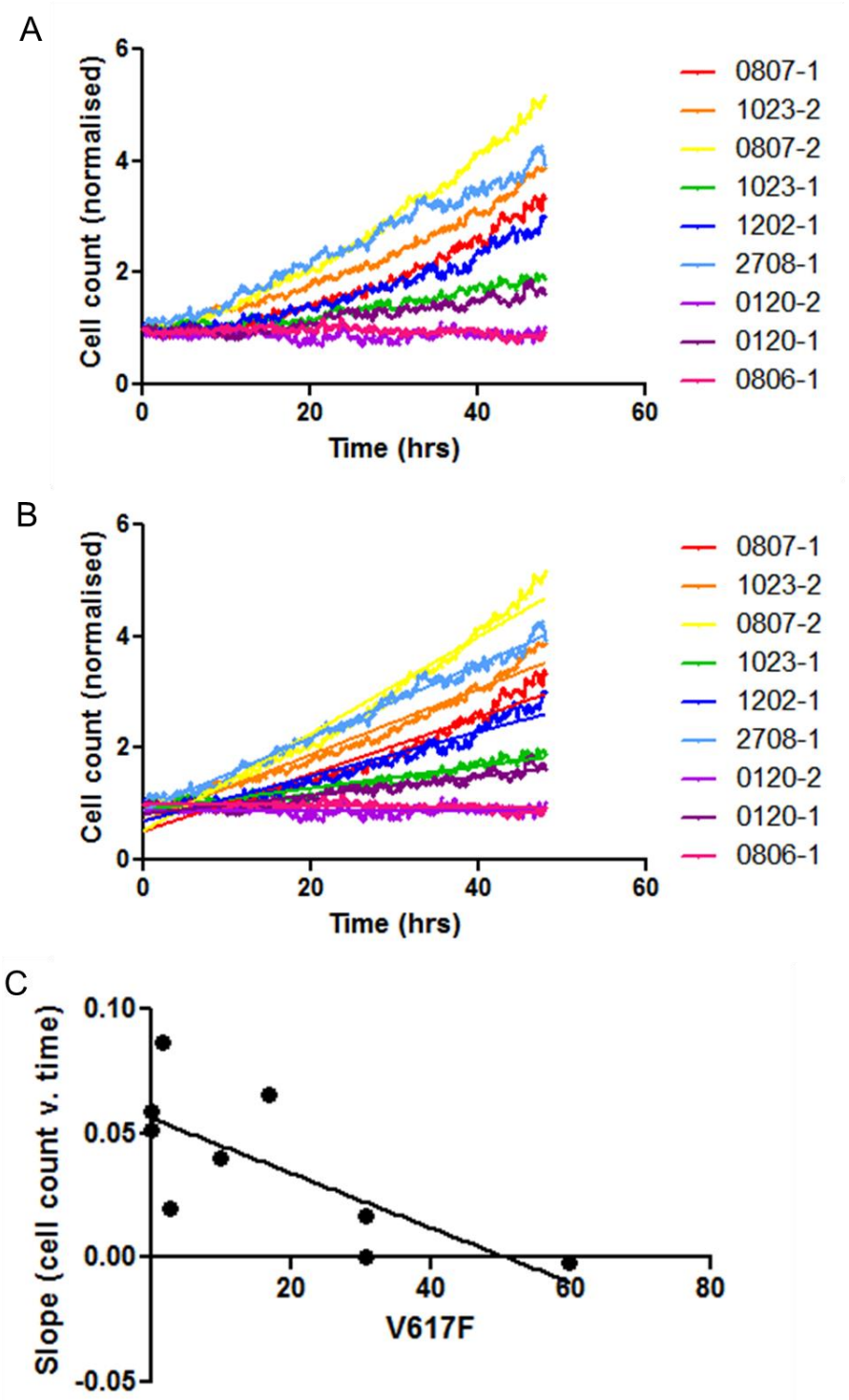

Figure 5.20 Analysis of BOEC proliferation by phase focus microscopy
Cell tracking was completed by phase focus imaging and segmentation and cells were counted in each frame. (A) Cell counts were normalised to initial cell count and plotted against time for each count. (B) These graphs were then fitted to linear regression models and (C) the slopes of each model were graphed versus percent $JAK2^{V617F}$ allelic burden. Increase in $JAK2^{V617F}$ allelic burden caused a decrease in cell proliferation capacity (linear regression, $p<0.001$).

there was very little or zero proliferation occurring in this sample (Figure 5.20B). Moreover, slopes were determined to be significantly different from each other, confirming that different BOEC samples had different proliferation rates ($p<0.0001$). When slopes of each linear model were plotted against $JAK2^{V617F}$ allelic burden, a negative linear regression was determined to be significant ($p=0.027$, Figure 5.20C). This suggests that $JAK2^{V617F}$ allelic burden can be used to predict proliferation potential of BOECs.

Linear regression models were used to determine change in cell number over time and slopes were used to determine if $JAK2^{V617F}$ could be a predictor of cell proliferation. On closer examination, it appeared that some BOEC samples might better fit a polynomial regression model. To this end, each BOEC sample was fitted to both linear and quadratic regression models to determine which model best fit each data set (Figure 5.21). Indeed, it appears that samples 0807-1, 1023-2, 0807-2, 1023-1, 1202-1 and 0120-1 exhibit non-linear growth, as they were better fit by the quadratic models. Samples 0120-2 and 0806-1were more difficult to analyse as neither model appeared to fit the data appropriately. When R^2 values were compared between linear and quadratic regression models for sample 2708-1, they appeared to be approximately equal which suggests that both models fit the data equally. Goodness-of-fit was determined by R^2 values (Table 5.6).

5.4 Discussion

The York Tissue Bank (YTB) and the Haematological Malignancy Research Network (HMRN), both located at the University of York were used to access patient samples from York Hospital and relative patient information. Patient samples were variable from all aspects, from whole blood separation by Ficoll gradient on day 1 to analysis of gene expression and phenotypic differences in BOECs. Inter-individual patient differences are not completely unexpected. Patients are unrelated and are likely subjected to individual environmental influences based on habit and preference. These factors cannot be controlled for in the laboratory. However, several observations were made throughout BOEC generation that were later quantified and compared to allelic burden of $JAK2^{V617F}$.

Isolating EPC and EC populations from PBMCs by FACS proved to be challenging and ultimately an unreliable source of endothelial cells for the proposed

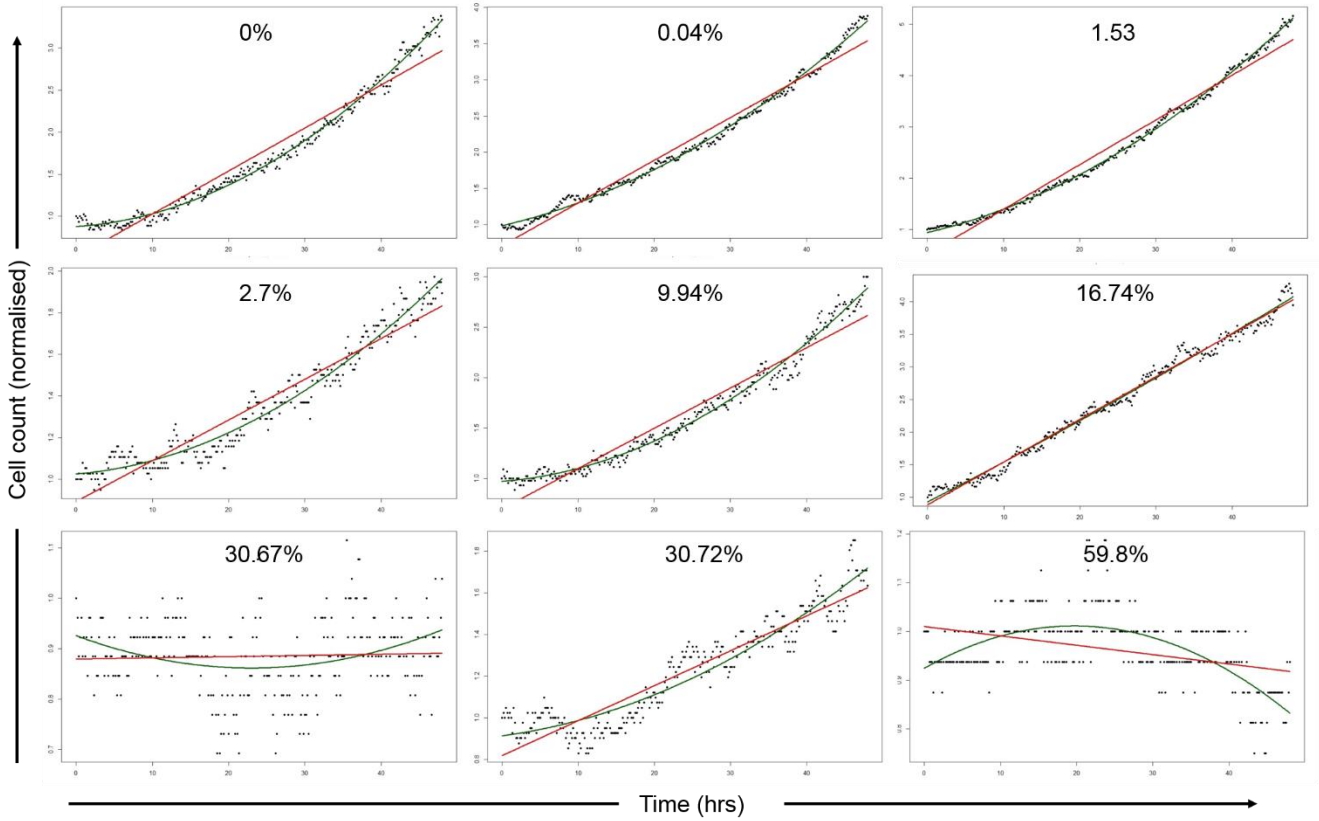

Figure 5.21 Analysis of BOEC proliferation by linear and quadratic regression models

Proliferation of each sample was originally analysed by linear regression, however some samples appeared to have non-linear growth. To investigate this in more depth, each sample was analysed by both linear (red) and quadratic (green) regression using the R Foundation. Indeed, samples 0807-1, 1023-2, 0807-2, 1023-1, 1202-1 and 0120-1 were better fit to quadratic regression models, indicating they were exhibiting non-linear growth. Samples 0120-2 (30.67%) and 0806-1 (59.8%) were poorly fitted to both models, as these samples did not proliferate. Each samples is labelled with percent $JAK2^{V617F}$ allelic burden.

Table 5.6 Values for Linear and Quadratic Regression Models
Purple indicates R^2 values which best fit the data, blue indicates similar R^2 values, red indicates poor R^2 values.

Patient	%V617F	R^2 Linear	R^2 Quadratic
0807-1	0.00	0.941200	0.99090
1023-2	0.04	0.972200	0.99470
0807-2	1.53	0.973800	0.99770
1023-1	2.70	0.913800	0.95770
1202-1	9.94	0.937200	0.98350
2708-1	16.74	0.987300	0.98770
0120-2	30.67	-0.001413	0.07813
0120-1	30.72	0.864400	0.89320
0806-1	59.80	0.141300	0.44310

experiments. EPCs and ECs constitute a small percentage of PBMCs, which undoubtedly makes isolation of these populations difficult; however BOEC samples with high $JAK2^{V617F}$ allelic burden gave rise to fewer EPC colonies in CFU-Hill assay suggesting that isolation of these cell types from PV patients might be even more challenging. Although, CFU-Hill assay results are preliminary; some patients were venesected on multiple dates and the CFU-Hill assay could be repeated whilst other patients were venesected only once throughout the study. Additional patient samples are needed to confirm EPC enumeration by CFU-Hill assay because limited patient samples could potentially skew the results.

Similar to EPC/EC isolation by FACS, generation of BOECs appeared to vary among patient samples. The first sample used in BOEC generation yielded its first colony within 1 week of culture, however most samples generated colonies between 1-3 weeks of culture. During passaging, some samples were expanded with ease whilst other samples failed to re-attach and expand. In the beginning, cells were kept in culture long enough to determine purity of endothelial cell cultures by morphology and flow cytometry and to collect DNA, RNA and cryo-preserved cell samples. Length in culture varied from 3 weeks to nearly 2 months depending on how quickly cells expanded. Moreover, cells which appeared to struggle with expansion also appeared to have changes in morphology. These cells were more flat and round and over time, instead of dividing and growing in number they grew in size. In contrast, proliferating BOECs maintained a cobblestone morphology characteristic of healthy endothelial cells.

Three methods of mutation detection were used to determine the presence of $JAK2^{V617F}$ in BOECs. Ultimately, QuASA was determined to be the most successful because by amplifying both $JAK2^{V617F}$ and $JAK2^{WT}$ alleles, percent $JAK2^{V617F}$ allelic burden could be calculated. Allelic burden of $JAK2^{V617F}$ ranged from 0-59.8%; however it was not clear whether this burden was the result of clonal derivation of one cell or a polyclonal population, with some cells having more or less burden of $JAK2^{V617F}$. XCIP assay for clonality suggested that BOECs generated were not completely polyclonal. Samples 0807-2 and 0120-1 displayed unequal band expression and 1023-2 displayed only 1 band, when digested with *Hpa*II. This suggests that BOECs were either clonal or becoming clonal in female patients. A caveat to this result is the nature of BOEC generation in culture. EPCs which give rise

to BOECs are already a rare cell population in peripheral blood and typically very few colonies give rise to BOEC cultures. This may promote clonal derivation of BOECs regardless of $JAK2^{V617F}$ status. However, it is still a relevant question to investigate, given the various ratios of $JAK2^{V617F}$ to $JAK2^{WT}$ expression in different samples. Another caveat to the XCIP assay performed in this study is the use of HUMARA over other hyper-methylated regions. The HUMARA assay is commonly used to determine clonality in myeloid malignancies, however there are other genes used in clonality assays and it is possible a different gene might be better suited for determining clonality in endothelial cells.

Phase focus microscopy allowed for the quantification of individual cell parameters which could be used to determine sample morphology, motility and proliferation. The use of ptychography to produce images according to diffraction patterns and the further analysis of these images to generate information about individual samples and cells is a relatively new technology. Therefore, development of the corresponding software and analysis programmes is ongoing. Collaborations between Phasefocus in Sheffield, UK and University of York allowed ongoing optimisation of data to investigate parameters which were important to this study.

Differences were observed in all 3 parameters among patient BOEC samples. $JAK2^{V617F}$ allelic burden appeared to correlate with a decrease in cell motility and an increase in cell size. Further, $JAK2^{V617F}$ allelic burden appeared to cause changes in cell proliferation. Samples with low or 0% mutation allelic burden displayed non-linear growth; cell counts in these samples quadrupled during the 48hr time period. Samples 0120-2 and 0806-1, 2 with higher allelic burden of $JAK2^{V617F}$ displayed no growth which is supported by the lack of fit of both linear and quadratic regression models of growth. Slopes of linear regression models were determined to be significantly different from each other and moreover, when slopes were compared to $JAK2^{V617F}$ allelic burden, linear regression analysis resulted in a significant, negative, non-zero slope. These results show that $JAK2^{V617F}$ has a negative impact on BOEC proliferation. Further, IF analysis suggests the negative effect of $JAK2^{V617F}$ on proliferation may be due to enhanced senescence or defects in mitosis. Previous reports of large, multinucleated ECs in atherosclerosis have been characterised.[261-263] Phenotypes such as these were attributed to EC senescence in atherosclerosis. This hypothesis warrants further investigation into cell cycle analysis and features of

senescence in different BOEC samples. Changes in cell morphology and motility appear to also correlate with $JAK2^{V617F}$ allelic burden; however it is not known whether allelic burden causes these changes or if they are a result of the impact of $JAK2^{V617F}$ on proliferation. Testing additional patient samples with varying levels of $JAK2^{V617F}$ allelic burden will confirm whether these changes are a direct or indirect result of mutation expression.

The data reported in this chapter includes observations and quantification from 9 different patient samples, most of which had minimal expression of $JAK2^{V617F}$. Therefore, these results can only be interpreted as a pilot study and additional samples are needed to validate the conclusions reported. There are limitations to the generation of BOECs, particularly when using samples from patients with MPNs. Firstly, previous groups report difficulty in generating BOECs from elderly patients and recommend using young patient blood samples.[79] Patients with MPNs are generally older in age, although some cases of paediatric MPNs do exist no patients in this category could be included in this study. Additionally, the phenotype of BOECs observed in this pilot study predict that patients with high $JAK2^{V617F}$ allelic burden in ECs will generate poorly proliferating BOECs. This will present many challenges to future studies because the pool of cells available for study will be limited. In particular, there are limitations to quantitative phase focus microscopy experiments performed on poorly proliferating BOECs. During experimental set-up, a specific area in the culture plate is selected for time-lapse imaging. Areas are carefully selected to accurately represent the confluence of the plate at the time, however when imaging samples that proliferate slowly it is difficult to ensure that the area selected will be representative of growth throughout the entire sample. One method to control for this would be to collect several images post-time lapse imaging from different regions, to ensure that the area imaged was representative of the sample.

There are many challenges associated with isolating human ECs for research. Different methods of cell sorting are time consuming, costly and yield small sample sizes that are often contaminated by other cell types. BOECs offer a more feasible mechanism for studying human ECs and data shows that BOECs indeed retain characteristics of mature ECs.[79,264,265] Additionally, evidence suggests that BOECs have therapeutic potential.[266,267] Future research into $JAK2^{V617F}$-positive EC

phenotype will benefit from the ability to generate expanded cell cultures of BOECs that are free from contaminating cell types.

CHAPTER 6 GENERAL DISCUSSION

ECs contribute to a variety of functions, including haemostasis, angiogenesis and vessel permeability. Consequently, aberrant EC function can have significant effects on physiological circulation. ECs are dynamic; during normal blood flow they express factors which are anti-thrombotic, helping to maintain platelet quiescence and adequate blood flow. On injury, ECs express pro-thrombotic factors and promote platelet adhesion, activation and thrombus formation. In contrast to haematopoietic cells, ECs do not proliferate continuously as they do not have to reconstitute the entire vasculature as regularly. However, they can be stimulated to proliferate during certain conditions such as angiogenesis, which can be harnessed by physiological mechanisms as in wound healing or in generation of the uterine lining during menstrual cycle or by pathological processes such as cancer.[268] Similarly, permeability of ECs can be modified to enhance or inhibit cell transmigration in response to processes such as inflammation.[269]

Patients with MPNs often suffer complications due to aberrant haemostasis and thrombosis events. These complications, manifesting as either blood clots, leading to infarction or stroke, or conversely, bleeding diatheses, can be life-threatening and so treatment is mainly focused at preventing these complications. Currently, treatment is non-specific and is limited to venesection, to decrease blood viscosity and red blood cell burden, aspirin, to inhibit platelet activation and hydroxycarbamide, to decrease cell proliferation.[270] Although effective in some patients, these treatments can have adverse effects particularly in patients who are at-risk for haemorrhagic complications. There is currently no method for stratifying patients with MPNs into groups which are at-risk for thrombosis versus haemorrhage. Therefore, global treatment for thrombosis complications may inadvertently increase risk for haemorrhagic complications in a subset of patients with MPNs. Understanding the mechanisms behind haemostasis and thrombosis complications in patients with MPNs may help to identify which patients are at risk for certain complications and may reveal new therapeutic targets.

The primary aim of this work was to elucidate the mechanisms of aberrant thrombohaemorrhagic complications in $JAK2^{V617F}$ MPNs. Secondary aims were

focused on identifying the mechanisms behind JAK2^{V617F} activation in ECs and how mutation burden affects ECs of patients with PV. The results described here have led to the development of several working hypotheses as to the mechanisms and effects of JAK2^{V617F} expression in ECs, which require further investigation.

6.1 JAK2^{V617F}-ECs are Critical in MPN Mouse Model Clot Instability

Tie2-Cre/FF1 transgenic mice exhibit an inability to form an occlusive thrombus in response to ferric chloride carotid injury or tail vein injury. Restricted expression of JAK2^{V617F} to either haematopoietic or ECs revealed that the contribution of JAK2^{V617F} expression in ECs is more important in causing this phenotype than mutant expression in haematopoietic cells. JAK2^{V617F}-haematopoietic only mice form occlusive thrombi in response to both injuries. In contrast, JAK2^{V617F}-endothelial only mice fail to form an occlusive thrombus in response to ferric chloride carotid artery injury, but form occlusive thrombi in response to tail injury. Data has shown that JAK2^{V617F}-ECs express increased levels of TFPI and CD39 and decreased levels of functional vWF. TFPI and CD39 both contribute to the anti-thrombotic surface of ECs and functional vWF is necessary for platelet adhesion during the initial phase of haemostasis.[22,57,60] Additional factors of JAK2^{V617F}-ECs likely contribute towards the observed phenotype as well.

Over the last few decades, mouse models have proven to be useful tools in studying disease in the context of a whole organism. However, an important consideration in all mouse studies must be the inherent differences between mice and humans. In particular mice and men differ in blood composition and susceptibility to thrombus formation. Compared to human platelets, mouse platelets are smaller and more numerous and contain more heterogeneous α and dense granule distribution.[271] In humans, neutrophils account for the majority of leukocytes in circulation, however in mice lymphocytes are a more common cell type.[272] Despite these inherent differences in blood composition, mouse models have proven to be indispensable tools in studying blood and thrombus formation. Gene-specific disruption in mice has led to the identification of the specific roles of agonists and receptors in platelet activation and thrombus formation.[273]

In addition to differences in blood composition, mice are intrinsically resistant to atherosclerosis, a disease of chronic inflammation and arterial thrombus formation.[274] Factors which may contribute to this are elevated heart rate, lower plasma cholesterol and elevated levels of high density lipoprotein (HDL) in mice, compared to humans. To accelerate atherosclerotic development in mice, apolipoprotein E (*apoE*) knockout mice were generated.[275] These mice have elevated cholesterol mostly in the form of low density lipoprotein (LDL), the form of lipoprotein that increases risk of cardiovascular-related complications, when fed a standard chow diet.[276] When fed a high-fat diet, *apoE*$^{-/-}$ mice develop even higher levels of LDL accumulation and suffer greater risk of developing atherosclerosis.

In the *Tie2-Cre/FF1* mouse model, the defect in thrombus propagation despite elevated platelet counts does seem paradoxical. However, experiments using chimeric mice showed that EC JAK2^{V617F} contributes more to this defect than platelet JAK2^{V617F}. Still, known differences in susceptibility to thrombus formation and atherosclerosis between mice and humans cannot be discounted. One possibility could be that, similar to atherosclerosis mouse models, haemostasis and thrombosis complications in MPN mouse models would be more aptly studied when JAK2^{V617F} expression is combined with a mouse which is more susceptible to these complications. Breeding *Tie2-Cre/FF1* mice, to *apoE*$^{-/-}$ mice, for example, would yield progeny that have JAK2^{V617F} expression in endothelial and haematopoietic cells and have a heightened susceptibility to develop atherosclerotic disease. Using *in vivo* thrombosis assays, the combined effects of JAK2^{V617F} expression and atherosclerosis on haemostasis can be determined. *ApoE*$^{-/-}$ mice on high fat diet exhibit increased thrombosis with faster occlusion times.[277] Given that *Tie2-Cre/FF1* mice have reduced thrombosis, it will be interesting to determine whether this remains true when combined with atherosclerosis development. Furthermore, atherosclerosis is a co-morbid condition in some MPN patients , therefore this model is biologically relevant to elderly patients who commonly exhibit features of both MPNs and atherosclerosis.[278]

In addition to differences between mice and humans and their ability to clot, the type of vessel and injury method used to study thrombosis in mice must be carefully considered. Several methods of vessel injury exist which include photochemical, laser, mechanical and ferric chloride induced injuries.[279,280] In the

photochemical model, a dye such as Rose Bengal is infused into mice and is activated on exposure to green light at 540nm. This causes oxidative damage to the endothelium and initiates thrombosis. Laser-induced injury is caused by direct exposure of vessels to ruby or argon-ion lasers. This technique is often coupled with fluorescently labelled platelets and intravital microscopy to visualise thrombus formation. Lastly, mechanical injury requires manual denudation of the endothelial layer and therefore might be considered the most technically challenging of the injury methods. In one model, a wire is inserted into carotid or femoral arteries using angioplasty techniques. Separately, microvascular thrombosis can be studied by collagen-epinephrine infusion, resulting in systemic thrombus formation.

All methods of injury differ quite extensively from biological vessel injury. Ferric chloride injury is the most commonly used technique, however it is considered a more severe form of injury which results in EC damage through cell necrosis.[279] Alternatively, methods which result in oxidative damage as in photochemical injury are considered to be more biologically relevant, especially when studying inflammation.[281] Still, the acute effects of both methods are not biological, as most pathological thrombus formation occurs in response to chronic inflammation or perturbations to flow. Ferric chloride remains to be one of the most commonly used techniques because equipment needed is minimal and the technique is more easily applied when compared to mechanical-induced injury models.

Despite the lack of physiological relevance of ferric chloride injury itself, thrombi which develop in response to this type of injury have been shown to be similar in structure to thrombi which develop in humans.[282] More recently, however, *in vitro* microfluidic investigation of the mechanism of ferric chloride-induced injury showed that neutralisation of charge due to Fe^{3+} in solution may result in increased interactions among blood cells, leading to aggregation.[283] These data suggest that aggregation was mainly blood cell-driven as opposed to blood cell-EC interaction driven, which is more physiologically relevant. This information does not undermine the data presented here, but may actually highlight the importance of ECs in promoting thrombus formation on injury. Vessel injury and blood cell activation indeed occurred in the *Tie2-Cre/FF1* mouse model, as evidenced by histological analysis of injured carotid arteries which displayed platelet plug formation. Therefore, ferric chloride is able to initiate thrombus

formation in *Tie2-Cre/FF1* mice; however JAK2^{V617F}-ECs are inadequate to support thrombus propagation.

Heterogeneity among ECs from different vessel types and vascular beds is known to influence location-specific mechanisms of haemostasis and thrombosis.[50,51] Data presented here describe two vessel injury models: carotid artery and tail vessel. Indeed, responses of chimeric mice to both injury types were variable. In JAK2^{V617F}-endothelial only mice, clot instability was shown in response to ferric chloride-induced carotid artery injury; however thrombus formation was unperturbed in response to tail injury. Future experiments aimed at investigating other vessel types and vascular beds will determine whether JAK2^{V617F}-ECs are anti-thrombotic globally or whether this effect is specific to the carotid artery. The effects of ferric chloride-induced carotid artery injury described in Chapter 3 were measured first by monitoring blood flow rate with a Doppler flow probe. This limited the application of the assay to vessels which fit inside the probe; as the probe used was the smallest available measuring flow rate in smaller vessels was not possible. However, the limitations of this experimental set-up can be overcome with other methods for studying thrombosis. Intravital microscopy allows direct visualisation of thrombus formation after laser-induced injury in real time.[281] Applying this technique will enable the study of JAK2^{V617F}-ECs on thrombus formation in veins and in the microcirculation.

Heterogeneity can also be investigated by isolating ECs from different vascular beds in mice. Expression of TFPI and CD39 was determined by isolating ECs from mouse lungs and lysing the cells for protein. Similar methods can be used to isolate ECs from other organs, such as the liver, spleen and heart, and RNA and protein samples can be collected from these organ-specific ECs. RNA sequencing of these samples will help identify additional changes in JAK2^{V617F} -ECs of different vascular beds and protein samples can help confirm these changes.

Section 3.1.1 discussed the development of the *FF1* mouse and its purpose for studying allelic burden of JAK2^{V617F} in MPNs. *FF1* mice were bred with both *VavCre* and interferon-inducible *MxCre* mice.[189] *VavCre/FF1* mice and *MxCre/FF1* mice treated with polyinosine-polycytosine (pIpC) were shown to have different levels of JAK2^{V617F} allelic burden, which corresponded to ET and PV disease phenotypes, respectively. It is currently not known whether allelic burden of JAK2^{V617F} in ECs

affects aberrant haemostasis and thrombosis. The presence of 9 copies of the transgene in *FF1* provide the opportunity for inducing expression of JAK2^{V617F} at varying levels when *FF1* mice are bred to inducible-*Cre* mice. To this end, *FF1* mice can be bred with *VE-cadherin-CreERT2* mice, which expresses a tamoxifen-inducible *Cre-recombinase* under the vascular endothelial cadherin promoter (*VE-cad*).[284] Investigating the effects of JAK2^{V617F} allelic burden on thrombosis are particularly relevant given the varying levels of JAK2^{V617F} allelic burden determined in the BOEC samples generated in Chapter 5.

6.2 JAK2^{V617F} -positive ECs have a Pro-inflammatory Phenotype

Inflammation is a natural response to infection or injury. Similar to haematopoiesis, inflammation is regulated by an intricate network of cytokine-receptor signalling and induction of specific gene expression patterns. One such cytokine-receptor pair involved in inflammation is IFN-γ/IFN-γR.[285] This cytokine-receptor pair transmits signal through JAK1 and JAK2 and further downstream through STAT1 homodimers. In haematopoiesis, IFN-γ is dispensable for homeostatic blood cell production; however during infection IFN-γ signalling can enhance HSC activation and differentiation of immature lymphoid cells to mature cells. During leukocyte migration, IFN-γ can enhance the production of chemokines, including CCL2. RNA sequencing data showed an increase in expression of both STAT1 and CCL2 in JAK2^{V617F}-HUVECs, which was later confirmed by western blot and qPCR, respectively.

RNA sequencing analysis of JAK2^{V617F}-HUVECs compared to JAK2^{WT}-HUVECs revealed an overall increase in genes related to inflammation. However, in the HUVEC system, lentivirus was used to generate cells which express either JAK2^{WT} or JAK2^{V617F} and it is unclear whether lenti-infection is responsible for the observed increase in inflammatory genes. To generate HUVECs with equal total JAK2 levels, larger volumes of JAK2^{V617F} lentivirus were required compared to volumes of JAK2^{WT} lentivirus. In the future, gene expression patterns of JAK2^{V617F}-HUVECs and JAK2^{WT}-HUVECs should be compared to gene expression patterns in HUVECs infected with empty lentivirus of similar volumes. Alternatively, RNA sequencing of JAK2^{V617F}-positive ECs from different organs in mice may provide insight as to whether this gene expression pattern is a result of JAK2^{V617F} expression or an artefact

of lentivirus infection. If a similar inflammatory profile is observed in JAK2^{V617F}-positive ECs obtained from mice, which would not have been exposed to lentivirus, these data would support that JAK2^{V617F} is causing the observed inflammatory gene expression profile. If a similar gene expression pattern is observed in ECs from *Tie2-Cre/FF1* mice, this may also suggest that increased inflammation contributes to the clot instability observed in the mouse model. Analysis of JAK2^{V617F}-positive ECs from mice by RNA sequencing will support or challenge this hypothesis.

EC permeability is one consequence of inflammation, allowing for transmigration of leukocytes and other myeloid cells. Thrombin, the potent platelet agonist in haemostasis, is also an agonist for EC permeability.[286] Similar to platelet activation, thrombin binds to PARs on ECs and causes a calcium ion influx, leading to cytoskeletal rearrangement and disruption of adherens junctions. Zona occludens-2 (ZO-2), also called TJP2, is important in establishing both adherens and tight junctions between ECs.[287] Increased TJP2 expression in JAK2^{V617F}-HUVECs was identified in RNA sequencing and confirmed by qPCR. *In vitro* permeability assay showed that HUVECs which expressed JAK2^{V617F} were more permeable in response to the agonist thrombin.

The effects of JAK2^{V617F} on inflammation and permeability require further investigation. *In vitro*, HUVECs expressing JAK2^{V617F} can be treated with anti-inflammatory mediators to determine if the inflammatory and permeability effects of JAK2^{V617F} can be reversed. Similarly, treatment of JAK2^{V617F}-endothelial chimeric mice with anti-inflammatory drugs would help to determine the extent to which inflammation is involved in the EC dysfunction seen in these mice. The molecular underpinnings regulating inflammation will likely require *in vitro* investigation of transduced HUVECs. IFN-γ is a promising target, as it associates with JAK2 and transmits signal through STAT1. IFN-α/β signalling should also be considered, as genes regulating these pathways were shown to be increased in JAK2^{V617F}-HUVECs in the RNA sequencing experiment. Permeability can be assessed *in vivo* by Evans Blue infusion.[288] Evans Blue dye binds albumin in serum, which is contained within vessels normally but leaks into surrounding tissues when permeability is increased. Permeability can be measured at basal levels in WT and *Tie2-Cre/FF1* mice and in injured mice. *In vitro* data suggests that effects of JAK2^{V617F} on permeability are enhanced when ECs are activated, therefore it is predicted that similar activation

through vessel injury will be required to see a difference in permeability between WT and *Tie2-Cre/FF1* mice.

Given that thrombin is a potent agonist of both platelet activation and EC permeability, and that mechanisms of both processes are connected to the inflammatory process, it is possible that JAK2^{V617F}-ECs have effects on all three processes: inflammation, permeability and haemostasis. Indeed, RNA sequencing data shows a common theme of upregulation of inflammatory mediators, *in vitro* permeability assay shows that permeability is increased and *in vivo* thrombosis assays show EC haemostasis contributions are perturbed, when JAK2^{V617F} is expressed. Further investigation into inflammation, permeability and haemostasis in the context of JAK2^{V617F} expression will make these interactions more clear.

6.3 JAK2^{V617F} Drives EC Senescence

In vitro, primary ECs have a limited proliferative capacity. Once thought to be a feature of *in vitro* culture, EC senescence has been reported as an age-related and atherosclerotic phenotype and endothelial senescence is associated with pro-thrombotic and pro-inflammatory phenotypes. [262,289,290] Among other effects, senescent ECs produce less NO and prostacyclin, two factors which are anti-thrombotic, and produce more PAI and reactive oxygen species (ROS), which are both pro-thrombotic features. In contrast, evidence shows that a subset of senescent ECs can exhibit an anti-inflammatory phenotype.[290] These effects were elicited through p38 MAPK activation and resulted in decreased sensitivity of senescent ECs to inflammatory stimuli. In general, senescent ECs (both pro- and anti-inflammatory) by definition have decreased proliferation potential, leading to a decrease in angiogenesis and endothelial repair.

Certain BOEC samples generated in Chapter 5 displayed hallmarks of EC senescence in both morphology and phenotype. Morphologically, two samples displayed large, multinucleated cells with decreased motility and proliferation. Other samples appeared to retain proliferative capacity and remained smaller in size and were singly-nucleated. A number of factors may contribute to these observed differences. As discussed, EC senescence has been reported as a feature of both increased age and atherosclerotic disease. Patients were generally older; however patients of similar ages (~65-70years) generated BOECs of both the proliferative and

senescent phenotypes. Patient co-morbidities, such as atherosclerosis, were not known and it cannot be ruled out that this may influence BOEC phenotype. Importantly, senescent ECs were only observed in patients with higher JAK2^{V617F} allelic burden. Whether mutation burden caused EC senescence remains to be proven, as more samples are needed to definitively draw this conclusion. However, it was shown that an increase in JAK2^{V617F} allelic burden decreased the proliferative potential of BOECs significantly, which is one feature of EC senescence. Given the complexity of EC senescence and the contributions of senescence to dysfunctions in haematosis and thrombosis, it is worth investigating how this phenotype contributes to MPN development and associated complications.

Senescent ECs have been identified in clinical specimens by positive β-galactosidase stain.[262] Senescence-associated β-galactosidase (SA-βgal) activity was first identified in senescent dermal cells, which is distinguishable from both proliferative and quiescent cell types.[291] The function of SA-βgal is still unknown, however it has proved to be a useful marker of senescent cells. Senescent ECs were found in regions of atherosclerotic plaque formation, in particular of regions with altered flow patterns.[292] These regions often corresponded to regions of curved vasculature, which is subjected to turbulent flow and susceptible to plaque formation. Senescence in ECs was also found to be induced by oxidative stress and hypoxia.[289,290,293] In addition to the pathophysiology of senescent ECs, reports on changes in EC morphology were quite distinctive. Of interest, reports of giant, multinucleated ECs in atherosclerotic lesions suggest that these features may be a result of EC senescence.[261,263] Additionally, permeability of senescent ECs was reported to be increased, demonstrated by *in vitro* permeability assays and decreased expression of junction proteins.[294]

Future work will focus on confirming senescence in JAK2^{V617F} ECs *in vivo* and *in vitro*. As senescent ECs in clinical specimens were identified by SA-βgal activity, a similar method can be employed to determine senescence in JAK2^{V617F}-expressing cells.[295] In this assay, the chromogenic substrate 5-bromo-4-chloro-3-indoyl β-D-galactopyranoside (X-gal) is cleaved by βgal, and lysosomal βgal activity can be distinguished from SA-βgal activity by using citric acid/sodium phosphate buffer at pH 6.0. X-gal cleavage results in the formation of a blue precipitate which

identifies senescent cells. The SA-βgal assay can be used to determine senescence in transduced HUVECs, BOECs and in vascular beds of *Tie2-Cre/FF1* mice.

Endothelial senescence has been associated with oxidative stress and turbulent shear. These factors can be induced *in vitro* to mimic stress ECs undergo *in vivo*. Agents such as ethanol, tert-butyl hydroperoxide, hydrogen peroxide and exposure to ultraviolet light have all been used to induce oxidative stress *in vitro*.[296] Shear stress can be induced by common laboratory equipment, such as orbital shakers or by more complex *in vitro* flow pumps such as the microfluidic chips produced by SynVivo.[292,297] The effects of *in vitro* induced senescence can be compared to those observed in senescent BOEC samples to provide additional support that BOECs are indeed undergoing senescence. Ultimately, additional patient samples are needed to confirm that $JAK2^{V617F}$ allelic burden causes EC senescence.

Mechanisms driving $JAK2^{V617F}$-endothelial senescence require further investigation. A good starting point for investigating signalling mechanisms regulating senescence would be to determine expression of cell cycle proteins. In particular, p16 and p53 regulated pathways have been implicated in endothelial senescence.[292,298] Cell cycle analysis of transduced HUVECs and BOEC samples would be helpful in determining the extent to which these cells are undergoing senescence. This can be accomplished through propidium iodide staining and analysis by flow cytometry.

In section 1.7, two models for $JAK2^{V617F}$ acquisition were discussed. In the first, $JAK2^{V617F}$ is acquired in the HSC, conferring a proliferative advantage to haematopoietic cells resulting in myeloproliferation. In the second model, $JAK2^{V617F}$ is acquired in a more primitive cell type, the haemangioblast, which results in both myeloproliferation and endothelial expression of $JAK2^{V617F}$. The data presented here shows that $JAK2^{V617F}$ in ECs confers a proliferative disadvantage, leading to senescence. This supports the hypothesis that $JAK2^{V617F}$ is acquired in the haemangioblast and leads to myeloproliferation and EC expression of $JAK2^{V617F}$. However, given the impact of $JAK2^{V617F}$ -endothelial expression on EC proliferation and senescence, it is suspected that $JAK2^{V617F}$ expression in ECs leads to a decrease in ECs, not expansion as would be expected for $JAK2^{V617F}$ expression in haematopoietic cells (Figure 6.1).

6.4 Translational Impact

MPNs are diseases of haematopoiesis, but often patients suffer from complications due to dysfunction in haemostasis and thrombosis. MPNs are most commonly diagnosed in older patients, and incidental diagnosis often occurs when patients experience an adverse cardiac-related event due to a blood clot or bleed. Further, certain conditions such as atherosclerosis are frequent, as these become more common as patients age. Therefore, studying MPNs in patients can become difficult because of the common occurrence of co-morbidities.

Identifying ECs as a component of dysfunctional haemostasis in *Tie2-Cre/FF1* mice emphasizes the importance of understanding the specific mechanisms of haemostasis and thrombosis complications. A common treatment for MPNs is low-dose aspirin therapy, which targets platelet cyclooxygenase. Treatment may be improved with better understanding of the mechanisms of MPN complications, which may identify therapeutic targets in other cell types or protein factors. Further, the phenotype observed in *Tie2-Cre/FF1* mice was unstable clot propagation, not increased thrombosis. Patients with MPNs are at-risk for either clotting or bleeding abnormalities and there are no current methods for stratifying patients for these separate risks. In addition to increased bleeding risks associated with anti-thrombotic treatment, the effects of platelet inhibition combined with dysfunctional endothelial cells are not currently known. Research into the specific mechanisms of haemostasis and thrombosis complications, both pro-thrombotic and anti-thrombotic, will aid in developing more accurate patient diagnoses for the complications they are most at-risk for and in identifying alternative therapeutic targets.

A previous report identified $JAK2^{V617F}$ expression in endothelial colony forming-cells from peripheral blood in patients with high risk for thrombosis complications.[218] Data presented here shows that $JAK2^{V617F}$ expression in ECs produces an anti-thrombotic phenotype in mice, however hallmarks of BOECs with

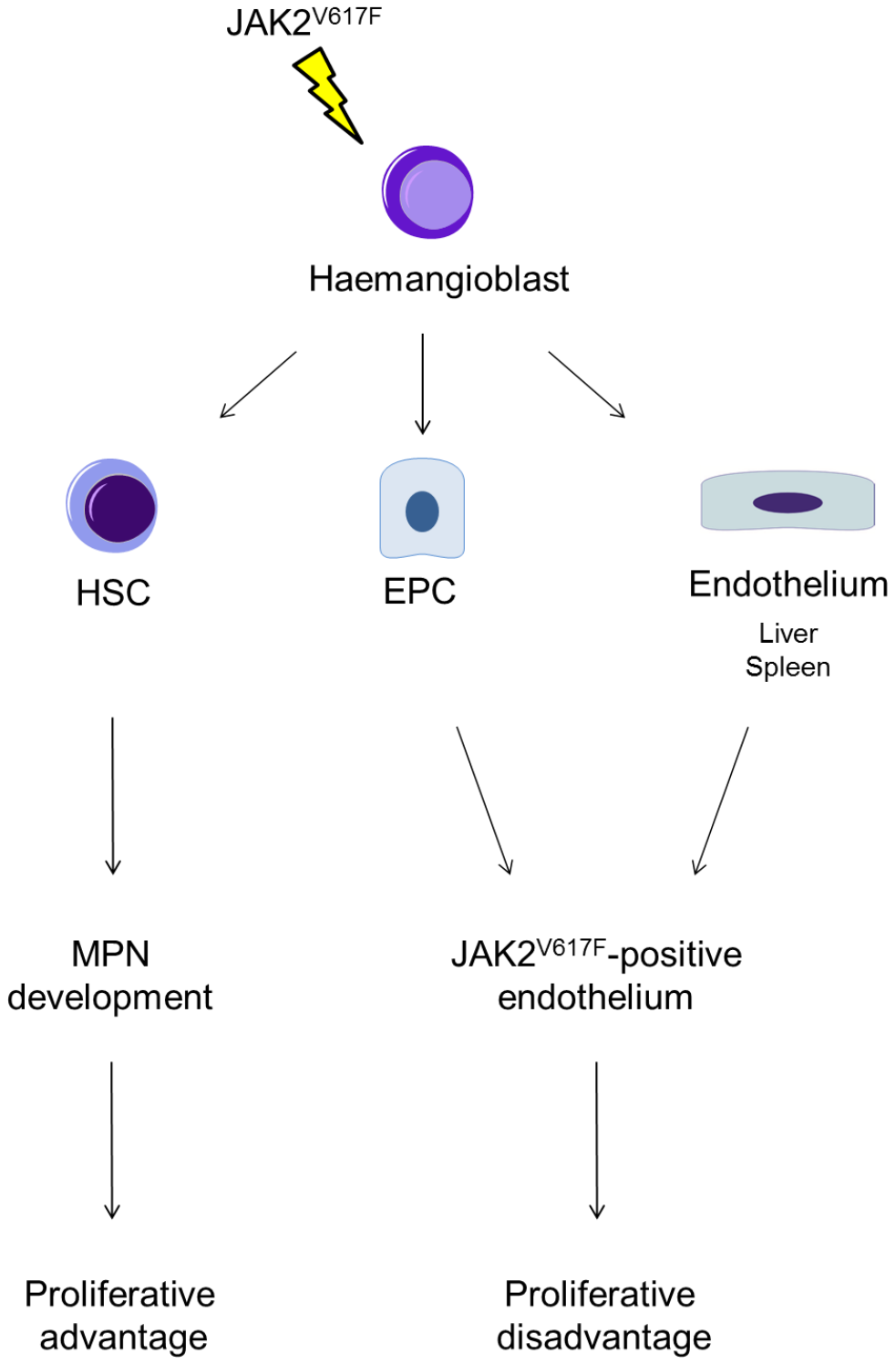

Figure 6.1 JAK2V617F expression in ECs leads to a decrease in EC proliferation

$JAK2^{V617F}$ expression has been identified in both haematopoietic and ECs, which suggests acquisition of the mutation in a primitive cell type leading to differentiation of both haematopoietic and ECs. It is known that $JAK2^{V617F}$ causes hyperproliferation of myeloid cells, which causes MPNs. However, data shows that endothelial expression of $JAK2^{V617F}$ leads to a decrease in EC proliferation and EC senescence. This suggests that EC expression $JAK2^{V617F}$ will lead to a decrease in EC numbers.

high JAK2^{V617F} allelic burden mimic ECs associated with atherosclerosis. It is possible, that similar to MPN patient variation for thrombotic or haemorrhagic risk, ECs which express JAK2^{V617F} vary in phenotype. However, if EC dysfunction, whether pro- or anti-thrombotic, is found to be dependent on JAK2^{V617F} expression patient stratification may be accomplished through screening for endothelial JAK2^{V617F}. Moreover, if allelic burden of JAK2^{V617F} is shown to have a direct correlation with increased thrombotic or haemorrhagic risk, treatment dosage can be altered accordingly. This would be especially important for younger patients who would experience life-long treatment for thrombotic or haemorrhagic risks. In these patients in particular, it might be possible to monitor JAK2^{V617F} allelic burden in ECs over time, and alter treatment accordingly. In doing this, excessive treatment would be avoided and consequently, risks for side effects would be kept at a minimum.

6.5 Concluding Remarks

Together, the work described here identifies that expression of JAK2^{V617F} in ECs causes dysfunction in this cell type. Initial experiments performed in mice showed endothelial dysfunction in response to vessel injury. Subsequent experiments *in vitro* suggested that JAK2^{V617F}-positive ECs express a pro-inflammatory phenotype and human ECs with high JAK2^{V617F} allelic burden exhibited dysfunction in growth and proliferation. Endothelial dysfunction manifested in various forms and it is unclear at the present time how dysfunction in clot stability, inflammation and proliferation are related in ECs. Previous reports of inflammation in MPNs and atherosclerosis suggest that these diseases are multi-faceted. Future studies should reflect the complexity of these diseases, investigating both the mechanisms of inflammation-induced dysfunction and the effects of inflammation on the normal function of endothelial and haematopoietic cells.

Haemostasis and thrombosis have been studied extensively on their own and in the context of many different diseases. Research into these processes has largely focused on platelets and specific coagulation factors. Sadly, ECs have for the most part been ignored. In addition to being in close proximity to blood cells, endothelial and haematopoietic cells share developmental origins. Although the concept of an adult haemangioblast remains controversial, the presence of an HSC mutation in ECs lends further support to the common developmental origin of haematopoietic and

endothelial cells. Given the similarities between endothelial and haematopoietic cell location and potential common developmental origin, the notion that both cell types work collectively to maintain physiological haemostasis and thrombosis is probable. Yet many groups ignore this cell type, its interactions with haematopoietic cells and its contributions towards haemostasis and thrombosis. The work presented here shows that not only do ECs contribute towards these functions, but they have the capacity to alter these functions, despite normal haematopoietic development. In the future, I hope that ECs are studied in more detail as their function and the underlying mechanisms driving these functions require extensive research to reach a parallel level of understanding compared to platelet functions. Further, the context of this work will apply broadly to diseases affected by dysfunctions in haemostasis and thrombosis. Research into ECs and the combined efforts of endothelial and haematopoietic cells in maintaining haemostasis and thrombosis will lead to a better understanding of how these processes can become perturbed. This will hopefully lead to more successful, targeted patient therapy, instead of blanket anti-thrombotic treatment, targeting platelets.

LIST OF SUPPLIERS

AD Instruments

Agilent Technologies

Applied Biosystems

BD Biosciences/BD Pharmingen

Beckman Coulter

BioLegend

Bio-Rad

BMG Labtech

Cellstar

Chronolog

Clontech

Dako

Denville Scientific

Drew Scientific Group, Erba Diagnostics, Inc

eBioscience

Eurofins Genomics

Enzyme Research Laboratories

GE Healthcare Life Sciences

Genesig

Goldenrod, MEDIpoint, Inc.

Jackson Laboratory

Life Technologies/Invitrogen

Lonza

Melford Technologies

Millipore

Miltenyi Biotec

Molecular Probes

New England Biolabs

Phasefocus

Promocell

QED Bioscience

Qiagen

Roche

Sarstedt

Scientific Laboratory Supplies

Severn Biotec Ltd.

Sigma

STEMCELL Technologies Inc.

Stovall

Syngene Bio Imaging System

Thermo Scientific

Transonic Systems Inc.

Vector Laboratories, Inc.

VWR

LIST OF ABBREVIATIONS

A

ACB-PCR	Allele-specific Competitive Blocker PCR
ADAMTS13	a disintegrin-like and metalloprotease domain with thrombospondin type-1 motif, number 13
ADP	adenosine diphosphate
AML	acute myeloid leukaemia
AMP	adenosine monophosphate
ANOVA	analysis of variance
APC	activated protein C
apoE	apolipoprotein E
AT	antithrombin
AvWD	acquired von Willebrand Disease

B

BHF	British Heart Foundation
BL-CFC	blast colony-forming cell
BOEC	blood outgrowth endothelial cell
BCR-ABL	break point cluster-Abelson tyrosine kinase
BCS	Budd Chiari Syndrome
BSA	bovine serum albumin

C

CALR	calreticulin

CCL2	chemokine ligand 2
CD39	ecto-ADPase
CDCP1	CUB domain containing protein 1
CEC	circulating EC
CEL	chronic eosinophilic leukaemia
CFU	colony forming unit
CML	chronic myelogenous leukaemia
CNL	chronic neutrophilic leukaemia
COX	cyclooxygenase

D

dHSC	definitive haematopoietic stem cell
DIC	disseminated intravascular coagulation
DLAR	Division of Laboratory Animal Resources
DMEM	Dulbecco's Modified Eagle Medium
DPBS	Dulbecco's Phosphate-Buffered Saline
DSP	dithiobis (succinimidylpropionate)
DVT	deep vein thrombosis

E

EC	endothelial cell
ECL	enhanced chemiluminescent
EDHP	endothelium derived hyperpolarizing factor
EMP	erythroid/myeloid progenitor
eNOS	endothelial NO synthase
EPCR	endothelial protein C receptor

EPO	erythropoietin
ET	essential thrombocythaemia
ET-1	endothelin-1

F

FBS	foetal bovine serum
FERM	4.1/ezrin/radixin/moesin
FF1	Flip-flop 1

G

G	L-glutamine
GH	growth hormone
GP	glycoprotein

H

HAEC	human aortic endothelial cell
HDL	high density lipoprotein
HEK293T	human embryonic kidney 293T cells
HEL	human erythroleukaemia cells
HMRN	Haematological Malignancy Research Network
HSC	haematopoietic stem cell
HUMARA	human androgen receptor gene
HUVEC	human umbilical vein endothelial cell

I

IACUC	Institutional Animal Care and Use Committee

ICAM-1	intercellular adhesion molecule-1
IF	immunofluorescence
IFN	interferon
IL	interleukin

J

JAK2	Janus kinase 2
JAK-STAT	Janus kinase-signal transducers and activators of transcription
JH	JAK homology

L

LDL	low density lipoprotein
LIFR	leukaemia inhibitory factor receptor
LOH	loss of heterozygosity

M

MACS	magnetic activated cell sorting
MEP	megakaryocyte/erythroid progenitor
MPN	myeloproliferative neoplasm

N

NO	nitric oxide
NP-40	nonidet P-40

O

OSMR	oncostatin M receptor

P

PAF	platelet activating factor
PAGE	polyacrylamide gel electrophoresis
PAR	protease-activated receptor
PBMC	peripheral blood mononuclear cells
PC	protein C
PCR	polymerase chain reaction
PE	pulmonary embolism
PECAM	platelet endothelial cell adhesion molecule
PGI2	prostacyclin
PH	pleckstrin homology
PMF	primary myelofibrosis
PTP1B	protein-tyrosine phosphatase 1B
PRP	platelet rich plasma
PS	penicillin-streptomycin
PV	polycythaemia vera
PVDF	polyvinylidene difluoride
PVSG	Polycythemia Vera Study Group

Q

qPCR	quantitative polymerase chain reaction
QuASA	quantitative allele specific amplification

R

RIPA	radioimmunoprecipitation assay

ROS	reactive oxygen species

S

SA-βgal	senescence-associated β-galactosidase
SCF	stem cell factor
SDS	sodium dodecyl sulfate
Serpin	serine protease inhibitor
SH2	Src homology 2
SHP	Src homology region 2 domain-containing phosphatase
SLE	systemic lupus erythematosus
SOCS	suppressor of cytokine signalling
STAT	signal transducers and activators of transcription

T

TAFI	thrombin-activatable fibrinolysis inhibitor
TBST	tris-buffered saline, 0.1% Tween-20
TET2	tet methylcytosine dioxygenase 2
TF	tissue factor
TFPI	tissue factor pathway inhibitor
TIE2	tunica intima endothelial kinase 2
TIRF	total internal reflection fluorescence
TJP2	tight junction protein 2
TM	thrombomodulin
TNF	tumour necrosis factor
tPA	tissue-type plasminogen activator
TPO	thrombopoietin

TxA2	thromboxane

U

UK	urokinase

V

VCAM-1	vascular cell adhesion molecule-1
VEGF	vascular endothelial growth factor
VEGFR	vascular endothelial growth factor receptor
VTE	venous thromboembolism
vWF	von Willebrand Factor

W

WT	wild-type

X

X-gal	5-bromo-4-chloro-3-indoyl β-D-galactopyranoside
XL10	XL10 Gold Ultracompetent cells
XCIP	X-chromosome inactivation pattern

Y

YTB	York Tissue Bank

Z

ZO-2	zona occludens-2

β-ME	2-mercaptoethanol

REFERENCES

1. Kyrle PA, Eichinger S. Is Virchow's triad complete? *Blood*. 2009;114(6):1138-1139.
2. Smalberg JH, Kruip MJ, Janssen HL, Rijken DC, Leebeek FW, de Maat MP. Hypercoagulability and hypofibrinolysis and risk of deep vein thrombosis and splanchnic vein thrombosis: similarities and differences. *Arterioscler Thromb Vasc Biol*. 2011;31(3):485-493.
3. Previtali E, Bucciarelli P, Passamonti SM, Martinelli I. Risk factors for venous and arterial thrombosis. *Blood Transfus*. 2011;9(2):120-138.
4. Franchini M, Mannucci PM. Venous and arterial thrombosis: different sides of the same coin? *Eur J Intern Med*. 2008;19(7):476-481.
5. Arboix A, Alio J. Cardioembolic stroke: clinical features, specific cardiac disorders and prognosis. *Curr Cardiol Rev*. 2010;6(3):150-161.
6. Righini M, Robert-Ebadi H, Le Gal G. Diagnosis of pulmonary embolism. *Presse Med*. 2015;44(12 Pt 2):e385-391.
7. Keaney J, Campbell M. The dynamic blood-brain barrier. *FEBS J*. 2015;282(21):4067-4079.
8. Boender J, Kruip MJ, Leebeek FW. A diagnostic approach to mild bleeding disorders. *J Thromb Haemost*. 2016.
9. Michiels JJ, Budde U, van der Planken M, van Vliet HH, Schroyens W, Berneman Z. Acquired von Willebrand syndromes: clinical features, aetiology, pathophysiology, classification and management. *Best Pract Res Clin Haematol*. 2001;14(2):401-436.
10. Townsend N, Bhatnagar P, Wilkins E, Wickramasinghe K, Rayner M. Cardiovascular Disease Statistics 2015. Vol. 146: British Heart Foundation; 2015.
11. Victor J. Marder WCA, Joel S. Bennett, Sam Schulman, Gilbert C. White, II. Hemostasis and Thrombosis (ed 6). Philadelphia, PA: Lippincott Williams & Wilkins, a Wolters Kluwer business; 2013.
12. Wang C, Luo Z, Kohan D, et al. Thromboxane prostanoid receptors enhance contractions, endothelin-1, and oxidative stress in microvessels from mice with chronic kidney disease. *Hypertension*. 2015;65(5):1055-1063.
13. Cohen RA. The role of nitric oxide and other endothelium-derived vasoactive substances in vascular disease. *Prog Cardiovasc Dis*. 1995;38(2):105-128.

14. Kaushansky K. Determinants of platelet number and regulation of thrombopoiesis. *Hematology Am Soc Hematol Educ Program*. 2009:147-152.

15. Italiano JE, Jr., Shivdasani RA. Megakaryocytes and beyond: the birth of platelets. *J Thromb Haemost*. 2003;1(6):1174-1182.

16. Reininger AJ. Function of von Willebrand factor in haemostasis and thrombosis. *Haemophilia*. 2008;14 Suppl 5:11-26.

17. Chen J, Lopez JA. Interactions of platelets with subendothelium and endothelium. *Microcirculation*. 2005;12(3):235-246.

18. Kanaji S, Fahs SA, Shi Q, Haberichter SL, Montgomery RR. Contribution of platelet vs. endothelial VWF to platelet adhesion and hemostasis. *J Thromb Haemost*. 2012;10(8):1646-1652.

19. Lopes da Silva M, Cutler DF. Von Willebrand Factor multimerization and the polarity of secretory pathways in endothelial cells. *Blood*. 2016.

20. Farndale RW, Sixma JJ, Barnes MJ, de Groot PG. The role of collagen in thrombosis and hemostasis. *J Thromb Haemost*. 2004;2(4):561-573.

21. Rand JH, Glanville RW, Wu XX, et al. The significance of subendothelial von Willebrand factor. *Thromb Haemost*. 1997;78(1):445-450.

22. Hassan MI, Saxena A, Ahmad F. Structure and function of von Willebrand factor. *Blood Coagul Fibrinolysis*. 2012;23(1):11-22.

23. De Ceunynck K, De Meyer SF, Vanhoorelbeke K. Unwinding the von Willebrand factor strings puzzle. *Blood*. 2013;121(2):270-277.

24. Massberg S, Gawaz M, Gruner S, et al. A crucial role of glycoprotein VI for platelet recruitment to the injured arterial wall in vivo. *J Exp Med*. 2003;197(1):41-49.

25. Gardner JM, Hynes RO. Interaction of fibronectin with its receptor on platelets. *Cell*. 1985;42(2):439-448.

26. Piotrowicz RS, Orchekowski RP, Nugent DJ, Yamada KY, Kunicki TJ. Glycoprotein Ic-IIa functions as an activation-independent fibronectin receptor on human platelets. *J Cell Biol*. 1988;106(4):1359-1364.

27. Kyriakides TR, Zhu YH, Smith LT, et al. Mice that lack thrombospondin 2 display connective tissue abnormalities that are associated with disordered collagen fibrillogenesis, an increased vascular density, and a bleeding diathesis. *J Cell Biol*. 1998;140(2):419-430.

28. Inoue O, Suzuki-Inoue K, McCarty OJ, et al. Laminin stimulates spreading of platelets through integrin alpha6beta1-dependent activation of GPVI. *Blood*. 2006;107(4):1405-1412.

29. Savage B, Saldivar E, Ruggeri ZM. Initiation of platelet adhesion by arrest onto fibrinogen or translocation on von Willebrand factor. *Cell*. 1996;84(2):289-297.

30. Golebiewska EM, Poole AW. Platelet secretion: From haemostasis to wound healing and beyond. *Blood Rev*. 2015;29(3):153-162.

31. Davie EW, Fujikawa K, Kisiel W. The coagulation cascade: initiation, maintenance, and regulation. *Biochemistry*. 1991;30(43):10363-10370.

32. Longstaff C, Kolev K. Basic mechanisms and regulation of fibrinolysis. *J Thromb Haemost*. 2015;13 Suppl 1:S98-105.

33. Levin EG, Loskutoff DJ. Cultured bovine endothelial cells produce both urokinase and tissue-type plasminogen activators. *J Cell Biol*. 1982;94(3):631-636.

34. Booth NA, Walker E, Maughan R, Bennett B. Plasminogen activator in normal subjects after exercise and venous occlusion: t-PA circulates as complexes with C1-inhibitor and PAI-1. *Blood*. 1987;69(6):1600-1604.

35. Larsson LI, Skriver L, Nielsen LS, Grondahl-Hansen J, Kristensen P, Dano K. Distribution of urokinase-type plasminogen activator immunoreactivity in the mouse. *J Cell Biol*. 1984;98(3):894-903.

36. Grau E, Moroz LA. Fibrinolytic activity of normal human blood monocytes. *Thromb Res*. 1989;53(2):145-162.

37. Manchanda N, Schwartz BS. Lipopolysaccharide-induced modulation of human monocyte urokinase production and activity. *J Immunol*. 1990;145(12):4174-4180.

38. Gross BS, Melford SK, Watson SP. Evidence that phospholipase C-gamma2 interacts with SLP-76, Syk, Lyn, LAT and the Fc receptor gamma-chain after stimulation of the collagen receptor glycoprotein VI in human platelets. *Eur J Biochem*. 1999;263(3):612-623.

39. Nieswandt B, Brakebusch C, Bergmeier W, et al. Glycoprotein VI but not alpha2beta1 integrin is essential for platelet interaction with collagen. *EMBO J*. 2001;20(9):2120-2130.

40. Bennett JS. Structure and function of the platelet integrin alphaIIbbeta3. *J Clin Invest*. 2005;115(12):3363-3369.

41. Kahn ML, Zheng YW, Huang W, et al. A dual thrombin receptor system for platelet activation. *Nature*. 1998;394(6694):690-694.

42. Kahn ML, Nakanishi-Matsui M, Shapiro MJ, Ishihara H, Coughlin SR. Protease-activated receptors 1 and 4 mediate activation of human platelets by thrombin. *J Clin Invest*. 1999;103(6):879-887.

43. Hechler B, Gachet C. P2 receptors and platelet function. *Purinergic Signal*. 2011;7(3):293-303.

44. Hirata M, Hayashi Y, Ushikubi F, et al. Cloning and expression of cDNA for a human thromboxane A2 receptor. *Nature*. 1991;349(6310):617-620.

45. Newman KD, Williams LT, Bishopric NH, Lefkowitz RJ. Identification of alpha-adrenergic receptors in human platelets by [3H]dihydroergocryptine binding. *J Clin Invest*. 1978;61(2):395-402.

46. Blair P, Flaumenhaft R. Platelet alpha-granules: basic biology and clinical correlates. *Blood Rev*. 2009;23(4):177-189.

47. Whiteheart SW. Platelet granules: surprise packages. *Blood*. 2011;118(5):1190-1191.

48. Furie B, Furie BC. Role of platelet P-selectin and microparticle PSGL-1 in thrombus formation. *Trends Mol Med*. 2004;10(4):171-178.

49. Gutensohn K, Geidel K, Brockmann M, et al. Binding of activated platelets to WBCs in vivo after transfusion. *Transfusion*. 2002;42(10):1373-1380.

50. Aird WC. Phenotypic heterogeneity of the endothelium: I. Structure, function, and mechanisms. *Circ Res*. 2007;100(2):158-173.

51. Aird WC. Phenotypic heterogeneity of the endothelium: II. Representative vascular beds. *Circ Res*. 2007;100(2):174-190.

52. Rondaij MG, Bierings R, Kragt A, van Mourik JA, Voorberg J. Dynamics and plasticity of Weibel-Palade bodies in endothelial cells. *Arterioscler Thromb Vasc Biol*. 2006;26(5):1002-1007.

53. Camussi G, Aglietta M, Malavasi F, et al. The release of platelet-activating factor from human endothelial cells in culture. *J Immunol*. 1983;131(5):2397-2403.

54. Liao JK. Linking endothelial dysfunction with endothelial cell activation. *J Clin Invest*. 2013;123(2):540-541.

55. Bajzar L. Thrombin activatable fibrinolysis inhibitor and an antifibrinolytic pathway. *Arterioscler Thromb Vasc Biol*. 2000;20(12):2511-2518.

56. Handt S, Jerome WG, Tietze L, Hantgan RR. Plasminogen activator inhibitor-1 secretion of endothelial cells increases fibrinolytic resistance of an in vitro fibrin clot: evidence for a key role of endothelial cells in thrombolytic resistance. *Blood*. 1996;87(10):4204-4213.

57. Wood JP, Ellery PE, Maroney SA, Mast AE. Biology of tissue factor pathway inhibitor. *Blood*. 2014;123(19):2934-2943.

58. Vincent LM, Tran S, Livaja R, Bensend TA, Milewicz DM, Dahlback B. Coagulation factor V(A2440G) causes east Texas bleeding disorder via TFPIalpha. *J Clin Invest*. 2013;123(9):3777-3787.

59. Marcus AJ, Broekman MJ, Drosopoulos JH, et al. The endothelial cell ecto-ADPase responsible for inhibition of platelet function is CD39. *J Clin Invest*. 1997;99(6):1351-1360.

60. Huttinger ZM, Milks MW, Nickoli MS, et al. Ectonucleotide triphosphate diphosphohydrolase-1 (CD39) mediates resistance to occlusive arterial thrombus formation after vascular injury in mice. *Am J Pathol*. 2012;181(1):322-333.

61. Levin EG, Santell L, Osborn KG. The expression of endothelial tissue plasminogen activator in vivo: a function defined by vessel size and anatomic location. *J Cell Sci*. 1997;110 (Pt 2):139-148.

62. Levin EG, Marzec U, Anderson J, Harker LA. Thrombin stimulates tissue plasminogen activator release from cultured human endothelial cells. *J Clin Invest*. 1984;74(6):1988-1995.

63. Gurewich V. Thrombolysis: A Critical First-Line Therapy with an Unfulfilled Potential. *Am J Med*. 2016;129(6):573-575.

64. Ornaghi S, Barnhart KT, Frieling J, Streisand J, Paidas MJ. Clinical syndromes associated with acquired antithrombin deficiency via microvascular leakage and the related risk of thrombosis. *Thromb Res*. 2014;133(6):972-984.

65. Thiyagarajan M, Cheng T, Zlokovic BV. Endothelial cell protein C receptor: role beyond endothelium? *Circ Res*. 2007;100(2):155-157.

66. Traub O, Berk BC. Laminar shear stress: mechanisms by which endothelial cells transduce an atheroprotective force. *Arterioscler Thromb Vasc Biol*. 1998;18(5):677-685.

67. Bark DL, Jr., Ku DN. Wall shear over high degree stenoses pertinent to atherothrombosis. *J Biomech*. 2010;43(15):2970-2977.

68. Ku DN, Giddens DP, Zarins CK, Glagov S. Pulsatile flow and atherosclerosis in the human carotid bifurcation. Positive correlation between plaque location and low oscillating shear stress. *Arteriosclerosis*. 1985;5(3):293-302.

69. Armulik A, Genové G, Mäe M, et al. Pericytes regulate the blood-brain barrier. *Nature*. 2010;468(7323):557-561.

70. Tkachenko E, Tse D, Sideleva O, et al. Caveolae, fenestrae and transendothelial channels retain PV1 on the surface of endothelial cells. *PLoS One*. 2012;7(3):e32655.

71. Yamamoto K, de Waard V, Fearns C, Loskutoff DJ. Tissue distribution and regulation of murine von Willebrand factor gene expression in vivo. *Blood*. 1998;92(8):2791-2801.

72. Asahara T, Murohara T, Sullivan A, et al. Isolation of putative progenitor endothelial cells for angiogenesis. *Science*. 1997;275(5302):964-967.

73. Takahashi M, Matsuoka Y, Sumide K, et al. CD133 is a positive marker for a distinct class of primitive human cord blood-derived

CD34-negative hematopoietic stem cells. *Leukemia*. 2014;28(6):1308-1315.

74. Yoder MC. Human endothelial progenitor cells. *Cold Spring Harb Perspect Med*. 2012;2(7):a006692.

75. Bogoslovsky T, Wang D, Maric D, et al. Cryopreservation and Enumeration of Human Endothelial Progenitor and Endothelial Cells for Clinical Trials. *J Blood Disord Transfus*. 2013;4(5).

76. Hristov M, Erl W, Weber PC. Endothelial progenitor cells: mobilization, differentiation, and homing. *Arterioscler Thromb Vasc Biol*. 2003;23(7):1185-1189.

77. Hill JM, Zalos G, Halcox JP, et al. Circulating endothelial progenitor cells, vascular function, and cardiovascular risk. *N Engl J Med*. 2003;348(7):593-600.

78. Basile DP, Yoder MC. Circulating and tissue resident endothelial progenitor cells. *J Cell Physiol*. 2014;229(1):10-16.

79. Ormiston ML, Toshner MR, Kiskin FN, et al. Generation and Culture of Blood Outgrowth Endothelial Cells from Human Peripheral Blood. *J Vis Exp*. 2015(106).

80. Schmidt DE, Manca M, Hoefer IE. Circulating endothelial cells in coronary artery disease and acute coronary syndrome. *Trends Cardiovasc Med*. 2015;25(7):578-587.

81. Goon PK, Lip GY, Boos CJ, Stonelake PS, Blann AD. Circulating endothelial cells, endothelial progenitor cells, and endothelial microparticles in cancer. *Neoplasia*. 2006;8(2):79-88.

82. Kraan J, Strijbos MH, Sieuwerts AM, et al. A new approach for rapid and reliable enumeration of circulating endothelial cells in patients. *J Thromb Haemost*. 2012;10(5):931-939.

83. Hirschi KK. Hemogenic endothelium during development and beyond. *Blood*. 2012;119(21):4823-4827.

84. Goldie LC, Lucitti JL, Dickinson ME, Hirschi KK. Cell signaling directing the formation and function of hemogenic endothelium during murine embryogenesis. *Blood*. 2008;112(8):3194-3204.

85. Kennedy M, Firpo M, Choi K, et al. A common precursor for primitive erythropoiesis and definitive haematopoiesis. *Nature*. 1997;386(6624):488-493.

86. Choi K, Kennedy M, Kazarov A, Papadimitriou JC, Keller G. A common precursor for hematopoietic and endothelial cells. *Development*. 1998;125(4):725-732.

87. Gordon-Keylock S, Sobiesiak M, Rybtsov S, Moore K, Medvinsky A. Mouse extraembryonic arterial vessels harbor precursors capable of maturing into definitive HSCs. *Blood*. 2013;122(14):2338-2345.

88. Rhodes KE, Gekas C, Wang Y, et al. The emergence of hematopoietic stem cells is initiated in the placental vasculature in the absence of circulation. *Cell Stem Cell*. 2008;2(3):252-263.

89. Zovein AC, Hofmann JJ, Lynch M, et al. Fate tracing reveals the endothelial origin of hematopoietic stem cells. *Cell Stem Cell*. 2008;3(6):625-636.

90. Loges S, Fehse B, Brockmann MA, et al. Identification of the adult human hemangioblast. *Stem Cells Dev*. 2004;13(3):229-242.

91. Sun Z, Zhang Y, Brunt KR, et al. An adult uterine hemangioblast: evidence for extramedullary self-renewal and clonal bilineage potential. *Blood*. 2010;116(16):2932-2941.

92. Lancrin C, Sroczynska P, Stephenson C, Allen T, Kouskoff V, Lacaud G. The haemangioblast generates haematopoietic cells through a haemogenic endothelium stage. *Nature*. 2009;457(7231):892-895.

93. Chen MJ, Li Y, De Obaldia ME, et al. Erythroid/myeloid progenitors and hematopoietic stem cells originate from distinct populations of endothelial cells. *Cell Stem Cell*. 2011;9(6):541-552.

94. Waters MJ, Brooks AJ. JAK2 activation by growth hormone and other cytokines. *Biochem J*. 2015;466(1):1-11.

95. Guilluy C, Bregeon J, Toumaniantz G, et al. The Rho exchange factor Arhgef1 mediates the effects of angiotensin II on vascular tone and blood pressure. *Nat Med*. 2010;16(2):183-190.

96. Banes-Berceli AK, Ketsawatsomkron P, Ogbi S, Patel B, Pollock DM, Marrero MB. Angiotensin II and endothelin-1 augment the vascular complications of diabetes via JAK2 activation. *Am J Physiol Heart Circ Physiol*. 2007;293(2):H1291-1299.

97. Yang P, Zhang Y, Pang J, et al. Loss of Jak2 impairs endothelial function by attenuating Raf-1/MEK1/Sp-1 signaling along with altered eNOS activities. *Am J Pathol*. 2013;183(2):617-625.

98. Wang JC, Bennett M. Aging and atherosclerosis: mechanisms, functional consequences, and potential therapeutics for cellular senescence. *Circ Res*. 2012;111(2):245-259.

99. Riva N, Donadini MP, Ageno W. Epidemiology and pathophysiology of venous thromboembolism: similarities with atherothrombosis and the role of inflammation. *Thromb Haemost*. 2015;113(6):1176-1183.

100. Palta S, Saroa R, Palta A. Overview of the coagulation system. *Indian J Anaesth*. 2014;58(5):515-523.

101. Levin A, Djurdjev O, Barrett B, et al. Cardiovascular disease in patients with chronic kidney disease: getting to the heart of the matter. *Am J Kidney Dis*. 2001;38(6):1398-1407.

102. Castillo R, Lozano T, Escolar G, Revert L, Lopez J, Ordinas A. Defective platelet adhesion on vessel subendothelium in uremic patients. *Blood*. 1986;68(2):337-342.

103. Falanga A, Panova-Noeva M, Russo L. Procoagulant mechanisms in tumour cells. *Best Pract Res Clin Haematol*. 2009;22(1):49-60.

104. Rice GE, Bevilacqua MP. An inducible endothelial cell surface glycoprotein mediates melanoma adhesion. *Science*. 1989;246(4935):1303-1306.

105. Hajjar KA. Cellular receptors in the regulation of plasmin generation. *Thromb Haemost*. 1995;74(1):294-301.

106. Levi M. Disseminated intravascular coagulation in cancer patients. *Best Pract Res Clin Haematol*. 2009;22(1):129-136.

107. Dameshek W. Some speculations on the myeloproliferative syndromes. *Blood*. 1951;6(4):372-375.

108. Vardiman JW, Thiele J, Arber DA, et al. The 2008 revision of the World Health Organization (WHO) classification of myeloid neoplasms and acute leukemia: rationale and important changes. *Blood*. 2009;114(5):937-951.

109. Haar JL, Ackerman GA. A phase and electron microscopic study of vasculogenesis and erythropoiesis in the yolk sac of the mouse. *Anat Rec*. 1971;170(2):199-223.

110. Medvinsky A, Dzierzak E. Definitive hematopoiesis is autonomously initiated by the AGM region. *Cell*. 1996;86(6):897-906.

111. Muller AM, Medvinsky A, Strouboulis J, Grosveld F, Dzierzak E. Development of hematopoietic stem cell activity in the mouse embryo. *Immunity*. 1994;1(4):291-301.

112. Boulais PE, Frenette PS. Making sense of hematopoietic stem cell niches. *Blood*. 2015;125(17):2621-2629.

113. Takahama Y. Journey through the thymus: stromal guides for T-cell development and selection. *Nat Rev Immunol*. 2006;6(2):127-135.

114. Akashi K, Reya T, Dalma-Weiszhausz D, Weissman IL. Lymphoid precursors. *Curr Opin Immunol*. 2000;12(2):144-150.

115. Cao X, Shores EW, Hu-Li J, et al. Defective lymphoid development in mice lacking expression of the common cytokine receptor gamma chain. *Immunity*. 1995;2(3):223-238.

116. Zhu J, Emerson SG. Hematopoietic cytokines, transcription factors and lineage commitment. *Oncogene*. 2002;21(21):3295-3313.

117. Ikonomi P, Rivera CE, Riordan M, Washington G, Schechter AN, Noguchi CT. Overexpression of GATA-2 inhibits erythroid and promotes megakaryocyte differentiation. *Exp Hematol*. 2000;28(12):1423-1431.

118. Parganas E, Wang D, Stravopodis D, et al. Jak2 is essential for signaling through a variety of cytokine receptors. *Cell*. 1998;93(3):385-395.

119. Nowell PC. Discovery of the Philadelphia chromosome: a personal perspective. *J Clin Invest*. 2007;117(8):2033-2035.

120. Druker BJ, Tamura S, Buchdunger E, et al. Effects of a selective inhibitor of the Abl tyrosine kinase on the growth of Bcr-Abl positive cells. *Nat Med*. 1996;2(5):561-566.

121. Titmarsh GJ, Duncombe AS, McMullin MF, et al. How common are myeloproliferative neoplasms? A systematic review and meta-analysis. *Am J Hematol*. 2014;89(6):581-587.

122. Hofmann I. Myeloproliferative Neoplasms in Children. *J Hematop*. 2015;8(3):143-157.

123. Stein BL, Williams DM, Wang NY, et al. Sex differences in the JAK2 V617F allele burden in chronic myeloproliferative disorders. *Haematologica*. 2010;95(7):1090-1097.

124. Mesa RA, Niblack J, Wadleigh M, et al. The burden of fatigue and quality of life in myeloproliferative disorders (MPDs): an international Internet-based survey of 1179 MPD patients. *Cancer*. 2007;109(1):68-76.

125. Falanga A, Marchetti M. Thrombotic disease in the myeloproliferative neoplasms. *Hematology Am Soc Hematol Educ Program*. 2012;2012:571-581.

126. Kiladjian JJ, Cervantes F, Leebeek FW, et al. The impact of JAK2 and MPL mutations on diagnosis and prognosis of splanchnic vein thrombosis: a report on 241 cases. *Blood*. 2008;111(10):4922-4929.

127. Turitto VT, Weiss HJ. Red blood cells: their dual role in thrombus formation. *Science*. 1980;207(4430):541-543.

128. Brown MM, Wade JP, Marshall J. Fundamental importance of arterial oxygen content in the regulation of cerebral blood flow in man. *Brain*. 1985;108 (Pt 1):81-93.

129. Barbui T, Finazzi MC, Finazzi G. Front-line therapy in polycythemia vera and essential thrombocythemia. *Blood Rev*. 2012;26(5):205-211.

130. Landolfi R, Ciabattoni G, Patrignani P, et al. Increased thromboxane biosynthesis in patients with polycythemia vera: evidence for aspirin-suppressible platelet activation in vivo. *Blood*. 1992;80(8):1965-1971.

131. Rocca B, Ciabattoni G, Tartaglione R, et al. Increased thromboxane biosynthesis in essential thrombocythemia. *Thromb Haemost*. 1995;74(5):1225-1230.

132. Musolino C, Alonci A, Bellomo G, et al. Myeloproliferative Disease: Markers of Endothelial and Platelet Status in Patients with Essential Thrombocythemia and Polycythemia Vera. *Hematology*. 2000;4(5):397-402.

133. Falanga A, Marchetti M, Evangelista V, et al. Polymorphonuclear leukocyte activation and hemostasis in patients with essential thrombocythemia and polycythemia vera. *Blood*. 2000;96(13):4261-4266.

134. Maldonado JE, Pintado T, Pierre RV. Dysplastic platelets and circulating megakaryocytes in chronic myeloproliferative diseases. I.

The platelets: ultrastructure and peroxidase reaction. *Blood*. 1974;43(6):797-809.

135. Gordon N, Thom J, Cole C, Baker R. Rapid detection of hereditary and acquired platelet storage pool deficiency by flow cytometry. *Br J Haematol*. 1995;89(1):117-123.

136. Berger S, Aledort LM, Gilbert HS, Hanson JP, Wasserman LR. Abnormalities of platelet function in patients with polycythemia vera. *Cancer Res*. 1973;33(11):2683-2687.

137. Le Blanc K, Lindahl T, Rosendahl K, Samuelsson J. Impaired platelet binding of fibrinogen due to a lower number of GPIIB/IIIA receptors in polycythemia vera. *Thromb Res*. 1998;91(6):287-295.

138. Budde U, Schaefer G, Mueller N, et al. Acquired von Willebrand's disease in the myeloproliferative syndrome. *Blood*. 1984;64(5):981-985.

139. Budde U, Dent JA, Berkowitz SD, Ruggeri ZM, Zimmerman TS. Subunit composition of plasma von Willebrand factor in patients with the myeloproliferative syndrome. *Blood*. 1986;68(6):1213-1217.

140. Tefferi A, Pardanani A. Myeloproliferative Neoplasms: A Contemporary Review. *JAMA Oncol*. 2015;1(1):97-105.

141. Geyer HL, Mesa RA. Therapy for myeloproliferative neoplasms: when, which agent, and how? *Hematology Am Soc Hematol Educ Program*. 2014;2014(1):277-286.

142. Vainchenker W, Delhommeau F, Constantinescu SN, Bernard OA. New mutations and pathogenesis of myeloproliferative neoplasms. *Blood*. 2011;118(7):1723-1735.

143. Klampfl T, Gisslinger H, Harutyunyan AS, et al. Somatic mutations of calreticulin in myeloproliferative neoplasms. *N Engl J Med*. 2013;369(25):2379-2390.

144. Nangalia J, Massie CE, Baxter EJ, et al. Somatic CALR mutations in myeloproliferative neoplasms with nonmutated JAK2. *N Engl J Med*. 2013;369(25):2391-2405.

145. Elf S, Abdelfattah NS, Chen E, et al. Mutant Calreticulin Requires Both Its Mutant C-terminus and the Thrombopoietin Receptor for Oncogenic Transformation. *Cancer Discov*. 2016;6(4):368-381.

146. Staerk J, Lacout C, Sato T, Smith SO, Vainchenker W, Constantinescu SN. An amphipathic motif at the transmembrane-cytoplasmic junction prevents autonomous activation of the thrombopoietin receptor. *Blood*. 2006;107(5):1864-1871.

147. Scott LM, Tong W, Levine RL, et al. JAK2 exon 12 mutations in polycythemia vera and idiopathic erythrocytosis. *N Engl J Med*. 2007;356(5):459-468.

148. Pietra D, Li S, Brisci A, et al. Somatic mutations of JAK2 exon 12 in patients with JAK2 (V617F)-negative myeloproliferative disorders. *Blood*. 2008;111(3):1686-1689.

149. Kralovics R, Passamonti F, Buser AS, et al. A gain-of-function mutation of JAK2 in myeloproliferative disorders. *N Engl J Med*. 2005;352(17):1779-1790.

150. Baxter EJ, Scott LM, Campbell PJ, et al. Acquired mutation of the tyrosine kinase JAK2 in human myeloproliferative disorders. *Lancet*. 2005;365(9464):1054-1061.

151. James C, Ugo V, Le Couedic JP, et al. A unique clonal JAK2 mutation leading to constitutive signalling causes polycythaemia vera. *Nature*. 2005;434(7037):1144-1148.

152. Levine RL, Wadleigh M, Cools J, et al. Activating mutation in the tyrosine kinase JAK2 in polycythemia vera, essential thrombocythemia, and myeloid metaplasia with myelofibrosis. *Cancer Cell*. 2005;7(4):387-397.

153. Rodig SJ, Meraz MA, White JM, et al. Disruption of the Jak1 gene demonstrates obligatory and nonredundant roles of the Jaks in cytokine-induced biologic responses. *Cell*. 1998;93(3):373-383.

154. Macchi P, Villa A, Giliani S, et al. Mutations of Jak-3 gene in patients with autosomal severe combined immune deficiency (SCID). *Nature*. 1995;377(6544):65-68.

155. Russell SM, Tayebi N, Nakajima H, et al. Mutation of Jak3 in a patient with SCID: essential role of Jak3 in lymphoid development. *Science*. 1995;270(5237):797-800.

156. Shimoda K, Kato K, Aoki K, et al. Tyk2 plays a restricted role in IFN alpha signaling, although it is required for IL-12-mediated T cell function. *Immunity*. 2000;13(4):561-571.

157. Ihle JN, Gilliland DG. Jak2: normal function and role in hematopoietic disorders. *Curr Opin Genet Dev*. 2007;17(1):8-14.

158. Pelletier S, Gingras S, Funakoshi-Tago M, Howell S, Ihle JN. Two domains of the erythropoietin receptor are sufficient for Jak2 binding/activation and function. *Mol Cell Biol*. 2006;26(22):8527-8538.

159. Funakoshi-Tago M, Pelletier S, Matsuda T, Parganas E, Ihle JN. Receptor specific downregulation of cytokine signaling by autophosphorylation in the FERM domain of Jak2. *EMBO J*. 2006;25(20):4763-4772.

160. Feng J, Witthuhn BA, Matsuda T, Kohlhuber F, Kerr IM, Ihle JN. Activation of Jak2 catalytic activity requires phosphorylation of Y1007 in the kinase activation loop. *Mol Cell Biol*. 1997;17(5):2497-2501.

161. Saharinen P, Takaluoma K, Silvennoinen O. Regulation of the Jak2 tyrosine kinase by its pseudokinase domain. *Mol Cell Biol*. 2000;20(10):3387-3395.

162. Shan Y, Gnanasambandan K, Ungureanu D, et al. Molecular basis for pseudokinase-dependent autoinhibition of JAK2 tyrosine kinase. *Nat Struct Mol Biol*. 2014;21(7):579-584.

163. Livnah O, Stura EA, Middleton SA, Johnson DL, Jolliffe LK, Wilson IA. Crystallographic evidence for preformed dimers of erythropoietin receptor before ligand activation. *Science*. 1999;283(5404):987-990.

164. Defour JP, Itaya M, Gryshkova V, et al. Tryptophan at the transmembrane-cytosolic junction modulates thrombopoietin receptor dimerization and activation. *Proc Natl Acad Sci U S A*. 2013;110(7):2540-2545.

165. Villarino AV, Kanno Y, Ferdinand JR, O'Shea JJ. Mechanisms of Jak/STAT signaling in immunity and disease. *J Immunol*. 2015;194(1):21-27.

166. Mascarenhas MI, Bacon WA, Kapeni C, et al. Analysis of Jak2 signaling reveals resistance of mouse embryonic hematopoietic stem cells to myeloproliferative disease mutation. *Blood*. 2016;127(19):2298-2309.

167. Schuringa JJ, Chung KY, Morrone G, Moore MA. Constitutive activation of STAT5A promotes human hematopoietic stem cell self-renewal and erythroid differentiation. *J Exp Med*. 2004;200(5):623-635.

168. Wierenga AT, Vellenga E, Schuringa JJ. Maximal STAT5-induced proliferation and self-renewal at intermediate STAT5 activity levels. *Mol Cell Biol*. 2008;28(21):6668-6680.

169. Huang Z, Richmond TD, Muntean AG, Barber DL, Weiss MJ, Crispino JD. STAT1 promotes megakaryopoiesis downstream of GATA-1 in mice. *J Clin Invest*. 2007;117(12):3890-3899.

170. Gough DJ, Messina NL, Hii L, et al. Functional crosstalk between type I and II interferon through the regulated expression of STAT1. *PLoS Biol*. 2010;8(4):e1000361.

171. Seki Y, Kai H, Shibata R, et al. Role of the JAK/STAT pathway in rat carotid artery remodeling after vascular injury. *Circ Res*. 2000;87(1):12-18.

172. Duan W, Yang Y, Yi W, et al. New role of JAK2/STAT3 signaling in endothelial cell oxidative stress injury and protective effect of melatonin. *PLoS One*. 2013;8(3):e57941.

173. Babon JJ, Lucet IS, Murphy JM, Nicola NA, Varghese LN. The molecular regulation of Janus kinase (JAK) activation. *Biochem J*. 2014;462(1):1-13.

174. Alicea-Velazquez NL, Jakoncic J, Boggon TJ. Structure-guided studies of the SHP-1/JAK1 interaction provide new insights into phosphatase catalytic domain substrate recognition. *J Struct Biol*. 2013;181(3):243-251.

175. Shultz LD, Rajan TV, Greiner DL. Severe defects in immunity and hematopoiesis caused by SHP-1 protein-tyrosine-phosphatase deficiency. *Trends Biotechnol*. 1997;15(8):302-307.

176. You M, Yu DH, Feng GS. Shp-2 tyrosine phosphatase functions as a negative regulator of the interferon-stimulated Jak/STAT pathway. *Mol Cell Biol*. 1999;19(3):2416-2424.

177. Irie-Sasaki J, Sasaki T, Matsumoto W, et al. CD45 is a JAK phosphatase and negatively regulates cytokine receptor signalling. *Nature*. 2001;409(6818):349-354.

178. Yasukawa H, Misawa H, Sakamoto H, et al. The JAK-binding protein JAB inhibits Janus tyrosine kinase activity through binding in the activation loop. *EMBO J*. 1999;18(5):1309-1320.

179. Yoshimura A, Naka T, Kubo M. SOCS proteins, cytokine signalling and immune regulation. *Nat Rev Immunol*. 2007;7(6):454-465.

180. Velazquez L, Cheng AM, Fleming HE, et al. Cytokine signaling and hematopoietic homeostasis are disrupted in Lnk-deficient mice. *J Exp Med*. 2002;195(12):1599-1611.

181. Kralovics R, Guan Y, Prchal JT. Acquired uniparental disomy of chromosome 9p is a frequent stem cell defect in polycythemia vera. *Exp Hematol*. 2002;30(3):229-236.

182. Najfeld V, Montella L, Scalise A, Fruchtman S. Exploring polycythaemia vera with fluorescence in situ hybridization: additional cryptic 9p is the most frequent abnormality detected. *Br J Haematol*. 2002;119(2):558-566.

183. Bandaranayake RM, Ungureanu D, Shan Y, Shaw DE, Silvennoinen O, Hubbard SR. Crystal structures of the JAK2 pseudokinase domain and the pathogenic mutant V617F. *Nat Struct Mol Biol*. 2012;19(8):754-759.

184. Vannucchi AM, Antonioli E, Guglielmelli P, et al. Clinical profile of homozygous JAK2 617V>F mutation in patients with polycythemia vera or essential thrombocythemia. *Blood*. 2007;110(3):840-846.

185. Ungureanu D, Wu J, Pekkala T, et al. The pseudokinase domain of JAK2 is a dual-specificity protein kinase that negatively regulates cytokine signaling. *Nat Struct Mol Biol*. 2011;18(9):971-976.

186. Toms AV, Deshpande A, McNally R, et al. Structure of a pseudokinase-domain switch that controls oncogenic activation of Jak kinases. *Nat Struct Mol Biol*. 2013;20(10):1221-1223.

187. Tefferi A, Lasho TL, Schwager SM, et al. The clinical phenotype of wild-type, heterozygous, and homozygous JAK2V617F in polycythemia vera. *Cancer*. 2006;106(3):631-635.

188. Beer PA, Delhommeau F, LeCouedic JP, et al. Two routes to leukemic transformation after a JAK2 mutation-positive myeloproliferative neoplasm. *Blood*. 2010;115(14):2891-2900.

189. Tiedt R, Hao-Shen H, Sobas MA, et al. Ratio of mutant JAK2-V617F to wild-type Jak2 determines the MPD phenotypes in transgenic mice. *Blood*. 2008;111(8):3931-3940.

190. Godfrey AL, Chen E, Pagano F, et al. JAK2V617F homozygosity arises commonly and recurrently in PV and ET, but PV is characterized by expansion of a dominant homozygous subclone. *Blood*. 2012;120(13):2704-2707.

191. Chen E, Beer PA, Godfrey AL, et al. Distinct clinical phenotypes associated with JAK2V617F reflect differential STAT1 signaling. *Cancer Cell*. 2010;18(5):524-535.

192. Duek A, Lundberg P, Shimizu T, et al. Loss of Stat1 decreases megakaryopoiesis and favors erythropoiesis in a JAK2-V617F-driven mouse model of MPNs. *Blood*. 2014;123(25):3943-3950.

193. Tefferi A, Pardanani A, Lim KH, et al. TET2 mutations and their clinical correlates in polycythemia vera, essential thrombocythemia and myelofibrosis. *Leukemia*. 2009;23(5):905-911.

194. Delhommeau F, Dupont S, Della Valle V, et al. Mutation in TET2 in myeloid cancers. *N Engl J Med*. 2009;360(22):2289-2301.

195. Schaub FX, Looser R, Li S, et al. Clonal analysis of TET2 and JAK2 mutations suggests that TET2 can be a late event in the progression of myeloproliferative neoplasms. *Blood*. 2010;115(10):2003-2007.

196. Scott LM, Rebel VI. JAK2 and genomic instability in the myeloproliferative neoplasms: a case of the chicken or the egg? *Am J Hematol*. 2012;87(11):1028-1036.

197. Wang X, Prakash S, Lu M, et al. Spleens of myelofibrosis patients contain malignant hematopoietic stem cells. *J Clin Invest*. 2012;122(11):3888-3899.

198. Ishii T, Zhao Y, Sozer S, et al. Behavior of CD34+ cells isolated from patients with polycythemia vera in NOD/SCID mice. *Exp Hematol*. 2007;35(11):1633-1640.

199. Lacout C, Pisani DF, Tulliez M, Gachelin FM, Vainchenker W, Villeval JL. JAK2V617F expression in murine hematopoietic cells leads to MPD mimicking human PV with secondary myelofibrosis. *Blood*. 2006;108(5):1652-1660.

200. Bumm TG, Elsea C, Corbin AS, et al. Characterization of murine JAK2V617F-positive myeloproliferative disease. *Cancer Res*. 2006;66(23):11156-11165.

201. Wernig G, Mercher T, Okabe R, Levine RL, Lee BH, Gilliland DG. Expression of Jak2V617F causes a polycythemia vera-like disease with associated myelofibrosis in a murine bone marrow transplant model. *Blood*. 2006;107(11):4274-4281.

202. Li J, Kent DG, Godfrey AL, et al. JAK2V617F homozygosity drives a phenotypic switch in myeloproliferative neoplasms, but is insufficient to sustain disease. *Blood*. 2014;123(20):3139-3151.

203. Akada H, Akada S, Hutchison RE, Mohi G. Erythroid lineage-restricted expression of Jak2V617F is sufficient to induce a myeloproliferative disease in mice. *Haematologica*. 2012;97(9):1389-1393.

204. Mullally A, Lane SW, Ball B, et al. Physiological Jak2V617F expression causes a lethal myeloproliferative neoplasm with differential effects on hematopoietic stem and progenitor cells. *Cancer Cell*. 2010;17(6):584-596.

205. Mullally A, Poveromo L, Schneider RK, Al-Shahrour F, Lane SW, Ebert BL. Distinct roles for long-term hematopoietic stem cells and erythroid precursor cells in a murine model of Jak2V617F-mediated polycythemia vera. *Blood*. 2012;120(1):166-172.

206. Li J, Spensberger D, Ahn JS, et al. JAK2 V617F impairs hematopoietic stem cell function in a conditional knock-in mouse model of JAK2 V617F-positive essential thrombocythemia. *Blood*. 2010;116(9):1528-1538.

207. Kent DG, Li J, Tanna H, et al. Self-renewal of single mouse hematopoietic stem cells is reduced by JAK2V617F without compromising progenitor cell expansion. *PLoS Biol*. 2013;11(6):e1001576.

208. Tefferi A, Thiele J, Vardiman JW. The 2008 World Health Organization classification system for myeloproliferative neoplasms: order out of chaos. *Cancer*. 2009;115(17):3842-3847.

209. Harrison C, Kiladjian JJ, Al-Ali HK, et al. JAK inhibition with ruxolitinib versus best available therapy for myelofibrosis. *N Engl J Med*. 2012;366(9):787-798.

210. Vainchenker W, Favale F. Myelofibrosis, JAK2 inhibitors and erythropoiesis. *Leukemia*. 2013;27(6):1219-1223.

211. Pietras K, Ostman A. Hallmarks of cancer: interactions with the tumor stroma. *Exp Cell Res*. 2010;316(8):1324-1331.

212. Mesa RA, Hanson CA, Rajkumar SV, Schroeder G, Tefferi A. Evaluation and clinical correlations of bone marrow angiogenesis in myelofibrosis with myeloid metaplasia. *Blood*. 2000;96(10):3374-3380.

213. Barosi G, Rosti V, Massa M, et al. Spleen neoangiogenesis in patients with myelofibrosis with myeloid metaplasia. *Br J Haematol*. 2004;124(5):618-625.

214. Gunsilius E, Duba HC, Petzer AL, et al. Evidence from a leukaemia model for maintenance of vascular endothelium by bone-marrow-derived endothelial cells. *Lancet*. 2000;355(9216):1688-1691.

215. Rigolin GM, Fraulini C, Ciccone M, et al. Neoplastic circulating endothelial cells in multiple myeloma with 13q14 deletion. *Blood*. 2006;107(6):2531-2535.

216. Streubel B, Chott A, Huber D, et al. Lymphoma-specific genetic aberrations in microvascular endothelial cells in B-cell lymphomas. *N Engl J Med*. 2004;351(3):250-259.

217. Sozer S, Fiel MI, Schiano T, Xu M, Mascarenhas J, Hoffman R. The presence of JAK2V617F mutation in the liver endothelial cells of patients with Budd-Chiari syndrome. *Blood*. 2009;113(21):5246-5249.

218. Teofili L, Martini M, Iachininoto MG, et al. Endothelial progenitor cells are clonal and exhibit the JAK2(V617F) mutation in a subset of thrombotic patients with Ph-negative myeloproliferative neoplasms. *Blood*. 2011;117(9):2700-2707.

219. Rosti V, Villani L, Riboni R, et al. Spleen endothelial cells from patients with myelofibrosis harbor the JAK2V617F mutation. *Blood*. 2013;121(2):360-368.

220. Sozer S, Ishii T, Fiel MI, et al. Human CD34+ cells are capable of generating normal and JAK2V617F positive endothelial like cells in vivo. *Blood Cells Mol Dis*. 2009;43(3):304-312.

221. Zhang Z, Lutz B. Cre recombinase-mediated inversion using lox66 and lox71: method to introduce conditional point mutations into the CREB-binding protein. *Nucleic Acids Res*. 2002;30(17):e90.

222. Kisanuki YY, Hammer RE, Miyazaki J, Williams SC, Richardson JA, Yanagisawa M. Tie2-Cre transgenic mice: a new model for endothelial cell-lineage analysis in vivo. *Dev Biol*. 2001;230(2):230-242.

223. Tang Y, Harrington A, Yang X, Friesel RE, Liaw L. The contribution of the Tie2+ lineage to primitive and definitive hematopoietic cells. *Genesis*. 2010;48(9):563-567.

224. Etheridge SL, Roh ME, Cosgrove ME, et al. JAK2V617F-positive endothelial cells contribute to clotting abnormalities in myeloproliferative neoplasms. *Proc Natl Acad Sci U S A*. 2014;111(6):2295-2300.

225. Tiedt R, Schomber T, Hao-Shen H, Skoda RC. Pf4-Cre transgenic mice allow the generation of lineage-restricted gene knockouts for studying megakaryocyte and platelet function in vivo. *Blood*. 2007;109(4):1503-1506.

226. Carstairs KC. The identification of platelets and platelet antigens in histological sections. *J Pathol Bacteriol*. 1965;90(1):225-231.

227. Lamrani L, Lacout C, Ollivier V, et al. Hemostatic disorders in a JAK2V617F-driven mouse model of myeloproliferative neoplasm. *Blood*. 2014;124(7):1136-1145.

228. Papadakis E, Hoffman R, Brenner B. Thrombohemorrhagic complications of myeloproliferative disorders. *Blood Rev*. 2010;24(6):227-232.

229. Matsushita K, Morrell CN, Cambien B, et al. Nitric oxide regulates exocytosis by S-nitrosylation of N-ethylmaleimide-sensitive factor. *Cell*. 2003;115(2):139-150.

230. Qian Z, Gelzer-Bell R, Yang Sx SX, et al. Inducible nitric oxide synthase inhibition of weibel-palade body release in cardiac transplant rejection. *Circulation*. 2001;104(19):2369-2375.

231. Pfeiffer S, Leopold E, Schmidt K, Brunner F, Mayer B. Inhibition of nitric oxide synthesis by NG-nitro-L-arginine methyl ester (L-NAME): requirement for bioactivation to the free acid, NG-nitro-L-arginine. *Br J Pharmacol*. 1996;118(6):1433-1440.

232. Charrier S, Ferrand M, Zerbato M, et al. Quantification of lentiviral vector copy numbers in individual hematopoietic colony-forming cells shows vector dose-dependent effects on the frequency and level of transduction. *Gene Ther*. 2011;18(5):479-487.

233. Ramana CV, Chatterjee-Kishore M, Nguyen H, Stark GR. Complex roles of Stat1 in regulating gene expression. *Oncogene*. 2000;19(21):2619-2627.

234. Stephanou A, Latchman DS. STAT-1: a novel regulator of apoptosis. *Int J Exp Pathol*. 2003;84(6):239-244.

235. Knupfer H, Preiss R. sIL-6R: more than an agonist? *Immunol Cell Biol*. 2008;86(1):87-91.

236. Müller-Newen G, Küster A, Hemmann U, et al. Soluble IL-6 receptor potentiates the antagonistic activity of soluble gp130 on IL-6 responses. *J Immunol*. 1998;161(11):6347-6355.

237. Pelletier S, Duhamel F, Coulombe P, Popoff MR, Meloche S. Rho family GTPases are required for activation of Jak/STAT signaling by G protein-coupled receptors. *Mol Cell Biol*. 2003;23(4):1316-1333.

238. Min W, Pober JS, Johnson DR. Interferon induction of TAP1: the phosphatase SHP-1 regulates crossover between the IFN-alpha/beta and the IFN-gamma signal-transduction pathways. *Circ Res*. 1998;83(8):815-823.

239. Zhang J, Alcaide P, Liu L, et al. Regulation of endothelial cell adhesion molecule expression by mast cells, macrophages, and neutrophils. *PLoS One*. 2011;6(1):e14525.

240. Whitman SC, Ravisankar P, Elam H, Daugherty A. Exogenous interferon-gamma enhances atherosclerosis in apolipoprotein E-/- mice. *Am J Pathol*. 2000;157(6):1819-1824.

241. Denny MF, Thacker S, Mehta H, et al. Interferon-alpha promotes abnormal vasculogenesis in lupus: a potential pathway for premature atherosclerosis. *Blood*. 2007;110(8):2907-2915.

242. Lu M, Xia L, Liu YC, et al. Lipocalin produced by myelofibrosis cells affects the fate of both hematopoietic and marrow microenvironmental cells. *Blood*. 2015;126(8):972-982.

243. Fleischman AG, Aichberger KJ, Luty SB, et al. TNFα facilitates clonal expansion of JAK2V617F positive cells in myeloproliferative neoplasms. *Blood*. 2011;118(24):6392-6398.

244. Wolf MJ, Hoos A, Bauer J, et al. Endothelial CCR2 signaling induced by colon carcinoma cells enables extravasation via the JAK2-Stat5 and p38MAPK pathway. *Cancer Cell*. 2012;22(1):91-105.

245. He R, Yang X, Lin Y, et al. FAP promotes immunosuppression by cancer-associated fibroblasts in the tumor microenvironment via STAT3-CCL2 signaling. *Cancer Res*. 2016.

246. Charo IF, Taubman MB. Chemokines in the pathogenesis of vascular disease. *Circ Res*. 2004;95(9):858-866.

247. Schecter AD, Berman AB, Yi L, et al. MCP-1-dependent signaling in CCR2(-/-) aortic smooth muscle cells. *J Leukoc Biol*. 2004;75(6):1079-1085.

248. Kusch A, Tkachuk S, Tkachuk N, et al. The tight junction protein ZO-2 mediates proliferation of vascular smooth muscle cells via regulation of Stat1. *Cardiovasc Res*. 2009;83(1):115-122.

249. Mitchell K, Yang HY, Berk JD, Tran JH, Iadarola MJ. Monocyte chemoattractant protein-1 in the choroid plexus: a potential link between vascular pro-inflammatory mediators and the CNS during peripheral tissue inflammation. *Neuroscience*. 2009;158(2):885-895.

250. Spassov DS, Ahuja D, Wong CH, Moasser MM. The structural features of Trask that mediate its anti-adhesive functions. *PLoS One*. 2011;6(4):e19154.

251. Hooper JD, Zijlstra A, Aimes RT, et al. Subtractive immunization using highly metastatic human tumor cells identifies SIMA135/CDCP1, a 135 kDa cell surface phosphorylated glycoprotein antigen. *Oncogene*. 2003;22(12):1783-1794.

252. Law ME, Ferreira RB, Davis BJ, et al. CUB domain-containing protein 1 and the epidermal growth factor receptor cooperate to induce cell detachment. *Breast Cancer Res*. 2016;18(1):80.

253. Assi TB, Baz E. Current applications of therapeutic phlebotomy. *Blood Transfus*. 2014;12 Suppl 1:s75-83.

254. Tan AY, Westerman DA, Dobrovic A. A simple, rapid, and sensitive method for the detection of the JAK2 V617F mutation. *Am J Clin Pathol*. 2007;127(6):977-981.

255. Pan L, Peng H. Polymerase chain reaction clonality assays based on x-linked genes. *Methods Mol Med*. 2001;49:73-79.

256. Boudewijns M, van Dongen JJ, Langerak AW. The human androgen receptor X-chromosome inactivation assay for clonality diagnostics of natural killer cell proliferations. *J Mol Diagn*. 2007;9(3):337-344.

257. Faulkner JMRaHML. A phase retrieval algorithm for shifting illumination. *Applied Physics Letters*. 2004;85(4795).

258. Suman R, Smith G, Hazel KE, et al. Label-free imaging to study phenotypic behavioural traits of cells in complex co-cultures. *Sci Rep*. 2016;6:22032.

259. Khan SS, Solomon MA, McCoy JP, Jr. Detection of circulating endothelial cells and endothelial progenitor cells by flow cytometry. *Cytometry B Clin Cytom*. 2005;64(1):1-8.

260. Quentmeier H, MacLeod RA, Zaborski M, Drexler HG. JAK2 V617F tyrosine kinase mutation in cell lines derived from myeloproliferative disorders. *Leukemia*. 2006;20(3):471-476.

261. Watanabe T, Tokunaga O. Multinucleated variant endothelial cell. Its characterization and relation to atherosclerosis. *Ann N Y Acad Sci*. 1990;598:217-222.

262. Minamino T, Miyauchi H, Yoshida T, Ishida Y, Yoshida H, Komuro I. Endothelial cell senescence in human atherosclerosis: role of telomere in endothelial dysfunction. *Circulation*. 2002;105(13):1541-1544.

263. Burrig KF. The endothelium of advanced arteriosclerotic plaques in humans. *Arterioscler Thromb*. 1991;11(6):1678-1689.

264. Martin-Ramirez J, Hofman M, van den Biggelaar M, Hebbel RP, Voorberg J. Establishment of outgrowth endothelial cells from peripheral blood. *Nat Protocols*. 2012;7(9):1709-1715.

265. Lin Y, Weisdorf DJ, Solovey A, Hebbel RP. Origins of circulating endothelial cells and endothelial outgrowth from blood. *J Clin Invest*. 2000;105(1):71-77.

266. Fuchs S, Motta A, Migliaresi C, Kirkpatrick CJ. Outgrowth endothelial cells isolated and expanded from human peripheral blood progenitor cells as a potential source of autologous cells for endothelialization of silk fibroin biomaterials. *Biomaterials*. 2006;27(31):5399-5408.

267. Dauwe D, Pelacho B, Wibowo A, et al. Neovascularization Potential of Blood Outgrowth Endothelial Cells From Patients With Stable Ischemic Heart Failure Is Preserved. *J Am Heart Assoc*. 2016;5(4):e002288.

268. Carmeliet P. Angiogenesis in health and disease. *Nat Med*. 2003;9(6):653-660.

269. Sukriti S, Tauseef M, Yazbeck P, Mehta D. Mechanisms regulating endothelial permeability. *Pulm Circ*. 2014;4(4):535-551.

270. Vannucchi AM. How I treat polycythemia vera. *Blood*. 2014;124(22):3212-3220.

271. Schmitt A, Guichard J, Masse JM, Debili N, Cramer EM. Of mice and men: comparison of the ultrastructure of megakaryocytes and platelets. *Exp Hematol*. 2001;29(11):1295-1302.

272. Peters LL, Cheever EM, Ellis HR, et al. Large-scale, high-throughput screening for coagulation and hematologic phenotypes in mice. *Physiol Genomics*. 2002;11(3):185-193.

273. Jirouskova M, Shet AS, Johnson GJ. A guide to murine platelet structure, function, assays, and genetic alterations. *J Thromb Haemost*. 2007;5(4):661-669.

274. Getz GS, Reardon CA. Animal models of atherosclerosis. *Arterioscler Thromb Vasc Biol*. 2012;32(5):1104-1115.

275. Piedrahita JA, Zhang SH, Hagaman JR, Oliver PM, Maeda N. Generation of mice carrying a mutant apolipoprotein E gene inactivated by gene targeting in embryonic stem cells. *Proc Natl Acad Sci U S A*. 1992;89(10):4471-4475.

276. Meir KS, Leitersdorf E. Atherosclerosis in the apolipoprotein-E-deficient mouse: a decade of progress. *Arterioscler Thromb Vasc Biol*. 2004;24(6):1006-1014.

277. Schafer K, Muller K, Hecke A, et al. Enhanced thrombosis in atherosclerosis-prone mice is associated with increased arterial expression of plasminogen activator inhibitor-1. *Arterioscler Thromb Vasc Biol*. 2003;23(11):2097-2103.

278. Barbui T, Finazzi G, Falanga A. Myeloproliferative neoplasms and thrombosis. *Blood*. 2013;122(13):2176-2184.

279. Day SM, Reeve JL, Myers DD, Fay WP. Murine thrombosis models. *Thromb Haemost*. 2004;92(3):486-494.

280. Westrick RJ, Winn ME, Eitzman DT. Murine models of vascular thrombosis (Eitzman series). *Arterioscler Thromb Vasc Biol*. 2007;27(10):2079-2093.

281. Furie B, Furie BC. Thrombus formation in vivo. *J Clin Invest*. 2005;115(12):3355-3362.

282. Farrehi PM, Ozaki CK, Carmeliet P, Fay WP. Regulation of arterial thrombolysis by plasminogen activator inhibitor-1 in mice. *Circulation*. 1998;97(10):1002-1008.

283. Ciciliano JC, Sakurai Y, Myers DR, et al. Resolving the multifaceted mechanisms of the ferric chloride thrombosis model using an interdisciplinary microfluidic approach. *Blood*. 2015;126(6):817-824.

284. Monvoisin A, Alva JA, Hofmann JJ, Zovein AC, Lane TF, Iruela-Arispe ML. VE-cadherin-CreERT2 transgenic mouse: a model for inducible recombination in the endothelium. *Dev Dyn*. 2006;235(12):3413-3422.

285. Rauch I, Muller M, Decker T. The regulation of inflammation by interferons and their STATs. *JAKSTAT*. 2013;2(1):e23820.

286. Tiruppathi C, Minshall RD, Paria BC, Vogel SM, Malik AB. Role of Ca2+ signaling in the regulation of endothelial permeability. *Vascul Pharmacol*. 2002;39(4-5):173-185.

287. Tsukita S, Katsuno T, Yamazaki Y, Umeda K, Tamura A, Tsukita S. Roles of ZO-1 and ZO-2 in establishment of the belt-like adherens and tight junctions with paracellular permselective barrier function. *Ann N Y Acad Sci*. 2009;1165:44-52.

288. Radu M, Chernoff J. An in vivo assay to test blood vessel permeability. *J Vis Exp*. 2013(73):e50062.

289. Erusalimsky JD. Vascular endothelial senescence: from mechanisms to pathophysiology. *J Appl Physiol (1985)*. 2009;106(1):326-332.

290. Coleman PR, Chang G, Hutas G, Grimshaw M, Vadas MA, Gamble JR. Age-associated stresses induce an anti-inflammatory senescent phenotype in endothelial cells. *Aging (Albany NY)*. 2013;5(12):913-924.

291. Dimri GP, Lee X, Basile G, et al. A biomarker that identifies senescent human cells in culture and in aging skin in vivo. *Proc Natl Acad Sci U S A*. 1995;92(20):9363-9367.

292. Warboys CM, de Luca A, Amini N, et al. Disturbed flow promotes endothelial senescence via a p53-dependent pathway. *Arterioscler Thromb Vasc Biol*. 2014;34(5):985-995.

293. Erusalimsky JD, Skene C. Mechanisms of endothelial senescence. *Exp Physiol*. 2009;94(3):299-304.

294. Krouwer VJ, Hekking LH, Langelaar-Makkinje M, Regan-Klapisz E, Post JA. Endothelial cell senescence is associated with disrupted cell-cell junctions and increased monolayer permeability. *Vasc Cell*. 2012;4(1):12.

295. Debacq-Chainiaux F, Erusalimsky JD, Campisi J, Toussaint O. Protocols to detect senescence-associated beta-galactosidase (SA-betagal) activity, a biomarker of senescent cells in culture and in vivo. *Nat Protoc*. 2009;4(12):1798-1806.

296. Wang Z, Wei D, Xiao H. Methods of cellular senescence induction using oxidative stress. *Methods Mol Biol*. 2013;1048:135-144.

297. Smith AM, Prabhakarpandian B, Pant K. Generation of shear adhesion map using SynVivo synthetic microvascular networks. *J Vis Exp*. 2014(87).

298. Minamino T, Komuro I. Vascular cell senescence: contribution to atherosclerosis. *Circ Res*. 2007;100(1):15-26.